Non-Linear Motion Response Simulation of Floating Vessels in Waves

by

Nuno Fonseca, B.Sc.

A Thesis submitted for the degree of
Master of Science

Department of Naval Architecture and Ocean Engineering
University of Glasgow

December 1993

ProQuest LLC.
789 East Eisenhower Parkway
P.O. Box 1346
Ann Arbor, MI 48106 – 1346

TABLE OF CONTENTS

DECLARATION

Except where reference is made to the work of others,
this thesis is believed to be original.

ACKNOWLEDGEMENTS

The author would like to thank the following;

Professor D. Faulkner, Head of Department, for allowing him to carry out this study.

Professor C. G. Soares for the strong encouragement given to begin this M.Sc., and for his continuous guidance and assistance during the first phase of the work in Lisbon.

Dr. A. Incecik for his excellent supervision, contribution to many aspects of the research, and for his always immediate assistance whenever help was needed, whether the matter was related to the thesis work or not.

Dr. L. Tamborskyi for his excellent and unique lectures, for the long hours spent teaching and discussing, and for providing some of the computer routines used in this work. The research was very much influenced by him.

All the technicians at the Hydrodynamic Laboratory for their help during the experiments.

Mr. D. Percival for his assistance during the analysis of the experimental results.

Financial support during the course of this work has been provided by the Portuguese Government represented by the "Junta Nacional de Investigação Científica e Tecnológica", for which the author is very grateful.

ABSTRACT

The subject of this thesis is the prediction of non-linear motions of floating bodies subjected to waves by a time domain method. Two steps are followed in the research, the first one consists of developing and applying a method able to calculate the hydrodynamic forces associated with non-linear unsteady motions in the time domain, since the ordinary frequency domain hydrodynamic coefficients are restricted to sinusoidal motions. Once this method is validated one non-linear term is studied and introduced to the motion equations. The non-linearity arises from the evaluation of the hydrostatic forces and moments taking into account the instantaneous wetted surface. The linear free surface elevation on the sides of the body contributes to the wetted surface. All time domain numerical results are compared with the corresponding linear frequency domain results, thus it is easy to verify improvements or discrepancies predicted by the non-linear model.

On the first part of the thesis the two-dimensional motion of cylinders with arbitrary cross sections and subjected to beam waves is studied. The motions are the sway, heave, and roll. The frequency domain radiation forces are evaluated by the "Frank Close Fit Method", while in the time domain the same forces are evaluated using Fourier transforms of the frequency domain solution. The exciting forces in both models are calculated by the "Frank Close Fit Method". Finally numerical results are compared with experimental data corresponding to several wave amplitudes and a wide range of wave frequencies.

On the second part of the thesis, the motion of ship forms travelling with an arbitrary heading angle relative to linear waves is studied. A modern strip theory is used to calculate the radiation and exciting forces, and the sectional forces are evaluated by the methods studied in the first part of the thesis. Again in the time domain model the radiation forces are evaluated using fourier transforms of the frequency domain solution. The development of the computer program which applies the time domain model was not completed during the period of the thesis work, thus results are presented only for the heave and pitch motions for the condition head waves and zero forward speed. The responses of a large

container ship are investigated for a wide range of wave frequencies. Also the influence of the wave steepness on the non-linear solution is investigated.

LIST OF FIGURES

NONEMCLATURE

A_{wl} Water plane area.

A_{kj} Ship added mass coefficient.

A_{kj}^{∞} Ship added mass coefficient at infinity frequency.

A_S Sectional area

B_{kj} Ship damping coefficient.

B_{kj}^{t} Time domain ship damping coefficient.

C_{kj} Ship restoring coefficient, and represents the force in k-direction when the ship is subjected to a unit motion in j-mode.

C_{kj}^{t} Time domain radiation restoring force in k-direction, when the ship with forward speed is subjected to a unit motion in j-mode.

$\overline{GM}_L$ Longitudinal metacentric height.

$\overline{GM}_T$ Transversal metacentric height.

$G(\overline{QP})$ Green function.

$G^*(\overline{QP})$ Contribution to the Green function due to the boundary conditions.

F Total oscillatory pressure force acting upon the ship.

F^E Ship exciting force.

F^I Ship incident part of the exciting force, or Froud Krilov force.

F^D Ship diffraction part of the exciting force.

F^R Ship radiation force or reactive hydrodynamic force.

F^H Ship hydrostatic force.

F^B Ship restoring force.

F^M Ship body mass force, or inertial force.

F^W Ship weight force.

F_k^E Ship complex amplitude of the exciting force in 'k' direction. The same follows for all other ship forces presented above.

$(F_k^E)^C$, $(F_k^E)^S$ Cosine and sine amplitudes of the ship exciting forces.

$\hat{F}_{kj}^R$ Ship radiation force in k-direction due to an unit imposed motion in j-mode.

Kh_j Retardation function of the free-surface elevation due to the radiated waves.

I_{ji} Body moments and products of inertia, i,j=1,...,6.

$K_{kj}(t)$ Retardation function representing the memory effects.

L_w Wave length.

M Ship mass.

M^H Ship hydrostatic moment.

N_2, N_3, N_4 Notation for the two-dimensional unit normal vector used in the ship motion problem.

P Generic point in the fluid, the influenced point.

Q Fundamental source point, the influencing point.

S Exact body wetted surface.

S_0 Mean body wetted surface, assumed equal to the wetted surface with the body in static equilibrium in still water.

S_F Free surface boundary of the fluid.

S_R Surface inside the fluid and approaching infinity.

$S_\zeta(\omega_0)$ Spectral density of wave energy.

U Ship forward speed.

V Fluid velocity vector.

V_0 Time independent steady fluid velocity vector.

V_1 Time dependent unsteady fluid velocity vector.

V_S Body velocity.

$V_{wl}(t)$ Body volume under the water line.

$X_0(x_0, y_0, z_0)$ Global fixed Cartesian co-ordinate system.

$X'(x', y', z')$ Body fixed Cartesian co-ordinate system.

$X(x, y, z)$ Cartesian co-ordinate system fixed on the mean position of the body.

a_{kj} Sectional added mass coefficient.

a_{kj}^{∞} Sectional added mass coefficient at infinite frequency.

b_{kj} Sectional damping coefficient.

b_{44}^{v} Sectional roll damping coefficient due to viscous effects.

b_{44}^{*} Equivalent roll damping coefficient, which contains the wave making and viscous effects.

c_{kj} Sectional restoring coefficient, and represents the force in k-direction which the body is subjected to due to a unit motion in j-mode.

f Total oscillatory pressure force acting upon a section.

f^{E} Sectional exciting force.

f^{I} Sectional incident part of the exciting force, or Froud Krilov force.

f^{D} Sectional diffraction part of the exciting force.

f^{R} Sectional radiation force or reactive hydrodynamic force.

f^{H} Sectional hydrostatic force.

f^{B} Sectional restoring force.

f^{M} Sectional body mass force, or inertial force.

f_k^{E} Sectional complex amplitude of the exciting force in 'k' direction. The same follows for all other Sectional forces presented above.

$\hat{f}_{kj}^{R}$ Sectional radiation force in k-direction due to a unit amplitude motion in j-mode.

$\hat{f}_k^{E}$ Sectional exciting force in k-direction due to an incident wave of unit amplitude. The same follows for $\hat{f}_k^{I}$ and $\hat{f}_k^{D}$.

$(f_k^{E})^{C}$, $(f_k^{E})^{S}$ Sectional amplitudes of the cosine and sine parts of the exciting force in k-direction.

g Gravitational acceleration.

k_0 Wave number.

m Sectional mass.

m_{kj} Sectional body inertia coefficients.

m^H Sectional hydrostatic moment.

$\tilde{m}$ Six component vector representing some characteristics of the steady flow in the neighbourhood of the body surface.

n Unit normal vector to the body mean wetted surface, S_0, with components (n_1, n_2, n_3).

n^{wl} Unit normal vector to the surface defined by the intersection of the free surface with the body volume, $n^{wl} = (n_1^{wl}, n_2^{wl}, n_3^{wl})$.

$\tilde{n}$ Six component normal vector to the body mean wetted surface, $(n_1, n_2, n_3) = n$, $(n_4, n_5, n_6) = n \times r$.

n^S Instantaneous unit normal vector to the exact wetted body surface, and directed outwards, with components (n_1^S, n_2^S, n_3^S).

p Fluid pressure.

p_a Atmospheric pressure.

p_h Hydrostatic pressure.

$q(Q,t)$ Source strength.

$\hat{q}_j(Q)$ Source strength in point Q, due to a sinusoidal motion of unit amplitude in j-mode.

$q^*_j(Q)$ Source strength non-dimensionalised with respect to $\omega\xi^a$.

r Vector displacement of any point on the body surface represented on the co-ordinate system X′.

t Time variable.

x_B, y_B, z_B Co-ordinates of the immersed volume centre.

x_G, y_G, z_G Co-ordinates of the gravity centre.

x'_G, y'_G, z'_G Co-ordinates of the gravity centre represented on the reference system fixed in the body.

Φ Fluid velocity potential expressed on the reference system fixed on the ship mean position.

Φ_0 Time independent steady potential, $\Phi_0 = -Ux + \Phi_S$.

Φ_1 Time dependent unsteady potential.

Φ_S Contribution to the steady potential due to ship's presence.

Φ^I Incident wave potential.

$\hat{\Phi}^I$ Incident wave potential due to a wave of unit amplitude.

Φ^D Diffracted wave potential.

$\hat{\Phi}^D$ Diffracted wave potential due to an incident wave of unit amplitude.

Φ^R Radiation potential.

$\hat{\Phi}_j^R$ Radiation potential due to an unit amplitude motion in j-mode. This potential can be separated into a speed independent component, $\hat{\Phi}_j^0$, and a speed dependent component, $\hat{\Phi}_j^U$.

ϑ_j Time domain radiation potential, normalised by the body velocity, due to a motion in j-mode.

Θ Fluid velocity potential expressed on the fixed reference system.

$\Omega(t) = (\xi_4(t), \xi_5(t), \xi_6(t))$ Unsteady rotation of the body represented on the co-ordinate system X.

$\alpha(r,t)$ Vector displacement of any point on the body surface, represented on the co-ordinate system X.

$\dot{\alpha}(r,t)$ Time derivative of $\alpha(r,t)$.

χ_j Normalised time domain radiation potential of a decaying fluid motion.

$\delta_k^B(t)$ Contribution to the restoring force in k-direction due to non-linear effects.

ε_n Random phase of the sinusoidal incident wave component n.

ϕ_j^v Time domain radiation potential, proportional to the body instantaneous velocity.

ϕ_j^r Time-domain radiation potential of a decaying fluid motion.

$\eta(t) = (\xi_1(t), \xi_2(t), \xi_3(t))$ Unsteady translation of the body.

$\hat{\varphi}^I$ Complex amplitude of the potential correspondent to an unit amplitude incident wave. This is a 2D part of a general 3D potential.

$\hat{\varphi}^D$ Two-dimensional diffraction potential corresponding to a unit amplitude incident wave. This is a 2D part of a general 3D potential.

μ Reyleigh viscosity.

θ_j Phase angle of the sinusoidal motion in j-mode.

ρ Fluid density.

ρ_B Body density.

τ Time variable.

ω Encounter frequency.

ω_0 Incident wave frequency.

ω_{0n} Incident wave frequency of the component n.

$\xi_j(t)$ Rigid body motions, where ξ_1, ξ_2, ξ_3 represent the surge, sway, and heave displacements respectively, and ξ_4, ξ_5, ξ_6 represent the roll, pitch, and yaw rotations respectively.

$\dot{\xi}_j(t)$ Body velocities.

$\ddot{\xi}_j(t)$ Body accelerations.

ξ_j^A Complex amplitude of the sinusoidal motion in 'j' mode.

ξ_j^a Real amplitude of the sinusoidal motion in 'j' mode.

ξ_j^C, ξ_j^S Amplitudes of the cosine and sine parts of the sinusoidal motion in j-mode.

$\zeta(t)$ Instantaneous free-surface elevation.

ζ^a Sinusoidal wave amplitude.

ζ_n^a Wave amplitude of the sinusoidal component n.

$\zeta^I, \zeta^D, \zeta^R$ Free-surface elevation respectively due to the incident wave, diffracted wave, and radiated wave.

$\zeta^{R}_{j_{FD}}$ Frequency domain amplitude of the radiated wave due to an unit amplitude motion in j-mode.

∇ Gradient operator.

$\mathfrak{I}\{f\}$ Fourier transform of the function f.

$\mathfrak{I}_c\{f\}, \mathfrak{I}_s\{f\}$ Fourier cosine and sine transforms of the function f.

1. INTRODUCTION

1.1 - Ship Motions in a seaway

Nowadays the accurate prediction and reduction of seakeeping and wave load problems are indispensable steps in the ship design procedure. Examples of these problems are: Vertical accelerations which contribute to extra load on cargo and equipment and cause seasickness on the crew and passengers, the exaggeration of relative vertical motions between the ship and the waves which can cause damage due to slamming, and the water on the deck or propeller emergence. Following waves can cause situations where the ship become statically unstable, and the directional stability can also be affected. For some particular ships the roll motion is of great importance from the operational point of view, and can even be a critical and dangerous motion. For larger ships wave induced bending moments, shear forces and torsional moments are determinant for design purposes. In addition as a consequence of ship motions and wave loads the speed may be significantly reduced, affecting the economic viability of cargo ships.

Although the application of linear strip theory in the frequency domain together with the probabilistic tools gives reliable predictions in certain conditions and is widely used, some of the described practical seakeeping and structural loading problems are not well analysed by such methods. These arise from behaviours with non-linear characteristics, for example the strong and small duration impact due to slamming, the non-linear restoring moment associated with large roll motions, the differences between the dynamic sagging and hogging moments, etc. To take account of these effects new time domain ship motion theories must be developed and tested.

Ships generally experience oscillatory motions as they travel with forward speed in waves. In the study of oscillatory motion, a ship may be regarded as an unrestrained rigid body with six degrees of freedom. The three components of translational motion vector are the "surge" parallel to the longitudinal axis of the ship, the "heave" in the vertical direction, and the "sway" in the lateral direction . The rotational motions about the longitudinal, vertical and lateral axes are respectively the "roll", the "yaw", and the "pitch".

The dynamics of the oscillatory ship motions are governed by equations which balance the external forces acting on the ship, with the internal forces due to gravity and inertia (forces refer to forces and moments). As external forces will be considered as those result from interactions between the fluid and the hull, and the fluid is normally assumed inviscid.

In order to derive the external forces the fluid flow around the hull must be analysed. This problem can be treated as a superposition of the steady flow induced by the forward speed with the oscillatory flow that result from the interactions of the waves with the vessel. However interactions between the steady and oscillatory flow fields exist and complicate the general problem.

If it is assumed that the oscillatory motions and the wave amplitudes are small enough then the linear superposition can be applied to formulate the fluid-ship interaction problem. The following force components are formulated independently; the "hydrostatic problem", where the oscillatory forces are function of the ship's position in relation to the equilibrium position, the "radiation problem", where the ship has a oscillatory motion in otherwise calm water, and the "exciting forces problem", where incident waves act upon the ship in its equilibrium position. Interactions between these problems are of higher order and may be neglected.

Once the several terms of the motion equations are identified there are two methods for their solutions.

In the first method it is assumed that the exciting forces are sinusoidal in time, the restoring (or hydrostatic) forces are linearly proportional to the displacements and the radiation forces may be decomposed into components which are linearly proportional to the velocity and acceleration of the motion. With these assumptions the mathematical model will represent motions which vary sinusoidaly in time. The radiation force components proportional to the velocity are the "damping" terms, which are related to the energy dissipated in the waves radiated by the ship's oscillatory motions. The constant which relates the velocities to forces is named "damping coefficient" and its value depends on the frequency of motion. The components proportional to the accelerations are the "added inertia". The constant which relates the accelerations to forces is named "added mass" and its value is also dependent of the frequency.

Once these hydrodynamic coefficients are known the solution of the motion equations is trivial, the main difficulty is in fact on the evaluation of the coefficients and the exciting forces.

As a resume, the exciting force has a sinusoidal character, associated with a sinusoidal wave. The exciting force is also function of the ship's forward speed, and wave direction with respect to ship's direction of travel. This is the so called "Frequency Domain Solution", that has been extensively studied in the last three decades.

In an irregular sea, St. Denis and Pierson (1953), proposed the superposition principle that any response of a ship would be equal to the sum of the corresponding responses in each of the sinusoidal waves in which the irregular sea could be decomposed.

Another major step in this linear approach is the application of statistical methods, which permit to estimate the most probable largest responses in an irregular sea.

Another way of solving the motion equations is by a numerical time integration procedure. The solution will be built in the time-domain, step by step. In this case, as the solution is numerical, the equations have no restrictions, and this means that:

- the hydrodynamic forces do not need to be given by coefficients dependent on one frequency and one underwater form at still water level.
- the restoring forces do not need to be linearly proportional to the displacements
- the exciting forces do not need to be sinusoidal and, in principle, may be of any form.

The principal difficulty is in the calculation of the radiation forces, because of the complicated time dependence of the corresponding pressure forces.

Having presented the background to the forces and motion equations, each mode of motion will be discussed in detail.

The damping of heave and pitch motions are due principally to the radiation of wave energy. These motions are generally of small amplitude and the inertial effects of these modes are important, so in most cases a linearized theory which assumes small unsteady motions and inviscid fluid can be applied.

In most cases heave and pitch are of greatest practical importance, especially in head and bow seas if the wave-length is comparable to the ship length and the forward speed is high. In this case the exciting forces are significant and the responses can be such that causes bow emergence, propeller emergence or deck wetness. High motion amplitudes necessitate speed reduction and cause uncomfortable accelerations, and can cause the ship hull to experience significant structural loads.

The roll motions are oposed by small restoring moments in the case of conventional ship forms. In addition the damping due to radiated waves is weak, especially at low frequencies near resonance. Therefore roll motions have large amplitudes and significant non-linear restoring, viscous damping, and geometric characteristics.

Although an understanding of roll motions is fundamental when studying dynamic stability, no satisfactory method exists for predicting the roll motion with accuracy. It is known that many ships, especially small ships, were lost by capsizing as a result of excessive rolling.

In contrast, the remaining three motions in the horizontal plane do not have hydrostatic restoring forces. The response is non-resonant and motions of large amplitude may occur at low frequencies in following and quartering seas, especially when ship's speed is high. Combined effects of dynamic and static instability may also occur, and as a result dangerous roll angles may happen. Directional stability can be affected.

Surge, sway and yaw motions can be influenced significantly by non-linear and viscous effects.

1.2 - Study Objectives

The objective of this study is to develop a time-domain formulation to predict the non-linear motion of floating bodies in waves.

To achieve this, the first step is to develop and apply a method able to predict linear radiation forces in the time domain due to non-sinusoidal motions. For the exciting force problem stated above the exciting forces do not have dependency on the past history of the motion thus the frequency domain solution can be used. Once the first problem is solved non-linearities can be introduced. The only non-linearity studied arises from the restoring force term. Here the hydrostatic forces are evaluated with no initial assumptions about the body shape or motion amplitudes since these forces are computed over the "exact" wetted surface. The linear free surface elevation at the sides of the body as well as its intersection with the body surface is calculated in the time domain.

Two problems are studied in this thesis, and for both the time domain results at each step are compared with the correspondent linear frequency domain solution, which is known to give reliable results within its applicability limits.

The first problem studied is the two-dimensional motion of cylinders of arbitrary cross section, subjected to sinusoidal or irregular beam waves and oscillating on the free-surface in sway, heave and roll. There is no forward speed. All the formulations from the basic principles to the solution of the motion equations are derived for both the frequency domain and the time domain solutions. Each mathematical model is applied to a computer program. Here the author used existing routines for the "Frank Close Fit Method", and extended a two-dimensional program. Results are analysed for a cylinder with a particular cross section shape, and compared with experimental data obtained from tests conducted at the Hydrodynamics Laboratory of the University of Glasgow.

The second problem studied is the non-linear motion of ship forms with forward speed, subjected to sinusoidal or unidirectional irregular waves with arbitrary heading angle. A modern strip theory is used to evaluate the forces arising from the interactions fluid-hull. Again all the formulations are derived, and the two-

dimensional solutions achieved in the first problem are used here. Two computer programs were developed, corresponding to the frequency domain and time domain models. Due to the limited time available for programming, the time domain numerical solution is restricted to the heave and pitch motions of ships with no forward speed.

In summary the objective of this study is to derive a method which enables the prediction of non-sinusoidal motions of ships with forward speed, in which the hydrodynamic forces are treated with realism, and on the other hand the computational effort is much less than for the other equivalent existing method, which is the three-dimensional time-domain panel-method. If this objective is not completely achieved during the period of this thesis work at least all the derivations and the main tools are prepared.

1.3 - Structure of the Thesis

Chapter-2 presents the ship motion problem in general and gives several general approaches to the solution. A historical review is given to illustrate the evolution of the solution. A description of the methods actually in use and being developed is also given, together with a summary of their advantages and limitations.

In Chapter-3 the general approach and formulation of ship motion problem is presented. First the exact boundary value problem is presented and in the next step the problem is linearized. The formulation of the forces resulting from the interaction between the ship-fluid and acting upon the hull is also presented.

The former results are then simplified for the case of two-dimensional motions of semi-submerged cylinders having arbitrary cross sections.

In Chapter-4 all the frequency-domain formulations are presented, for the two-dimensional motions of cylinders subjected to sinusoidal waves and oscillating on the free-surface. First the "Frank Close Fit Method" used to compute the radiation and exciting forces is derived. The same method is then modified in order to calculate the infinity frequency added masses. The restoring force and moment formulations are presented. A method to estimate the viscous moment for roll motions is also presented. The derivation and solution of the equations of motion are also discussed.

In Chapter-5 all the time-domain formulations are presented for the same problem. Here the radiation forces are derived in the time-domain and then related to the frequency-domain solution. The exciting forces arising from irregular waves are derived. The formulation necessary to evaluate the hydrostatic forces over the exact wetted surface is developed. The viscous moment in roll motions is also estimated. Finally the time domain equations of motion are presented.

In Chapter-6 the computer programs are presented. Details of the experimental model tests and their results are explained. The results obtained from two different numerical models and those obtained from the measurements are presented and comparisons between the three sets of results discussed.

In Chapter 7 a modern frequency domain strip theory is presented. The ship's added mass and damping coefficients are derived and the result comes in terms of the sectional coefficients obtained in Chapter 4. The diffraction part of the exciting forces is derived by two methods, the first solves the diffraction problem directly and the other uses the Haskind's relations to represent these forces in terms of the motions induced potentials. Then the ship restoring coefficients are deduced, as well as the coefficients of the ship mass matrix, and finally the equations of motion are discussed and the equations corresponding to the heave and pitch presented.

In Chapter 8 a time domain strip theory is deduced, where the geometric and frequency range limitations arise from the same assumptions used to develop the frequency domain strip theory. Thus in some aspects the two models are very similar. The radiation forces are deduced in the time domain and then related to the frequency domain solution. The exciting forces due to sinusoidal waves are evaluated by the frequency domain model, however the same forces resulting from unidirectional irregular waves can be introduced and a method to predict them is presented. All the formulations are developed to obtain the non-linear hydrostatic forces, where the "exact" wetted surface is taken into account by calculating the intersection of the fluid free surface with the ship's hull. Finally the time domain equations of motion corresponding to the heave and pitch motions are presented and discussed.

Chapter 9 begins by presenting the frequency domain and the time domain computer programs. Then the ship used in the numerical computations is introduced. Frequency domain results are compared with two other ship motion theories together with experimental data obtained from the Netherlands Ship Research Centre. Finally the heave and pitch predictions by the time domain model are compared with the frequency domain solutions, for the condition head waves and zero forward speed. All the results are discussed.

In Chapter 10 overall conclusions are given as well as recommendations for future research.

2. State of the Art

2.1 - Presentation of the General Problem

In order to develop a theoretical method to predict ship motions one has to start with the formulation of the appropriate hydrodynamic boundary value problem.

The "exact" formulation leads to the non-linear free-surface problem, the kinematic and dynamic conditions applied on the boundaries in their instantaneous positions, and the appropriate conditions at infinity, with all the flow governed by the three-dimensional Laplace equation. (Here "exact" means exact in the ideal fluid and irrotational flow formulation). This very complex problem must then be simplified to the point where it can be solved numerically, with practical computational effort. There are several ways of achieving this, and the choice depends on the initial assumptions. This assumptions generally involve restrictions on basic parameters governing the solution, which are; the amplitude and frequency of oscillation of boundaries, steady forward speed and geometrical shape of the hull.

The first step is to remove the non-linearities from the boundary conditions. The next one is related to the three-dimensional aspects of the problem. With the objective of linearising the problem it will be assumed that the oscillation amplitude of the boundaries is sufficiently small and the ship form must be thin or slender. (A ship form is named as 'thin' when her length is much larger then her beam, while it is 'slender' when her length is much larger then her beam and draft. The ratio of beam and draft to length is normally referred as the slenderness parameter , ε=B,T/L.)

After linearisation four general approaches to the formulation of ship motions theory can be summarised as follows:

- Strip theory analysis, in which two-dimensional boundary-value problems are formulated at the start. Some three-dimensional corrections are introduced in the final formulas.

- Analysis based on the three-dimensional boundary-value problem, and the strip theory approximations are introduced only into the final formulas.

- Systematic perturbation analysis that may lead to several forms depending on what assumptions are made initially, and depending on the relative orders of magnitude of the governing parameters.

- Application of the Green theorem for the unknown three-dimensional potentials and numerical solution of the resulting boundary integral equation formulated at the body surface.

The evolution of these four general approaches will be better understood after reading the next Section, where a brief historical outline and the actual state of the art are presented.

2.2 - Historical Review and State of the Art

In this Section briefly will be described the theory of ship motion development, and concise evaluation of the methods currently used or being developed will be given.

First Years

The modern study of ship motions began with William Froude (1861) during the first years of steam ships. He investigated the rolling of ships. Some years latter Krylov (1896) studied the pitch and heave motions of a ship.

Froude and Krylov derived differential equations of motion which include the inertial and restoring forces acting on a ship. Only the pressure field of the undisturbed incident waves was considered, assuming that the ship does not perturbate the surrounding fluid. The wave force acting on the ship due to incident waves have became known as the Froude-Krylov exciting forces.

Thin Ship Approach

Michell (1898) was the first studying in a realistic way the hydrodynamic disturbance due to the ship hull, although he was concerned only with the steady perturbation and wave resistance theory. In order to simplify the problem Michell imposed a geometrical restriction when the beam of the ship was assumed small compared with the length and draught. This way the boundary condition can be satisfied on the centreplane. Thus Michell introduced the "Thin-Ship Theory" in hydrodynamics.

Lewis (1929) was another pioneer in the analysis of hydrodynamic perturbation. He calculated the added mass of a ship vibrating vertically. In this problem the characteristic frequency is very large and inertial effects are dominant, so radiated waves may be neglected, greatly simplifying the analysis. Lewis assumed the ship with a much larger length than the beam, which does not necessarily means that the ship is thin. A strip-theory approach was used to

integrate the ship added mass in terms of the two-dimensional characteristics of each section. Some correction factors were also used to simulate the three-dimensional characteristics of the flow.

The heave and pitch motions were analysed by Haskind (1946) using an innovative method. The velocity potential due to the unsteady motions of the ship was calculated using the Green theorem, and the necessary Green function was derived. Physically the Green function represents the potential of an oscillatory source, located under the free-surface, and the unsteady flow can be represented by a suitable distribution of this functions. To the date this seems to be the best way of solving the ship motions problem in a consistent manner. The thin-ship approximation was used to solve the resulting integral equation. Haskind was the first to derive the velocity potential in such a way that the diffraction and radiation problems can be solved separately in each modes of motion.

Peters and Stoker (1957) first, and Newman (1961) some years latter applied perturbation methods to the thin ship approximation assuming that the ship's beam and the unsteady motions are of same small order of magnitude. Comparisons of damping coefficients between computations and measurements showed that results did not correlate well.

The thin ship model was applied to ship motions in longitudinal waves, however there were some problems like; ship forms were not thin, the draft was of the same order of the beam and not of the length, and the first order theory induced unbounded resonance in pitch and heave while the second order theory was extremely complex. Sooner researchers gave up of the thin ship models.

Slender Body Theory

The "slender-body theory" of aerodynamics was adapted to the predict the ship motions in waves by several authors; Ursell (1962), Joosen (1964), Newman (1964), Newman and Tuck (1964), and Maruo (1967). This theory is based on the assumption that the beam and the draft are both small compared with the length of the ship, which is a reasonable assumption for conventional ships. The smallness parameter 'ε' is defined as the beam-length ratio of the ship. The slender-body theory accounts for the longitudinal changes in the flow, due to

interference effects between transversal sections of the ship, and also due to the effects of steady forward motion. The linearized potential theory is used, so the wave amplitude and the unsteady motion amplitudes are assumed small. Furthermore the length of the incident wave is assumed to be of the same order or greater than the ship's length.

Now the approach proposed by Newman and Tuck will be explained as an example. The potential is derived to satisfy two distinctive domains, one is near to the ship within a distance typically of the same order as the beam. This is the "near-field", and the other is the "far-field" which includes all domains outside the near field. In the near-field the radiation problem is treated as two-dimensional and the potential must satisfy the body boundary condition in its mean position and the very simple "rigid-wall" free-surface boundary condition. This rigid-wall condition means that there are no wave effects in the near-field. In the far-field the three-dimensional effects are considered in the Laplace equation and the linearized free-surface boundary condition, and the potential is simulated by a suitable distribution of three-dimensional singularities on the longitudinal axis of the ship. Once the body boundary condition do not exist in the far-field the Green function to be calculated is not so complex. These two separate solutions are then required to match in a suitable overlap domain. A method of matched asymptotic expansions has been applied.

This theory is valid for slender ships and, given the simplified free-surface condition in the near-field, it is limited to low frequencies (or the wave-length must be at least of the same order of ship's length). In addition the forward speed must be slow.

Strip Theory

While some researchers were trying to represent and calculate the three-dimensional flow, work was carried out to study the oscillatory motions of cylinders in the free-surface with zero forward speed. This problem is two-dimensional and, in principle, there are no restrictions to the cylinder shape and oscillation frequency.

This type of problem was first solved rigorously by Urssel (1949) for the heaving motion of a half-immersed circular cylinder. The velocity potential was

represented as a sum of an infinite set of sources, each one satisfying the free-surface boundary condition and being multiplied by a coefficient in order to satisfy the body boundary condition.

Some years latter Grim (1953), Tasai (1959) and Porter (1960) used a variation of Ursell's method, by applying a conformal mapping of a given section onto a circle they computed the hydrodynamic coefficients for cylinders of several shapes.

W. Frank (1970) represented the velocity potential by a distribution of sources over the mean submerged cross section. Green functions are applied to represent the potential of the unit strength sources. The density of the sources is an unknown function, of the position along the contour, to be determined from integral equations derived by applying the kinematic boundary condition on the submerged part of the cylinder. This method allows the computation of hydrodynamic coefficients of cylinders with non-regular shapes with much more accuracy than the others.

Korvin-Kroukovsky (1955) was the first to apply the two-dimensional results in a three-dimensional strip-theory to predict the heave and pitch motions. In the strip-theories approach the hydrodynamic, hydrostatic, and exciting forces are calculated for each section and then integrated over the length of the ship. Korvin-Kroukovsky used some concepts from slender-body theory, in particular it was assumed that the ship was slender and the wavelength was of the same order as the beam. The forward speed effects were derived by intuitive physical insight, and for this reason theoretical workers were slow to accept the strip-theory approach of Korvin-Kroukovsky. In his work the wave-induced force on the ship was computed in the same way as the motion induced hydrodynamic force, using the concept of 'relative velocity' between the hull and the water surface. He assumed that the flow characteristics around the hull remains the same when the hull is moving down into the water, or when the water is moving up around the hull. In the years following this idea of avoiding to solve the diffraction problem was widely used, althout the concept of relative velocity was abandoned.

Several other methods were developed based on the strip-theory approach. The basic assumption of the strip-theory on the shape geometry is the same as the slender body theory. However both theories differ in the characteristic wave-

length assumed, since the strip-theory works with small length incident waves. The strip-theory assumes that the oscillatory flow is two-dimensional in each transverse section of the ship, which is reasonable only if the wave-length is small compared with the ship length. In this case, interference arising from bow and stern three-dimensional shapes will be negligible since there are many wave lengths between them, and the problem can be reduced to a sequence of two-dimensional problems. The short waves do not have to be so short as the name suggests, as Ogilvie (1974) showed they may be almost as long as the ship that generates them.

Among the several strip-theory methods developed the solution of Salvesen, Tuck and Faltinsen (1970) will be cited since it treats the forward speed effects in the most consistent way, and the strip-theory approximations are introduced only into the final formulas. Here the linearized free-surface boundary condition is simplified by assuming that frequency is high. The body boundary condition is simplified assuming that the steady disturbance due to the steady flow passing the ship may be neglected.

This method is suitable for (very) thin ships, high frequency oscillations, and slow forward speed. The results are especially good for heave and pitch motions, even for low frequencies where in this case the hydrostatic forces are dominant, and therefore a poor prediction of hydrodynamic forces is not so important.

The "rational strip-theory" developed by Ogilve and Tuck (1969) should also be reviewed, because the effects of slenderness 'ε' were not neglected. They developed a systematic perturbation analysis assuming that the frequency of oscillation is high. Ogilvie and Tuck used two small parameters in their perturbation analysis, the slenderness parameter and a motion amplitude parameter. Use of the later permits the linearization of the problem with respect to the motion amplitude without introducing restrictions on ship slenderness. The higher order terms related to the slenderness were consistently retained. Therefore this method, in addition to the former, is valid for ships which are not "very thin".

It should be noted that in general the theories valid for ships which are not very thin are also valid for higher forward speeds, since some of the problems arising from the forward speed effects are similar to those due to form effects.

Finally it should be referred that among the several strip-theories only the Salvesen, Tuck and Faltinsen (1970) and Ogilvie and Tuck (1969) evaluate the interactions between the oscillatory motion of the ship and the incident uniform stream in a way that the Timman-Newman (1962) symmetry theorem is satisfied.

Unified Slender Body Theory

Newman (1978) with the "Unified Slender-Body Theory" achieved another step forward in the study of ship motions. The objective was to develop a method based on the slender-body theory and valid for the whole range of frequencies. Here the free-surface boundary condition in the near-field is more general than the one from the ordinary slender-body theory, since some of the wave effects are taken into account. To achieve the objective of the unified theory a careful analysis of the matching error must be carried out, and the overlap region, between the near-field and far-field, is chosen to minimise this error. This approach have no restrictions on the frequency, but the ship must be slender and the forward speed not high.

For zero forward speed, calculations of heave and pitch hydrodynamic coefficients by Mays (1978) showed good agreement with "exact" three-dimensional computations for slender spheroids with L/B=0.25. Computations of added mass and damping at zero forward speed also have been done by Maruo and Tokura (1978), and compared with experimental data. The agreement found was good, and the results showed improvement relative to the ordinary slender-body theory and the strip theory.

While these strip-theory and slender-body theory are still in use to predict the linear small motions of thin ships with limited forward speed in regular waves, other methods have been developed in order to better represent the responses of; ships which are "not so thin", ships subjected to non-linear forces, high speed crafts, bodies with non-conventional ship forms and ships with large amplitude motions.

Tamborski (unpublished) developed a solution valid in the whole range of wave frequencies (wave lengths), for ships which are "not very thin", advancing with low forward speed. He developed the perturbation slender-body model to the

second order with respect to the slenderness parameter. Simultaneously the basic concept of the unified theory was adopted to make the solution valid in the whole frequency range.

Three-dimensional Panel Methods

With the objective of avoiding the use of undesirable higher order approximations for speed effects on hydrodynamic pressure, methods based on a three-dimensional potential theory were developed. These are the so called "three-dimensional boundary integral methods".

Chang (1977) was the first to report success with the direct numerical solutions for this problem. This was followed by Inglis and Price (1982), and Nakos and Sclavounos (1990). The method is based on a three-dimensional linearized potential theory. The mean wetted surface is discritized by a set of panels, and over this surface an oscillating source distribution is fitted, where in each panel the source intensity is constant. The free-surface boundary condition is linearized by assuming that the geometry of the ship is such that the steady disturbance is small. There is no frequency limitation in this boundary condition. The body boundary condition is simplified by assuming that the effects of the steady perturbation in the uniform flow, due to the presence of the ship, may be neglected. For this reason the ship must be thin. The Green theorem is used to obtain the three-dimensional integral equation applied on the body surface. Given the linearized free-surface boundary condition the method is restricted to thin ships, high frequency and limited forward speed, however these limitation cover now wide range then that covered by slender-body and strip theories.

Chan (1992) added to the three-dimensional formulation the cross-flow approach for taking into account viscous effects, and applied the 3-D method to the case of twin-hull vessels with forward speed in regular waves. As he showed, for this type of ships with very thin water plane area, the motions in the vertical plane are associated with viscous forces which are of the same order as the damping forces resulting from radiated waves. An empirical method based on the steady cross-flow assumption was used to calculate the fluid forces due to viscous effects.

Non-Linear Strip Theories

During recent years several non-linear strip-theories have been developed with the objective of taking into account the effects of non-linear variation of the wave exciting, restoring and hydrodynamic forces, as well as the forces arising from slamming and deck wetness. As an example, it is well known there is a difference in bending moment amplitude between the sagging and hogging conditions, when the sea state is severe. The linear theories are not able to predict this difference.

Several attempts were made in order to solve the non-linear equations of motion, which can be divided into the frequency-domain and time-domain solutions. (All the solutions presented here so far are frequency domain solutions.)

Belik, Bishop and Price (1980) developed a frequency-domain theory to predict transient response of ships to slamming loads. The theory is basically a linear theory as ship motions are determined from linear equations. Non-linearities are treated as transient forces decoupled from the linear terms. The non-linear transient response is calculated in the time domain by applying a convolution integral and is then superimposed on linear response to obtain the total response.

Jensen and Pederson (1979) developed a frequency-domain quadratic theory to predict the non-linear heave and pitch motions, which is based on a perturbation procedure. The linear terms are identical to those of the classical linear strip theories. The quadratic terms arise from the non-linearity of the exciting waves, the non-vertical sides of the ship, and the non-linear hydrodynamic forces. The theory takes into account the flexibility of the ship, which also makes possible investigation of springing vibrations that may occur for fast and/or large ships.

The calculation of the slamming forces is simply based on time derivation of the momentum of the added mass. In addition the damping and restoring terms depend on the relative motions.

The theory produces solutions in the frequency domain that compare well with full scale measurements of wave induced bending moments.

Several authors solved the non-linear equations of motion in the time-domain, based on the concept of relative motions for the prediction of forces acting on

the hull. This means that the instantaneous water line is considered instead of the mean water line.

Paulling and Wood (1974) developed a time-domain numerical method to predict the large amplitude motions and capsizing of ships advancing in following and quartering seas. Experiments were carried out with radio-controlled ship models in the waters of San Francisco Bay. The experiments showed that the capsizing occurred most frequently at high speed in either following or quartering seas. In this condition the encounter frequency is low, and so the hydrostatic and Froude-Krylov forces are dominant. For this reason in the solution of the problem the hydrodynamic forces were not calculated with high accuracy. In addition, the forces resulting from steering and control were taken into account. Finally as the method was developed to predict large motions, the viscous effects were estimated by coefficients of quadratic damping. The equations were derived with the non-linear terms in the angular motions and velocities, necessary to represent the large amplitude angular motions, in agreement with the Euler equations.

The same equations were solved numerically using a fifth-order Glauz-Adams predictor-corrector algorithm. The numerical results agreed with the experimental measurements.

Elsimillawy and Miller (1986) proposed a numerical method to solve the equations of motion in time-domain, and to predict the large amplitude oscillatory motions for a ship advancing in regular waves. A strip theory was used to integrate the external forces over the length of the ship. An approximate water line in each section is used to calculate the hydrodynamic, hydrostatic, and exciting forces, so the variation of all these forces with motions is taken into account. The non-linear waves were also considered. The equations of motions were solved by applying the Runge-Kutta method.

The influence of oscillatory motions on righting moment was studied and found to be important. The influence of linear and non-linear wave shapes on ship's righting arm was also studied.

Petersen (1992) presented a non-linear strip theory in time domain for a ship advancing in head seas. All forces acting on the hull were calculated by summing the forces on each section using the instantaneous "Smith correction"

immersion. Due to the circular motion of the water particles in a wave the pressure distribution on the hull can not be taken as the hydrostatic pressure alone, so the immersion is corrected. Using this corrected immersion there is no distinction between the hydrostatic and exciting forces. The damping term and inertia of water were calculated using corrected relative velocity and acceleration. The time derivative of the momentum of added mass was used to predict the slamming forces.

The two equations of dynamic equilibrium were solved by numerical time integration procedure. Adam's predictor corrector method where the time step is adjusted by an error estimate was used.

The use of the Smith correction is questionable in ship motion problem, since the steady flow, all the unsteady motions, and the diffracted wave will certainly change much the orbital velocity of the water particles of the incident wave in a way difficult to quantify.

There are also studies for the heave and pitch motions and loads of high-speed crafts advancing in head sea. As an example, Chin and Fujino developed a time-domain non-linear strip-theory procedure where the lift forces and impact forces were introduced. Furthermore the non-linear terms derived from the angular pitch motions were taken into account. They compared the numerical results with experimental results from model tests, and the agreement was good.

Offshore Floating Platforms

A particular case that has been studied in recent years is the seakeeping of offshore floating platforms. The external forces acting on the platform are; hydrodynamic forces, hydrostatic forces, exciting forces due to waves, forces transmitted by the mooring cables, and other external forces like wind forces. The existing methods to predict the exciting forces on offshore structures are mainly based on one of the following:

Morison equation in which the total force is divided in two components. The first is an inertial force that is proportional to the water acceleration, and an inertial coefficient is used to predict it. The other is a drag force which is due to

a wake region behind the body. The drag is proportional to the square of water velocity, and a drag coefficient is used.

The other two methods are the two-dimensional and three-dimensional source distribution technics, which are similar to those used in ship motion problem. Here the problem is much simplified since the problem does not involve forward speed, so the Green functions to be derived are simpler, and in principle there are no restrictions to the hull form. These methods do not account for the drag forces, however the free surface effects are account for. The three-dimensional method is more suitable for structures with large structural members.

In the case of studying the linear motions resulting from calm to moderate seas the frequency-domain approach is adequate. The three-dimensional panel methods are popular, and the predictions are quite accurate. But when studying non-linear large amplitude motions, motions resulting from non-linear forces, motions of damaged platforms, etc, a time-domain procedure is required. Some accurate results have been obtained in this field.

Time-Domain Solution of the Boundary Value Problem

Finally the study carried out using the time domain formulation of the forces will be described. It should be noted that all presented methods to solve the motion equations in time-domain use hydrodynamic coefficients which were derived and indicated for frequency-domain solution, since they are frequency dependent. About this subject, Golovato (1959) for example, gave direct experimental proof that the classical second order equations with frequency dependent coefficients, cannot be used to describe non-sinusoidal motions. He conducted transient tests with a ship model, allowing it to do pitch motions from an initial angle until it reached the equilibrium position. He found that the response could not be represented by differential equations with frequency dependent coefficients. Ursell (1964) reached the same conclusion analytically for the case of transient heave motions.

The existence of radiated waves implies there is a complicated time dependence of the fluid motion and hence of the pressure force. Waves generated by the ship at time 't' will persist, in principle, for an infinite time thereafter, as well as the

associated pressure force on the hull. This situation can be described mathematically by a convolution integral, with the fluid motion and pressure force at a given time dependent on the previous history of the motion. In this case the equations of motion will not have frequency dependent coefficients, and in addition the differential equations are solved numerically, so the exciting forces do not need to be sinusoidal, and the hydrostatic forces do not need to be linearly proportional to the ship displacement since they can be computed "exactly" whatever is the shape of the hull.

This method is correct, within the limitations of linear potential theory, to predict the ship motions when the exciting frequency is not well defined and the forces applied are non-linear .In addition the ship do not need to have constant speed or course.

Formulation of the Problem

Finkelstein (1957), and Stoker (1957) were the first who discussed the time-domain direct solutions for the problem of generated water waves.

Cummins (1962) derived a formulation of the radiation forces in the time-domain, where the basic assumption is the linearity of the forces. Assuming the oscillatory motion velocity to be decomposed in a sequence of impulsive displacements, Cummins derived the related velocity potential. Each individual impulsive displacement induce a potential which must satisfy the boundary conditions during and after the impulse is finished. The formula for the potential obtained is a hydrodynamic analogue to the impulse response function. Cummins assumed that this impulse response function exists but did not calculate it. From the radiation velocity potential the radiation forces were derived and equations of motion were proposed. The equations are valid for any excitation, as long as it results in permissible motions. The inertial properties of the fluid are represented by coefficients which are independent from the frequency, the previous history of the motion and the ship's forward speed. Cummins called them "legitimate added masses". The effect of past history is represented by a convolution integral over the oscillatory velocity.

Ogilvie (1964) also discussed the use of time-domain analysis to solve unsteady ship motion problem. He derived the motion equations for ships moving with

forward speed and oscillatory motions in a different manner from Cummins, however the final equations are similar. Furthermore the relations between frequency-domain and time-domain equations were studied using Fourier analysis.

The zero forward speed problem was examined in detail by Wehausen (1971).

Two-Dimensional Results

Results in time-domain were obtained both for bodies with zero-speed and non-zero speed. Ursell (1964), and Maskell and Ursell (1970) developed solutions in time-domain for a floating semi-circle using the Fourier transform of the frequency-domain solution.

Two-dimensional direct solutions in time-domain were presented by Ikebuchi (1981), for the hydrodynamic forces on a body oscillating in the free-surface, and Yeung (1982) for the transient heaving motion of floating cylinders. In the direct solution the integral equations are solved in time-domain to obtain the velocity potential or source strength.

Kim and Hwang (1986) developed a method to solve the two-dimensional transient motions with large amplitude in time-domain. The numerical calculations were done for several problems, and the more interesting is the case of forced harmonic large amplitude motions with forward speed. In the solution the body boundary condition is satisfied exactly at the instantaneous position, so this condition do not impose restrictions in the motion amplitudes. The free-surface boundary condition is linearized. This kind of approach seems appropriate only if the motion amplitudes are large but the generated waves are small. In the approach the velocity potential is devided into two parts, one represents the instantaneous effect of the body, and the other represents the wave field. A method of spectral free-surface representation is used to compute the wave field part of the potential, while the other potential is represented by a suitable distribution of sources on the body surface. The integral equation for the source strength distribution is calculated directly in time-domain. The method was first used by Chapman (1979,1981), in addition, the present authors, introduced an artificial restriction on the inner free-surface to remove the irregular frequency effect.

Results were compared with experiments and other theories for the forced heave motion, and in general good agreement was found. It is interesting that discrepancy was found between the results by linear and non-linear (body exact condition) computations, even when the amplitude of the body motions is small. The authors concluded that the interaction between the disturbed steady flow and the body oscillation is significant in the values of added mass and damping coefficients for bluff bodies in heave motion.

Three-Dimensional Results

Newman (1985) has used time-domain analysis to determine the impulse response function for a vertical circular cylinder.

Beck and Liapis (1987) used a linear time-domain approach to solve the radiation problem for arbitrary bodies at zero forward speed. The linear potential theory was used, and both the free-surface condition and the body boundary condition used were linear, thus the unsteady motions were assumed small. The velocity potential due to an impulsive velocity was obtained by the solution of a pair of integral equations. These equations were solved numerically using a panel method. The results of radiation forces for arbitrary motions were evaluated by a convolution integral of the impulse response function and the time derivatives of the motion. This approach is similar to the one developed by Cummins (1962). Comparisons between the time-domain computations and known results for a sphere, and a vertical circular cylinder oscillating in the free-surface showed very good agreement. Some experiments were carried out to measure the heave motions of a sphere released from an initial displacement, and the measurements were compared with the theoretical results. Correlation between the calculations and the measurements were very good.

In the next step of their work Liapis and Beck (1985) solved the problem of a ship travelling with constant forward speed and experiencing arbitrary oscillatory motions using linear time-domain analysis. The only addition in relation to the former work, is that the effects on the velocity potential of the ship forward speed were taken into account. The free-surface boundary condition and the body boundary condition are simplified assuming that the interactions between the steady and the unsteady potentials may be neglected,

which means that the ship must be thin. In addition the linear potential theory assumes small unsteady motions.

The three-dimensional panel method was first applied in frequency-domain, however the method encounters difficulties in the case of ships with forward speed because the Green function required is complicated and difficult to calculate when forward speed is included. In the case of time-domain approach the Green function is easier to derive and compute regardless of ship speed.

The major disadvantage of this method is the very large computational effort necessary to obtain results. Since the potential in each panel depends on the influence of all the others, a very large system of integral equations, with the corresponding Green functions, must be solved at each time step. This disadvantage is especially relevant if statistic properties are required, because long time histories of the responses must be calculated. Another difficulty is the possible instability in the computation of the time-domain impulse response function over large period of times. This problem was found to be related with the irregular frequencies in the frequency-domain solution.

King, Beck and Magee (1988) derived and computed the radiation, exciting and restoring forces in time-domain for ships with forward speed. The linear potential flow theory was adopted and three-dimensional effects in the flow were accounted by using a panel method to compute the potential at the surface of the ship. The Green theorem was used to derive the integral equations to be solved in order to obtain the velocity potential. As the hydrodynamic problem has been linearized the impulse response function can be used, however in this work non-impulsive inputs have been used, because it was found that some numerical problems can be eliminated. The non-impulsive inputs in addition to the body boundary condition are used to solve the integral equations at each time step. With the resultant potential the radiation and exciting forces can be computed.

It should be remembered that even the method used is three-dimensional, as a consequence of the linearized potential, linearized free-surface and body boundary conditions, the ship must be thin, the forward speed can not be high and the oscillatory motions must be small enough.

Numerical results were compared with the results of other theories and experimental measurements. In conclusion we can say that in some cases the time-domain calculations compare better with experiments and on other the time domain predictions are worse. In general the coupling coefficients are predicted with more accuracy, and the variation of the coefficients with forward speed tend to be better predicted.

Recently Beck and Magee (1991), following the work already described here, presented the solution of the problem considering the body boundary condition satisfied on the instantaneous exact position of the body, while the linearized free-surface boundary condition was maintained. This is a necessary step in order to formulate in a consistent way a method to predict the large amplitude motions, however this problem may be solved only in time-domain.

This paper did not give numerical results for the non-linear model of ships, however the authors compared results of the linear model with experiments, and the conclusions are similar to those obtained by King et al. (1988).

3. THE BOUNDARY-VALUE PROBLEM

3.1 - Ship Motion Problem

Two co-ordinate systems will be defined, the first $X_0 = (x_0 , y_0 , z_0)$ is fixed in space, and the other $X = (x , y , z)$ is fixed with respect to the mean position of the ship, with 'z' in the vertical upward direction and passing through the centre of gravity of the ship, 'x' in the direction of forward speed, and 'y' perpendicular to the former and in the port direction. The origin is in the plane of the undisturbed free-surface.

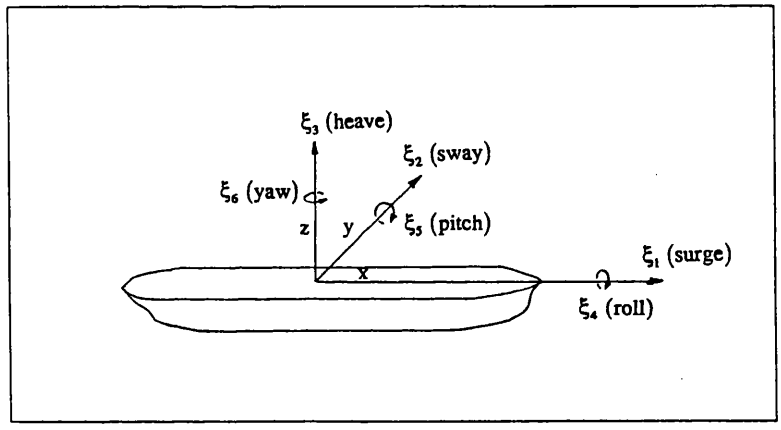

Figure 3.1 The co-ordinate system and six modes of ship motion

Let us consider a ship advancing in waves and oscillating as a unrestrained rigid body. The oscillatory motions will consist of three translations and three rotations. The translatory displacements in the x, y, and z directions are respectively the "surge (ξ_1)", the "sway (ξ_2)", and the "heave (ξ_3)". The rotational displacements about the x, y, and z axes are respectively the "roll (ξ_4)", the "pitch (ξ_5)", and the "yaw (ξ_6)". The co-ordinate system and the linear and angular displacements are shown in figure-3.1.

If we assume that the viscous effects are negligible and consequently the fluid motion is irrotational, the problem can be formulated in terms of potential flow theory. This means that the fluid velocity vector, $V(x_0 ,y_0 ,z_0 ,t)$, may be represented by the gradient of the velocity potential, $\Theta(x_0 ,y_0 , z_0 ,t)$;

$$V = \nabla\Theta \qquad (3.1.1)$$

The Laplace equation, which expresses conservation of fluid mass for potential flows, provides the governing partial differential equation to be solved for the potential Θ;

$$\nabla^2\Theta = 0 \qquad (3.1.2)$$

Once the velocity potential is known the fluid pressure, $p(x_0, y_0, z_0, t)$, is given by the Bernoulli equation;

$$p = -\rho\left(\frac{\partial\Theta}{\partial t} + \frac{1}{2}|\nabla\Theta|^2 + gz_0\right) \qquad (3.1.3)$$

where 'ρ' represents the fluid density and 'g' is the gravitational acceleration.

Integrating the pressure over the ship's wetted surface the total hydrodynamic forces acting upon the hull are obtained. The main difficulty is to find the solution of the Laplace equation for the velocity potential. In order to achieve this the two boundary conditions will be used.

Boundary Conditions

The kinematic body boundary condition states that, on the submerged portion of the body surface, the normal component of the adjacent fluid velocity must be equal to the normal velocity of the boundary surface itself.

$$V_S \cdot n^s = V \cdot n^s \qquad \text{, on} \quad S \qquad (3.1.4)$$

where 'S' is the ship's wetted surface and 'V_S' the ship's velocity, 'V' is the fluid velocity, and 'n^s' is the unit normal vector directed outwards. This vector is normal to the body surface at its exact position.

At the free-surface the kinematic boundary condition is similar, that is, in this surface the normal velocity of fluid motion must be equal to the normal velocity of the surface itself. But since the position of the free-surface is unknown, an additional dynamic boundary condition must be imposed, that is the pressure on the free-surface is atmospheric. Bernoulli's equation is used. The joint condition is the free-surface boundary condition to be satisfied by the velocity potential;

$$\frac{\partial^2\Theta}{\partial t^2}+2\nabla\Theta.\frac{\partial\Theta}{\partial t}+\frac{1}{2}\nabla\Theta.\nabla(\nabla\Theta.\nabla\Theta)+g\frac{\partial\Theta}{\partial z_0}=0 \qquad \text{, on } z_0=\zeta \quad (3.1.5)$$

where '$\zeta(x_0, y_0, t)$' is the free-surface elevation.

From now on the independent variables will appear as subscripts to indicate partial differentiation. So the formula (3.1.5) becomes;

$$\Theta_{tt}+2\nabla\Theta.\nabla\Theta_t+\frac{1}{2}\nabla\Theta.\nabla(\nabla\Theta.\nabla\Theta)+g\Theta_{z_0}=0 \qquad \text{, on } z_0=\zeta \quad (3.1.5b)$$

These are the two boundary conditions of the problem, valid on the ship hull and on the free-surface.

In addition the fluid must satisfy the bottom condition, that is when the distance from the free-surface tends to minus infinity the fluid tends to be in rest;

$$V \to 0 \quad \text{, when } z_0 \to -\infty \qquad (3.1.6)$$

Finally a radiation condition at infinity, near the free-surface, is imposed. This states that the waves on the free-surface, other than the incident waves, are also due to the presence of the body. First the ship is an obstacle to the incident waves, and so some diffraction will occur, second the oscillating ship will generate perturbations. Both these effects take the form of waves that must be radiated away from the body. The incident wave is by definition excluded from this radiation condition. This condition will be introduced latter.

In conclusion, the "exact" problem consists of finding the velocity potential of the flow around the ship's hull knowing that it must satisfy;

(L) the Laplace equation (3.1.2)

(F) the non-linear free-surface boundary condition (3.1.5)

(K) the non-linear body kinematic boundary condition (3.1.4)

(B) the bottom condition (3.1.6)

(R) the appropriate free-surface radiation condition at infinite

The problem presented above is exact within the limitations of an ideal incompressible fluid, however in order to solve this very complex problem some simplifications must be made. The first step is to remove the non-linearities from the boundary conditions.

Linearized Free-Surface Boundary Condition

In the co-ordinate system moving with the ship the velocity potential may be defined in the form;

$$\Theta(x_0, y_0, z_0, t) = \Theta(x + Ut, y, z, t) = \Phi(x, y, z) \tag{3.1.7}$$

where 'U' is the forward speed of the ship.

The flow field will consist of a steady flow due to the presence of the ship advancing through the free-surface, an oscillatory flow due to the incident wave, and an oscillatory flow due to interactions between the incident wave and the ship hull being present in the flow. The steady and oscillatory potential flows can be assumed superposed, neglecting the interferences between each other;

$$\Phi(x, y, z, t) = \Phi_0(x, y, z) + \Phi_1(x, y, z, t) \tag{3.1.8}$$

The steady part can be further decomposed as follows;

$$\Phi_0(x, y, z) = -Ux + \Phi_S(x, y, z)$$

where the first term is the potential due to the constant speed of the fluid passing the reference system, and 'Φ_S' represents the steady contribution due to the ship's presence in steady flow. 'Φ_1' represents the unsteady potential and is assumed small.

How linearizing the free-surface boundary condition takes two steps :

- First the potential given by (3.1.8) is substituted in the free-surface condition (3.1.5b), and as the unsteady potential was assumed small, the higher order terms in Φ_1 are neglected.

- Second if the perturbation of the steady flow due to the ship is neglected $(\Phi_S \cong 0)$, the condition (3.1.5b) in the reference system advancing with the ship becomes;

$$\frac{\partial^2\Phi}{\partial t^2} - 2U\frac{\partial^2\Phi}{\partial x \partial t} + U^2\frac{\partial^2\Phi}{\partial x^2} + g\frac{\partial\Phi}{\partial z} = 0 \qquad , \text{ on } z_0 \tag{3.1.9}$$

This linearized free-surface boundary condition is imposed on the mean position of the free-surface, because the difference between the value of the potential or its derivatives on $z = \zeta$ and $z = 0$ is of the same order of the terms already neglected.

To derive this condition it was necessary to assume that;

- the unsteady potential is small, so it means small incoming waves, and small oscillatory motions.
- the effects of the steady potential created by the ship on the free-surface can be neglected, so the ship's hull must be thin, and/or the forward speed must be low.

Linearized Body Kinematic Boundary Condition

Now it will be necessary to define one more co-ordinate system, $X' = (x', y', z')$, fixed in the ship. The axes are oriented as shown in figure-3.1 (substituting x,y,z by x',y',z').

The vector displacement in the co-ordinate system moving with the ship's forward speed, X(x,y,z), is :

$$\alpha(r,t) = \eta(t) + \Omega(t) \times r \tag{3.1.10}$$

where '$\eta(t)$' and '$\Omega(t)$' are the unsteady translation and rotation of the ship represented on X(x,y,z).

$$\begin{cases} \eta(t) = (\xi_1(t), \xi_2(t), \xi_3(t)) \\ \Omega(t) = (\xi_4(t), \xi_5(t), \xi_6(t)) \end{cases} \tag{3.1.11}$$

The symbol '×' represents the vector product and 'r' is the position vector on $X' = (x', y', z')$. The co-ordinate systems and the vectors are shown in figure-3.2.

If the oscillatory motions of the ship are small we can assumed that the transformation between the exact Eularian angles on $X' = (x', y', z')$, which represent the real angular motions of the ship, and the angles on $X = (x, y, z)$, is affected by the unit transformation matrix. This means that the angles on both co-ordinate systems are set equal to each other. The associated error may be neglected for small angular motions.

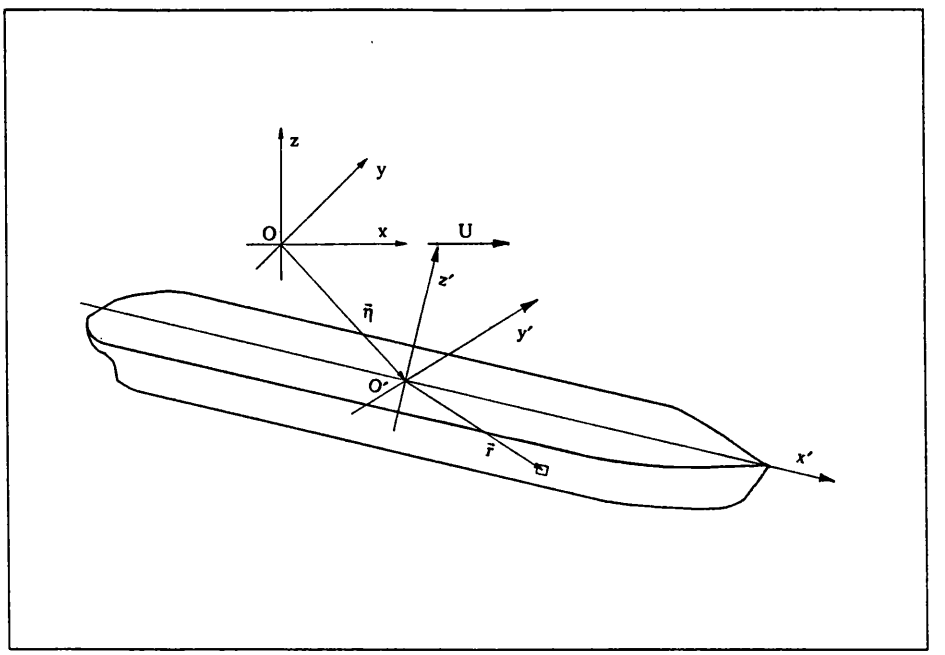

Figure 3.2 Co-ordinate systems and position vector

The exact kinematic boundary condition on the surface of the body is;

$$V_s \cdot n^s = V \cdot n^s \qquad \text{, on } S \tag{3.1.4}$$

It is remembered that 'S' is the exact position of the ship's wetted surface, and '$n^s = (n_1^s, n_2^s, n_3^s)$' is the outward unit normal vector to the instantaneous exact body surface.

It would be very convenient if the body boundary condition could be satisfied on the mean position of the body, and in fact same authors in the past made this

assumption. However Timman and Newman (1962) have proved that a consistent first order theory must take into account some interferences between the steady velocity potential and the oscillatory motions. The purpose of the linearisation is to obtain an expression representing the boundary condition, which can be satisfied on the known mean position of the body surface.

Linearisation of the body boundary condition takes four steps;

1 Use of the simplified vector displacement (α) given by (3.1.10) to obtain the velocity of the body surface (V_S) so the condition can be written as;

$$-\dot{\alpha}\cdot n^s + V\cdot n^s = 0 \qquad , \quad \text{on} \quad S \tag{3.1.12}$$

where the overdot indicates differentiation in the reference system X=(x,y,z).

2 Expansion in a Taylor series of the fluid velocity vector (V) about the mean hull position. The quadratic and higher order terms are neglected;

$$V(x',y',z') \cong V|_{S_0} + (\alpha\cdot\nabla)V|_{S_0} \qquad , \quad \text{on} \quad S_0 \tag{3.1.13}$$

'S_0' represents the surface defined by the mean hull wetted surface.

This way the fluid velocity vector on the exact position of the body surface, is represented in terms of the same vector on the mean body surface. The associated error is proportional to the neglected terms on the expansion.

3 Like the fluid velocity vector, the unit normal vector to the body surface at its exact position, 'n^s', must be represented in terms of the unit normal vector to the mean surface, 'n'.

$$n^s = [D]n$$

where, assuming again small angular displacements, the general transformation matrix with the Eulerian angles is simplified, and given in terms of the angular displacements represented in the co-ordinate system X=(x,y,z) by;

$$[D]=\begin{bmatrix} 1 & -\xi_6 & \xi_5 \\ \xi_6 & 1 & -\xi_4 \\ -\xi_5 & \xi_4 & 1 \end{bmatrix}$$

The unit normal vector to the body surface at its exact position, 'n^s', can alternatively be represented in terms of the displacement vector, α;

$$n^s=[D]n=n+(n\cdot\nabla)\alpha \qquad (3.1.14)$$

where 'n' is the unit normal vector to the hull mean surface, S_0. The associated error is of the order of the Eulerian angles squares.

4 The linearized kinematic body boundary condition applied at the mean position of the hull, 'S_0', can be obtained by substituting the expanded velocity vector (3.1.13) and the transformed unit normal vector (3.1.14) into equation (3.1.12);

$$V\cdot n=\left[\dot{\alpha}+(V\cdot\nabla)\alpha-(\alpha\cdot\nabla)V\right]\cdot n \quad , \text{ on } S_0 \qquad (3.1.15)$$

and as $V\cdot n=\dfrac{\partial\Phi}{\partial n}=\Phi_n$ it becomes;

$$\Phi_n=\left[\dot{\alpha}+(V\cdot\nabla)\alpha-(\alpha\cdot\nabla)V\right]\cdot n \quad , \text{ on } S_0 \qquad (3.1.15b)$$

In summary, the simplified transformation matrices used, and the terms neglected in the expanded fluid velocity imply that the ship motions are assumed small when the body boundary condition is derived.

Remembering that the potential is linearly superposed (see equation (3.1.8)) the fluid velocity takes the form;

$$V=V_0+V_1$$

where 'V_0' is the steady velocity and 'V_1' the oscillatory velocity.

Substituting the later expression into (3.1.15), and as the steady flow have only tangential velocity near the body surface, it results;

$$V_0\cdot n=0 \quad , \text{ on } S_0 \qquad (3.1.16)$$

Furthermore since the steady potential is $\Phi_0 = -Ux + \Phi_S$, and $V_0 = \nabla\Phi_0$, the kinematic boundary condition to be satisfied by the steady potential on the hull at mean position is;

$$\frac{\partial\Phi_S}{\partial n} = Un_1 \qquad , \text{ on } S_0 \tag{3.1.17}$$

For the unsteady flow velocity and potential the condition becomes;

$$V_1 \cdot n = \left[\dot{\alpha} + (V_0 \cdot \nabla)\alpha - (\alpha \cdot \nabla)V_0\right] \cdot n \qquad , \text{on } S_0 \tag{3.1.18}$$

or

$$\frac{\partial\Phi_1}{\partial n} = \left[\dot{\alpha} + (V_0 \cdot \nabla)\alpha - (\alpha \cdot \nabla)V_0\right] \cdot n \qquad , \text{on } S_0 \tag{3.1.18b}$$

The boundary condition (3.1.18) was derived by Timman and Newman (1962) to account in a consistent manner the interaction between the steady and oscillatory flow fields. In some ship motion theories an incomplete form of this condition is used, which results in coupling coefficients between heave and pitch which do not satisfy the symmetry requirement.

Decomposition of the unsteady potential

Since the wave amplitude and the oscillatory motions have been assumed small, the unsteady potential Φ_1 can be decomposed linearly into separate components due to incident wave, diffracted wave because of body presence, and radiated wave for each of the six rigid body motions;

$$\Phi_1 = \Phi^I + \Phi^R + \Phi^D \tag{3.1.19}$$

where $\Phi^R = \sum_{j=1}^{6} \Phi_j^R$

Haskind (1946a,b) was the first to decompose the velocity potential into a canonical form which permits the solution of the several hydrodynamic problems separately.

Substituting eq. (3.1.19) into eq. (3.1.18b) we obtain two conditions for the unsteady potential to be satisfied at mean hull position. The first is related to the "radiation problem", and the second to the "diffraction problem".

$$\frac{\partial \Phi^R}{\partial n} = \left[\dot{\alpha} + (\nabla\Phi_0 \cdot \nabla)\alpha - (\alpha \cdot \nabla)\nabla\Phi_0\right] \cdot n \qquad , \text{ on } S_0 \tag{3.1.20}$$

$$\frac{\partial \Phi^D}{\partial n} = -\frac{\partial \Phi^I}{\partial n} \qquad , \text{ on } S_0 \tag{3.1.21}$$

The condition (3.1.20) is normally presented in a more compact way by defining the '$\tilde{n}$' and '$\tilde{m}$' vectors in a manner very similar to Ogilvie and Tuck (1969);

$$\tilde{n} = \begin{cases} (n_1, n_2, n_3) = n \\ (n_4, n_5, n_6) = r \times n \end{cases} \tag{3.1.22}$$

$$\tilde{m} = \begin{cases} (m_1, m_2, m_3) = -\dfrac{(n \cdot \nabla)\nabla\Phi_0}{U} \\ (m_4, m_5, m_6) = -\dfrac{(n \cdot \nabla)(r \times \nabla\Phi_0)}{U} \end{cases} \tag{3.1.23}$$

where 'r' is the position vector with respect to the origin of the co-ordinate system.

The quantity '$\tilde{m}$' is related to the rate of change, in the neighbourhood of the ship, of an steady incident velocity flow past the body and having unit velocity at infinity. It is dependent only on the shape of the hull.

With this definition and remembering that the radiation potential is assumed equal to the linear superposition of each body motion mode, it can be proved that the equation (3.1.20) reduces to;

$$\frac{\partial \Phi^R}{\partial n} = \sum_{j=1}^{6} \frac{\partial \Phi_j^R}{\partial n} = \sum_{j=1}^{6} \left(\dot{\xi}_j n_j + \xi_j U m_j\right) \qquad , \text{ on } S_0 \tag{3.1.24}$$

which is the final form of the kinematic body boundary condition to be satisfied by the radiation problem.

Linearized problem

In conclusion we can say that in order to linearize the boundary conditions it was necessary to restrict some basic parameters that govern the solution, being more specific;

- incoming waves must be of small amplitude
- the ship oscillatory motions must be small
- the ship hull must be thin
- the steady forward speed must be slow

The linearized boundary conditions are, the free-surface boundary condition, the body boundary condition to be satisfied by the radiation problem, and the body boundary condition to be satisfied by the diffraction problem, which can be formulated respectively as follows;

$$\Phi_{tt} - 2U\Phi_{xt} + U^2\Phi_{xx} + g\Phi_z = 0 \quad , \text{ on } z = 0 \tag{3.1.9}$$

$$\frac{\partial \Phi_j^R}{\partial n} = \dot{\xi}_j n_j + \xi_j U m_j \quad , j = 1,...,6 \text{ , on } S_0 \tag{3.1.24b}$$

$$\frac{\partial \Phi^D}{\partial n} = -\frac{\partial \Phi^I}{\partial n} \quad , \text{ on } S_0 \tag{3.1.20}$$

The "exact" problem stated in the beginning of the Chapter has been simplified and now consists of finding the velocity potential of the flow around the ship hull knowing that it must satisfy:

(L) $\Phi_{xx} + \Phi_{yy} + \Phi_{zz} = 0$ (3.1.2b)

(F) $\Phi_{tt} - 2U\Phi_{xt} + U^2\Phi_{xx} + g\Phi_z = 0 \quad , \text{ on } z = 0$ (3.1.9)

(K) $$\frac{\partial \Phi_j^R}{\partial n} = \dot{\xi}_j n_j + \xi_j U m_j \quad , \; j = 1,...,6 \; , \text{ on } \; S_0 \qquad (3.1.24b)$$

$$\frac{\partial \Phi^D}{\partial n} = -\frac{\partial \Phi^I}{\partial n} \quad , \text{ on } \; S_0 \qquad (3.1.20)$$

(B) $$\nabla \Phi \rightarrow 0 \quad , \text{ on } z \rightarrow -\infty \qquad (3.1.6)$$

(R) Appropriate radiation condition at infinite

These conditions are the basis for almost all the consistent ship motion theories actually in use, however to solve the problem further simplifications are necessary to deal with the three-dimensional aspects involved. This last remaining step distinguish the several approaches developed to solve the ship motion problem.

Equations and forces

As explained in the introduction, the dynamics of ship motions are governed by equations of motion which balance the external forces acting upon the hull with the internal forces due to gravity and inertia.

Once the problem of the previous Section is solved and the velocity potential is known, the application of Bernoulli's equation will give the pressure on the hull, and integration of the pressure over the wetted surface will give the external forces acting on the hull.

In the reference system advancing with the ship's forward speed the Bernoulli equation is;

$$\frac{p - p_a}{\rho} = -\frac{\partial \Phi}{\partial t} - \frac{1}{2}|\nabla \Phi|^2 - zg + \frac{1}{2}U^2 \qquad (3.1.25)$$

where 'p' is the fluid pressure, 'p_a' is the atmospheric pressure, and 'ρ' is the fluid density. Substituting the potential decomposition (3.1.8) into (3.1.25) and neglecting the higher order terms in Φ_1, two groups of terms can be distinguished; one represent the steady pressure due to the steady flow, and the

other represent the oscillatory pressure. We are concerned here only with the oscillatory part, so the linearized time-dependent pressure is;

$$\frac{p-p_a}{\rho}=-\left(\frac{\partial\Phi_1}{\partial t}+\nabla\Phi_0\cdot\nabla\Phi_1+zg\right) \tag{3.1.26}$$

It should also be referred that in spite of the fact that one of the pressure terms is steady in time, its contribution to the hydrodynamic forces is not steady, because the wetted surface, over which the pressure should be integrated, is changing. However, within the accuracy of the linearization the pressure will not be evaluated at the exact wetted surface. We will return to this particular subject latter on.

The total oscillatory force acting upon the hull is obtained by integration of the pressure (3.1.26);

$$F=\iint_S(p-p_a)\tilde{n}ds \tag{3.1.27}$$

$$F=-\iint_{S_0}\left(\frac{\partial\Phi_1}{\partial t}+\nabla\Phi_0\cdot\nabla\Phi_1\right)\tilde{n}ds-\rho g\iint_S(z\tilde{n})ds \tag{3.1.28}$$

Where according to the boundary value problem stated, the forces due to the unsteady potentials are evaluated at the mean wetted surface 'S_0'. The last term on the right side of equation (3.1.28) represents the hydrostatic force which will be studied latter on.

The first term can be further simplified by applying a variation of the Stokes theorem as derived by Ogilvie and Tuck (1969);

Theorem

Let $\Phi_1(x,y,z)$ *be a differentiable scalar function. Then the following is true;*

$$\iint_{S_0}\left[-\Phi_1(\tilde{n}\cdot\nabla)V_0+(V_0\cdot\nabla\Phi_1)\tilde{n}\right]ds=-\oint_{C_0}\left[\Phi_1(e_z\cdot V_0)\tilde{n}\right]d\ell$$

where 'C_0' is the intersection of the surface S_0 with the still water line, and is followed in a counterclokcwise direction looking down on the ship (see figure-3.3).

Ogilvie and Tuck proved that for the motion modes of heave and pitch the line integral vanishes if the ship is wall-sided around the water line level $(n_3 = n_5 = 0)$. For the other motion modes the line integral will be negligible if the ship is slender $(e_z \cdot n \cong 0)$. Thus the former relation can be used in the following form;

$$\iint_{S_0} \left[-\Phi_1 (\tilde{n} \cdot \nabla) \nabla \Phi_0 + (\nabla \Phi_0 \cdot \nabla \Phi_1) \tilde{n} \right] ds = 0 \qquad (3.1.29)$$

where $V_0 = \nabla \Phi_0$.

Using this theorem we can convert the surface integral involving derivatives of Φ_1 (see eq. (3.1.28)) into a surface integral which involve only the values of Φ_1, thus we avoid the necessity of evaluating differentiation of the unsteady potential with respect to the space co-ordinates.

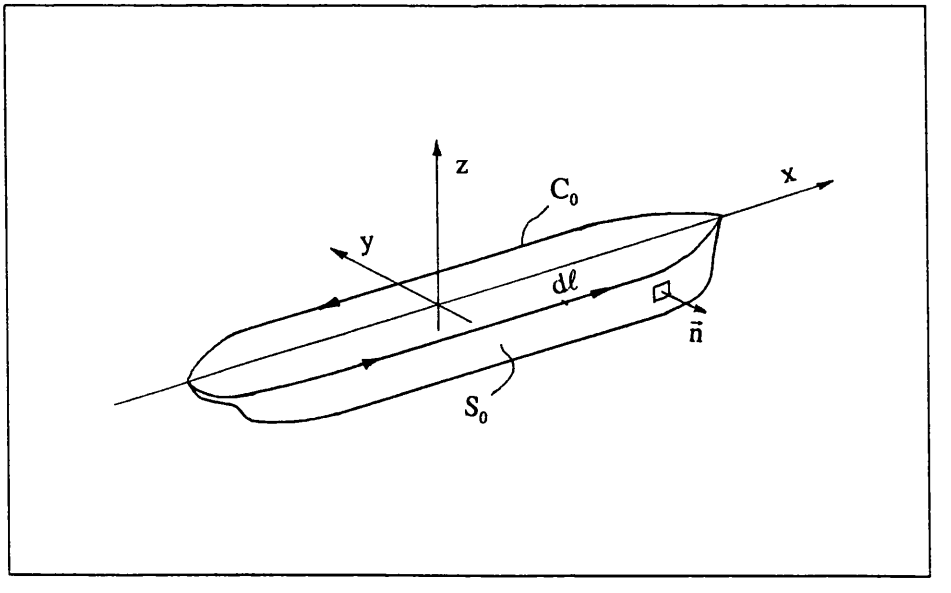

Figure 3.3 Application of Tuck's theorem

Using (3.1.29) to simplify the first term on the right side of (3.1.28) results;

$$F = -\rho \iint_{S_0} \left(\frac{\partial \Phi_1}{\partial t} \tilde{n} - \Phi_1 U \tilde{m} \right) ds \tag{3.1.30}$$

where the $\tilde{n}$ and $\tilde{m}$ vectors have been defined in (3.1.23).

As the unsteady potential was linearly decomposed we are able to distinguish the exciting force and the radiation force:

-The total exciting force is;

$$F^E = -\rho \iint_{S_0} \left(\frac{\partial (\Phi^I + \Phi^D)}{\partial t} \tilde{n} - (\Phi^I + \Phi^D) U \tilde{m} \right) ds \tag{3.1.31}$$

which represent the unsteady force that the body is subjected to, other than the hydrostatic force, when it is fixed at it's static equilibrium position and the waves are incident on it.

-The total radiation force is;

$$F^R = -\rho \iint_{S_0} \left(\frac{\partial \Phi^R}{\partial t} \tilde{n} - \Phi^R U \tilde{m} \right) ds \tag{3.1.32}$$

Which represent the unsteady force that the body is subjected to, other than the hydrostatic force, when the body is undergoing unsteady motions in otherwise calm water.

So the linearized exciting force and radiation force are evaluated independently, and the interference effects between each other are neglected.

-Finally the second term in (3.1.28) represents the hydrostatic force;

$$F^H = -\rho g \iint_S (z\tilde{n}) ds \tag{3.1.33}$$

Which represent the hydrostatic force that the body is subjected to, when it is at some general position. 'S' is the wetted surface of the ship.

It is now possible to express the motion equation for free oscillations of the ship in waves, by equating the above forces to the inertial forces associated with accelerations of the body mass. The body is unrestrained and assumed rigid. The inertial forces and moments associated with ship's mass are given by the rate of change of linear momentum and angular momentum. The equation of motion is;

$$F^M + F^R + F^B = F^E \qquad (3.1.34)$$

The restoring forces, 'F^B' are the result of combining the effects of the hydrostatic forces and the weight of the body.

3.2 - Cylinder Motion Problem

In this study, two-dimensional motion of cylinders with arbitrary cross section, subjected to beam waves and oscillating on the free-surface is investigated. There is no forward speed and the flow is two-dimensional.

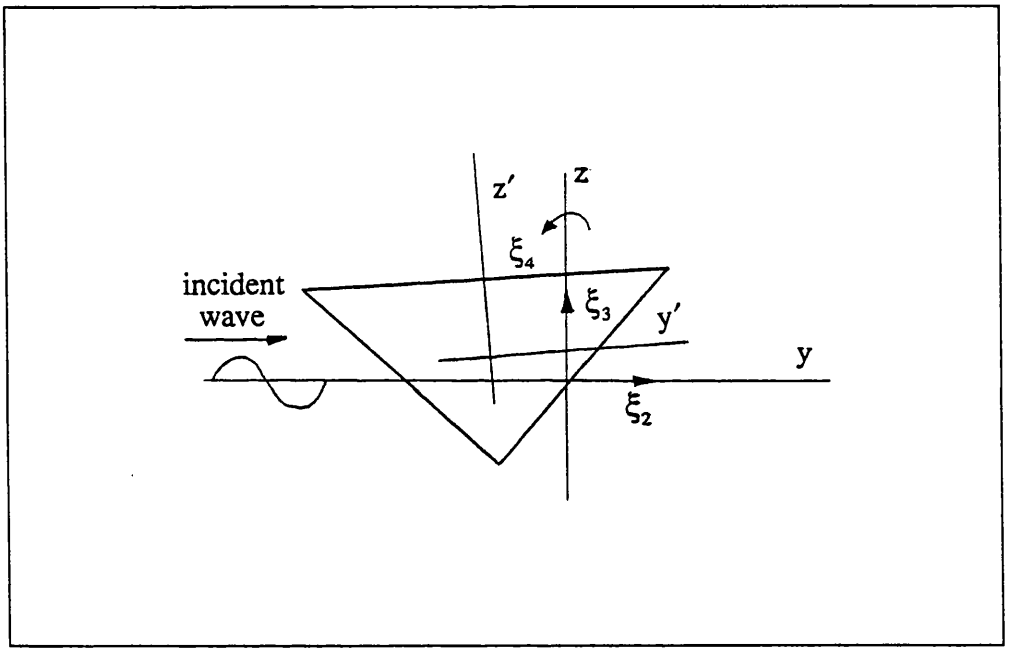

Figure 3.4 Reference Systems and Sign Convention for the Displacements

Two reference systems must be defined. The first one, $X=(y,z)$, is fixed in space, with the origin located on the still water line, on same vertical as the centre of gravity of the cylinder at its mean position. All the forces acting on the cylinder are represented in this reference system. The other reference system, $X'=(y',z')$, is fixed on the body. The origin location is defined with the body on the static equilibrium position, on the intersection of the still water line with the same vertical as the gravity centre. This system is used to evaluate the inertial properties of the body.

The cylinder will oscillate in three degrees of freedom. Namely it will have two translatory motions in the y and z directions, respectively the sway and heave, and one angular motion in the y-z plane, the roll motion. The reference systems and the several motions are represented in figure 3.4.

In the cylinder motion problem the unit vector normal to the body surface has only two components, $n=(n_2,n_3)$. The correspondent vector with the auxiliary component necessary to evaluate the moments is, $\tilde{n}=(n_2,n_3,n_4)$.

Boundary Value Problem

The general linearized boundary value problem stated on the previous Section is now simplified to derive the velocity potential of the flow around the cylinder surface knowing that it must satisfy;

(L) The two-dimensional Laplace equation

$$\Phi_{yy}+\Phi_{zz}=0 \tag{3.2.1}$$

(F) The linearized free-surface boundary condition

$$\Phi_{tt}+g\Phi_z=0 \quad , \quad \text{on} \quad z=0 \tag{3.2.2}$$

(K) The linearized body kinematic boundary conditions to be satisfied by the radiation problem and the diffraction problem

$$\begin{cases} \dfrac{\partial\Phi_j^R}{\partial n}=\dot{\xi}_j n_j & (3.2.3) \\ \dfrac{\partial\Phi^D}{\partial n}=-\dfrac{\partial\Phi^I}{\partial n} & (3.2.4) \end{cases} \quad , \; j=2,3,4 \quad , \; \text{on} \quad S_0$$

(B) The bottom condition

$$\nabla\Phi\to 0 \quad , \quad \text{on} \quad z\to-\infty \tag{3.2.5}$$

(R) The appropriate radiation condition at infinite for the radiation and diffraction potentials

Forces and Motion Equation

Once the potential is known the two-dimensional forces acting upon the cylinder are;

- The exciting force

$$f^E = -\rho \iint_{S_0} \left(\frac{\partial}{\partial t} (\Phi^I + \Phi^D) \tilde{n} \right) ds \qquad (3.2.6)$$

- The radiation force

$$f^R = -\rho \iint_{S_0} \left(\frac{\partial \Phi^R}{\partial t} \tilde{n} \right) ds \qquad (3.2.7)$$

- The hydrostatic force

$$f^H = -\rho g \iint_{S} (z\tilde{n}) ds \qquad (3.1.28)$$

The equation of motions can now be presented by equating the above forces with the body-mass forces in the usual way;

$$f^M + f^R + f^B = f^E \qquad (3.2.8)$$

The restoring forces, 'f^B' are the result of combining the effects of the hydrostatic forces and the weight of the body.

4. Frequency-Domain Solution of the Cylinder Motion Problem

4.1 - Introduction

In this Chapter we will restrict the general linearized problem presented in Section 3-2 to sinusoidal excitations and linear and harmonic responses of the cylinder. The mathematical model represents inertial, damping and restoring forces which are linearly proportional respectively to the amplitudes of the ship oscillatory acceleration, velocity and displacement, and as the oscillatory motions are sinusoidal the amplitudes of forces are linearly proportional to the amplitude of motions. A more practical consequence of the linearity of the system can be stated as follows; if the cylinder is subjected to a sum of two excitations, both sinusoidal at the same frequency , the total response would be the sum of the separate responses.

The exciting forces in k-direction and the motions in j-mode are now given by;

$$f_k^E(t) = \mathrm{Re}\left[f_k^E e^{i\omega t}\right] \quad , \quad k = 2,\ldots,4 \tag{4.1.1}$$

$$\xi_j(t) = \mathrm{Re}\,\xi_j^A e^{i\omega t} \quad , \quad j = 2,\ldots,4 \tag{4.1.2}$$

Where 'f_k^E' are the complex amplitudes of the exciting forces, and 'ξ_j^A' are the complex amplitudes of the sinusoidal motions. (From now on only the real part will be taken in all terms involving $e^{i\omega t}$.)

The reference systems, $X = (x,y)$, and $X' = (x',y')$, have been defined in Section-3.2.

In order to obtain the several terms in the motion equations (3.2.8) it will be necessary to solve the linearized boundary value problem and evaluate the integrals for the forces, as presented in Section 3-2. To solve the boundary value problem, the well known "Frank Close Fit Method" developed by W. Frank (1970) is used. Both radiation and exciting forces are calculated by this method. Basically Frank represented the velocity potential by a distribution of sources over the mean submerged cross section. The Green functions are applied to represent the potential of the unit strength sources. The density of the sources, placed along the contour, is an unknown function to be determined from the integral equations derived by applying the kinematic boundary condition on the

submerged part of the cylinder. In the numerical solution the contour of the section is descritized in a number of segments, and on each one a singularity is placed. This method was chosen because it allows the computation of hydrodynamic coefficients of cylinders with non-regular shapes with much more accuracy than the other available methods.

4.2.1 - Radiation Forces at Finite Frequencies

Solution of the Boundary Value Problem

As explained in Section-3.1, under certain assumptions, the linearized radiation potential problem can be treated as an independent problem, neglecting the interferences with the incident and diffracted potentials. This way the problem consists of evaluating the forces, other than hydrostatic, associated with oscillatory motion of the section in otherwise calm water. (From now on we will refer to the cylinder as "section", because it is more appropriate to associate it with the two-dimensional flow.)

Under the former assumption, and given the conditions stated in Section-3.2, the boundary value problem is: for the section having sinusoidal oscillation on the free-surface with frequency 'ω', in otherwise calm water, the evaluation of the radiation potential on the hull mean surface that satisfy the following conditions;

(L) The two-dimensional Laplace equation

$$\Phi^R_{yy} + \Phi^R_{zz} = 0 \qquad (4.2.3)$$

(F) The linearized free-surface boundary condition

$$-\frac{\omega^2}{g}\Phi^R + \Phi^R_z = 0 \quad , \text{ on } z=0 \qquad (4.2.4)$$

(K) The linearized body kinematic boundary condition

$$\frac{\partial \Phi^R_j}{\partial n} = i\omega\xi_j n_j \quad , j = 2,3,4 \quad , \text{ on } S_0 \qquad (4.2.5)$$

(B) The bottom condition

$$\nabla\Phi^R \to 0 \quad , \text{ on } z \to -\infty \qquad (4.2.6)$$

(R) The radiation condition at infinity

$$\nabla\Phi^R - i\frac{\omega^2}{g}\Phi^R = 0 \qquad , \text{ on } |y| \to \infty \tag{4.2.7}$$

The deduction of the last condition can be found in Wehausen and Laitone (1960).

In figure 4.1 the section and all the boundaries where boundary conditions must be satisfied are shown. These surfaces bound a Laplacian fluid volume, and 'S_0' represents the mean hull surface, 'S_F' is the free-surface, and 'S_R' is a surface inside the fluid and approaching infinity. In addition, 'Q' is a point on the surface of the body, fundamental source point or influencing point, and 'P' is a point in the fluid domain, the influenced point.

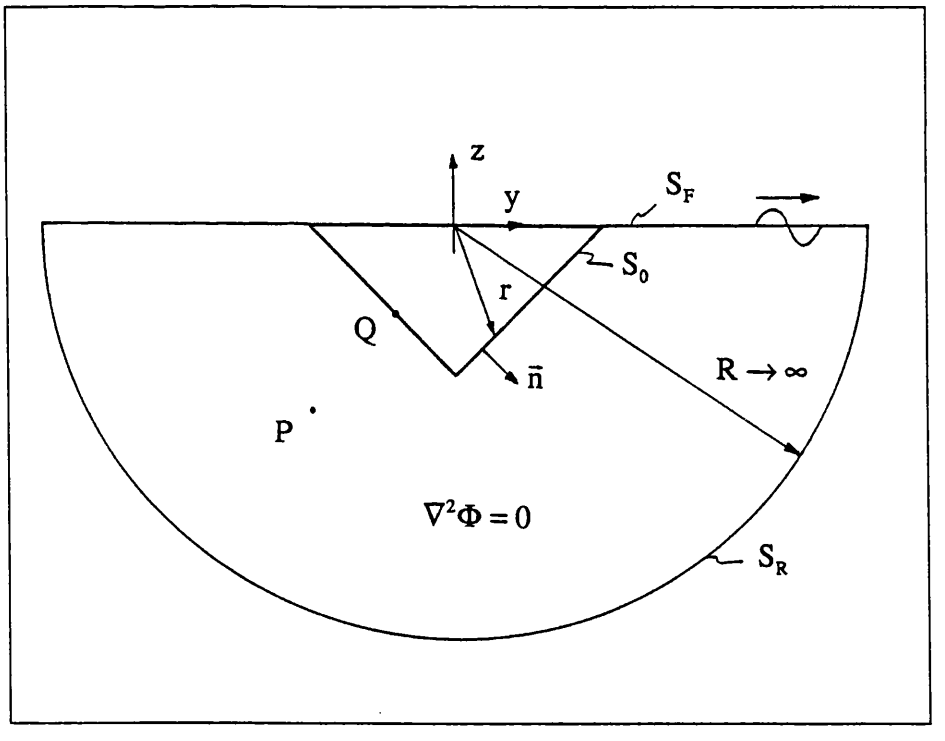

Figure 4.1 The Boundary Value Problem

Applying the Green theorem to the fluid volume, we find that the velocity potential '$\Phi(P,t)$' at a general point 'P(y,z)' in the fluid can be represented in terms of a dipole distribution of moment '$\Phi(Q,t)$', and a source distribution of

strength '$-\partial\Phi/\partial n$' distributed over the boundary surfaces (see Newman (1977), sec-4.11);

$$\Phi(P,t) = -\frac{1}{2\pi}\iint_{S_0+S_F+S_R}\left[G(\overline{QP})\frac{\partial\Phi(Q,t)}{\partial n} - \Phi(Q,t)\frac{\partial G(\overline{QP})}{\partial n}\right]ds \qquad (4.2.8)$$

Here $Q(\eta,\zeta)$ is a point on the surface of the body. $G(\overline{QP})$ is a function representing a source potential which satisfy the same Laplace equation (4.2.3), and the boundary conditions on the free-surface (4.2.4) and at infinity (4.2.6), (4.2.7). This function exhibits the characteristic of having a singular point when $P \to Q$, and is named as Green function. Its form was deducted by Wehausen and Laitone (1960) and is given by;

$$G(\overline{QP}) = \left[\ln d - \ln \bar{d} + G^*(QP)\right] \qquad (4.2.9)$$

Where: d, is the distance between the points $Q(\eta,\zeta)$ and $P(y,z)$

$\bar{d}$, is the distance between the points $\bar{Q}(\eta,-\zeta)$ and $P(y,z)$

$\ln d$, is the fundamental solution of the Laplace equation in unbounded fluid

$\ln \bar{d}$, is the contribution due the solution only in half plane

$G^*(QP)$, is the contribution due to the boundary conditions that the Green function must satisfy, and is given by;

$$G^* = -2\lim_{\mu\to 0^+}\int_0^\infty \frac{e^{s(z+\zeta)}\cos\left[s(y-\eta)\right]}{s - \frac{(\omega - i\mu)^2}{g}}ds \qquad (4.2.10)$$

where 'μ' can be interpreted as a Rayleigh viscosity coefficient, representing a fictitious dissipation which suppresses radiated waves at infinity.

Thus, in general, the flow can be represented by a suitable distribution of dipoles and sources on the boundary of the fluid volume.

The integral in (4.2.8) can be reduced to an integral over the body surface by using the boundary conditions stated above;

(L) $\Phi^R_{yy} + \Phi^R_{zz} = 0$	$G_{yy} + G_{zz} = 0$
(F) $\Phi^R_z - k_0\Phi^R = 0$ on $z = 0$	$G_z - k_0 G = 0$ on $z = 0$
(R) $\Phi^R_r - ik_0\Phi^R = 0$ when $\lvert y\rvert \to \infty$	$G_r - ik_0 G = 0$ when $\lvert y\rvert \to \infty$
(B) $\nabla\Phi^R = 0$ when $z \to -\infty$	$G_r = 0$ when $z \to -\infty$

Where 'k_0' is the wave number defined as $k_0 = \frac{\omega_0^2}{g}$, and ω_0 is the wave frequency.

If now the integral in (4.2.8) is devided in three integrals over the three boundary surfaces, and the equations presented are used, we find that the integrals over S_F and S_R vanish, leaving only the one over the surface of the body;

$$\Phi^R(P,t) = -\frac{1}{2\pi}\iint_{S_0}\left[G(\overline{QP})\frac{\partial\Phi^R(Q,t)}{\partial n} - \Phi^R(Q,t)\frac{\partial G(\overline{QP})}{\partial n}\right]ds \qquad (4.2.11)$$

Remembering that 'n' is the normal to the body surface, it is easy to conclude that the term $\partial\Phi^R / \partial n$ represents a flux per unit of area, so this term can be identified with a source strength;

$$\frac{\partial\Phi^R(Q,t)}{\partial n} \Leftrightarrow q(Q,t) \qquad (4.2.12)$$

A similar reasoning can be given to conclude that the term Φ^R is equivalent to the moment of a dipole.

However in order to simulate immersed and semi-immersed bodies, normally a distribution of sources is enough to evaluate the velocity potential, thus equation (4.2.11) reduces to;

$$\Phi^R(P,t) = \frac{1}{2\pi}\iint_{S_0}\left[q(Q,t)G\left(\overline{QP}\right)\right]ds \qquad (4.2.13)$$

Finally the body boundary condition (4.2.5) is applied, which will result in the Fredholm integral equation of the second kind;

$$2\pi q(P,t) + \iint_{S_0}\left[q(Q,t)\frac{\partial G\left(\overline{QP}\right)}{\partial n}\right]ds = \frac{\partial \dot{\alpha}(t)}{\partial n} \qquad (4.2.14)$$

As the radiation potential is the linear superposition of the contributions of the three motion modes, we can work separately with the equation relative to each motion. In addition all the terms in the equation (4.2.14) are sinusoidal in time, thus we can work only with the complex amplitudes. This way the Fredholm equation for each mode of motion becomes;

$$2\pi q_j(P) + \iint_{S_0}\left[q_j(Q)\frac{\partial G_j\left(\overline{QP}\right)}{\partial n}\right]ds = i\omega\xi_j^A n_j \qquad j=2,3,4 \qquad (4.2.15)$$

In the radiation problem the motions are the "input" to obtain the solution, thus, for simplicity, we can say that the motions are cosine functions;

$$\xi_t(t) = \xi_j^a \cos\omega t \quad , \quad j=2,3,4 \qquad (4.2.16)$$

$$\dot{\xi}_j(t) = -\omega\xi_j^a \sin\omega t \quad , \quad j=2,3,4 \qquad (4.2.17)$$

$$\ddot{\xi}_j(t) = -\omega\xi_j^a \cos\omega t \quad , \quad j=2,3,4 \qquad (4.2.18)$$

where 'ξ_j^a' is the real amplitude of the j-motion.

Using these relations in (4.2.15), and separating the real and imaginary parts, the equations to be solved for the source strengths given unit amplitude motions are;

$$\mathrm{Re}\left\{2\pi\hat{q}_j(P)+\iint_{S_0}\left[\hat{q}_j(Q)\frac{\partial G_j(\overline{QP})}{\partial n}\right]ds\right\}=0\ ,\quad j=2,3,4 \tag{4.2.19}$$

$$\mathrm{Im}\left\{2\pi\hat{q}_j(P)+\iint_{S_0}\left[\hat{q}_j(Q)\frac{\partial G_j(\overline{QP})}{\partial n}\right]ds\right\}=-\omega n_j\ ,\ j=2,3,4 \tag{4.2.20}$$

Where '$\hat{q}_j(Q)$' is the source strength in point Q of the body surface, due to a sinusoidal motion of unit amplitude in j-direction.

With the values of the source strength along the contour of the section, the velocity potentials relative to sinusoidal motions of unit amplitude can be obtained by using equation (4.2.13).

In the numerical solution of the integral equations, the contour of the section is divided on a finite number of segments, 'N'. On each segment the distribution of sources have an unknown constant strength, while the normal velocity is known. Thus the integral equations (4.2.19) and (4.2.20) reduce to a set of 2N linear algebraic equations. The major difficulty is on the evaluation of the integrals for the Green functions, and also here is the weakness of the method since some instabilities may occur in certain frequencies, and disparate results arise. Frequencies at which instabilities occur are the so called irregular frequencies, however there are ways of avoiding this instability problem.

Radiation Forces

Once the radiation potentials are known, the pressure on the section surface is obtained by the use of the Bernoulli equation, then the integration over the body surface gives the radiation forces. These steps have been derived in Chapter-3, and the equation for the radiation forces is;

$$f^R=-\rho\iint_{S_0}\left(\frac{\partial\Phi^R}{\partial t}\tilde{n}\right)ds \tag{3.2.7}$$

If the sinusoidal characteristics of the potential are used, and we decompose the force in three directions of the reference system, we obtain;

$$f_k^R = -i\omega\rho \iint_{S_0} (\Phi^R n_k) ds \qquad , \quad k = 2,3,4 \tag{4.2.21}$$

As the potential is linearly decomposed in contributions from each mode of motion, the radiation force in k-direction due to a motion in j-direction is;

$$f_{kj}^R = -i\omega\rho\xi_j \iint_{S_0} (\hat{\Phi}_j^R n_k) ds \qquad , \quad k,j = 2,3,4 \tag{4.2.22}$$

Where $\hat{\Phi}_j^R$ is the radiation potential due to an unit amplitude motion in the j-mode. These are the potentials we obtain from the solution of the boundary value problem as described in the last pages.

The same force as (4.2.22) for the unit amplitude motion is;

$$\hat{f}_{kj}^R = -i\omega\rho \iint_{S_0} (\hat{\Phi}_j^R n_k) ds \qquad , \quad k,j = 2,3,4 \tag{4.2.23}$$

This force can be divided in real and imaginary parts;

$$\mathrm{Re}(\hat{f}_{kj}^R) = -\omega\rho\, \mathrm{Re}\left\{ i \iint_{S_0} (\hat{\Phi}_j^R n_k) ds \right\} \qquad , \quad k,j = 2,3,4 \tag{4.2.24}$$

$$\mathrm{Im}(\hat{f}_{kj}^R) = -\omega\rho\, \mathrm{Im}\left\{ i \iint_{S_0} (\hat{\Phi}_j^R n_k) ds \right\} \qquad , \quad k,j = 2,3,4 \tag{4.2.25}$$

In the numerical solution of equations (4.2.24) and (4.2.25), the hydrodynamic force on each segment is calculated assuming the pressure over the segment is constant and equal to the pressure in the mid-point.

If now we define the following constants;

$$a_{kj} = \frac{\rho}{\omega} \mathrm{Re}\left\{ i \iint_{S_0} \left(\hat{\Phi}_j^R n_k \right) ds \right\} \quad , \quad k,j = 2,3,4 \tag{4.2.26}$$

$$b_{kj} = -\rho \, \mathrm{Im}\left\{ i \iint_{S_0} \left(\hat{\Phi}_j^R n_k \right) ds \right\} \quad , \quad k,j = 2,3,4 \tag{4.2.27}$$

Then equation (4.2.23) can be written in the compact form;

$$\hat{f}_{kj}^R = -\omega^2 a_{kj} + i\omega b_{kj} \quad , \quad k,j = 2,3,4 \tag{4.2.28}$$

The radiation force in the 'k' direction due to a sinusoidal motion of arbitrary amplitude in j-direction is;

$$f_{kj}^R = \xi_j \left(-\omega^2 a_{kj} + i\omega b_{kj} \right) \quad , \quad k,j = 2,3,4 \tag{4.2.29}$$

We have now an equation which is analogues to the linear dynamic motion equation which consists of mass and damping forces;

$$f_{kj}^R = a_{kj} \ddot{\xi} + b_{kj} \dot{\xi} \quad , \quad k,j = 2,3,4 \tag{4.2.30}$$

We find that the radiation forces have two components, one in phase with the acceleration of the motion, and the other in phase with the velocity of the motion. These forces are linearly proportional to the acceleration and velocity, and the constants of proportionality are the "added mass coefficient", 'a_{kj}', and the "damping coefficient", 'b_{kj}'. A more complete analysis of these terms is made in Section-7.2.

Final Remarks

Some assumptions were made to obtain numerical solutions for the boundary value problem. First, it was assumed that the cross section of the cylinder can be approximated by a polygon defined by a finite number of points. Then it was assumed that in each segment the source distribution was constant, which permits to convert the integral equation to a set of linear algebraic equations.

Finally the mean hydrodynamic pressure over each segment was taken into account for the computation of the total hydrodynamic forces.

This method have advantages in relation to the conformal mapping techniques, specially when the hydrodynamic coefficients of sections with non-regular forms are modelled. In this case, the conformal mapping method needs a large number of terms to make the mapping of the section onto the unit circle. The Frank Close-Fit Method is applicable to any shape of the cross section, even those with bulbs, sharp corners, bilge keels, etc.

4.2.2 - Radiation Forces at High Frequency

In the former sub-Section the forces induced by the motions of the body, when it is oscillating with finite frequencies, have been studied. In the present sub-Section the same forces are studied by assuming that the body is oscillating on the free-surface with high frequencies, such that physically it can be assumed that these oscillations are occurring at infinite frequency. This means that the inertial effects of the fluid are dominant, and gravitational forces can be neglected. Thus the wave effects are ignored, which means that in this problem there are no damping forces.

The free-surface boundary condition is;

$$-\frac{\omega^2}{g}\Phi^R + \Phi_z^R = 0 \qquad , \text{ on } z=0 \tag{4.2.4}$$

To satisfy this equation, as the frequency approaches infinity we must impose that the radiation potential on the free-surface at mean level approaches the zero value;

$$\frac{\omega^2}{g} = \infty \Rightarrow \Phi^R = 0 \qquad , \text{ on } z=0 \tag{4.2.31}$$

This free-surface condition implies that the radiation potential, Φ^R, is anti symmetric with respect to the z=0 plane. We can interpret the phenomena physically as if the body would be extended by having its mirror-image added to it, and the whole space outside of the body being filled with fluid (see figures 4.4 and 4.5).

The potential flow around a moving body with geometrical symmetry, has the characteristic of having itself a symmetric distribution of the velocity module, in relation to the symmetry plane of the body. However the normal components of the fluid velocity vector on the body surface, at correspondent points on both sides in relation to the symmetry plane, can be both pointing out to the fluid (or pointing in to the body), or one pointing to the fluid and the other to the body.

The heave motions correspond the first case, and the sway and roll motions are identified with the second case (see figures 4.2 and 4.3).

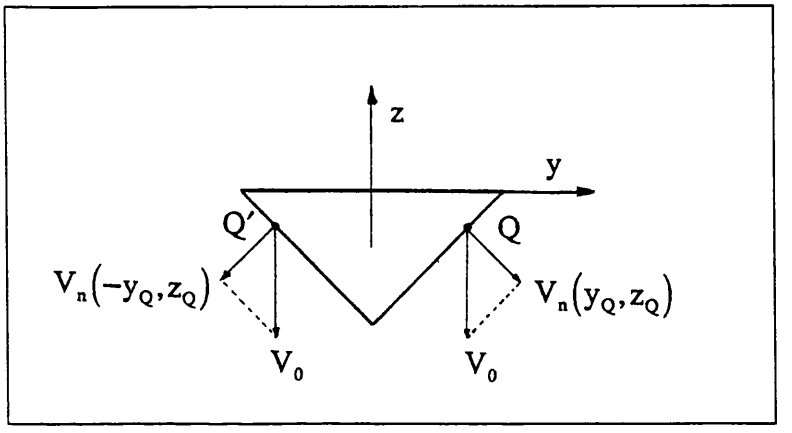

Figure 4.2 Fluid velocity vector at the body surface for the heave motion

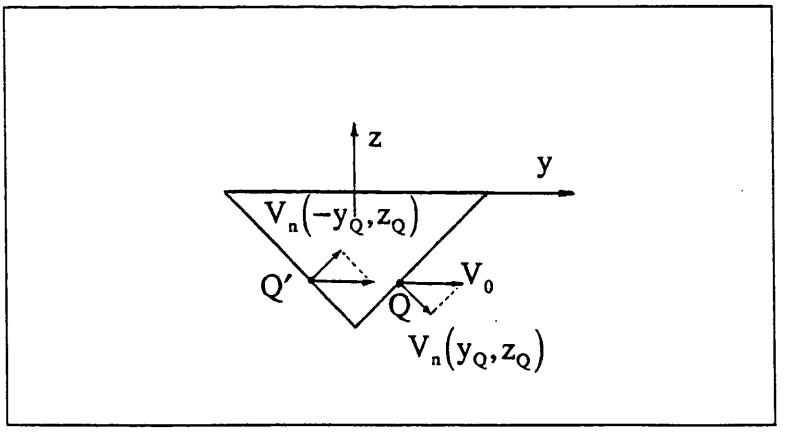

Figure 4.3 Fluid velocity vector at the body surface for the sway and roll motions

The sign (positive or negative) of velocity potential evaluated at the body surface, is dependent if the fluid normal velocity vector is pointing out to the fluid or out of the fluid. Thus we can say that the heave motion has a symmetrical distribution of Φ^R;

$$\Phi^R(y', z') = \Phi^R(-y', z') \quad , \text{ on } S_0 \tag{4.2.32}$$

where x′ and y′ are the co-ordinates of a general point on the body surface, represented on the reference system fixed at the body.

The extended body and the associated potential, which satisfy the anti symmetrical condition (4.2.31) in relation to the plane z=0, and the symmetrical condition (4.2.32) in relation to the plane y=0, are drawn in fig.4.4.

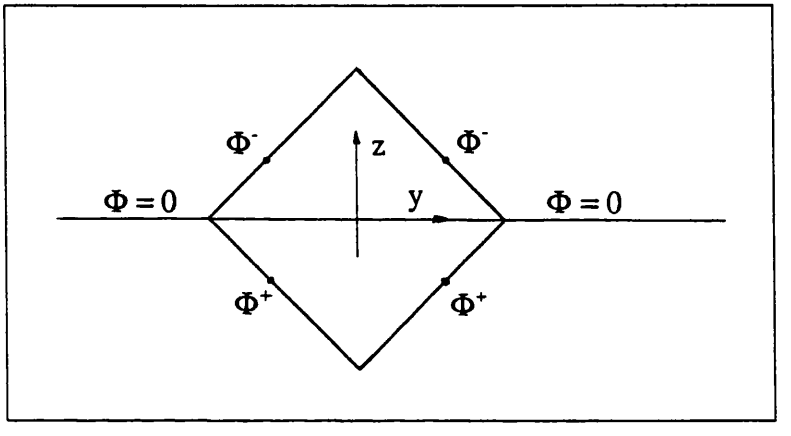

Figure 4.4 Extended body for the heave motion

Thus in the case of heave motion, the extended body now moves as a unit, with oscillatory motion in an unbounded fluid region.

The sway and roll motions have anti symmetrical distribution of Φ^R;

$$\Phi^R(y',z') = -\Phi^R(-y',z') \quad , \text{ on } S_0 \tag{4.2.33}$$

The extended body and the associated potential, which satisfy the anti symmetrical condition (4.2.31) in relation to the plane z=0, and the anti symmetrical condition (4.2.33) in relation to the plane y=0, are shown in fig.4.5.

The simulation of the roll motion problem is similar to the case of heave motion problem, the extended body now moves as a unit. However to simulate the sway motion the body must be completed by having its mirror-image added to it, but the reflected half-body must move in opposite direction to the real body.

The evaluation of the velocity potential for this problem, is much simpler than the previous case applied to finite frequencies of oscillation. The main reason is

that now there is no free-surface, thus the Green function necessary to use the Green theorem is simply given by;

$$G(QP) = \ln r \qquad (4.2.34)$$

where 'r' is the distance between the points Q and P (see Section-4.2.1).

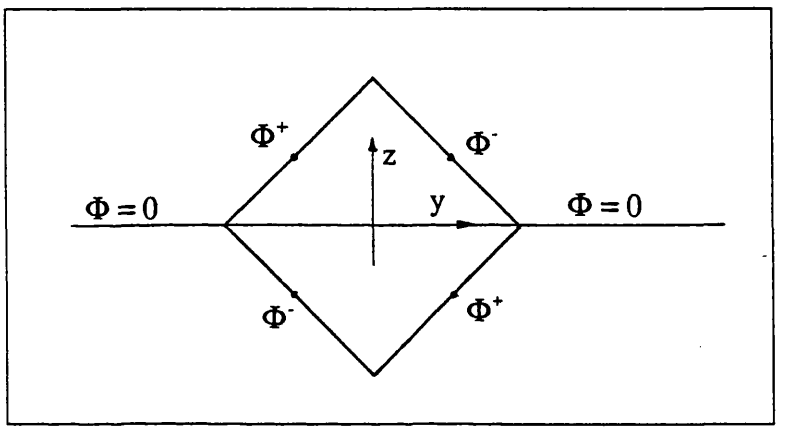

Figure 4.5 Extended body for the sway and roll motions

The conditions to be used to evaluate the radiation potential are;

(L) The two-dimensional Laplace equation

$$\Phi^R_{yy} + \Phi^R_{zz} = 0 \qquad (4.2.3)$$

(F) The infinite frequency free-surface boundary condition

$$\Phi^R = 0 \quad , \text{ on } z=0 \qquad (4.2.31)$$

(K) The linearized body kinematic boundary condition

$$\frac{\partial \Phi^R_j}{\partial n} = i\omega \xi_j n_j \quad , \; j = 2,3,4 \quad , \text{ on } S_0 \qquad (4.2.5)$$

(B) The radiation condition at infinity

$$\nabla \Phi^R \to 0 \quad , \text{ on } |y+z| \to \infty \qquad (4.2.35)$$

The steps followed to obtain first the velocity potential and then the associated forces, are similar to those described in Section-4.3.1. However there are some particular differences which simplify the problem, thus these are explained here again.

The Green theorem can be applied to the fluid volume to evaluate the velocity potential. But, now the appropriate closed surface bounding the fluid volume consists of the body surface, S_0, plus a control surface, S_C, surrounding the extended body and approaching infinity everywhere else.

$$\Phi(P,t) = -\frac{1}{2\pi}\iint_{S_0+S_C}\left[G(\overline{QP})\frac{\partial\Phi(Q,t)}{\partial n} - \Phi(Q,t)\frac{\partial G(\overline{QP})}{\partial n}\right]ds \qquad (4.2.36)$$

Using the condition at infinity, (4.2.35), we find that the integral over the surface S_C vanishes in the limit where this surface is at an infinite distance from the body surface. In addition, in order to simulate the flow around immersed bodies, a distribution of sources is enough to evaluate the velocity potential, hence equation (4.2.36) reduces to;

$$\Phi^R(P,t) = \frac{1}{2\pi}\iint_{S_0}\left[q(Q,t)G(\overline{QP})\right]ds \qquad (4.2.13)$$

which is the equation deducted in Section-4.2.1. Applying the body boundary condition (4.2.5) to each mode of motion separately, results in the Fredholm integral equation of the second kind related with each mode of motion;

$$2\pi q_j(P,t) + \iint_{S_0}\left[q_j(Q,t)\frac{\partial G_j(\overline{QP})}{\partial n}\right]ds = i\omega\xi_j^A e^{i\omega t}n_j \qquad j=2,3,4 \qquad (4.2.15)$$

For convenience, the source distribution of strength is dimensionalised with respect to $\omega\xi^a$, becoming;

$$q_j^*(Q) = \frac{q_j(Q)}{\omega\xi^a} \quad , \; j=2,3,4 \qquad (4.2.37)$$

The displacements, velocities, and accelerations are given by;

$$\xi_t(t) = \xi_j^a \cos\omega t \quad , \quad j = 2,3,4 \tag{4.2.16}$$

$$\dot{\xi}_j(t) = -\omega\xi_j^a \sin\omega t \quad , \quad j = 2,3,4 \tag{4.2.17}$$

$$\ddot{\xi}_j(t) = -\omega^2\xi_j^a \cos\omega t \quad , \quad j = 2,3,4 \tag{4.2.18}$$

We have concluded, at the beginning of the Section that there are no damping forces in the infinite frequency radiation problem, hence the source distribution of strength and distribution of potential have the same phase angle as the velocity of the motion, thus we can work with real quantities instead of complex, and eq. (4.2.15) can be rewritten as;

$$2\pi q_j^*(P,t) + \iint_{S_0}\left[q_j^*(Q,t)\frac{\partial G_j(\overline{QP})}{\partial n}\right]ds = -\sin(\omega t)n_j \quad , j = 2,3,4 \tag{4.2.38}$$

Solving the equation (4.2.38) we obtain the non-dimensional source distribution of strength, $q_j^*(Q)$, which is used in equation (4.2.13) to find the velocity potential distribution over the body surface, Φ^{*R}, which is also non-dimensionalised with respect to $\omega\xi^a$.

Following Section-3.2 the radiation force is given by;

$$F^R = -\rho\iint_{S_0}\left(\frac{\partial\Phi^R(t)}{\partial t}\tilde{n}\right)ds \tag{3.2.7}$$

The forces can be separated in three directions and contributions from each motion mode. In addition the potential is a sine function of time, thus we can write;

$$F_{kj}^R = -\omega\cos(\omega t)\rho\iint_{S_0}\left(\Phi_j^R n_k\right)ds \quad , \quad k,j = 2,3,4 \tag{4.2.39}$$

Or using the non-dimensional radiation potential;

$$F_{kj}^{R} = -\omega^2 \cos(\omega t)\xi_j^a \rho \iint_{S_0} \left(\Phi_j^{*R} n_k\right) ds \quad , \quad k, j = 2,3,4 \tag{4.2.40}$$

Rewriting in a more compact form;

$$F_{kj}^{R} = a_{kj}^{\infty} \ddot{\xi}_j(t) \quad , \quad k, j = 2,3,4 \tag{4.2.41}$$

where 'a_{kj}^{∞}' is the infinite frequency added mass coefficient, given by;

$$a_{kj}^{\infty} = \rho \iint_{S_0} \left(\Phi_j^{*R} n_k\right) ds \tag{4.2.42}$$

4.3 - Exciting Forces

Solution of the Boundary Value Problem

As explained in Section-3.1, under certain assumptions, the linearized exciting potential problem can be treated as an independent problem, neglecting the interactions with the radiation potential.

Given the former assumption, and the conditions stated in Section-3.2, the boundary value problem will be solved for the section fixed on the free-surface at its static equilibrium position, and being subjected to sinusoidal waves of frequency 'ω_0'. The incident wave potential and the diffraction potential on the hull surface must satisfy the following conditions;

(L) The Laplace equation

$$\Phi^I_{yy} + \Phi^I_{zz} = 0 \tag{4.3.1}$$

$$\Phi^D_{yy} + \Phi^D_{zz} = 0 \tag{4.3.2}$$

(B) The body boundary condition on the hull at mean position

$$\frac{\partial \Phi^D}{\partial n} = -\frac{\partial \Phi^I}{\partial n} \quad , \text{ on } S_0 \tag{4.3.3}$$

(F) The free-surface boundary condition

$$-\omega^2 \Phi^I + g\frac{\partial}{\partial z}\Phi^I = 0 \quad , \text{ on } z = 0 \tag{4.3.4}$$

$$-\omega^2 \Phi^D + g\frac{\partial}{\partial z}\Phi^D = 0 \quad , \text{ on } z = 0 \tag{4.3.5}$$

(B) The bottom condition

$$\nabla \Phi^I \rightarrow 0 \quad , \text{ on } z \rightarrow -\infty \tag{4.3.6}$$

$$\nabla\Phi^D \to 0 \quad , \text{ on } z \to -\infty \tag{4.3.7}$$

(R) The diffraction potential must satisfy the radiation condition at infinity

$$\frac{\partial\Phi^D}{\partial r} - i\frac{\omega^2}{g}\Phi^D = 0 \quad \text{as} \quad |r| \to \infty \tag{4.3.8}$$

The incident wave potential by definition do not need to satisfy the radiation condition at infinity.

Here we are going to use incident linear waves, and in accordance with the linear gravity-wave theory, the incident wave potential corresponding to a wave travelling in the positive y-direction is given by;

$$\Phi^I(y,z,t) = \frac{ig\zeta^a}{\omega_0}\left(e^{k_0 z}\right)\left(e^{-ik_0 y}\right)\left(e^{i\omega t}\right) \tag{4.3.9}$$

Where ζ^a is the wave amplitude, and $k_0 = \omega_0^2 / g$ is the wave number.

The incident wave potential already satisfies the Laplace equation, the free-surface and the bottom conditions.

The diffracted potential will be evaluated with a method very similar to the one presented in the previous Section which describes the radiation potential. Thus the application of the Green theorem and the same boundary conditions as defined before are used to derive an equation, which gives the diffracted potential in terms of a suitable distribution of sources on the section surface;

$$\Phi^D(P,t) = \frac{1}{2\pi}\iint_{S_0}\left[q(Q,t)G\left(\overline{QP}\right)\right]ds \tag{4.3.10}$$

The sources strength, $q(Q)$, are the unknowns to be evaluated. The Green function must satisfy the same boundary conditions as the diffraction potential (4.3.2), (4.3.5), (4.3.7), and (4.3.8), except the kinematic body condition. In the following the kinematic body boundary condition is used to derive the fredholm equation, solution of which will yield the source strength distribution.

$$\frac{\partial \Phi^I}{\partial n} = -\frac{\partial \Phi^D}{\partial n} \quad , \text{ on } S_0 \tag{4.3.3}$$

$$\frac{\partial \Phi^D}{\partial n} = 2\pi q(P,t) + \iint_{S_0}\left[q(Q,t)\frac{\partial G(\overline{QP})}{\partial n}\right] ds \tag{4.3.11}$$

$$\frac{\partial \Phi^I}{\partial n} = (n_3 - in_2)k_0\Phi^I \tag{4.3.12}$$

Where n_2 and n_3 are the components, in the directions y and z, of the unit vector normal to the body surface.

Using relations (4.3.3), (4.3.11), and (4.3.12), we obtain an equation where the unknown is the source strength distribution;

$$2\pi q(P,t) + \iint_{S_0}\left[q(Q,t)\frac{\partial G(\overline{QP})}{\partial n}\right] ds = -(n_3 - in_2)k_0\Phi^I(t) \tag{4.3.13}$$

All the terms in the equation (4.3.13) are sinusoidal in time, thus we can work only with the complex amplitudes. Furthermore the equation can be divided in real and imaginary parts, so the source strength distribution given an incident wave of unit amplitude becomes;

$$\mathrm{Re}\left\{ 2\pi\hat{q}(P) + \iint_{S_0}\left[\hat{q}(Q)\frac{\partial G(\overline{QP})}{\partial n}\right] ds \right\} = -\mathrm{Re}\left\{ (n_3 - in_2)k_0\hat{\Phi}^I \right\} \tag{4.3.14}$$

$$\mathrm{Im}\left\{ 2\pi\hat{q}(P) + \iint_{S_0}\left[\hat{q}(Q)\frac{\partial G(\overline{QP})}{\partial n}\right] ds \right\} = -\mathrm{Im}\left\{ (n_3 - in_2)k_0\hat{\Phi}^I \right\} \tag{4.3.15}$$

Where $\hat{\Phi}^I$ is the amplitude of the incident wave potential due to a wave of unit amplitude.

We can say that the "input" for the diffraction problem is the incident wave, so for simplicity, the incident wave can be considered a pure cosine wave, without phase lag in time.

Having obtained the source strength distribution, the diffraction potential due to a wave of unit amplitude, $\hat{\Phi}^D$, can be calculated using equation (4.3.10).

The numerical approach to the solution is similar to the one described for the radiation problem, so the computer routines for the calculation of the Green function are the same as those used. Also the routines are the same to solve the linear algebraic equations given in equations (4.3.14) and (4.3.15), and finally to calculate the diffraction potential given in equation (4.3.10). Only the right hand side of the algebraic equations is calculated by different routines.

Exciting forces

Once the diffraction and incident wave potentials are known, the pressure on the hull is obtained from the Bernoulli equation. The equation for the exciting forces can be written as (see Section-3.2);

$$f^E = -\rho \iint_{S_0} \left(\frac{\partial}{\partial t} (\Phi^I + \Phi^D) \tilde{n} \right) ds \qquad (4.3.16)$$

The potentials are sinusoidal in time, so the derivative can be substituted by '$i\omega$', in addition the force can be decomposed in the three directions of the reference system, thus the exciting force in k-direction due to an incident wave of unit amplitude becomes;

$$\hat{f}_k^E = -i\omega\rho \iint_{S_0} \left(\hat{\Phi}^I + \hat{\Phi}^D \right) n_k ds \quad , \quad k = 2,3,4 \qquad (4.3.17)$$

And the exciting force in k-direction due to an incident wave of arbitrary amplitude is;

$$f_k^E = -i\omega\rho\zeta^a \iint_{S_0} \left(\hat{\Phi}^I + \hat{\Phi}^D \right) n_k ds \quad , \quad k = 2,3,4 \qquad (4.3.18)$$

We can see easily from these equations that the exciting forces are linearly proportional to the amplitude of the incident linear waves.

Normally the exciting forces are devided in two parts. One is the incident wave exciting force, or Froude Krylov force, and the other is the diffraction exciting force;

$$f_k^I = -i\omega\rho\zeta^a \iint_{S_0} \hat{\Phi}^I n_k ds \qquad , \quad k = 2,3,4 \tag{4.3.19}$$

$$f_k^D = -i\omega\rho\zeta^a \iint_{S_0} \hat{\Phi}^I n_k ds \qquad , \quad k = 2,3,4 \tag{4.3.20}$$

The exciting force is sinusoidal in time, with frequency ω, and can be represented in each direction as;

$$f_k^E(t) = \mathrm{Re}\left[f_k^E e^{i\omega t}\right] \qquad , \quad k = 2,3,4 \tag{4.3.21}$$

It is understood that the real part is to be taken in all expressions involving $e^{i\omega t}$, so from now on we will write;

$$f_k^E(t) = f_k^E e^{i\omega t} \qquad , \quad k = 2,3,4 \tag{4.3.22}$$

Here f_k^E is the amplitude of the total exciting force, and it represents a complex number which have the information about the absolute value of the force, and the corresponding phase angle. 'ω' is the encounter frequency.

Alternatively (4.3.20) can be written as;

$$f_k^E(t) = \left(f_k^E\right)^C \cos\omega t + \left(f_k^E\right)^S \sin\omega t \qquad , \quad k = 2,3,4 \tag{4.3.23}$$

So we have the exciting force divided in a cosine part and a sine part.

The numerical solution of equation (4.3.18) is similar to the one used in the computation of the radiation forces, so the same computer routines, with small modifications, can be used.

The advantages and limitations of this method to solve the boundary value problem stated in the beginning of the Section, are identical to those described for the radiation problem in Section-4.2.

4.4 - Restoring Forces

The restoring forces are the result of hydrostatic pressure action upon the hull, together with the effects of the body weight. The expression to evaluate the hydrostatic forces have been deducted in Chapter-3, and is;

$$f^H = -\rho g \iint_S (z\tilde{n}) ds \qquad (3.1.28)$$

Where 'S' is the instantaneous wetted surface.

In this Chapter we will maintain the linear characteristic of the system, so it is assumed that the effects of the radiation and exciting perturbation do not interfere with the hydrostatic force. We are referring to the changes in the wetted surface, due to the radiated and diffracted waves. Furthermore the free-surface elevation due to the incident waves is also neglected. Thus the hydrostatic forces will be evaluated assuming the Section oscillating in still water.

In Section-7.4 it is proved that for a ship form, under certain assumptions of the hull shape and amplitude of angular motions, the restoring forces in still water are linearly proportional to the displacements. The constants of proportionality are the restoring coefficients, 'c_{kj}', and the restoring force in k-direction due to a displacement in j-direction, ξ_j, is given by;

$$f^B_{kj} = c_{kj}\xi_j \qquad , \quad k,j = 2,3,4 \qquad (4.4.1)$$

In the case of oscillating cylinders there are no coupling coefficients. The only non-zero coefficients are associated with the heave and roll motions, and are given by;

$$c_{33} = \rho g A_f \qquad (4.4.2)$$

$$c_{44} = mg\overline{GM_T} \qquad (4.4.3)$$

Where 'ρ' is the density of the fluid, 'g' is the gravitational acceleration, 'A_f' is the water plane area, 'm' is the mass of the section, and '$\overline{GM_T}$' is the lateral metacentric height.

To use these coefficients we have to assume that, the sides of the section are vertical near the water line, the roll motion is of small amplitude, and the heave motion has a small amplitude.

A more detailed analysis of the restoring forces is given in Section-7.4.

4.5 - Body-Mass Force

In this Section we are concerned with the internal forces, proportional to the sectional inertia characteristics, and motion acceleration. These are the inertial forces and moments, given by the rate of change of linear momentum and angular momentum of the body. The derivations are given in Section-7.5, for the more general case of the ship.

The inertial force in k-direction due to an acceleration in j-direction is given by;

$$f_{kj}^{M} = m_{kj}\ddot{\xi}_{j} \qquad , \quad k,j = 2,3,4 \tag{4.5.1}$$

Where 'm_{kj}' are the coefficient from the matrix of body-inertia coefficients. For the present case of two-dimensional motion, if the section is symmetric with relation to the z-axis and the gravity centre is located at $(0, z'_G)$, the mass matrix is;

$$\left[m_{kj}\right] = \begin{bmatrix} m & 0 & -mz'_G \\ 0 & m & 0 \\ -mz'_G & 0 & I_{44} \end{bmatrix} \tag{4.5.2}$$

Where the moment of inertia for the roll mode is given by;

$$I_{44} = \iiint_{V_B} \rho_B \left(y'^2 + z'^2\right) dv \tag{4.5.3}$$

The vertical co-ordinate of gravity centre is;

$$z'_G = \frac{1}{m} \iiint_{V_B} (\rho_B z') dv \tag{4.5.4}$$

where the co-ordinates are represented on the reference system fixed on the section, $X' = (y', z')$.

We can conclude that the body inertial forces are linearly proportional to the motion rigid-body accelerations.

4.6 - Motion Equations and Solution

Equations of Motion

In the previous Sections of this Chapter the several components of the total pressure force, as well as the forces due to the mass-inertia of the ship have been discussed. Now the equations of motion for free oscillations of the cylinder in linear waves can be derived by equating the external pressure forces acting upon the body surface, with the internal forces due to gravity and internal forces associated with acceleration of the body mass. The cylinder will be assumed as an unrestrained body, and in state of equilibrium when in calm water.

Re-writing the three component vectors representing the various forces in each principal direction we have;

f_k^E , $k = 2,3,4$ For the sinusoidal exciting forces due to waves

$$f_k^M = \sum_{j=2}^{4} \left(m_{kj} \ddot{\xi}_j \right) \quad , \quad k = 2,3,4 \quad \text{For the body-mass inertial forces}$$

$$f_k^R = \sum_{j=2}^{4} \left(a_{kj} \ddot{\xi}_j + b_{kj} \dot{\xi}_j \right) \quad , \quad k = 2,3,4 \quad \text{For the radiation forces}$$

$$f_k^B = \sum_{j=2}^{4} c_{kj} \xi_j \quad , \quad k = 2,3,4 \quad \text{For the restoring forces}$$

The internal gravity force (the section weight) is already included in the restoring force term.

Equating the above terms in a appropriate way we finally obtain the equations of motion;

$$\sum_{j=2}^{4} \left\{ \left(m_{kj} + a_{kj} \right) \ddot{\xi}_j + b_{kj} \dot{\xi}_j + c_{kj} \xi_j \right\} = f_k^E \quad , \quad k = 2,3,4 \qquad (4.6.1)$$

Where the coefficients in the equations are sequentially; the body-inertia coefficients, the added mass coefficients, the damping coefficients and the restoring coefficients.

The generalised body-inertia matrix for sections with symmetry about the z-axis, and with the centre of gravity located at $(0, z'_G)$ is given by;

$$\left[m_{kj}\right] = \begin{bmatrix} m & 0 & -mz'_G \\ 0 & m & 0 \\ -mz'_G & 0 & I_{44} \end{bmatrix} \tag{4.5.2}$$

For sections with lateral symmetry it also follows that the added mass and damping coefficient matrices are;

$$\left[a_{kj}(\omega)\right] = \begin{bmatrix} a_{22} & 0 & a_{24} \\ 0 & a_{33} & 0 \\ a_{42} & 0 & a_{44} \end{bmatrix} \tag{4.6.2}$$

$$\left[b_{kj}(\omega)\right] = \begin{bmatrix} b_{22} & 0 & b_{24} \\ 0 & b_{33} & 0 \\ b_{42} & 0 & b_{44} \end{bmatrix} \tag{4.6.3}$$

These added-mass and damping coefficients are dependent of the encounter frequency and the section shape. The corresponding forces are also dependent of the unsteady motion amplitudes.

For sections with symmetry about the z-axis, and oscillating in the free-surface, the only non zero linear hydrostatic restoring coefficients are c_{33}, and c_{44}.

Substituting the mass matrix (4.5.2), the added mass and damping coefficients (4.6.2) and (4.6.3), and the restoring coefficients into the equations of motion (4.6.1), we find that for sections with lateral symmetry the three equations of motion, corresponding respectively to sway, heave, and roll, are;

$$\begin{cases}(m+a_{22})\ddot{\xi}_2+b_{22}\dot{\xi}_2+(a_{24}-mz'_G)\ddot{\xi}_4+b_{24}\dot{\xi}_4=f_2^E\\(m+a_{33})\ddot{\xi}_3+b_{33}\dot{\xi}_3+c_{33}\xi_3=f_3^E\\(a_{42}-mz'_G)\ddot{\xi}_2+b_{42}\dot{\xi}_2+(I_{44}+a_{44})\ddot{\xi}_4+b_{44}\dot{\xi}_4+c_{44}\xi_4=f_4^E\end{cases} \qquad (4.6.4)$$

The first and third equations are coupled through the body-inertia and radiation forces. The heave equation is independent of sway and roll motions.

Now a new set of equations, equivalent to (4.1.1) and (4.1.2), will be introduced to describe the sinusoidal exciting forces and motions;

$$f_k^E(t)=\left(f_k^E\right)^C\cos\omega t+\left(f_k^E\right)^S\sin\omega t \quad , \quad k=2,3,4 \qquad (4.6.5)$$

$$\xi_j(t)=\xi_j^C\cos\omega t+\xi_j^S\sin\omega t \quad , \quad j=2,3,4 \qquad (4.6.6)$$

$$\dot{\xi}_j(t)=-\omega\xi_j^C\sin\omega t+\omega\xi_j^S\cos\omega t \quad , \quad j=2,3,4 \qquad (4.6.7)$$

$$\ddot{\xi}_j(t)=-\omega^2\xi_j^C\cos\omega t-\omega^2\xi_j^S\sin\omega t \quad , \quad j=2,3,4 \qquad (4.6.8)$$

Where $\left(f_k^E\right)^C$ and ξ_j^C are respectively the amplitudes of the cosine parts of the exciting force in k-direction and motion in j-mode. The same follows for the sine parts.

Introducing these relations in (4.6.4), and separating the sine and cosine terms, the equations of motion become;

Sway Motion

$$\begin{cases}-\omega^2(m+a_{22})\xi_2^C+\omega b_{22}\xi_2^S-\omega^2(a_{24}-mz'_G)\xi_4^C+\omega b_{24}\xi_4^S=f_2^C\\-\omega^2(m+a_{22})\xi_2^S-\omega b_{22}\xi_2^C-\omega^2(a_{24}-mz'_G)\xi_4^S-\omega b_{24}\xi_4^C=f_2^S\end{cases} \qquad (4.6.9)$$

Roll Motion

$$\begin{cases} -\omega^2(a_{42} - mz'_G)\xi_2^C + \omega b_{42}\xi_2^S + \left[c_{44} - \omega^2(I_{44} + a_{44})\right]\xi_4^C + \omega b^*_{44}\xi_4^S = f_4^C \\ -\omega^2(a_{42} - mz'_G)\xi_2^S - \omega b_{42}\xi_2^C + \left[c_{44} - \omega^2(I_{44} + a_{44})\right]\xi_4^S - \omega b^*_{44}\xi_4^C = f_4^S \end{cases} \quad (4.6.10)$$

Heave Motion

$$\begin{cases} \left[c_{33} - \omega^2(m + a_{33})\right]\xi_3^C + \omega b_{33}\xi_3^S = f_3^C \\ \left[c_{33} - \omega^2(m + a_{33})\right]\xi_3^S - \omega b_{33}\xi_3^C = f_3^S \end{cases} \quad (4.6.11)$$

In the roll motion equations the wave damping coefficient was substituted by the equivalent damping coefficient which contains the viscous effects due to skin friction and eddy eddy damping. A procedure to evaluate these two viscous components is presented in Apendix-A.

Solving these very simple linear algebraic equations, we obtain the cosine and sine parts, ξ_j^C and ξ_j^S , $j = 2,3,4$. Then the real amplitudes of the motions, ξ_j^a, and the corresponding phase angles, 'θ_j', are;

$$\xi_j^a = \sqrt{\left(\xi_j^C\right)^2 + \left(\xi_j^S\right)^2} \quad , \quad j = 2,3,4 \quad (4.6.12)$$

$$\theta_j = tg^{-1}\left(\frac{\xi_j^S}{\xi_j^C}\right) \quad , \quad j = 2,3,4 \quad (4.6.13)$$

Finally the motions are given either by;

$$\xi_j(t) = \xi_j^C \cos\omega t + \xi_j^S \sin\omega t \quad , \quad j = 2,3,4 \quad (4.6.14)$$

or by;

$$\xi_j(t) = \xi_j^a \sin\left(\omega t + \theta_j\right) \quad , \quad j = 2,3,4 \quad (4.6.15)$$

This frequency-domain solution have some advantages and limitations, which are discussed for more general case of ship motions in Section-7.6.

5. TIME-DOMAIN SOLUTION OF THE CYLINDER MOTION PROBLEM

5.1 - Introduction

In the Chapter-4 the cylinder motion problem has been solved assuming that the exciting forces were sinusoidal in time, and the radiation forces were proportional to frequency dependent coefficients. Thus the model is appropriate only if the motion is strictly sinusoidal in time. In the present chapter we will present a method valid whatever is the nature of the exciting forces (as long as they result in small motions), and where some non-linearities can be introduced.

The cylinder motion problem will be solved in the time-domain, which means that the differential motion equations instead of being solved analytically, are solved numerically with a time-integration procedure and the solution will be built time step by time step. For implementing this method all the forces expressed in the motion equations must be represented in the time-domain.

This causes no major difficulty so far as the evaluation of the exciting and restoring forces are concern, since these forces do not have time dependency of the previous history of the fluid motion.

However the radiation forces behave in a different manner. The existence of radiated waves implies a complicated time dependence of the fluid motion and hence the resulting pressure forces. Waves generated by the body at time 't' will persist, in principle, for an infinite time thereafter, as well as the associated pressure force on the body surface. This situation is analogous to the case of a stone falling in still water, where we can observe waves moving away from the incident point for a very long time. If the fluid was not viscous, the waves would appear forever. This problem can be described mathematically by a convolution integral, with the fluid motion and pressure force at a given time dependent on the previous history of the motion. The convolution integral formulation is especially derived to calculate directly the motion response of the cylinder to non-sinusoidal exciting forces, and the non-linear restoring forces which appear when the sides of the section are non-vertical and the motion amplitudes are large can be incorporated to the formulation. When applying this method to solve the large amplitude motions problem, one should not forget that all the linearized potential theory assumes small motions. Otherwise we may end solving a problem where the neglected terms in the linearized theory are of the

some order, or even have more importance than the terms we are trying to include here.

5.2 - Radiation Forces

The formulation deducted by Cummins (1962) will be used to represent the radiation forces in terms of unknown velocity potentials. The basic assumption is the linearity of the radiation forces. That is, if the body is given an impulsive displacement of any kind, it will have a certain response lasting much more than the duration of the impulse, since the perturbation in the surrounding water will remain after the impulse. If the body experience a succession of impulses, its response at any time is assumed to be the sum of its responses to the individual impulses, each response being calculated with an appropriate time lag from the instant of the corresponding impulse. These impulses can be considered to occur so close together that the impulsive responses are integrated instead of sum, and the total response will be represented by a convolution integral. The impulsive responses being referred to here are velocity potentials in the form of impulse response functions.

Therefore, instead of calculating these potentials, the radiation forces in time-domain will be related to the radiation forces in frequency-domain using Fourier transforms.

As explained in Section-3.1, under certain assumptions, the linearized radiation potential problem can be treated as an independent problem, neglecting the interferences with the incident and diffracted potentials. This way the problem consists of evaluating the forces, other than the hydrostatic forces, associated with oscillatory motion of the section in otherwise calm water.

Boundary Value Problem

Under the former assumptions, and given the conditions stated in Section-3.2, the boundary value problem for the section having arbitrary oscillatory motion on the free-surface, in otherwise calm water, is to evaluate the radiation potential on the section mean surface that satisfy the following conditions;

(L) The two-dimensional Laplace equation

$$\Phi^R_{yy} + \Phi^R_{zz} = 0 \qquad (5.2.1)$$

(F) The linearized free-surface boundary condition

$$\Phi^R_{tt} + g\Phi^R_z = 0 \quad , \text{ on } z=0 \qquad (5.2.2)$$

(K) The linearized body kinematic boundary

$$\frac{\partial \Phi^R_j}{\partial n} = \dot{\xi}_j n_j \quad , j = 2,3,4 \quad , \text{ on } S_0 \qquad (5.2.3)$$

(B) The bottom condition

$$\nabla \Phi^R \to 0 \quad , \text{ on } z \to -\infty \qquad (5.2.4)$$

(R) The radiation condition at infinite

$$\nabla \Phi^R \to 0 \quad , \text{ on } |y| \to \infty \qquad (5.2.5)$$

The last two conditions are valid since the disturbances generating the unsteady potentials are originated in the neighbourhood of the origin, and this is an initial value problem.

The radiation potential has been linearly decomposed into conponents related to each motion mode (see Section-3.1). It will be studied the consequences of an oscillatory motion in the arbitrary j-direction, j=2,3,4. The reference system has been defined in Section-3.2.

Let us assume that at an initial instant 't_0' the section is given an impulsive displacement '$\Delta\xi_j$' in the j-direction. The displacement can be considered to have a constant velocity 'V_j', during a small time interval 'Δt', with the motion terminating abruptly at the end of this time interval.

<u>During the impulse</u> $(t_0 \le t \le t_0 + \Delta t)$:

The impulsive displacement is given by;

$$\Delta\xi_j = V_j \Delta t \qquad (5.2.6)$$

During the impulse the flow will have a velocity potential proportional to the impulsive velocity of the section;

$$\phi_j^v = V_j \vartheta_j \tag{5.2.7}$$

Where 'ϑ_j' is a normalised potential for the impulsive flow.

The potential ϑ_j must satisfy the body boundary condition (5.2.3), and the kinematic boundary condition on the free-surface;

$$\frac{\partial \phi_j^v}{\partial n} = V_j \cdot n \tag{5.2.8}$$

$$\frac{\partial \zeta_j}{\partial t} = \frac{\partial \phi_j^v}{\partial z} \Leftrightarrow \frac{\Delta \zeta_j}{\Delta t} = \frac{\partial}{\partial z}\left(V_j \phi_j^v\right) \tag{5.2.9}$$

These terms represent the vertical velocity of the free-surface, and 'ζ_j' is the free-surface elevation. From this relation we obtain the impulsive displacement contribution to the free-surface elevation during Δt;

$$\Delta \zeta_j = \frac{\partial \vartheta_j}{\partial t} \Delta \xi_j \tag{5.2.10}$$

<u>After the impulse</u> $(t \geq t_0 + \Delta t)$:

The free-surface elevation produced by the impulsive displacement will dissipate as a radiated perturbation, and, after a long time, the fluid near the section will not feel the perturbation any more. The velocity potential of this decaying fluid motion is given by;

$$\phi_j^r(t) = \chi_j(t) \Delta \xi_j \tag{5.2.11}$$

Where '$\chi(t)$' is the velocity potential normalised by $\Delta \xi_j$, which must satisfy the <u>initial conditions</u> at the instant $t = t_0 + \Delta t$;

- At this instant the potential $\chi(t)$ is still zero

$$\chi_j = 0 \quad , \text{ at } t = t_0 + \Delta t \tag{5.2.12}$$

- There must be continuity on the free-surface elevation at this instant;

$$\Delta\zeta_j^- = \Delta\zeta_j^+ \tag{5.2.13}$$

Just at the end of the impulse the free-surface elevation is given by (5.2.10);

$$\Delta\zeta_j^- = \frac{\partial \vartheta_j}{\partial z}\Delta\xi_j \quad , \; t^- \to t_0 + \Delta t \tag{5.2.14}$$

In order to obtain $\Delta\zeta_j^+$ the linearized dynamic condition on the free-surface will be used;

$$\zeta = -\frac{1}{g}\frac{\partial \phi}{\partial t} \quad , \; \text{on } z = \zeta \tag{5.2.15}$$

Since we are evaluating the equation on $z = \zeta$, this condition can be deducted directly from the Bernoulli equation (3.1.3), by substituting the pressure term, 'p', by the atmospheric pressure, 'p_a'. The higher order terms are neglected.

Substituting the velocity potential due to the radiated waves in eq. (5.2.15) we obtain;

$$\Delta\zeta_j^+ = -\frac{1}{g}\frac{\partial}{\partial t}\left(\chi_j \Delta\xi_j\right) \quad , \; \text{as } t^+ \to t_0 + \Delta t \tag{5.2.16}$$

Thus the relation (5.2.13) becomes;

$$\frac{\partial \chi_j}{\partial t} = -g\frac{\partial \vartheta_j}{\partial z} \quad , \; \text{at } t = t_0 + \Delta t \tag{5.2.17}$$

After the impulse has finished, $(t \geq t_0 + \Delta t)$, the potential of the perturbation, '$\chi(t)$', must satisfy the linear free-surface condition, and the kinematic condition on the body surface, being the section velocity equal to zero after the impulse;

$$\frac{\partial^2 \chi_j}{\partial t^2} + g\frac{\partial \chi_j}{\partial z} = 0 \quad , \; \text{on } z = 0 \tag{5.2.18}$$

$$\frac{\partial \chi_j}{\partial n} = 0 \qquad , \text{ on } S_0 \tag{5.2.19}$$

General motion in j-mode

Let us assume now that the body has a general motion in j-mode, $\xi_j(t)$. This motion can be represented as a succession of impulsive displacements, $\Delta\xi_{jn}(t)$, as represented in figure-5.1.

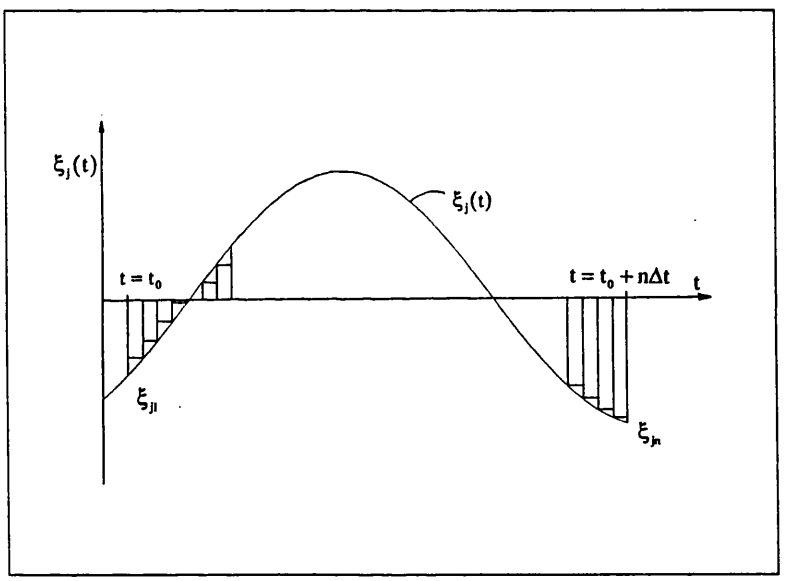

Figure 5.1 Discretized Body Motion in j-mode

Assuming that the radiation potential is linear, the response velocity potential associated with the general motion of the body, $\xi_j(t)$, can be represented as the sum of the response potentials to the individual impulses, each response being calculated with an appropriate time lag from the instant of the corresponding impulse. Thus the radiation potential at time 't' is given by;

$$\Phi_j^R = V_{jn}\vartheta_j + \sum_{i=1}^{n} \chi_j\left[t_0 + (n-i)\Delta t\right] V_{ji}\Delta t \tag{5.2.20}$$

When the time interval approaches the zero value $(\Delta t \to 0)$, the summation given by eq. (5.2.20) can be expressed as an integral equation. Hence the radiation potential due to oscillations in j-mode becomes;

$$\Phi_j^R(t) = \dot{\xi}_j(t)\vartheta_j + \int_{-\infty}^{t} \chi_j(t-\tau)\ddot{\xi}_j(\tau)d\tau \qquad (5.2.21)$$

This radiation potential must satisfy the free-surface condition given in eq. (5.2.2). First eq. (5.2.20) is introduced in eq. (5.2.2), then applying the conditions given in eqs. (5.2.12), (5.2.17), and (5.2.18) the following equation can be obtained;

$$\left(\Phi_{tt}^R\right)_j + g\left(\Phi_z^R\right)_j = \frac{\partial^2 \dot{\xi}_j}{\partial t^2}\vartheta_j$$

The radiation potential given in eq. (5.2.21) should satisfy the linear free-surface condition. This requires;

$$\vartheta_j = 0 \quad , \text{ on } z = 0 \qquad (5.2.22)$$

This is the free-surface condition appropriate for the problem of a body oscillating at high frequencies (see Section-4.2.2), so ϑ_j represents the velocity potential related with the body oscillating in j-mode with infinite frequency oscillation with a unit amplitude. An important characteristic of ϑ_j is that it represents the instantaneous fluid response to the motion of the body. If the body is moving and suddenly stops, the fluid motion associated with the ϑ_j potential stops.

The integral term in eq. (5.2.21) represents the effects of the free-surface, which last long after the occurrence of the impulses. Furthermore χ_j satisfies the free-surface condition given in eq. (5.2.18) and the kinematic body condition given in eq. (5.2.19). Thus this term represents the dispersion of waves caused by the impulse. It also follows that '$\chi_j(t-\tau)$' is proportional to a contribution for the free-surface elevation at time 't', from one impulsive displacement that occurs 'τ seconds' before. In the same way, it is proportional to the contribution for the

radiation potential at time 't', from one impulsive displacement that occurs 'τ seconds' before.

In the present work the boundary value problem will not be solved directly in time-domain, instead the radiation forces will be evaluated in terms of the unknown potentials (ϑ_j and χ_j), and then will be related to the radiation forces as formulated in the frequency-domain problem, for which the boundary value problem has been solved (see Section-4.2).

Radiation Forces

Once the radiation potentials are known, the pressure on the section surface is obtained by the use of Bernoulli's equation. The integration of the pressure over the body surface gives the radiation forces. The calculation procedure to obtain the radiation forces have been derived in Chapter-3, and the equation for the radiation forces is;

$$f^R(t) = -\rho \iint_{S_0} \left(\frac{\partial \Phi^R(t)}{\partial t} \tilde{n} \right) ds \qquad (3.2.7)$$

If we decompose the force in the principal three directions of the reference system, and the potential in contributions from each mode motion, the radiation force in k-direction due to a motion in j-direction is;

$$f^R_{kj}(t) = -\rho \iint_{S_0} \left(\frac{\partial \Phi^R_j(t)}{\partial t} n_k \right) ds \qquad , \quad k,j = 2,3,4 \qquad (5.2.23)$$

Where the time derivative of eq. (5.2.21) is;

$$\frac{\partial \Phi^R_j(t)}{\partial t} = \ddot{\xi}_j(t)\vartheta_j + \int_{-\infty}^{t} \frac{\partial}{\partial t}\left[\chi_j(t-\tau)\right]\dot{\xi}_j(\tau)d\tau \qquad , \quad j = 2,3,4 \qquad (5.2.24)$$

Introducing this relation in the expression for the radiation force given in eq. (5.2.23) it follows;

$$F_{kj}^{R}(t) = -\ddot{\xi}_j(t)a_{kj}^{\infty} - \int_{-\infty}^{t}\left\{K_{kj}(t-\tau)\dot{\xi}_j(t)\right\}d\tau \quad , \; k,j = 2,3,4 \tag{5.2.25}$$

Where 'a_{kj}^{∞}' is;

$$a_{kj}^{\infty} = \rho\iint_{S_0}\left\{\vartheta_j n_k\right\}ds \quad , \; k,j = 2,3,4 \tag{5.2.26}$$

In accordance with eq. (5.2.22) and the definition of added mass given in Section-4.2.2, a_{kj}^{∞} represents the infinite frequency added mass coefficient, which contributes to the forces in k-direction due to unsteady motion in j-mode.

The term '$K_{kj}(\tau)$' will be named the retardation function, and is given by;

$$K_{kj}(\tau) = \rho\iint_{S_0}\left(\frac{\partial\chi_j(\tau)}{\partial t}n_k\right)ds \quad , \; k,j = 2,3,4 \tag{5.2.27}$$

This coefficient represents the memory effects due to the radiated waves.

It can be stated that the second term in eq. (5.2.25) contains some or all of the damping force of the system. It is interesting to see that $K_{kj}(\tau)$ is similar to the impulse response function of any stable linear system.

It must be stressed that the quantities a_{kj}^{∞} and $K_{kj}(t)$ do not depend on the past history of the unsteady motions. This means that they only need to be calculated once for a given section, and then the radiation forces can be found for any arbitrary motion by the simple evaluation of a convolution integral and a product.

Finally the radiation force in k-direction is given by;

$$f_k^R(t) = \sum_{j=2}^{4} f_{kj}^R(t) \quad , \; k = 2,3,4$$

Final Remarks

The equations obtained for the radiation forces do not have coefficients dependent of the frequency, thus they are valid to evaluate the radiation forces associated with non-sinusoidal motions, like for example irregular motions. The only condition necessary to apply this method is the linearity of the radiation forces, and this means that the unsteady motions must be of small amplitude. So far in this thesis no procedure to evaluate the velocity potentials χ_{kj} has been developed, because instead of evaluating them the true radiation forces in time-domain will be related to the radiation forces of all of the frequency-domain range. This will be done in Section-5.6.

5.3 - Exciting Forces

Exciting Forces in Sinusoidal Waves

As explained in Section-3.1, under certain assumptions, the linearized exciting potential problem can be treated as an independent problem, neglecting the interferences with the radiation potential. In addition, noting that the formulated exciting forces problem consists of the body fixed at its mean position and linear waves acting on it, we can conclude that the linear exciting forces are not affected by the previous history of the fluid motion. The frequency-domain formulation deducted in Section-4.3 can be used to evaluate the time-domain exciting forces.

The time-domain sinusoidal exciting forces are given by;

$$f_k^E(t) = \left(f_k^E\right)^C \cos\omega t + \left(f_k^E\right)^S \sin\omega t \quad , \; k = 2,3,4 \tag{4.3.21}$$

Exciting Forces in Irregular Waves

As concluded in Section-4.3 the linear exciting forces, due to sinusoidal waves, are linearly proportional to the wave amplitude. Thus the superposition principle can be applied to obtain the exciting forces arising from irregular waves.

We will use a statistical description of the sea, assuming that the irregular water motion can be described as sum of many simple sinusoidal waves, each one described separately by the linear gravity-wave theory. Following St. Denis and Pierson (1953) the statistical nature of the sea can be expressed by allowing the phases of these components to take random values;

$$\zeta(t) = \sum_{n=1}^{\infty} \zeta_n^a \cos(\omega_{0n} t + \varepsilon_n) \tag{5.3.1}$$

Where '$\zeta(t)$' is the irregular free-surface elevation, 'ζ_n^a', 'ω_{0n}', and 'ε_n' are respectively the amplitude, the frequency, and the random phase of the sinusoidal component 'n'.

There is one practical way to take into account the irregularity of the waves, and that is to determine the total energy. This is obtained by adding together the energies of all of the small, sinusoidal waves that produce the seaway by their superposition. The severity of the seaway is then measured by the total energy of all the waves present. Thus any given sea state can be described by the energy distribution versus the frequency range. The frequency distribution of energy is called the "energy spectrum" for a particular seaway.

The energy of a sinusoidal wave is proportional to $1/2\zeta_n^2$. After superposing these values for every sinusoidal wave component, the frequency distribution of the "wave spectrum" is obtained, and the ordinates are represented by '$S_\zeta(\omega_0)$', which is called the "spectral density of wave energy". A picture with a general form of a wave spectrum is presented in figure-5.2.

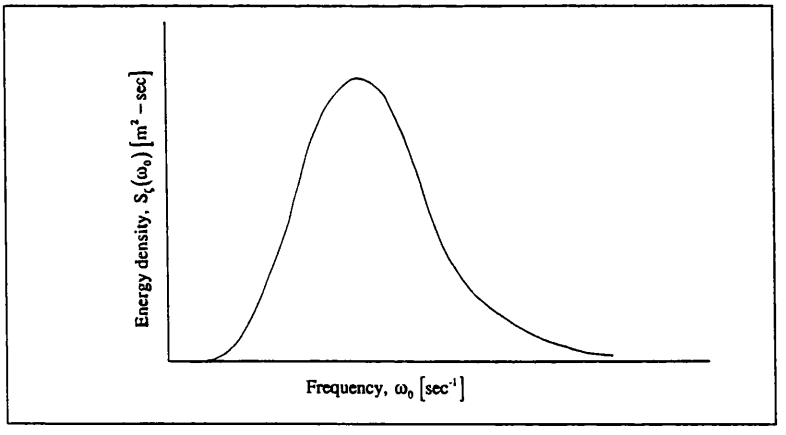

Figure 5.2 Wave Spectrum

If the wave spectrum is discritized in a finite number, 'N', of frequency intervals '$d\omega_0$', the relation between the free-surface elevation and the density of wave energy is given by;

$$\frac{(\zeta_n^a)^2}{2} = S_\zeta(\omega_{0n})d\omega_0 \qquad (5.3.2)$$

So from the wave spectrum we can obtain the sinusoidal components which can represent it;

$$\zeta_n^a = \sqrt{2S_\zeta(\omega_{0n})d\omega_0} \qquad (5.3.3)$$

Now by applying the superposition principle, the linear exciting forces resulting from an irregular seaway can be evaluated as described in the following;

1. Given the characteristics of the sea way, one of the known wave spectrums can be calculated.

2. The wave spectrum is decomposed in a large number of sinusoidal components (for example 100) using equation (5.3.2). Each component will be given a random phase;

$$\zeta_n(t) = \zeta_n^a \cos(\omega_n t + \varepsilon_n) \qquad (5.3.4)$$

3. Then the exciting forces, '$\hat{f}^E(t)$', for a unit wave amplitude at each sinusoidal wave frequency, are calculated using the procedure described in Section-4.3. The variation of the exciting forces with the wave frequency is a regular one (except for particular irregular frequencies), so it is enough to calculate about 15 or 20 components distributed over the frequency range, and the other components can be obtained by interpolation.

4. Finally the linear superposition assumption can be used to evaluate the exciting forces due to the irregular seaway;

$$f^E(t) = \sum_{n=1}^{N}\left\{\zeta_n^a \hat{f}^E(t)\cos(\omega_{0n} + \varepsilon_n)\right\} \qquad (5.3.5)$$

$$f^E(t) = \sum_{n=1}^{N}\left\{\left(\sqrt{2S_\zeta(\omega_{0n})d\omega}\right)\hat{f}^E(t)\cos(\omega_{0n}t + \varepsilon_n)\right\} \qquad (5.3.6)$$

And the exciting force in each principal direction of the reference system is;

$$f_k^E(t) = \sum_{n=1}^{N} \left\{ \left(\sqrt{2S_\zeta(\omega_{0n})d\omega} \right) \hat{f}_k^E(t) \cos(\omega_{0n} t + \varepsilon_n) \right\} \qquad (5.3.7)$$

Where $\hat{f}_k^E(t)$ is given by equation (4.3.17).

5.4 - Restoring Forces

The restoring forces (and moments) can be calculated adding the effects of the weight and the hydrostatic forces (or moments) .

Hydrostatic Forces

The hydrostatic forces are the result of hydrostatic pressure action upon the body surface. The expression to evaluate these forces have been deducted in Chapter-3, and is;

$$f^H = \iint_S (p_h \tilde{n}) ds \tag{5.4.1}$$

or separating the forces from the moments about the origin, we redefine;

$$f^H = \iint_S (p_h n) ds \tag{5.4.2}$$

$$m^H = \iint_S p_h (r \times n) ds \tag{5.4.3}$$

where 'S' is the instantaneous wetted surface, '$p_h = -\rho g z$' is the hydrostatic pressure, 'n' is the outer unit normal vector of S, and 'r' is the vector position of any point of the section surface.

In order to evaluate the surface integral in eq. (5.4.1) the divergence theorem of Gauss is used. The use of the Gauss theorem, and all the derivations are explained in detail in the Section-8.4.

After combining the weight with the hydrostatic forces, the resultant restoring forces are obtained as follows (see Section-8.4);

$$f_2^B = -\rho g \iint_{S_{wl}} (z n_2^{wl}) ds \tag{5.4.4}$$

$$f_3^B(t) = \rho g V_{wl} - \rho g \iint_{S_{wl}} (z n_3^{wl}) ds - mg \tag{5.4.5}$$

$$f_4^B(t) = \rho g V_{wl} y_B - \rho g \iint_{S_{wl}} z(y n_3^{wl} - z n_2^{wl}) ds - y_G mg \tag{5.4.6}$$

where 'V_{wl}' is the instantaneous immersed volume, 'S_{wl}' is defined by the intersection of the free-surface elevation with the body, 'n^{wl}' is the outward unit vector normal to S_{wl}, 'm' is the mass of the section, 'y_B' is the y-co-ordinate of the centre of the immersed volume, and 'y_G' is the y-co-ordinate of the mass gravity centre.

To evaluate the hydrostatic terms it is necessary to calculate the intersection of the free-surface with the body. Thus both the points on the surface of the body and the free-surface elevation must be represented on the fixed reference system. Assuming that the body rotates about the gravity centre, the transformation of the co-ordinates of the body surface points between moving reference system and the fixed reference system is given by;

$$\begin{aligned} y &= \xi_2 + y' \cos\xi_4 - (z' - z'_G) \sin\xi_4 \\ z &= \xi_3 + y' \sin\xi_4 + (z' - z'_G) \cos\xi_4 + z'_G \end{aligned} \tag{5.4.7}$$

where z'_G is the z-co-ordinate of the gravity centre on the fixed reference system.

The free-surface elevation on the neighbourhood of the section is given by the contribution of the incident wave, difracted wave, and radiated waves associated with the three modes of motion, respectively ζ^I, ζ^D, and ζ_j^R. In the linear potential theory the unsteady potential is linearly decomposed, thus the correspondent free-surface elevation is;

$$\zeta(t) = \zeta^I(t) + \zeta^D(t) + \sum_{j=2}^{4} \zeta_j^R(t) \tag{5.4.8}$$

The incident wave contribution given the incident potential used in this thesis is deducted in the Section-8.4 for the three-dimensional case. The simplified two-dimensional result is readily obtained;

$$\zeta^I(y,t) = \zeta^a\{\cos(k_0 y)\cos(\omega t) + \sin(k_0 y)\sin(\omega t)\} \qquad (5.4.9)$$

where ζ^a is the incident wave amplitude.

Also in Section-8.4 is deducted the expression for the free-surface elevation associated with a general unsteady potential. The correspondent two-dimensional result is;

$$\zeta(y,t) = -\frac{1}{g}\frac{\partial \Phi}{\partial t} \quad , \quad \text{on} \quad z=0 \qquad (5.4.10)$$

In Section-4.2 and Section-4.3 methods were presented to solve the boundary value radiation and diffracted problems and obtain the correspondent potentials in the surface of the body. The same methods can be used to evaluate the radiation and diffracted potentials at the mean level free-surface, $z=0$. Substituting the results in equation (5.4.10) the frequency domain free-surface radiated and diffracted wave elevations are obtained. Since the diffraction potential do not have time dependence the frequency domain diffracted wave can be used in the time domain solution. However the radiated waves, like the damping forces, have time dependence of the past history of the fluid motion, thus the free-surface elevation due to the radiation potential must be evaluated in the time-domain. Here again an impulse response function is used, which is the free-surface elevation due to an unit amplitude motion. This is obtained from the Fourie transform of the frequency domain results;

$$Kh_j(t) = \frac{2}{\pi}\int_0^\infty \zeta^R_{j_{FD}}(\omega)\cos(\omega t)d\omega \qquad (5.4.11)$$

where $Kh_j(t)$ is the free-surface elevation retardation function, and $\zeta^R_{j_{FD}}(\omega)$ is the frequency domain amplitude of the radiated wave due to an unit amplitude sinusoidal motion in the j-mode.

Applying the convolution integral the time domain free-surface elevation due to an arbitrary motion in the j-mode is;

$$\zeta^R_j(t) = \int_{-\infty}^{t} Kh_j(t-\tau)\xi_j(\tau)d\tau \qquad (5.4.12)$$

Finally it is assumed that the intersection of the free-surface with the body can be represented by a plane, which is fairly correct in the frequency range of interest.

5.5 - Body-Mass Force

This section is exactly identical to Section-4.5, however it was decided to repeat here because it may help the reading of the following text, and it also presents just final equations obtained from the fully formulation given in Section-7.5.

In this section we are concerned with the internal forces, proportional to the sectional inertia characteristics, and motion accelerations. These are the inertial forces and moment, given by the rate of change of linear momentum and angular momentum of the body.

The inertial force in k-direction due to an acceleration in j-direction is given by;

$$f_{kj}^{M} = m_{kj}\ddot{\xi}_j \qquad , \quad k,j = 2,3,4 \tag{5.5.1}$$

Where 'm_{kj}' are the coefficients from the mass matrix. For the present case of two-dimensional motion, if the section has symmetry with respect to the z'-axis and the gravity centre is located at $(0, z'_G)$, the mass matrix is;

$$\left[m_{kj}\right] = \begin{bmatrix} m & 0 & -mz'_G \\ 0 & m & 0 \\ -mz'_G & 0 & I_{44} \end{bmatrix} \tag{5.5.2}$$

Where the moment of inertia for the roll mode is given by;

$$I_{44} = \iiint_{V_B} \rho_B \left(y'^2 + z'^2\right) dv \tag{5.5.3}$$

The vertical co-ordinate of gravity centre is;

$$z'_G = \frac{1}{m} \iiint_{V_B} (\rho_B z') dv \tag{5.5.4}$$

where the co-ordinates are defined in the reference system fixed on the section $X' = (y', z')$.

5.6 - Motion Equations and Solution

Equations of Motion

In the previous Sections of this Chapter the several components of the total pressure force, as well as the forces associated to the mass of the cylinder have been discussed. Now the equations of motion for free oscillations of the cylinder in sinusoidal or irregular waves will be derived by equating the external pressure forces acting upon the body surface, with the internal forces due to gravity and internal forces associated with acceleration of the body mass. The cylinder will be assumed as an unrestrained body, and in state of equilibrium when in calm water.

Re-writing the three component vectors representing the various forces in each direction we obtain;

$$f_k^E(t) \quad , \quad k = 2,3,4$$

$$f_k^M(t) = \sum_{j=2}^{4} m_{kj}\ddot{\xi}_j(t) \quad , \quad k = 2,3,4$$

$$f_k^R(t) = -\sum_{j=2}^{4}\left\{\ddot{\xi}_j(t)a_{kj}^{\infty} + \int_{-\infty}^{t}\left[K_{kj}(t-\tau)\dot{\xi}_j(t)\right]d\tau\right\} \quad , \quad k = 2,3,4$$

$$f_k^B(t) \quad , \quad k = 2,3,4$$

The gravitional forces are already included in the restoring force terms.

The equations of motion can be obtained by combining the exciting forces with reaction forces within Newton's Second Law in usual way;

$$\sum_{j=2}^{4}\left\{\left(m_{kj}+a_{kj}^{\infty}\right)\ddot{\xi}_j(t)+\int_{-\infty}^{t}\left[K_{kj}(t-\tau)\dot{\xi}_j(\tau)\right]d\tau\right\}+f_k^B(t)=f_k^E(t) \qquad (5.6.1)$$

$$, \; k=2,3,4$$

Where 'a_{kj}^{∞}' is the infinite frequency added mass coefficient, and 'K_{kj}' are the retardation functions given by;

$$K_{kj}(\tau)=\rho\iint_{S_0}\left(\frac{\partial\chi_j(\tau)}{\partial t}n_k\right)ds \qquad , \; k,j=2,3,4 \qquad (5.2.27)$$

Relation with the Frequency-Domain Solution

As stated in the beginning of this Chapter, the problem will not be solved directly in the time domain, which means that the potentials χ_{kj} are not going to be calculated. Instead, following Ogilvie (1964), the equations of motion in time-domain and frequency-domain will be related using Fourier analysis. Then the inverse Fourier transform is used to obtain the retardation functions in terms of the damping coefficients corresponding to the whole frequency range.

The following relation will be used;

$$\int_{-\infty}^{t}\left\{K_{kj}(t-\tau)\dot{\xi}_j(\tau)\right\}d\tau=\int_{0}^{\infty}\left\{K_{kj}(\tau)\dot{\xi}_j(t-\tau)\right\}d\tau$$

Before applying the Fourier transforms equations (5.6.1) will be reduced to a suitable form. The restoring force can be decomposed in two parts;

$$f_k^B(t)=\sum_{j=2}^{4}c_{kj}\xi_j(t)+\delta_k^B(t) \qquad , \; k=2,3,4 \qquad (5.6.2)$$

The first term is the conventional linear restoring force, and the restoring coefficients, c_{kj}, are given by (4.4.2) and (4.4.3). The second term is the contribution due to non-linear effects (see Section-5.4.2).

Since the exciting force can be of any form, the non-linear contribution to the restoring force will be placed on the right side of equation (5.6.1), resulting;

$$\sum_{j=2}^{4}\left\{\left(m_{kj}+a_{kj}^{\infty}\right)\ddot{\xi}_j(t)+\int_0^{\infty}\left[K_{kj}(\tau)\dot{\xi}_j(t-\tau)\right]d\tau+c_{kj}\xi_j(t)\right\}=f_k^E(t)-\delta_k^B(t) \qquad (5.6.3)$$

$$, \; k=2,3,4$$

Ogilvie starts by assuming the unsteady motion to be transient, such that motion die out after some time and the body approaches the static equilibrium position (at least asymptotically). This makes the use of conventional Fourier transforms possible. Ogilvie also proved that if the ship is stable, the same result is valid for non-transient motions.

Thus taking Fourier transforms of eq. (6.5.3) we can obtain;

$$\sum_{j=2}^{4}\left[-\omega^2\left(m_{kj}+a_{kj}^{\infty}\right)+i\omega\Im\{K_{kj}\}+c_{kj}\right]\Im\{\xi_j\}=\Im\{f_k^E-\delta_k^B\} \qquad (5.6.4)$$

$$, \; k=2,3,4$$

Where the Fourier transform of '$f(t)$' is defined as;

$$\Im\{f\}=\int_{-\infty}^{\infty}e^{-i\omega t}f(t)dt \qquad (5.6.5)$$

If $f(t)=0$ for $t<0$, then;

$$\Im\{f\}=\Im_c\{f\}-i\Im_s\{f\} \qquad (5.6.6)$$

Where $\Im_c\{f\}$ and $\Im_s\{f\}$ are respectively the Fourier cosine and Fourier sine transforms, given by;

$$\Im_c\{f\}=\int_0^{\infty}f(t)\cos(\omega t)dt \qquad (5.6.7)$$

$$\Im_s\{f\} = \int_0^\infty f(t)\sin(\omega t)dt \tag{5.6.8}$$

Since the retardation functions, K_{kj}, satisfies the former condition, eq. (5.6.4) can be written as;

$$\sum_{j=2}^{4}\left[-\omega^2\left(m_{kj} + a_{kj}^{\infty} - \frac{1}{\omega}\Im_s\{K_{kj}\}\right) + i\omega\Im_c\{K_{kj}\} + c_{kj}\right]\Im\{\xi_j\} = \Im\{f_k^E - \delta_k^B\} \quad , k = 2,3,4 \tag{5.6.9}$$

These new equations represent one of the frequency components in which the general time-domain equations can be decomposed.

The equations of motion in frequency-domain, eq. (4.6.1), will be rewritten here, with different variables representing the motions and exciting forces just to distinguish them from the equivalent time-domain variables. The equations are;

$$\sum_{j=2}^{4}\left\{\left(m_{kj} + a_{kj}\right)\ddot{x}_j + b_{kj}\dot{x}_j + c_{kj}x_j\right\} = g_k^E \quad , \quad k = 2,3,4 \tag{5.6.10}$$

Where 'x_j' are the sinusoidal motions, and 'g_k^E' the sinusoidal exciting forces.

If we let the sinusoidal motion and exciting force be given by;

$$x_j(t) = e^{i\omega t}\Im\{\xi_j\} \tag{5.6.11}$$

$$g_k^E(t) = e^{i\omega t}\Im\{f_k^E - \delta_k^B\} \tag{5.6.12}$$

Then equation (5.6.10) will have the form;

$$\sum_{j=2}^{4}\left[-\omega^2\left(m_{kj} + a_{kj}\right) + i\omega b_{kj} + c_{kj}\right]\Im\{\xi_j\}e^{i\omega t} = \Im\{f_k^E - \delta_k^B\}e^{i\omega t} \quad , k = 2,3,4 \tag{5.6.13}$$

Now if in eq. (5.6.9) both sides are multiplied by $e^{i\omega t}$, we find that the Fourier transform of the motion equations in time-domain, eq. (5.6.9), is equivalent to the motion equations in the frequency-domain eq. (5.6.10).

As Ogilvie states, "This means that taking the Fourier transforms of the equations of motions (that is, of the true equations in time-domain) is equivalent to breaking the forcing function into its frequency components and determining the response to each of these components."

If the real and imaginary parts of equations (5.6.9) and (5.6.13) are combined together it results;

$$a_{kj}(\omega) = a_{kj}^{\infty} - \frac{1}{\omega}\int_0^{\infty}\{K_{kj}(t)\sin\omega t\}dt \qquad (5.6.14)$$

$$b_{kj}(\omega) = \int_0^{\infty}\{K_{kj}(t)\cos\omega t\}dt \qquad (5.6.15)$$

$$K_{kj}(t) = \frac{2}{\pi}\int\{b_{kj}(\omega)\cos\omega t\}d\omega$$

The inverse of the cosine transform is given by;

$$K_{ki}(t) = \frac{2}{\pi}\int_0^{\infty}\{b_{ki}(\omega)\cos\omega t\}d\omega \qquad (5.6.16)$$

$$K_{kj}(t) = \frac{2}{\pi}\int\{b_{kj}(\omega)\cos\omega t\}d\omega$$

Thus the retardation functions, $K_{kj}(t)$, can be obtained from the frequency domain damping coefficients, $b_{kj}(\omega)$, correspondent to the whole range of frequencies.

Resuming, the true equations of motion in time domain are given by;

$$\sum_{j=2}^{4}\left\{\left(m_{kj}+a_{kj}^{\infty}\right)\ddot{\xi}_j(t) + \int_{-\infty}^{t}\left[K_{kj}(t-\tau)\dot{\xi}_j(\tau)\right]d\tau\right\} + f_k^B(t) = f_k^E(t) \qquad (5.6.1)$$

$$, \; k = 2,3,4$$

$$K_{kj}(t) = \frac{2}{\pi}\int_0^{\infty}\{b_{kj}(\omega)\cos\omega t\}d\omega \qquad (5.6.16)$$

The equations (5.6.1) do not have frequency dependent coefficients, thus they are valid for non-sinusoidal motions. For the three motion modes considered in this study the motion equations become;

Sway Motion

$$\begin{aligned}(m+a_{22}^{\infty})\ddot{\xi}_2(t)+\int_{-\infty}^{t}\left[K_{22}(t-\tau)\dot{\xi}_2(\tau)\right]d\tau+(a_{24}^{\infty}-mz'_G)\ddot{\xi}_4(t)\\+\int_{-\infty}^{t}\left[K_{24}(t-\tau)\dot{\xi}_4(\tau)\right]d\tau-\rho g\iint_{S_{wl}}(zn_2^{wl})ds=f_2^E(t)\end{aligned}\qquad(5.6.17)$$

Heave Motion

$$\begin{aligned}(m+a_{33}^{\infty})\ddot{\xi}_3(t)+\int_{-\infty}^{t}\left[K_{33}(\tau)\dot{\xi}_3(t-\tau)\right]d\tau\\-\rho g\iint_{S_{wl}}(zn_3^{wl})ds+\rho gV_{wl}(t)-mg=f_3^E(t)\end{aligned}\qquad(5.6.18)$$

Roll Motion

$$(a_{24}^{\infty}-mz'_G)\ddot{\xi}_2(t)+\int_{-\infty}^{t}\left[K_{42}(t-\tau)\dot{\xi}_2(\tau)\right]d\tau+(I_{44}+a_{44})\ddot{\xi}_4(t)+b_{44}^{v}\dot{\xi}_4(t)+$$

$$\int_{-\infty}^{t}\left[K_{44}(t-\tau)\dot{\xi}_4(\tau)\right]d\tau-\rho g\iint_{S_{wl}}z(yn_3^{wl}-zn_2^{wl})ds+\rho gV_{wl}(t)y_B(t)-y_G(t)mg=f_4^E(t)$$

The term $b_{44}^{v}\dot{\xi}_4(t)$ represents the viscous effects due to the skin friction and eddy components of the roll damping, and the coefficient is determined according to the procedure described in Apendix-A.

These equations will be solved in time domain, by the numerical procedure known as "fourth order Runge Kutta method".

6. NUMERICAL AND EXPERIMENTAL RESULTS

6.1 - Computer Programs

One of the objectives of the research described in the thesis is to compare the predictions of the two-dimensional motion of floating cylinders with arbitrary cross section, and subjected to sinusoidal beam waves, by two different mathematical methods. The first method provides the well known linear frequency domain solution, which was explained in Section-4. The second method uses a time domain solution, and one non-linearity is introduced in the force restoring term. The latter was explained in Section-5. These mathematical models were implemented in two computer programs which will be briefly described now.

Frequency-Domain Program

The frequency domain equations which must be solved to obtain the sway, heave, and roll motions of the cylinder were derived in Section-4.6 and are;

Sway and Roll Motions

$$\begin{cases} -\omega^2(m+a_{22})\xi_2^C + \omega b_{22}\xi_2^S - \omega^2(a_{24}-mz'_G)\xi_4^C + \omega b_{24}\xi_4^S = f_2^C \\ -\omega^2(m+a_{22})\xi_2^S - \omega b_{22}\xi_2^C - \omega^2(a_{24}-mz'_G)\xi_4^S - \omega b_{24}\xi_4^C = f_2^S \\ -\omega^2(a_{42}-mz'_G)\xi_2^C + \omega b_{42}\xi_2^S + \left[c_{44}-\omega^2(I_{44}+a_{44})\right]\xi_4^C + \omega b^*_{44}\xi_4^S = f_4^C \\ -\omega^2(a_{42}-mz'_G)\xi_2^S - \omega b_{42}\xi_2^C + \left[c_{44}-\omega^2(I_{44}+a_{44})\right]\xi_4^S - \omega b^*_{44}\xi_4^C = f_4^S \end{cases}$$

Heave Motion

$$\begin{cases} \left[c_{33}-\omega^2(m+a_{33})\right]\xi_3^C + \omega b_{33}\xi_3^S = f_3^C \\ \left[c_{33}-\omega^2(m+a_{33})\right]\xi_3^S - \omega b_{33}\xi_3^C = f_3^S \end{cases}$$

The sway and roll motions are coupled, while the heave motion is independent. The equations presented are simple algebraic equations and once all coefficients are determined the solutions (ξ_j^C, ξ_j^S) are readily obtained.

- The added mass and damping coefficients (a_{kj}, b_{kj}) are computed using the "Frank Close Fit Method" described in Section-4.2. In addition the equivalent roll damping coefficient is obtained by adding together the wave making component with the friction and eddy components, $b_{44}^* = b_{44} + b_F + b_E$, as explained in Appendix-A. Since the viscous components are a function of the roll amplitude, the equivalent roll damping is estimated by an iterative process. The roll motion equation is solved several times, and in each iteration the viscous damping is evaluated using the roll amplitude obtained on the previous one. The process stops when the difference between two consecutive predictions is smaller than a pre-determined value. The convergence is obtained in a few cycles.

- The exciting forces due to sinusoidal incident waves are evaluated using also the "Frank Close Fit Method" according to Section-4.3.

- The restoring and inertia coefficients are computed using the expressions presented in Sections 4.4 and 4.5.

- Finally the equations are solved by the Gauss-Jordan method.

Time Domain Program

The time domain equations of motion were derived in Chapter-5, and are;

Sway and Roll Motions

$$\left(m + a_{22}^{\infty}\right)\ddot{\xi}_2(t) + \int_{-\infty}^{t}\left[K_{22}(t-\tau)\dot{\xi}_2(\tau)\right]d\tau + \left(a_{24}^{\infty} - mz'_G\right)\ddot{\xi}_4(t)$$

$$+ \int_{-\infty}^{t}\left[K_{24}(t-\tau)\dot{\xi}_4(\tau)\right]d\tau + f_2^B(t) = f_2^E(t)$$

$$\left(a_{24}^{\infty} - mz'_G\right)\ddot{\xi}_2(t) + \int_{-\infty}^{t}\left[K_{42}(t-\tau)\dot{\xi}_2(\tau)\right]d\tau + \left(I_{44} + a_{44}\right)\ddot{\xi}_4(t) + \int_{-\infty}^{t}\left[K_{44}(t-\tau)\dot{\xi}_4(\tau)\right]d\tau + f_4^B(t) = f_4^E(t)$$

Heave Motion

$$\left(m + a_{33}^{\infty}\right)\ddot{\xi}_3(t) + \int_{-\infty}^{t}\left[K_{33}(\tau)\dot{\xi}_3(t-\tau)\right]d\tau + f_3^B(t) = f_3^E(t)$$

These are integro-differential equations, with two non-linear terms both included in the restoring force term. Thus, given the nature of the equations, the solution must be numerical.

This is an initial value problem, since the characteristics of the motion are known at some starting point, t=0, and it is desired to find the same characteristics at some final point, or at some discrete list of points. The method chosen to solve the problem is the "fourth-order Runge-Kutta", which processes the integration of coupled first order ordinary differential equations, thus the first step is to reduce the second order differential equations presented above, to a set of equivalent first order differential equations;

$$\dot{y}_1 = \frac{\partial \xi_4}{\partial t} = \dot{\xi}_4(t)$$

$$\dot{y}_2 = \frac{\partial \dot{y}_1}{\partial t} = \ddot{\xi}_4(t) = \frac{\left(m + a_{22}^{\infty}\right)}{\left(m + a_{22}^{\infty}\right)\left(I_{44} + a_{44}^{\infty}\right) - \left(a_{42}^{\infty} - mz'_G\right)\left(a_{24}^{\infty} - mz'_G\right)} \times$$

$$\left\{ f_4^E(t) - f_4^B(t) - b_{44}^V(t)\dot{\xi}_4(t) - CV_{24}(t) - CV_{44}(t) - \frac{\left(a_{42}^{\infty} - mz'_G\right)}{\left(m + a_{22}^{\infty}\right)}\left[f_2^E(t) - CV_{24}(t) - CV_{22}(t)\right] \right\}$$

$$\dot{y}_3 = \frac{\partial \xi_2}{\partial t} = \dot{\xi}_2(t)$$

$$\dot{y}_4 = \frac{\partial \dot{y}_3}{\partial t} = \ddot{\xi}_2(t) = \frac{f_2^E(t) - f_2^B(t) - CV_{24}(t) - \left(a_{24}^{\infty} - mz'_G\right)\ddot{\xi}_4(t) - CV_{22}(t)}{\left(m + a_{22}^{\infty}\right)}$$

$$\dot{y}_5 = \frac{\partial \xi_3}{\partial t} = \dot{\xi}_3(t)$$

$$\dot{y}_6 = \frac{\partial \dot{y}_5}{\partial t} = \ddot{\xi}_3(t) = \frac{f_3(t) - CV_{33}(t) - f_3^B(t)}{\left(m + a_{33}^{\infty}\right)}$$

where the convolution integrals and restoring terms are given by;

$$CV_{kj}(t) = \int_{-\infty}^{t} \left\{K_{kj}(t-\tau)\dot{\xi}_j(\tau)\right\} d\tau$$

$$f_2^B(t) = -\rho g \iint_{S_{wl}} \left\{z(t) n_2^{wl}(t)\right\} ds$$

$$f_3^B(t) = -\rho g \iint_{S_{wl}} \left\{z(t) n_3^{wl}(t)\right\} ds + \rho g V_{wl}(t) - mg$$

$$f_4^B(t) = -\rho g \iint_{S_{wl}} z(t)\left\{y(t) n_3^{wl}(t) - z(t) n_2^{wl}(t)\right\} ds + \rho g V_{wl}(t) y_B(t) - y_G(t) mg$$

Basically the fourth-order Runge-Kutta method advances a solution from 't_n' to '$t_{n+1} = t_n + \Delta t$', using the derivative information in four points across the interval 'Δt'. Thus the method requires four evaluations of the right-hand side of the equations presented above per step. Then the derivative information is used to math a Taylor series expansion. The error obtained is of the order Δt^5.

The several terms in the equations of motion are evaluated as follows;

1. The body-inertia terms are known data to the problem.

2. The infinite frequency added masses, a_{kj}^{∞}, are computed using the method described in Section-4.2.

3. The exciting forces, $f_k^E(t)$, are calculated by the Frank Close Fit method presented in Section-4.3. These forces are computed four times during each time step at the instants required by the RK4 routine. The same follows for all the terms which are time dependent.

4. To compute the restoring forces several steps must be taken;

   - The exact free-surface elevation on both sides of the cylinder is calculated at every time instant, as well as the intersection of this surface with the body volume. The intersection is assumed to be a plane. The free surface elevation is given by five contributions; incident wave, diffracted wave, and radiated waves due to the three modes of motion. To the first two contributions the frequency-domain results are used, while the radiated waves are computed in the time-domain by a method similar to the one used to evaluate the damping forces which is explained further ahead.

   - The surface integral over the former intersection is evaluated.

   -The exact immersed volume of the body is calculated, as well as the centre of this volume.

   - Finally the hydrostatic and weight moments about the origin are calculated.

5. At last the convolution integrals, $CV_{kj}(t)$, are evaluated at each time instant. To do so the retardation functions, $K_{kj}(t)$, are computed before the routine which solves the motions equations is called for the first time. In fact these functions are computed by a different program since they are independent of the characteristics of the motion. This way, once we have got the retardation functions, several runs can be made with the motions program in different exciting conditions. The retardation functions are given by the cosine fourier transform of the damping coefficients corresponding to all the frequency domain range of frequencies;

$$K_{kj}(t) = \frac{2}{\pi}\int_{\hat{}}^{\infty}\{b_{kj}(\omega)\cos\omega t\}d\omega$$

$$K_{kj}(t) = \frac{2}{\pi}\int_{0}^{\infty}\{b_{kj}(\omega)\cos\omega t\}d\omega$$

   These functions are computed between the second '0' and the second '20', since for t>20 sec. the value of the functions is approximately zero, as is

shown by the graphics in Section-6.3. In practical terms this means that '$-\infty = -20$ sec.' in the convolution integrals, or in other words that the history of the fluid motion which occurred 20 seconds before is not affecting the actual fluid motion at the actual instant. The damping coefficients correspondent to all the frequency range are computed by the Frank Close Fit method described in Section-4.2.

In addition the roll motion equation has one term which represents the viscous effects due to the skin friction and eddy making. The method to obtain this components is presented in Appendix-A. Since the viscous component is a function of the roll amplitude, at each time instant, the program checks the local maximum and minimum roll angles which occurred during the previous period of the periodic motion. Then the absolute value of both angles are added together and divided by two. The result is used to estimate the viscous roll damping.

It was found that in certain cases the solution of the roll motion is very sensitive to sudden variations of the exciting force, thus an exponential ramp function was adopted to initiate the motion. This function increases in an exponential way the incident wave amplitude from a very small wave to the actual incident wave during a time equal to four times the period of the motion.

6.2 - Experiments

A series of experiments were carried out in order to validate the two-dimensional numerical models developed. In particular it was important to verify if the time-domain model was able to predict some non-linearities which the classical solution ignores. The experiments were conducted in the towing tank of the Hydrodynamic Laboratory at the University of Glasgow, which is 77m long, 4.6m wide, and 2.7m deep, and has a wave maker at one of the ends and an absorber beach at the other. The wave maker, which generates regular waves, is driven by an hydraulic pump controlled electronically by a micro-computer.

Characteristics of the Model

In order to obtain non-linear motions, even at moderate motion amplitudes, the model chosen was a cylinder with triangular cross section. A sketch of the model as well as the geometric characteristics is presented;

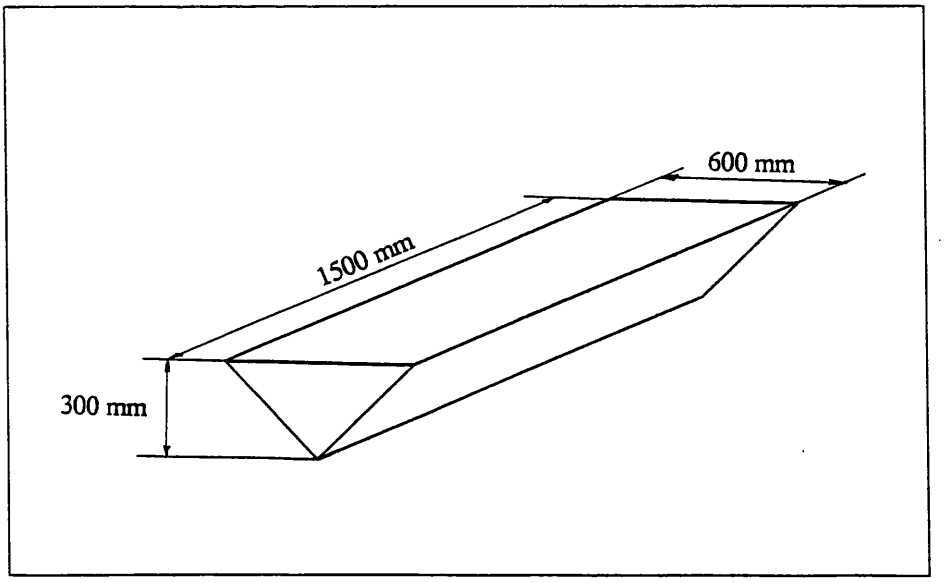

Figure-6.1 Test model

Length = 150,0 cm

Beam at the water line = 29,3 cm

Immersion = 14,65 cm

Weight of the hull = 11,9 Kg

Ballast = 20,25 Kg

Total weight = 32,15 Kg

Z_G = -4,0 cm (vertical position of the gravity centre, positive upwards)

$\overline{GM_T}$ = 8,9 cm (lateral metacentric height)

I_{44} = 0.79 Kg·m^2 (roll inertial moment about the gravity centre)

Preparation of the experiments

The model was ballasted in such a way that in the static equilibrium position it had zero heel and trim angles. Then the model was positioned laterally with respect to the length of the tank, at about 1/3 of the length from the wave maker, and moored to the sides of the tank by four lines with elastic at the ends. The mooring was prepared in a manner which allowed the body to undergo some swaying motions. The motions of the model were measured by a Selspot system, for which two light emitting diodes were mounted on each side of the model deck. The signals emitted by the diodes were received by one camera fixed on the side of the tank. In order to measure the incident wave heights three resistance type wave probes were mounted across the breadth of the tank between the wave maker and the model. If B is the breadth of the tank, the wave probes were installed at B/2, B/3, and B/4. These probes induce an electrical signal which intensity depends of its wetted height. Figure-6.2 shows the outline of the model in the tank prepared to be tested.

Before the experiments were carried out the wave probes and the Selspot system needed to be calibrated. This is a simple operation, however it must be precise or else the results may show large errors.

All the signals, detected by the wave probes and by the camera, were collected at a rate of 60 samples per second. Collections started when it was observed that the model was in steady oscillation. The signals were processed by specific

systems and then passed through the Data Collecting System by seven channels and recorded in a Macintosh micro-computer. The data could be immediately observed in the computer screen in the form of graphs. The specific channels recorded in the computer contained;

Channel-1 Horizontal motion of the port diode

Channel-2 Horizontal motion of the starboard diode

Channel-3 Vertical motion of the port diode

Channel-4 Vertical motion of the starboard diode

Channel-5 Free surface elevation collected by wave probe at B/2

Channel-6 Free surface elevation collected by wave probe at B/3

Channel-7 Free surface elevation collected by wave probe at B/4

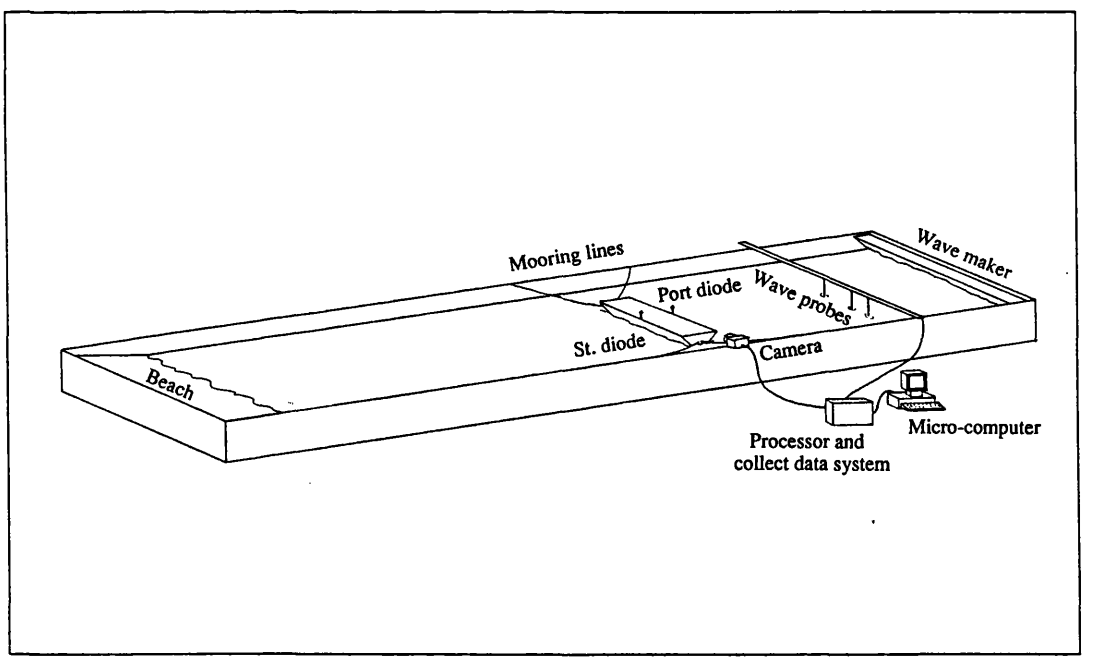

Figure-6.2 Layout of the facilities

Experiments

Three inclining tests were conducted in order to determine the lateral metacentric height and the vertical position of the gravity centre of the model. Basically a small weight was placed on the deck near the centre line and the

position recorded. Then the weight was transferred to the port side of the deck and again the model position recorded. Finally the weight was returned to the original centre line position. This procedure was repeated transferring for the starboard side.

Three extinction tests were carried out in order to obtain the natural period of roll.

Finally a series of experiments were conducted in order to measure the sway heave and roll motions of the body subjected to set of regular beam waves with different frequencies and heights. Seven frequencies were used from 3,77 rad/s to 8,80 rad/s, and six wave heights from 2,0 cm to 6,0 cm. Altogether 17 different cases were tested.

Results

The sway is calculated adding together the results recorded in channels 1 and 2 and dividing by 2.

The roll motion is computed using the results in channels 3 and 4 (C3, and C4) by the following expression;

$$\xi_4 = \sin^{-1}\left(\frac{C4 - C3}{dist}\right)$$

where 'dist' is the distance between the two diodes. One should not forget to use the sign convention adopted in the theoretical formulation.

The heave motion is calculated using the information in channels 3 and 4 by the following expression;

$$\xi_3 = \frac{C4 + C3}{2} - \overline{DG}(1 - \cos\xi_4)$$

where $\overline{DG}$ is the vertical distance between the diodes and the gravity centre in the fixed reference system.

6.3 - Results

Three types of final results of the cylinder two-dimensional motions, which consist of experimental results, linear frequency domain results, and non-linear time domain results are presented. While the experimental and frequency domain results can be presented readily, for the presentation of the time domain cases there are some intermediate steps which should be analysed more carefully. We are referring to the computation of the radiation forces, and free-surface elevation due to the radiated waves, where the first step to be done before solving the motion equations using the Runge-Kutta method is to determine the retardation functions, K_{kj}, Kh_j, which are given by;

$$K_{kj}(t) = \frac{2}{\pi}\int_0^\infty \{b_{kj}(\omega)\cos\omega t\}d\omega$$

$$Kh_j(t) = \frac{2}{\pi}\int_0^\infty \{\zeta^R_{j_{FD}}(\omega)\cos\omega t\}d\omega$$

The damping coefficients, b_{kj}, corresponding to the whole frequency range (from $\omega = 0$ to $\omega = \infty$) are computed by the "Frank Close Fit Method", while the radiated wave free surface elevations, $\zeta^R_{j_{FD}}$, corresponding to the same frequency range are computed by the same method and the expression derived in Section-8.4. The non-dimensional results are presented in figures 6.3 to 6.10, where the non-dimensionalising factors for each damping coefficient are as follows;

$$b_{22}, b_{33} \rightarrow \rho A_s\sqrt{\frac{2g}{b}}$$

$$b_{24}, b_{42} \rightarrow \rho A_s b\sqrt{\frac{2g}{b}}$$

$$b_{44} \rightarrow \rho A_s b^2\sqrt{\frac{2g}{b}}$$

where 'A_s' is the sectional area, and 'b' is the sectional beam.

The frequency domain free surface elevations, $\zeta^R_{j_{FD}}$, are non-dimensionelised by the motion amplitudes.

For high frequencies the "Frank method" is very unstable, thus the end parts of the damping coefficient curves presented have been smoothed out. In the case of the free surface elevation results for high frequencies, the instability is so drastic that it was decided to simply cut the end part of the curves. Perhaps this is the reason why the time domain free surface elevation due to the radiated waves is computed with a certain error, which is believed not to affect, significantly, the restoring force results since this is one of several contributions to the restoring forces.

The retardation functions, or impulse response functions, for the present time domain problem are presented in figures 6.11 to 6.18. They are non-dimensionalised with respect to the same factors presented above. These functions represent the influence of the past history of the fluid motion to the radiation forces acting on the body at the actual instant. Observing the graphs two conclusions are immediate, the actual instant and the instants just before are those which most contribute to the forces, and the history of the motion which occurred more than ten seconds before can be neglected.

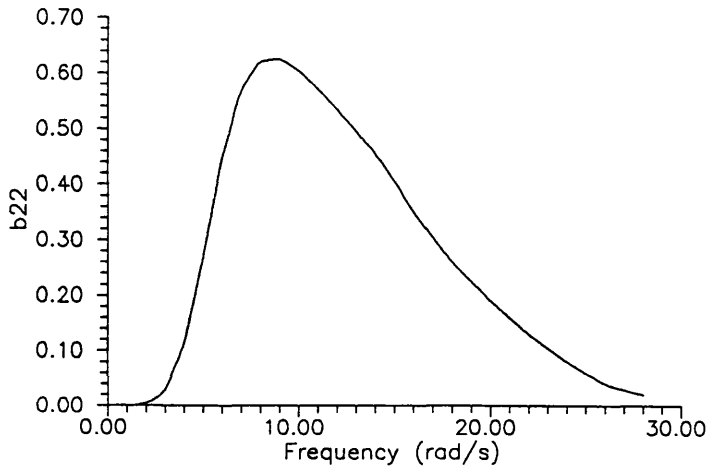

Figure 6.3 Damping coefficient in sway

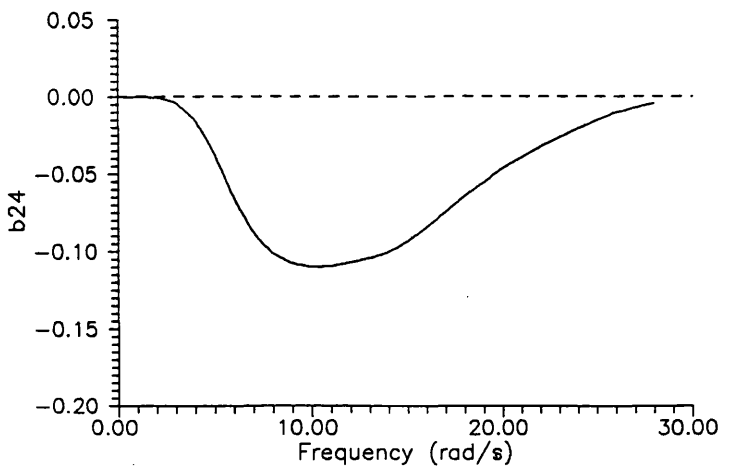

Figure 6.4 Coupling coefficient of roll into sway

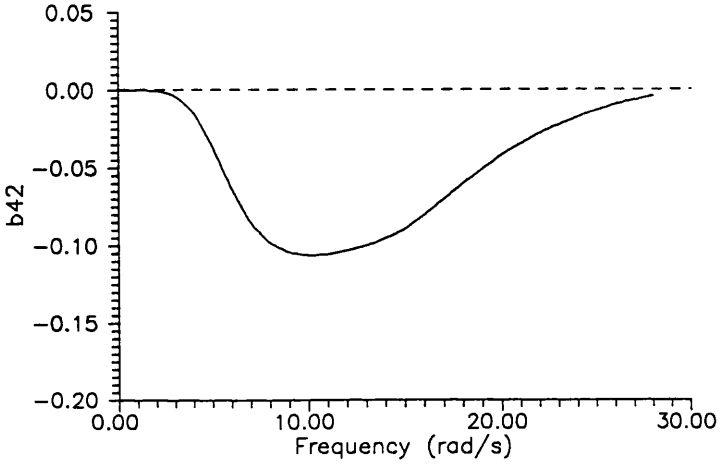

Figure 6.5 Coupling coefficient of sway into roll

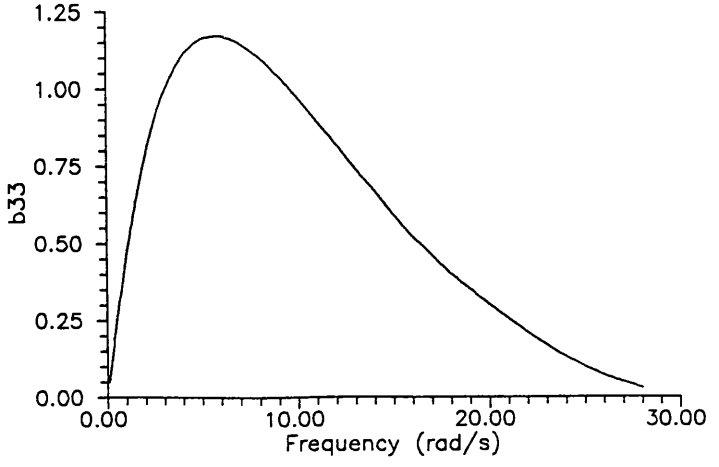

Figure 6.6 Damping coefficient in heave

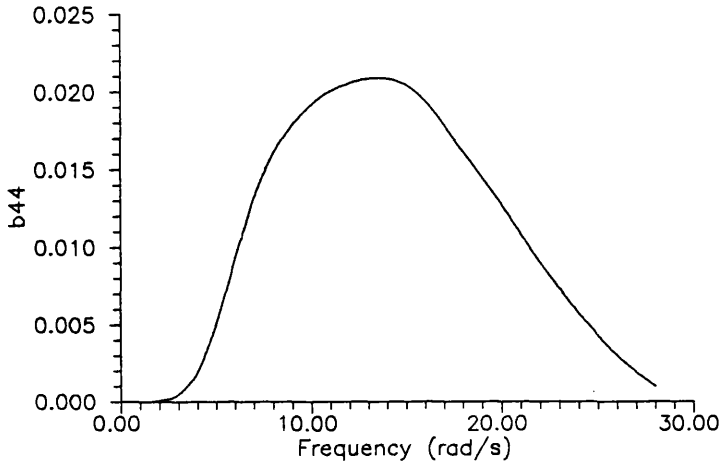

Figure 6.7 Damping coefficient in roll

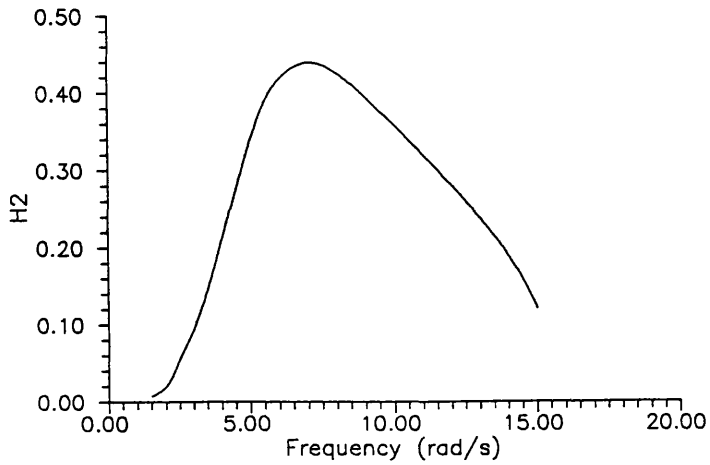

Figure 6.8 Wave amplitude ratio in sway

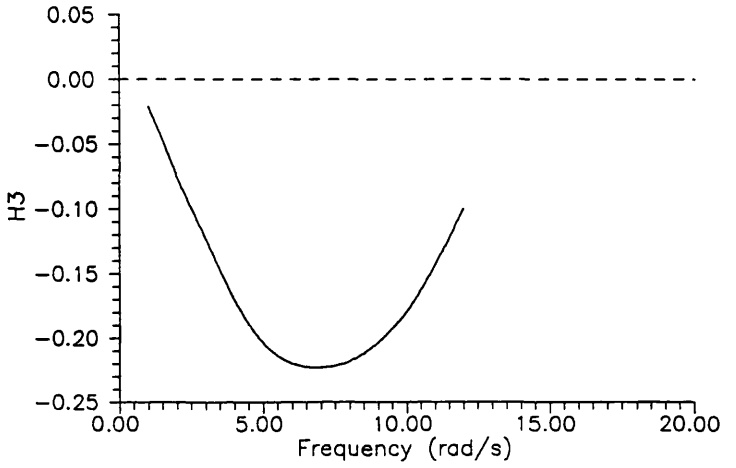

Figure 6.9 Wave amplitude ratio in heave

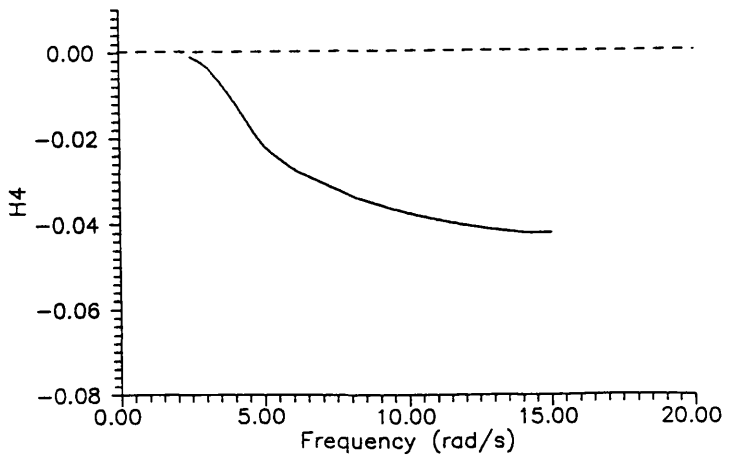

Figure 6.10 Wave amplitude ratio in roll

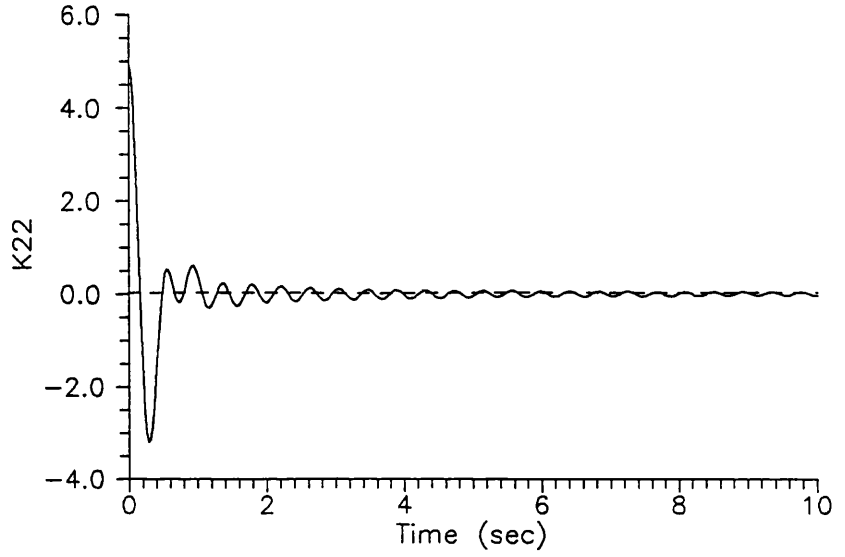

Figure 6.11 Retardation function for sway

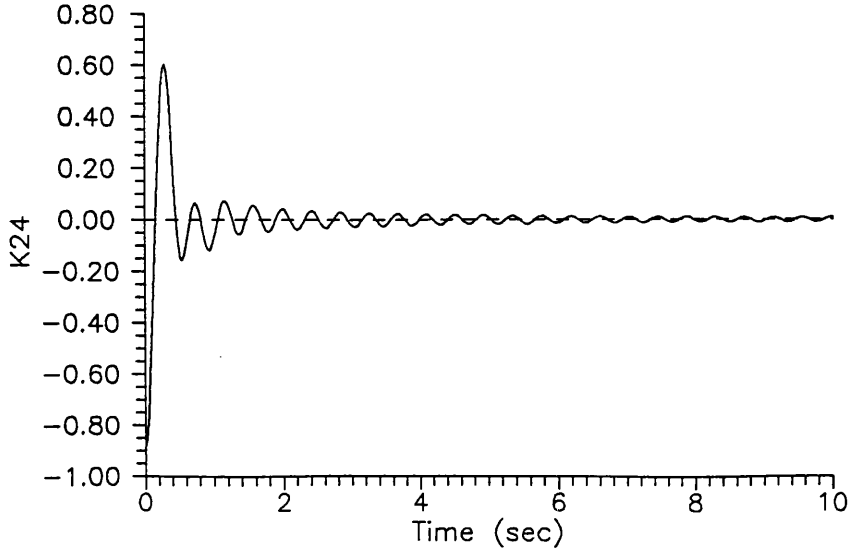

Figure 6.12 Retardation function for roll into sway

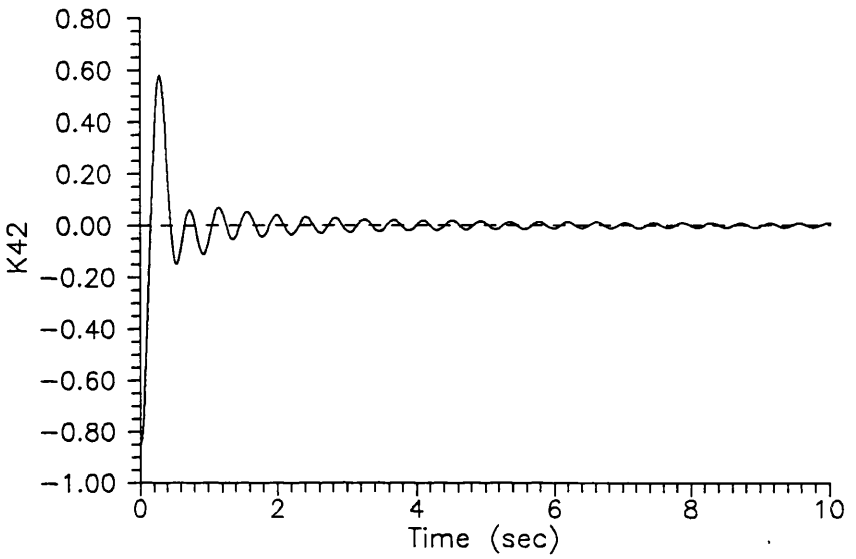

Figure 6.13 Retardation function for sway into roll

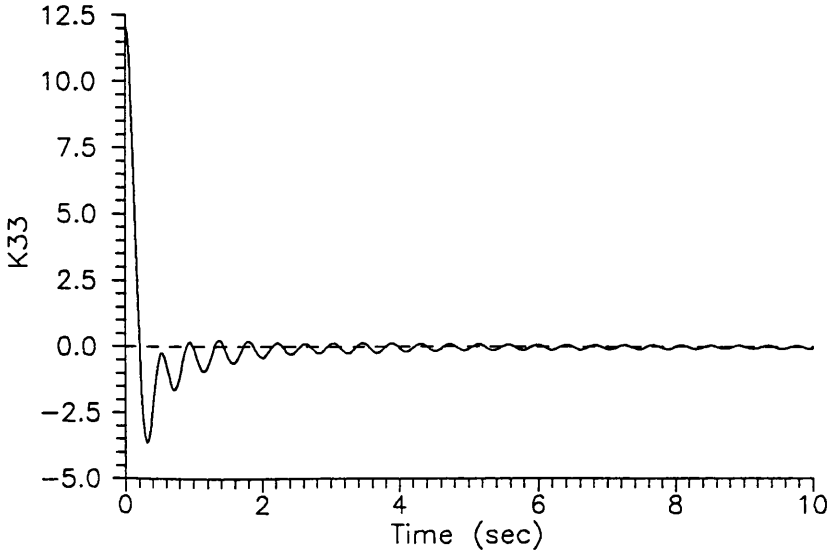

Figure 6.14 Retardation function for heave

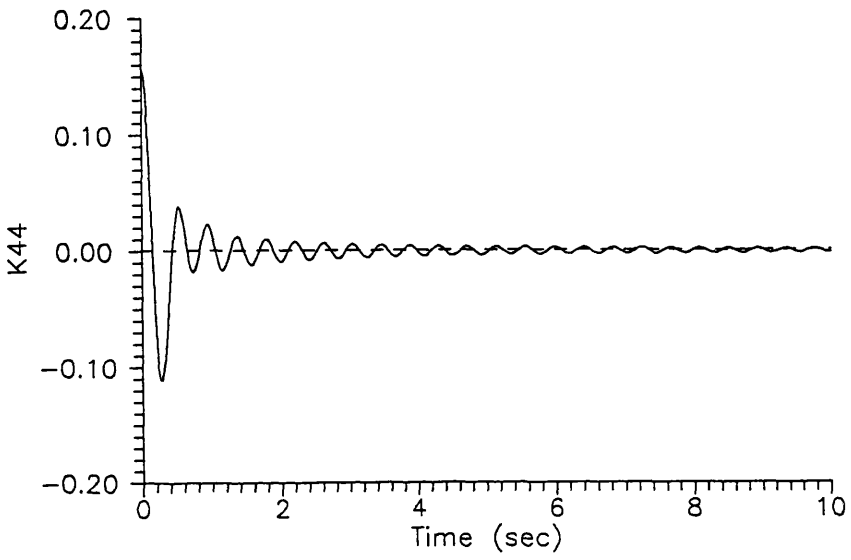

Figure 6.15 Retardation function for roll

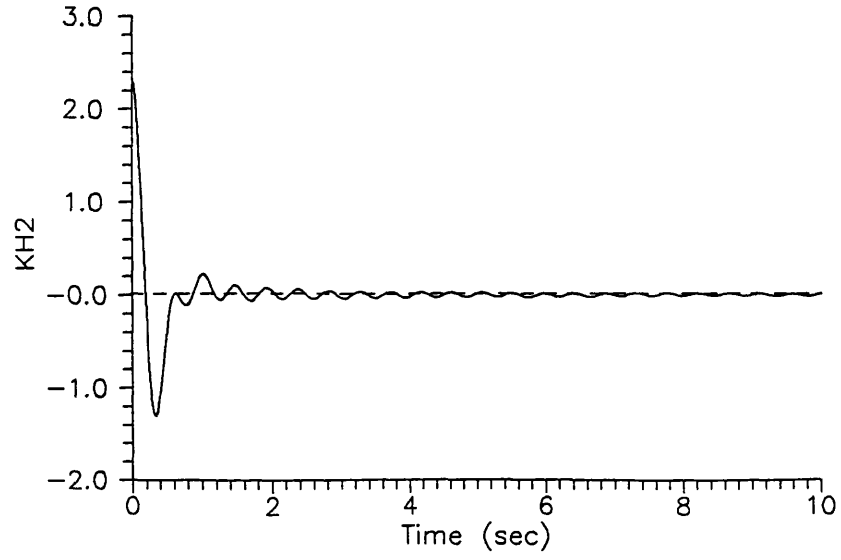

Figure 6.16 Retardation function of the wave amplitude ratio in sway

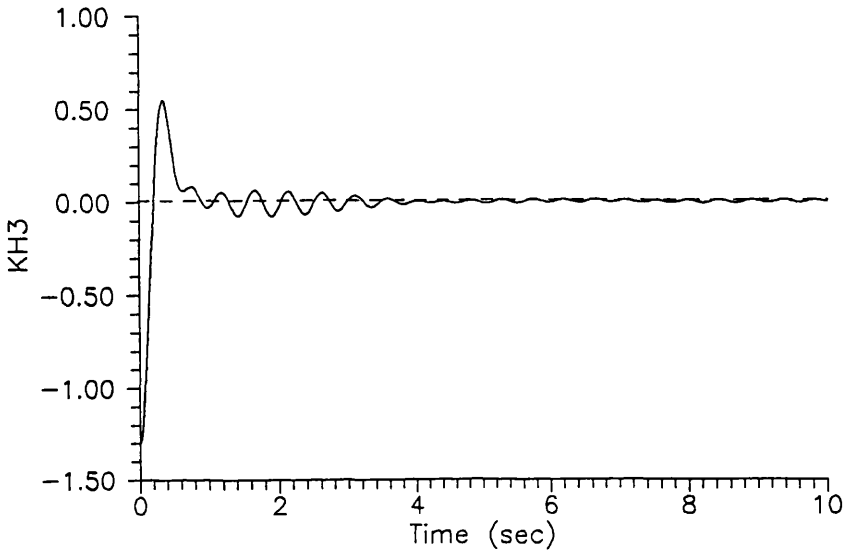

Figure 6.17 Retardation function of the wave amplitude ratio in heave

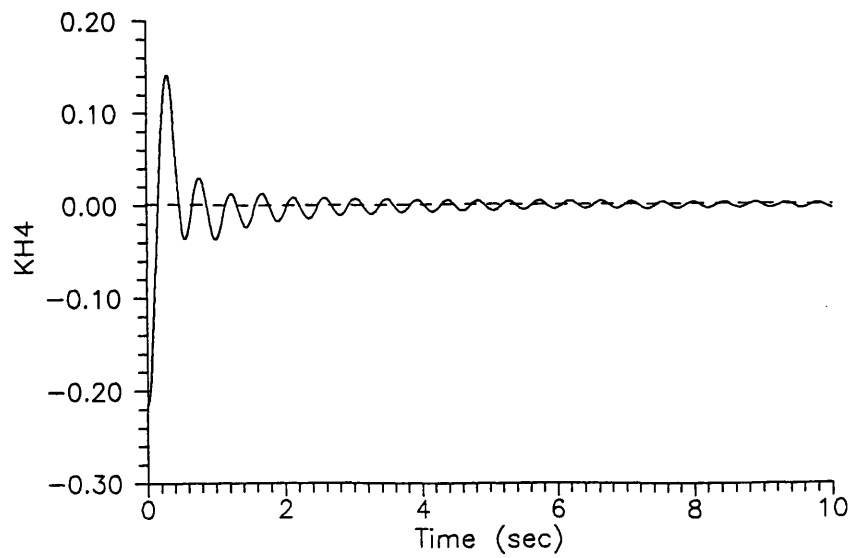

Figure 6.18 Retardation function of the wave amplitude ratio in roll

The first numerical results presented are linear for both models, frequency-domain and time-domain, which means that the time-domain restoring forces are computed using the restoring coefficients given in Section-4.4. This way all the terms in the time domain equations are linear, thus theoretically the predictions given by both models should be equal. Tests were made for a wide range of frequencies and amplitudes of the exciting forces, and the results were similar. The time histories of the sway, heave, and roll motions corresponding to two cases are presented, in figures 6.19 to 6.21 for a wave amplitude of 2 cm and wave frequency of 6.28 rad/sec, and figures 6.22 to 6.24 for the same wave amplitude with a frequency of 4.40 rad/sec. The frequency-domain results are represented by the dashed lines, while the time-domain results are represented by the solid lines. It can be observed that the predictions of the heave and roll motions by both methods tend to be exactly the same, but only after a transition period where the effects of the increasing amplitude of the exciting force stops affecting the time domain solution. In other words, when in practical terms the motion can be considered sinusoidal with constant amplitude since forever the time-domain and frequency-domain solutions are equal. The transition period is much longer and felt more strongly in the case of roll motion, since this motion is more sensitive to the variations of the damping. It is believed that the transition period predicted by the time-domain model is closer to the real case than the frequency-domain predictions. In fact it was observed during the experiments that in many cases the roll motion of the body experienced similar initial larger amplitude oscillations when the first waves reached it before the motion amplitudes become steady. A similar tendency was obtained in the numerical results, and there are significant differences between the time domain and frequency domain results. This may be a result with important practical applicability to predict the most probable larger roll amplitudes of small ships in irregular seas, since this kind of behaviour is found in those conditions. A small ship can be travelling and experiencing small to moderate roll amplitudes, but if it happens to encounter a set of waves with amplitudes high enough and at the right frequency the roll amplitudes will increase in a short period of time.

In the case of sway motion it can be observed that the predictions by both models are similar after the transition period, with the difference that the time domain solution has a steady sway. The reason for this behaviour was not found, but probably somewhere in the numerical computations there is an approximation error, which although small, creates an initial small steady velocity which is not opposed by any restoring force.

The important conclusion from these results is that the radiation forces can in fact be calculated in the time domain by the method presented in this thesis.

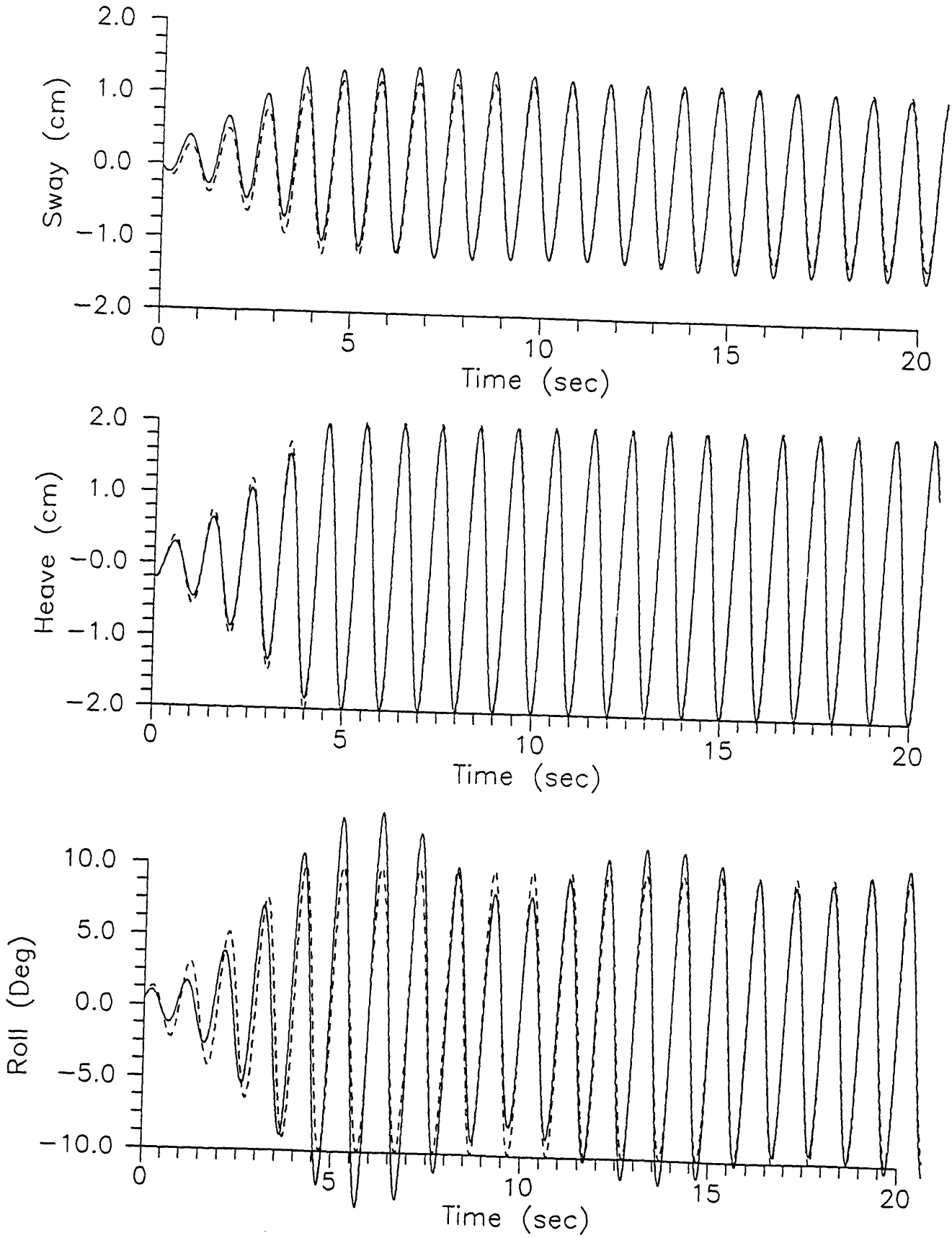

Fig. 6.19, 6.20, 6.21 Linear time-domain and frequency-domain solutions, $\zeta^a = 2$ cm, $\omega_0 = 6.28$ rad / s

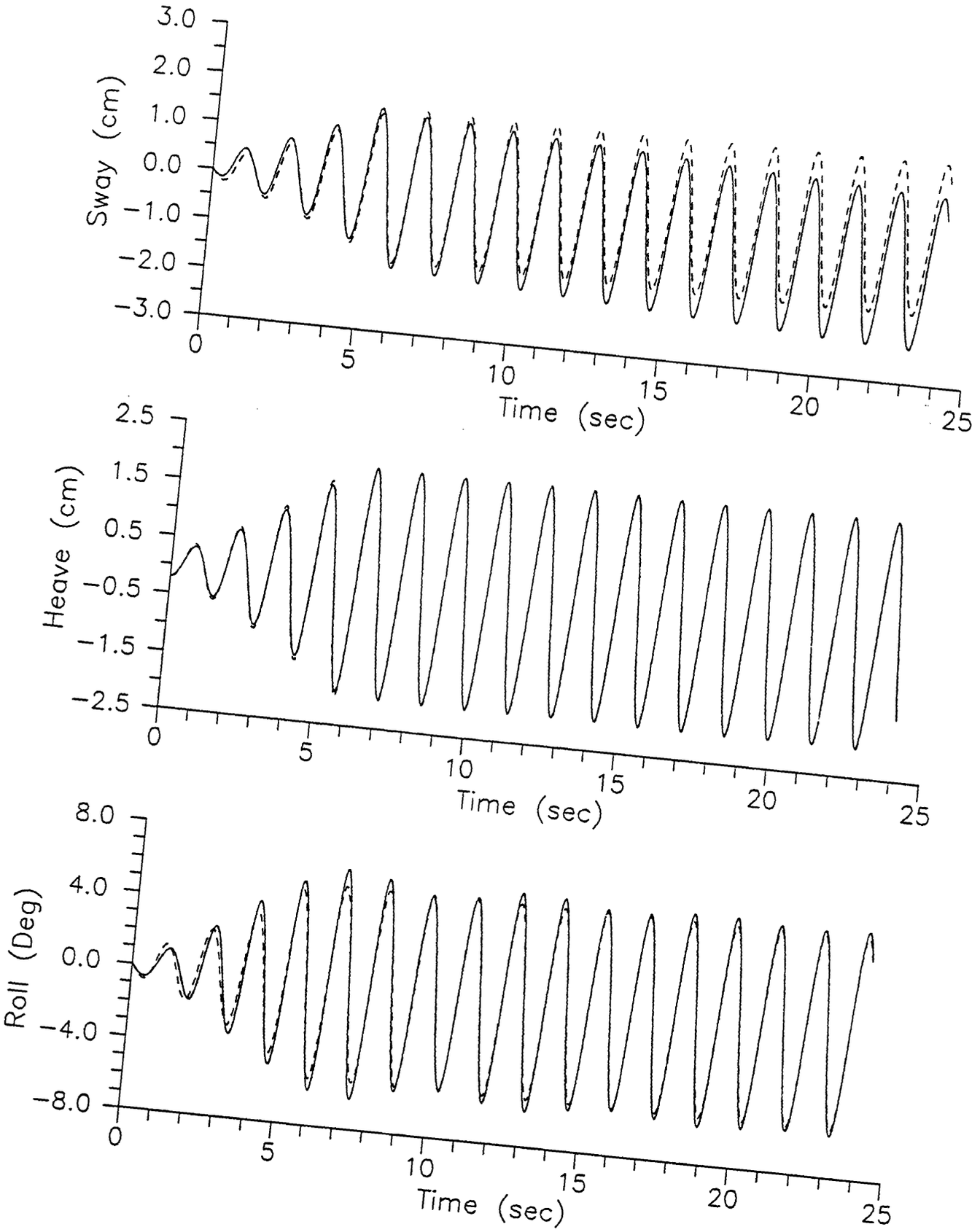

Fig. 6.22, 6.23, 6.24 Linear time-domain and frequency-domain solutions, $\zeta^a = 2$ cm, $\omega_0 = 4.40$ rad/s

In figures 6.25 to 6.143 the time histories of the motions measured during the experiments as well as the corresponding numerical results are presented. In addition the time history of the free surface elevation measured by the wave probe located at half the tank breadth is also presented. These last results are used to find the amplitude and frequency of the real incident waves, since the wave maker is not very accurate in producing the waves ordered by the computer. In fact the wave probes were located too close to the model, and the measured free surface elevations are affected by the waves radiated and diffracted from the model. This is specially amplified for higher frequencies and wave heights. However the locations chosen to position the model and wave probes were probably the best, since the wave probes were already close the wave maker, and on the other hand if the model were positioned closer to the beach (see figure 6.2) the time interval between the moment when the body reached steady motions and the moment when the waves diffracted from the beach reached the body would be very small. Concluding, some error is expected in the values of the wave amplitude used in the numerical computations.

Now the non-linear time-domain model is used, which means that the restoring force term is calculated according to the formulation derived in Section-5.4. Again in the graphs showing numerical results the frequency-domain and time-domain solutions are plotted together, so it is easy to verify whether the second model brings any improvements in the prediction of the motions. The dashed lines represent frequency domain results and the lines time domain results.

For the sway motion the linear and non-linear numerical results are similar, except that for the second case there is a small steady sway which arises from two effects: there is a sway hydrostatic force which in general is stronger for one of the directions due to the asymmetry of the free surface elevation on both sides of the body, and it was found that there is a small numerical error which induces a small steady sway velocity. Compared with the experimental data we find that for the lower frequencies the experimental amplitudes of the motion are smaller than the numerical results, but of the same order of magnitude. The smaller values can be explained by the fact that the mooring system, which restrains the motions, is not taken into account by the numerical models. However for the most of the cases the measured amplitudes are much higher than the predictions. No justification is found for the wrong predictions for the

forces associated with the sway motion when the same forces associated with the other modes of motion are nearly correct. One probable cause for these differences is inaccurate calibration of the Selspot system for the horizontal motions, however the author is not able to state that this is the reason or one of the reasons. More research is needed to validate the sway motion models.

The heave experimental results show a small non-linear behaviour, it can be observed that in general the positive amplitudes are higher than the module of the negative amplitudes. This is due to the coupling through the hydrostatic forces between the heave and roll motions, because of the v-shape of the body cross section when the model experiences a roll displacement the immersed volume increases thus an hydrostatic force pointing upwards is associated. This tendency is also present in the non-linear numerical results, however in many cases it is very exaggerated. Some tests were done with a modified time-domain model where the heave restoring force was computed ignoring the roll motion. Examples of the resultant heave motion are presented in figures 6.144 to 6.146, where it can be observed that the predictions are very similar to the ones of the linear model. The reason is because the relation 'water plane area/immersed volume' is very high for this body, and so the relative motion between the body and the free surface is not high enough to originate strong non-linearities on the heave restoring force and consequently on the heave motion. But the main purpose of presenting these figures is to show that the exaggerated heave amplitudes predicted by the non-linear model are associated with the roll motion, and in fact some of the runs where wrong heave amplitudes were obtained have simultaneous wrong roll motion predictions, in the sense that the roll amplitudes are too high (see for example figures 6.56 and 6.98). Some additional tests were carried out with one other modified time domain model, where nearly the roll motions measured in the experimental tests were used in the time domain simulation to predict heave motions. The propose was to verify if the heave results were improved. In fact some improvments were realised in heave motions when measured roll displacements were used in the simulations, but not enough that we can say the results are acceptable. In addition there are some cases where the roll motion predictions compare very well with the experiments, however the heave predictions are wrong (see figures 6.77 and 6.84). Assuming that the hydrostatic forces are well computed, and after a very long period of tests nothing indicates that they are not, the former steps lead to the conclusion that there is one or more neglected terms in the linear

assumptions of the other forces which should be included. It would be very interesting to calculate the Froude-Krylov force over the exact wetted surface of the body instead of using the mean wetted surface. This force is relatively easy to compute in the time domain, the run time would not be much increased, and it could be verified if the results were improved at least in the low frequency range where the hydrostatic and Froude-Krylov forces are dominant over the radiation and diffracted forces.

Turning now to the roll motion, in the moderate to high frequency range there is a tendency in the experimental results that the roll amplitude for one of the sides (the negative one) is higher than for the other side. In other words the side of the body "receiving" the incident waves turns down more than the other side. This tendency is predicted very well by the time domain model in some of the moderate frequencies (see figures 6.80 and 6.87), however for high frequencies the predicted asymmetry is for the opposite side (see figures 6.129 and 6.136). In the numerical model this kind of behaviour is created by the non-linear hydrostatic moment, which in turn have a higher amplitude for one of the sides because it is computed over the wetted surface up to the actual free surface elevation. In figures 6.147 to 6.150 are presented the time histories of the total free surface elevation on both sides of the body for four different frequencies, and it can be observed that the elevation on the side receiving the incident waves has a higher amplitudes than the other side. This is because the diffracted waves are much higher on this side.

Near the resonance frequency the time domain solution compares very well with the experimental results (see figures 6.80 and 6.87), however there are some other cases where the solution is wrong, like for example the results shown in figures 6.45, 6.59 or 6.101. It was found that the contribution for the hydrostatic moment of the layer between the still water line and the actual free surface elevation is responsible for the occurrence of these large amplitudes while on the other hand the linear model produces reasonable results. Again it is believed that the hydrostatic moment is properly evaluated and there is a neglected term which should be included. The Froude-Krylov moment evaluated in the time domain over the exact wetted surface could be easily introduced to verify if the numerical results were improved.

It was found that for the higher wave amplitude at high frequencies the solution is unstable (see figure 6.143). Some tests were carried out with the time domain

program but now using the frequency domain damping coefficients to calculate the damping forces, the solutions were still unstable. On the other hand the restoring forces are relatively small, thus it seems that this is a numerical problem occurring with large waves at high frequencies.

Finally the linear frequency domain model should be mentioned since it predicts the heave motions well, and the roll motions compare remarkably well with the experiments, except for the frequency range near the resonance. It seems that in the linear theory there are several terms neglected, which could be of significant importance, but they tend to cancel each other thus the final result is not much affected.

All the heave and roll results are condensed in the form of transfer functions in figures 6.151 to 6.158. The heave is non-dimensionalised with respect to the wave amplitude, while the roll is non-dimensionalised with respect to the product wave amplitude-wave number. As the negative amplitudes are not equal to the positive amplitudes two transfer function graphs are presented for each case. The first transfer function corresponds to the positive amplitudes and the second to the negative amplitudes. In figures 6.151 to 6.154 are the graphs corresponding to the wave amplitudes near to 2 cms, and in figures 6.155 to 6.158 are the graphs corresponding to the wave amplitudes near to 3 cms. The experimental results are represented by the black balls, the linear results by the dashed line, and the non-linear results by the solid line.

From the former graphs it can be concluded that at the present stage the method is not reliable to predict the heave motions of the cylinder if the hydrostatic coupling with the roll displacements is to be taken into account. In some cases the predictions compare well with the experiments but in some other cases the numerical solution is wrong. In addition for the cylinder used in this work, which has a cross section with very steep sides, the heave solution is very sensitive to the accuracy of the roll solution.

The roll motion predictions by the non-linear model for the smaller wave amplitude (2 cm) are encouraging since they compare very well with the experiments, even near the resonance frequency where the linear model completely fails. However for the higher wave amplitude (3 cm) there are some frequencies where the solution is wrong.

It is known that some modern ship motion programs use the stability arm curve in order to calculate the ship roll restoring moment at large roll angles. This is certainly an improvement in relation to the use of the linear metacentric theory. Thus the author was tempted to use the same method to evaluate the cylinder restoring moment. Again the time domain program was modified and the hydrostatic moment computed neglecting the coupling with the heave motion and the free surface elevation effects. At each time instant the moment is evaluated considering the cylinder in still water with the actual roll displacement and with zero heave displacement. All the runs were repeated and the resultant transfer functions are presented in figures 6.159 to 6.162, where in addition to the symbology already presented the new solution is represented by the triangles.

Observing the graphs two characteristics of the new model can be pointed out, first the spring term in the equations of motion is increased thus the resonance frequency is higher, consequently the amplitudes of motion for frequencies near the new resonance are higher than those predicted by the other models. The resonance frequency found in the experimental results compares better with the other two models. Secondly it seems that the new model tends to under-estimate the roll amplitudes corresponding to higher waves, perhaps because in these case the neglected effects of the free surface elevation become more important.

The results analysed are just a few to get conclusions, but if these tendencies are verified for other cases, especially for cylinders with cross sections with less steep sides, maybe we have to start taking into account the effects of the free surface elevation in order to obtain accurate predictions of the roll motion of ships.

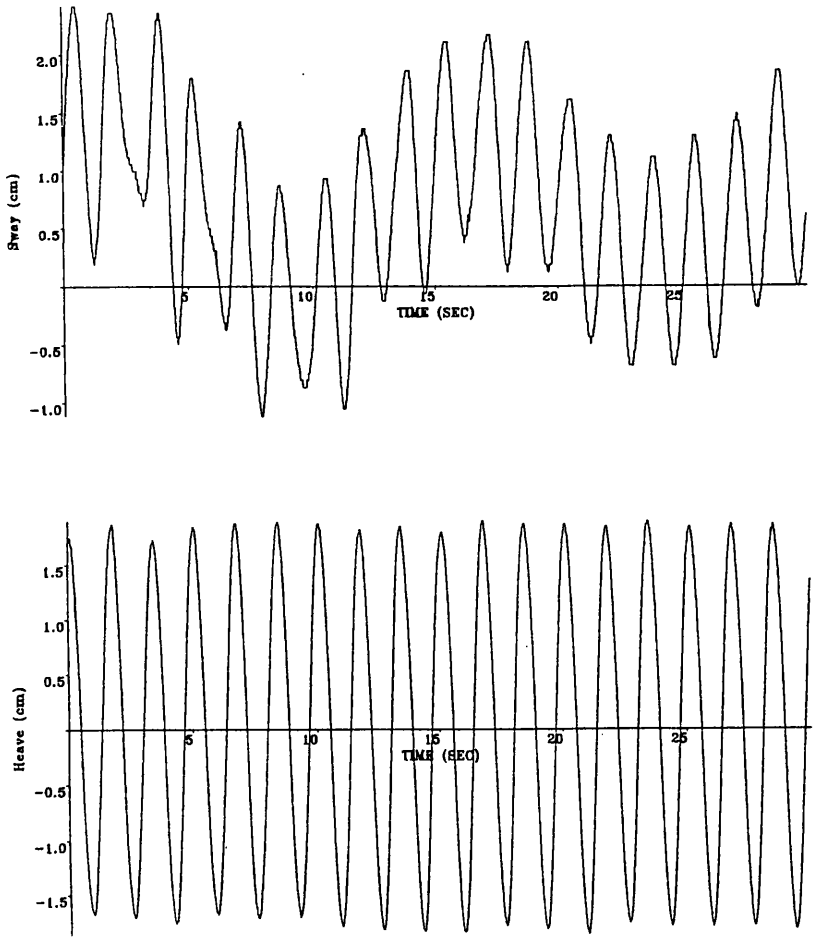

Fig. 6.25, 6.26 Experimental results, sway and heave time histories,
$\zeta^* = 1.9$ cm, $\omega_n = 3.77$ rad / s

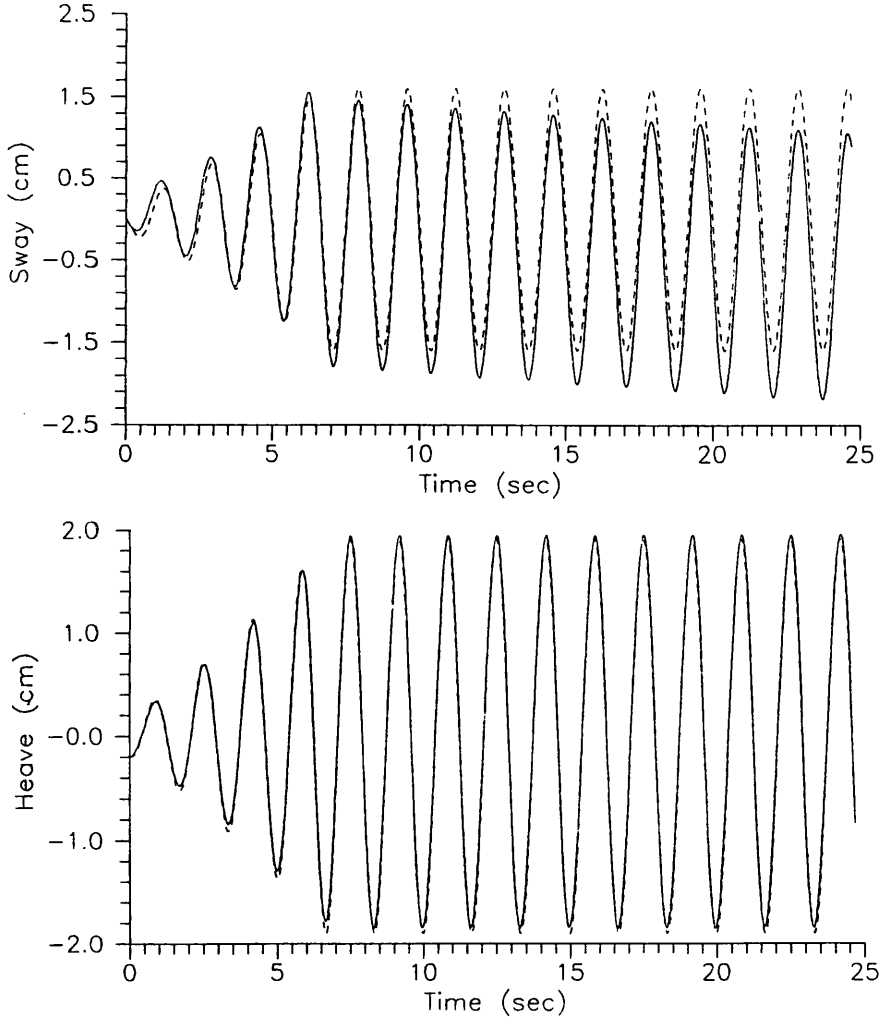

Fig. 6.27, 6.28 Numerical results, sway and heave time histories,
$\zeta^* = 1.9$ cm, $\omega_n = 3.77$ rad / s

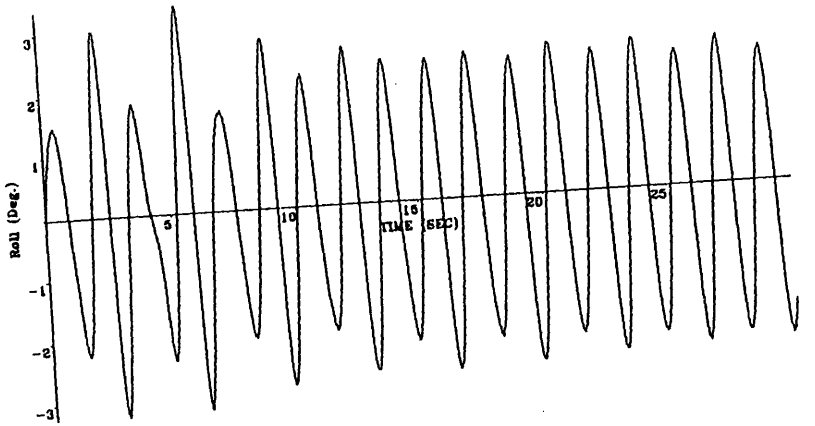

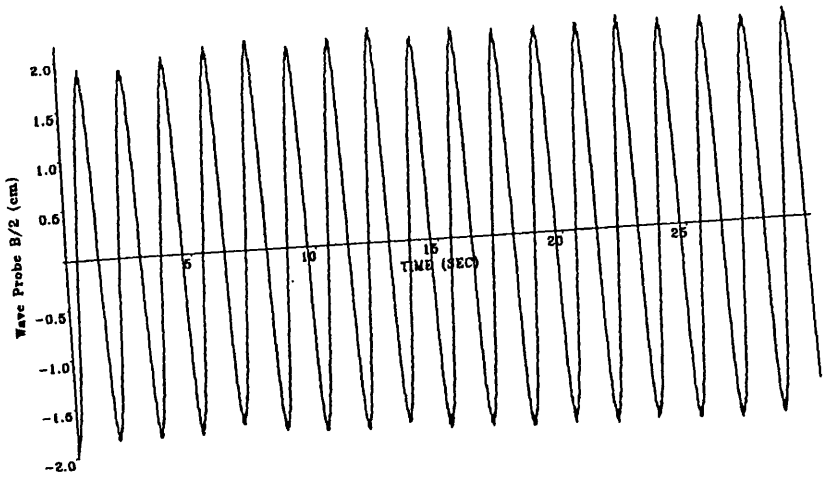

Fig. 6.29 Experimental result, roll time history,
$\zeta^* = 1.9$ cm, $\omega_o = 3.77$ rad / s

Fig. 6.30 Experimental result, free surface elevation

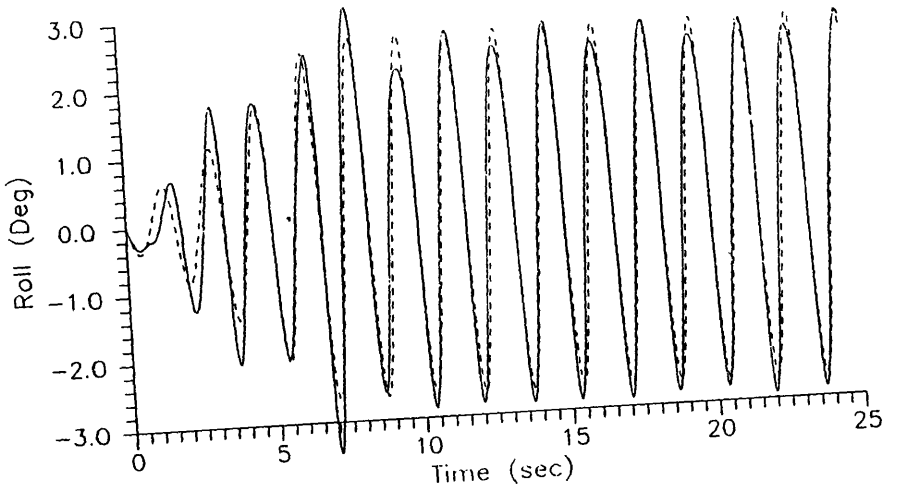

Fig. 6.31 Numerical results, roll time history,
$\zeta^* = 1.9$ cm, $\omega_o = 3.77$ rad / s

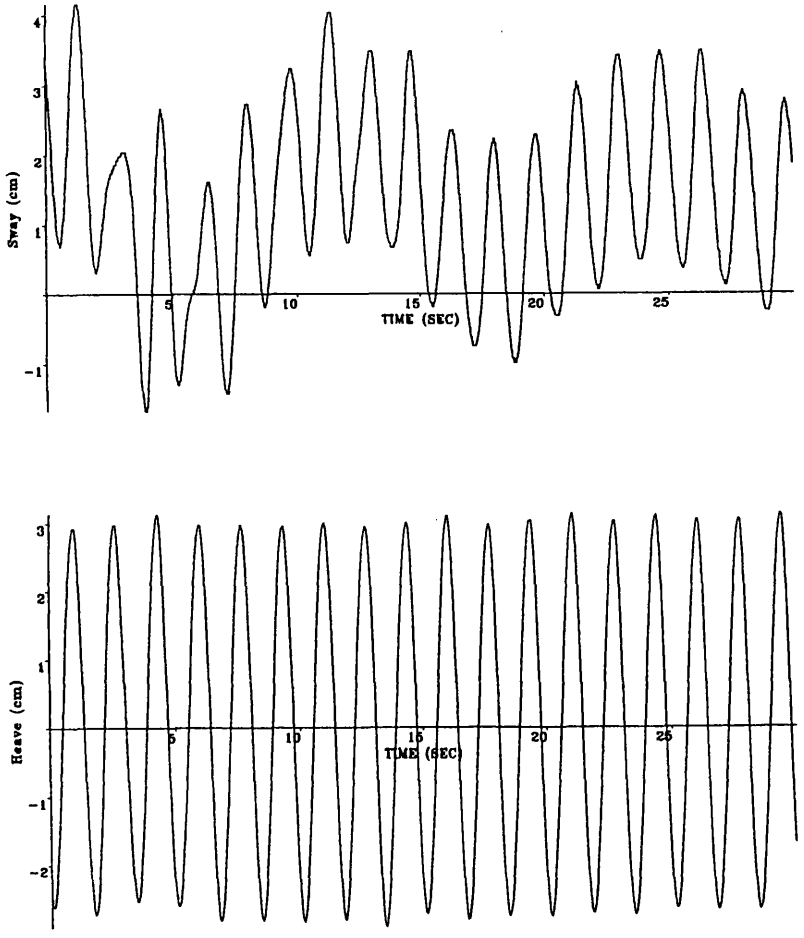

Fig. 6.32, 6.33 Experimental results, sway and heave time histories,
ζ^a = 3.1 cm, ω_n = 3.77 rad / s

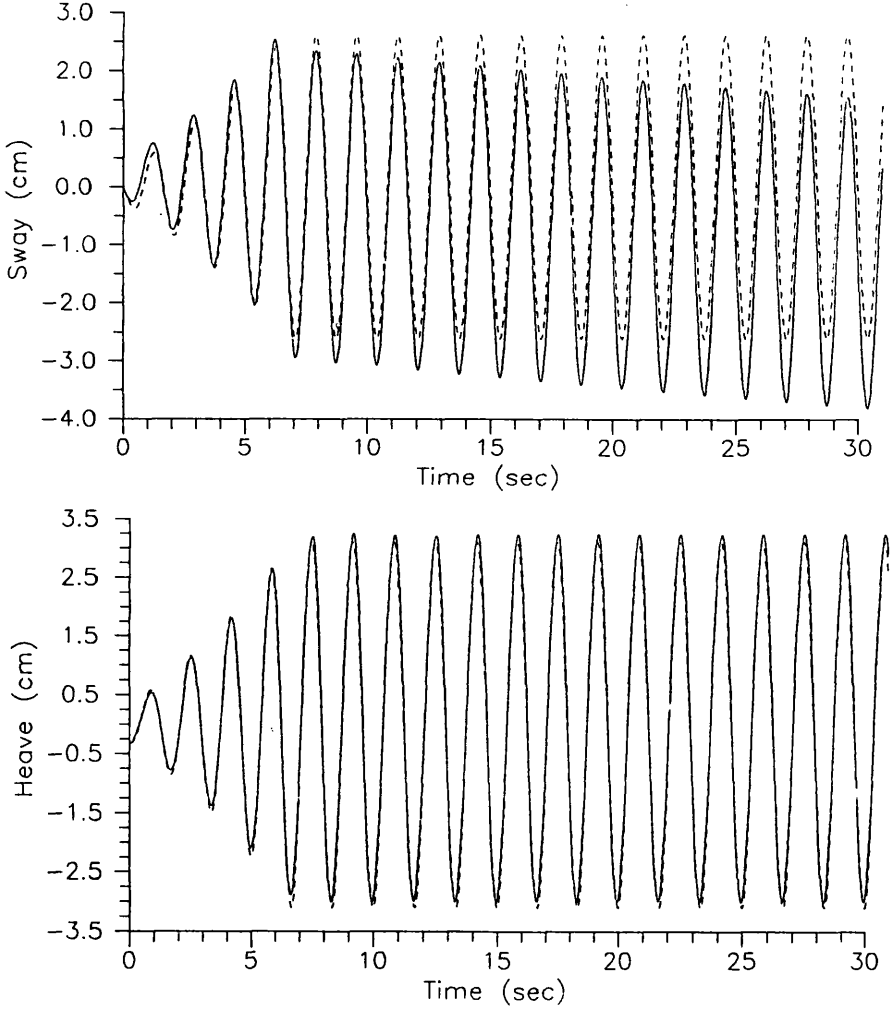

Fig. 6.34, 6.35 Numerical results, sway and heave time histories,
ζ^a = 3.1 cm, ω_n = 3.77 rad / s

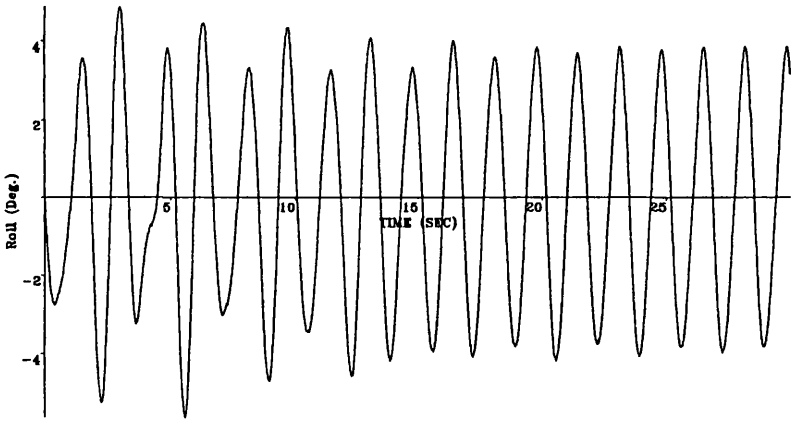

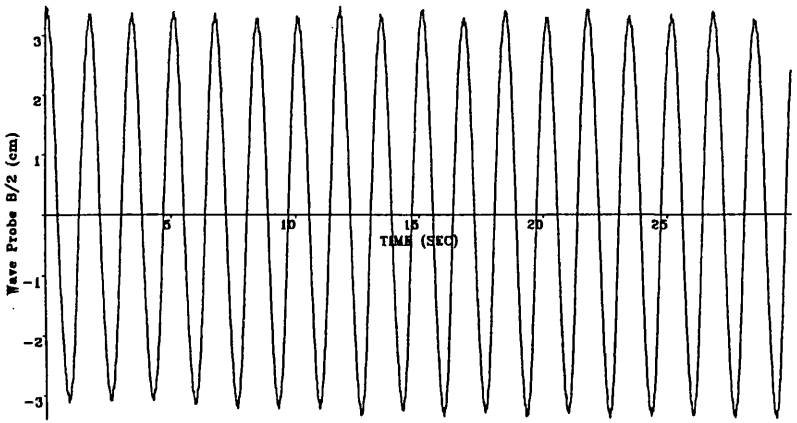

Fig. 6.36 Experimental result, roll time history,
$\zeta^* = 3.1$ cm, $\omega_n = 3.77$ rad / s

Fig. 6.37 Experimental result, free surface elevation

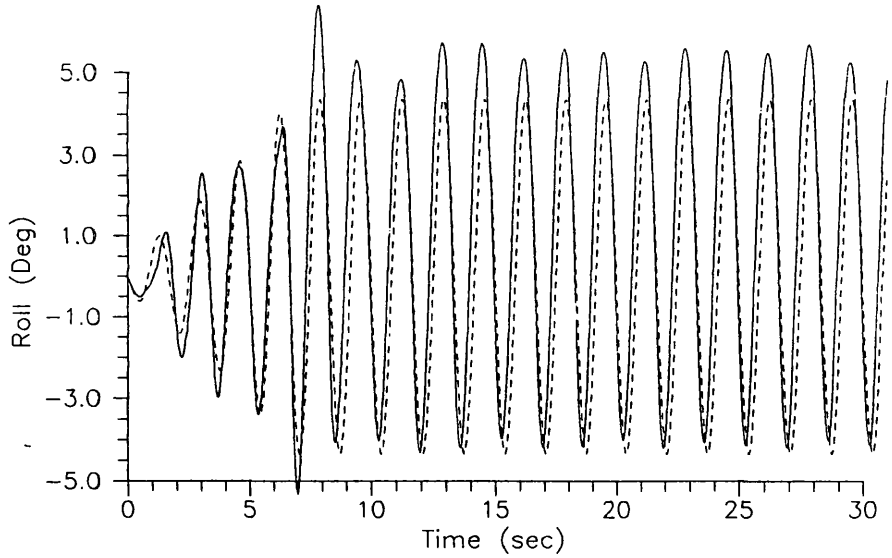

Fig. 6.38 Numerical results, roll time history,
$\zeta^* = 3.1$ cm, $\omega_n = 3.77$ rad / s

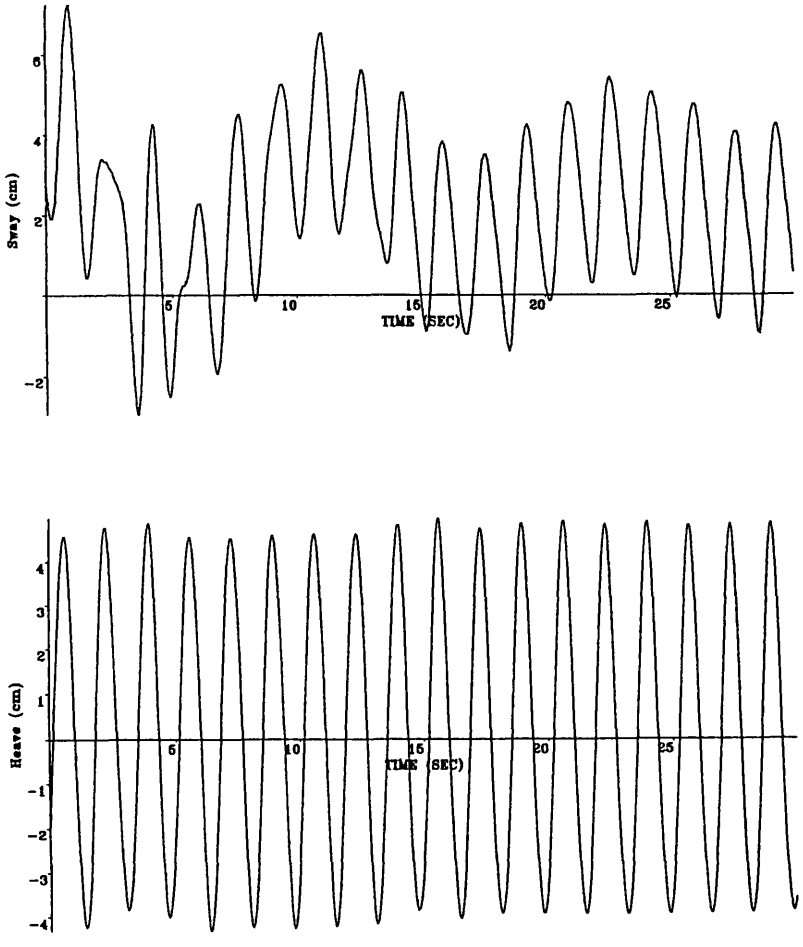

Fig. 6.39, 6.40 Experimental results, sway and heave time histories,
$\zeta^* = 4.3$ cm, $\omega_n = 3.77$ rad / s

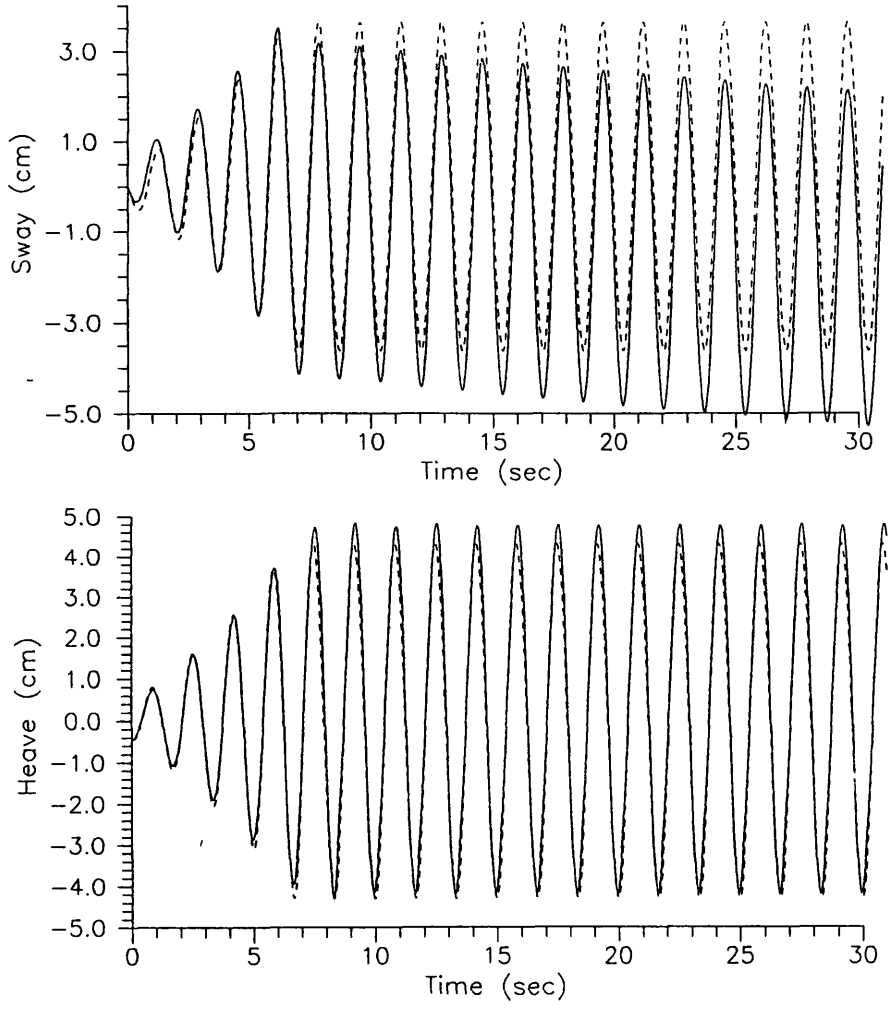

Fig. 6.41, 6.42 Numerical results, sway and heave time histories,
$\zeta^* = 4.3$ cm, $\omega_n = 3.77$ rad / s

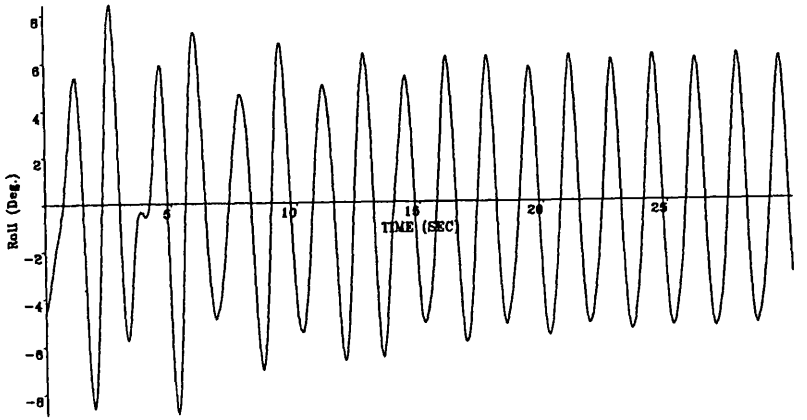

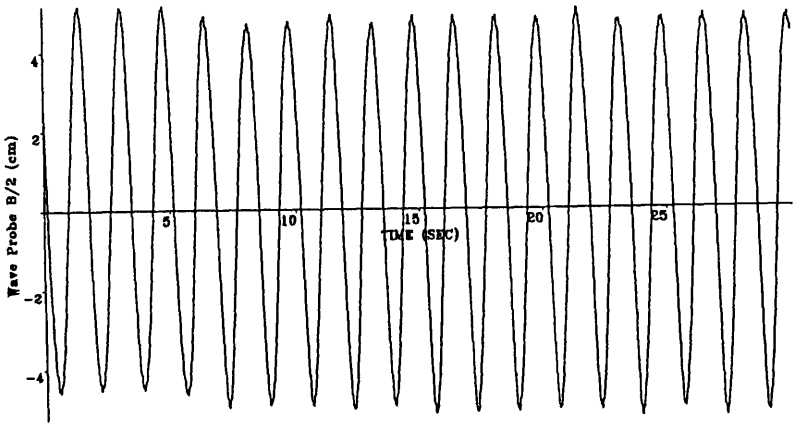

Fig. 6.43 Experimental result, roll time history,
$\zeta^* = 4.3$ cm, $\omega_n = 3.77$ rad / s

Fig. 6.44 Experimental result, free surface elevation

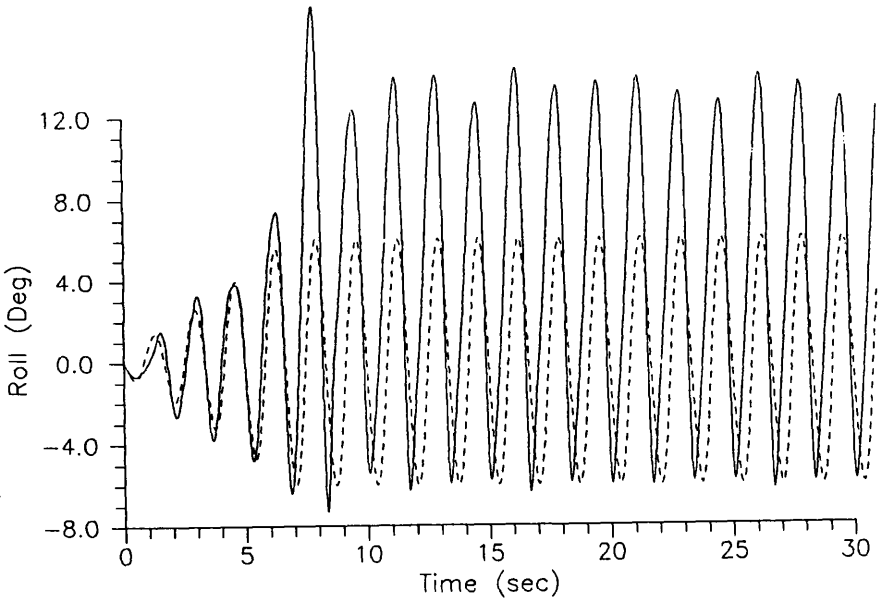

Fig. 6.45 Numerical results, roll time history,
$\zeta^* = 4.3$ cm, $\omega_n = 3.77$ rad / s

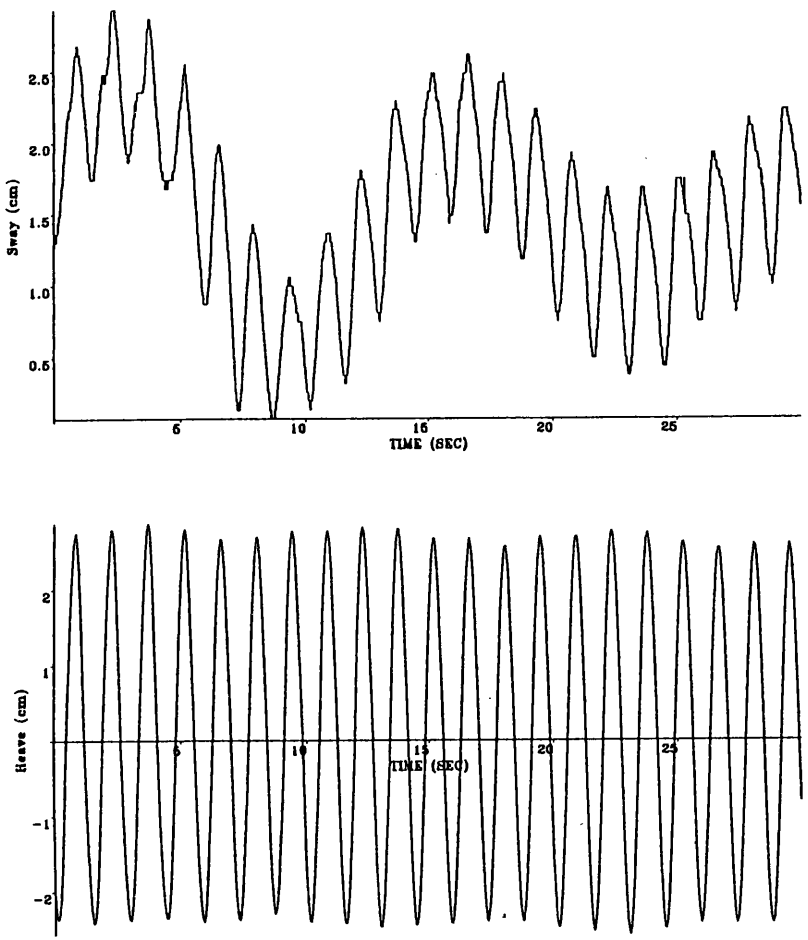

Fig. 6.46, 6.47 Experimental results, sway and heave time histories,
$\zeta^* = 2.4$ cm, $\omega_n = 4.40$ rad / s

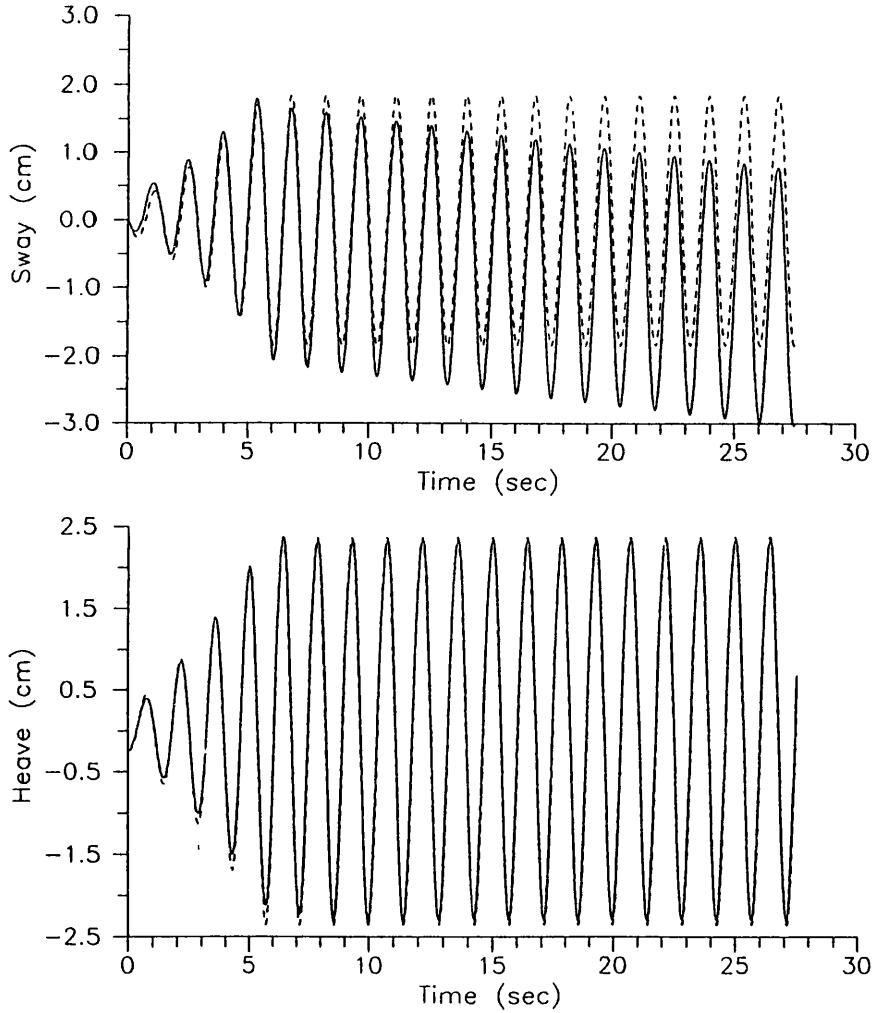

Fig. 6.48, 6.49 Numerical results, sway and heave time histories,
$\zeta^* = 2.4$ cm, $\omega_n = 4.40$ rad / s

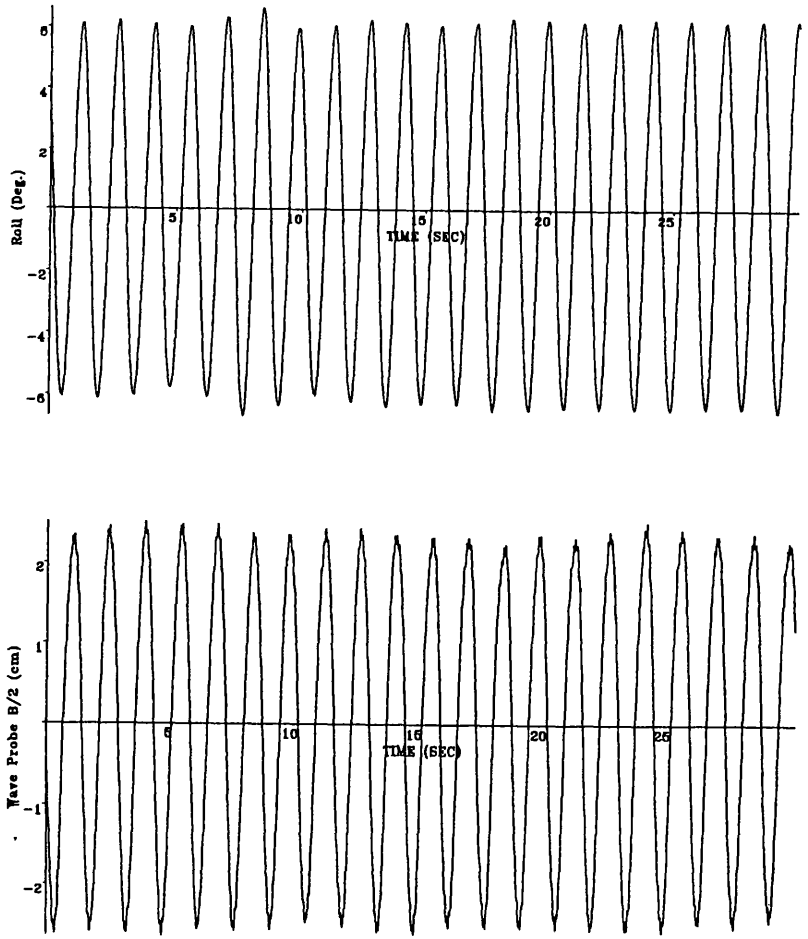

Fig. 6.50 Experimental result, roll time history,
$\zeta^* = 2.4$ cm, $\omega_n = 4.40$ rad / s

Fig. 6.51 Experimental result, free surface elevation

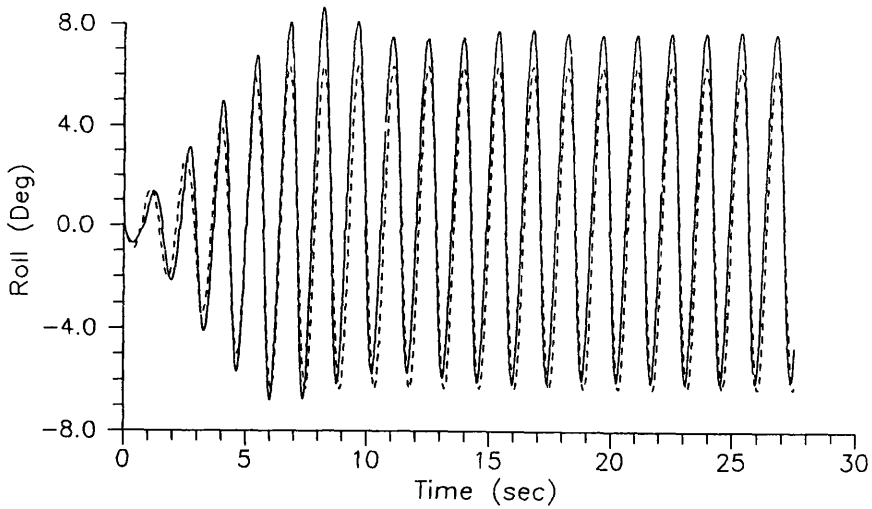

Fig. 6.52 Numerical results, roll time history,
$\zeta^* = 2.4$ cm, $\omega_n = 4.40$ rad / s

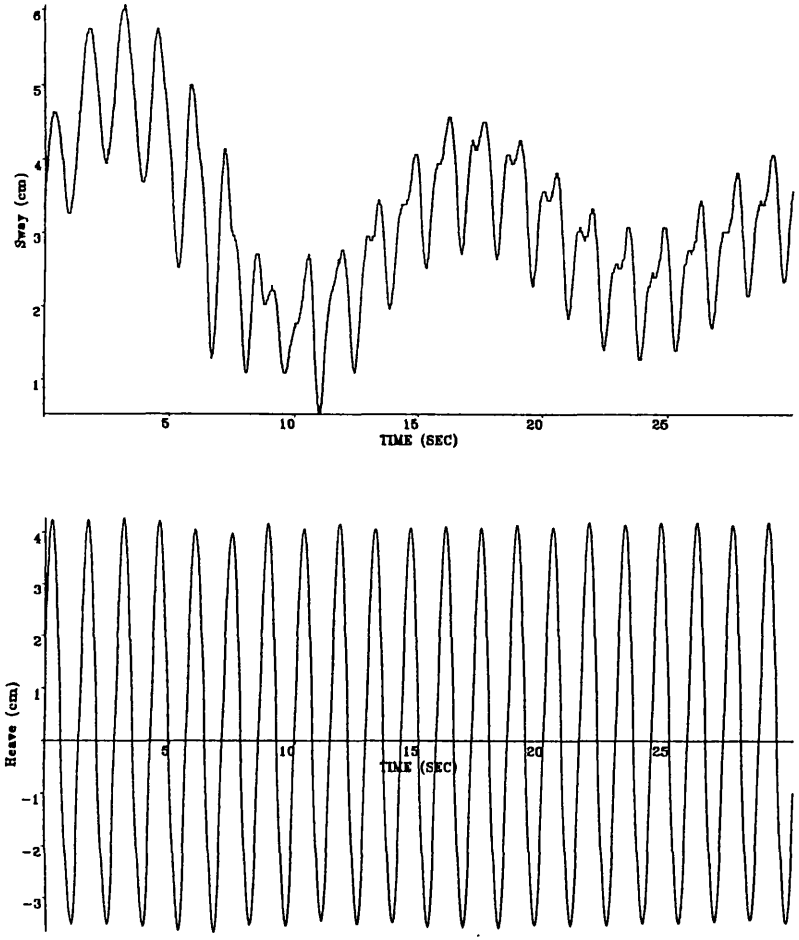

Fig. 6.53, 6.54 Experimental results, sway and heave time histories,
$\zeta^* = 3.6$ cm, $\omega_n = 4.40$ rad / s

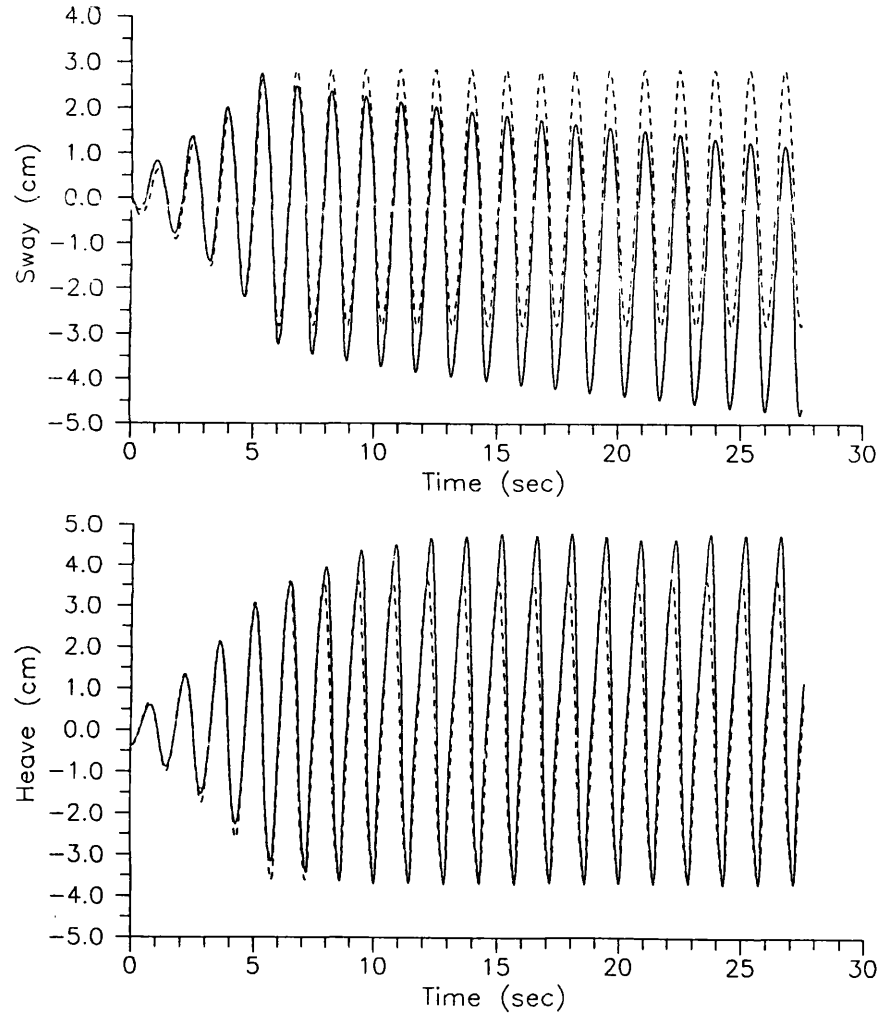

Fig. 6.55, 6.56 Numerical results, sway and heave time histories,
$\zeta^* = 3.6$ cm, $\omega_n = 4.40$ rad / s

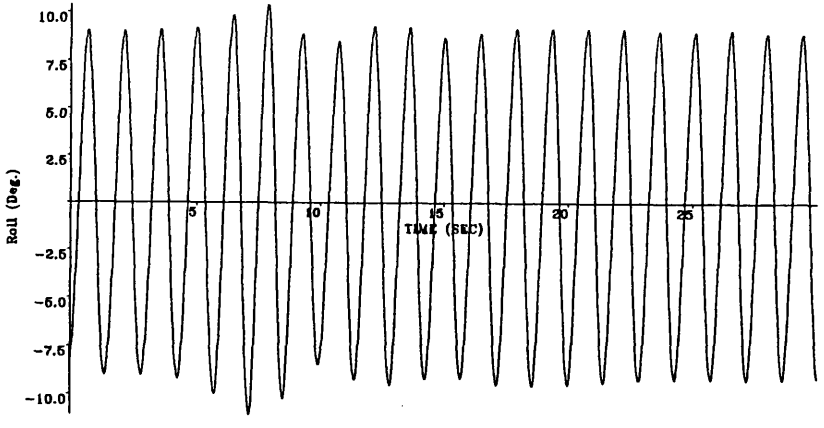

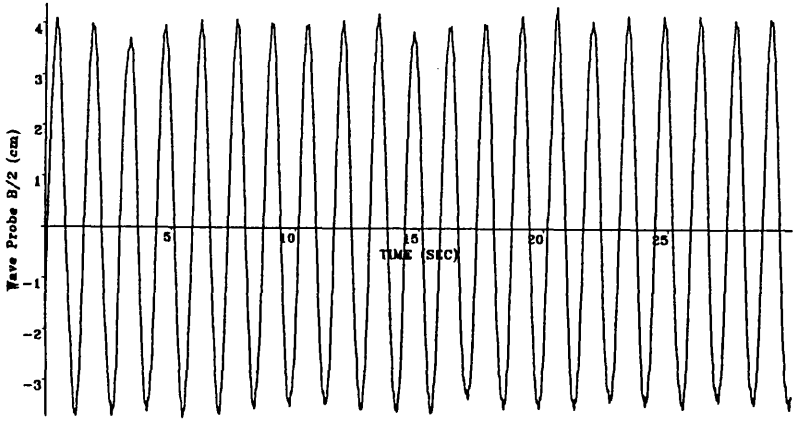

Fig. 6.57 Experimental result, roll time history,
$\zeta^* = 3.6$ cm, $\omega_n = 4.40$ rad / s

Fig. 6.58 Experimental result, free surface elevation

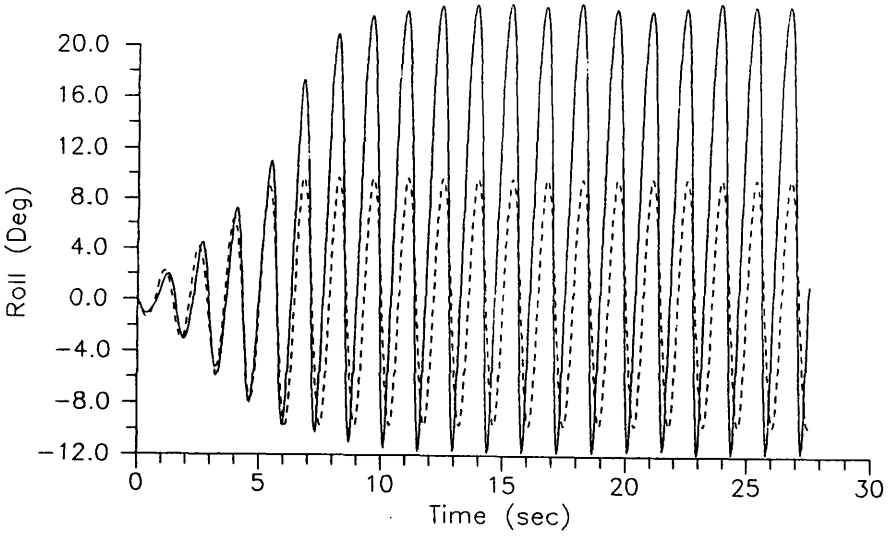

Fig. 6.59 Numerical results, roll time history,
$\zeta^* = 3.6$ cm, $\omega_n = 4.40$ rad / s

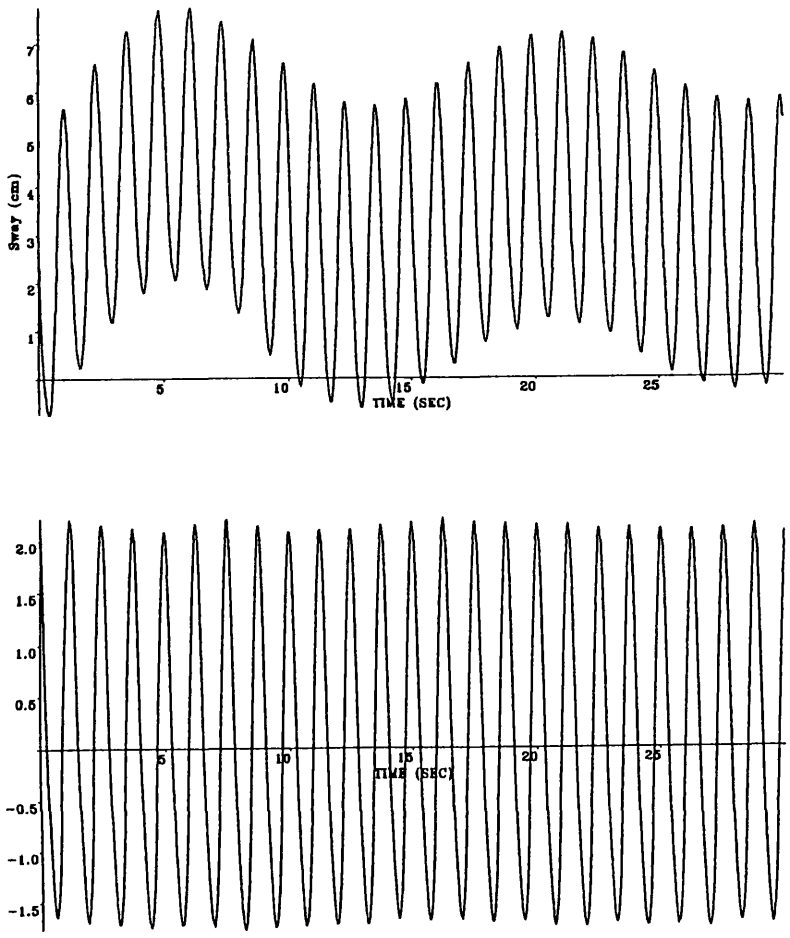

Fig. 6.60, 6.61 Experimental results, sway and heave time histories,
$\zeta^* = 2.0$ cm, $\omega_n = 5.03$ rad / s

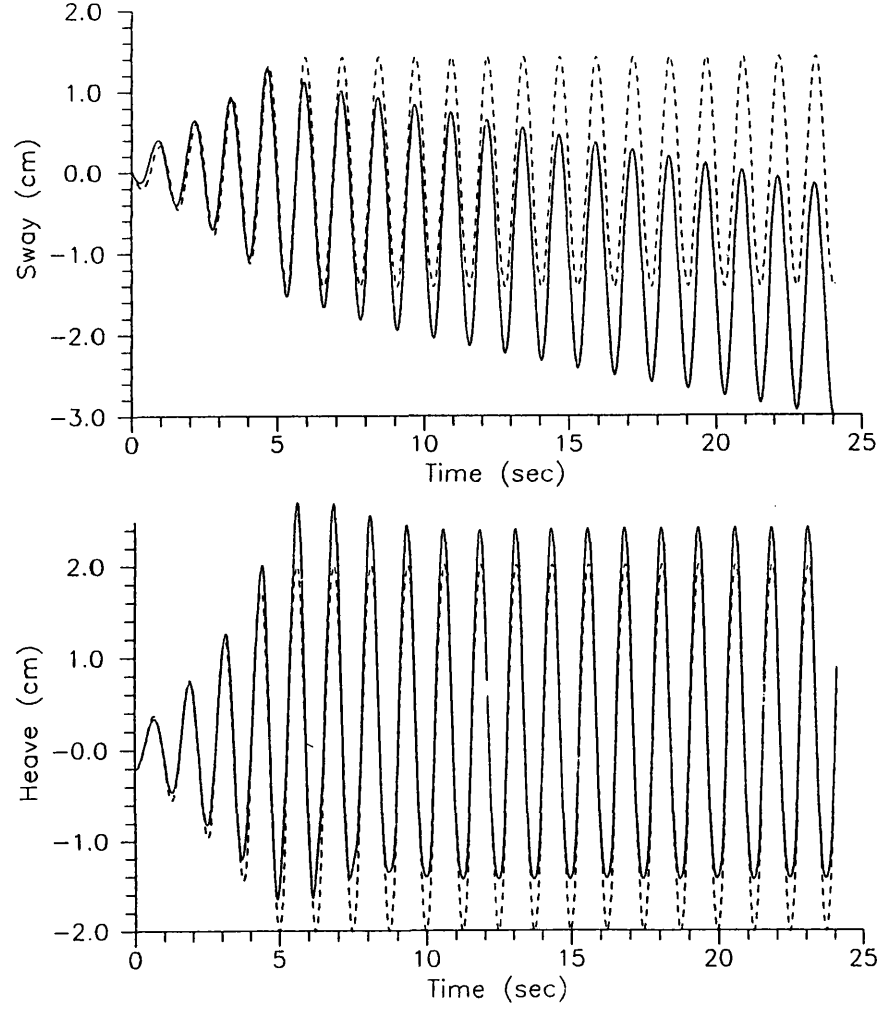

Fig. 6.62, 6.63 Numerical results, sway and heave time histories,
$\zeta^* = 2.0$ cm, $\omega_n = 5.03$ rad / s

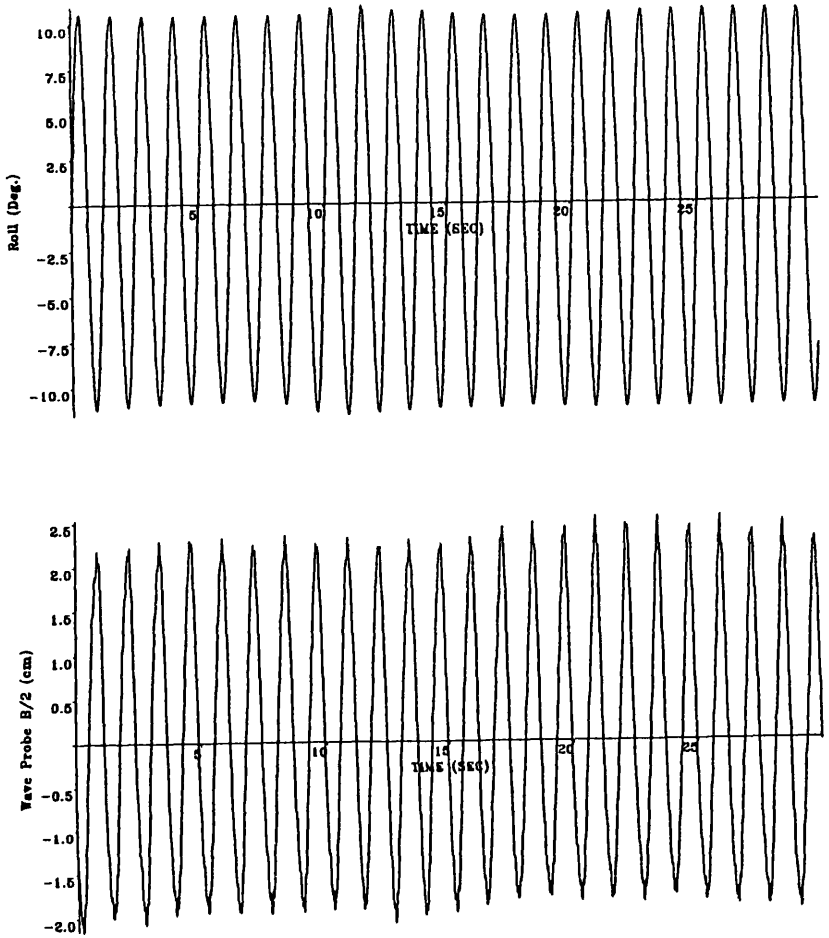

Fig. 6.64 Experimental result, roll time history,
$\zeta^a = 2.0$ cm, $\omega_n = 5.03$ rad / s

Fig. 6.65 Experimental result, free surface elevation

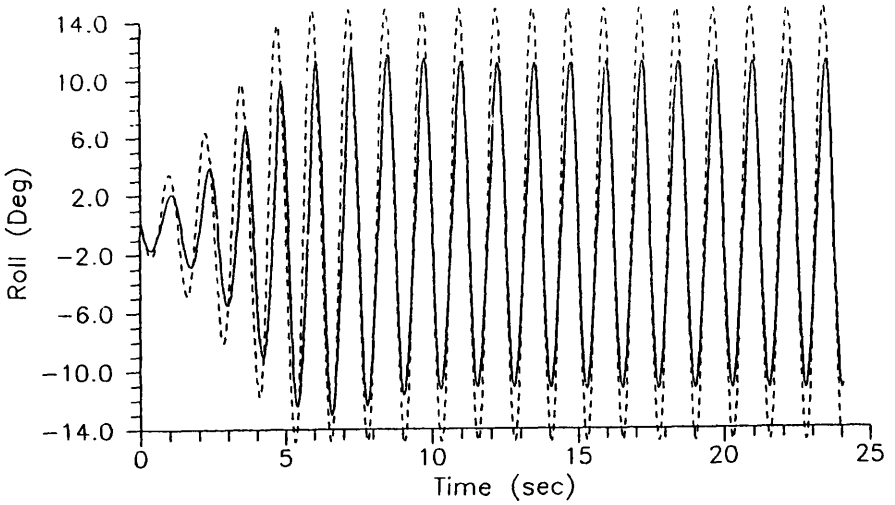

Fig. 6.66 Numerical results, roll time history,
$\zeta^a = 2.0$ cm, $\omega_n = 5.03$ rad / s

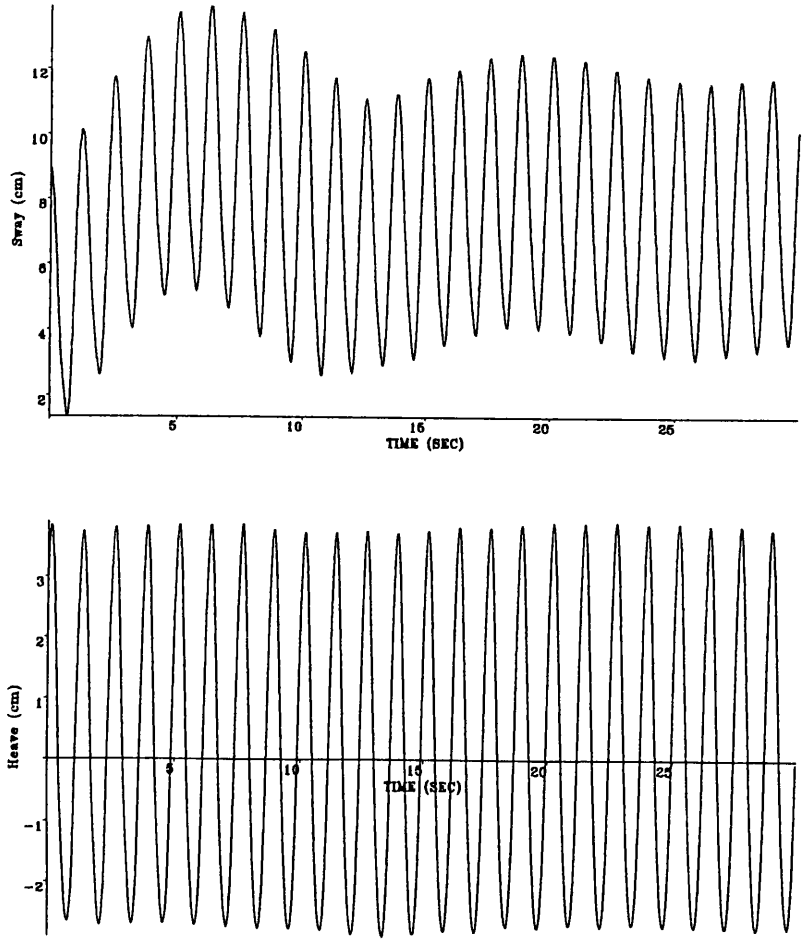

Fig. 6.67, 6.68 Experimental results, sway and heave time histories,
$\zeta^* = 3.4$ cm, $\omega_n = 5.03$ rad / s

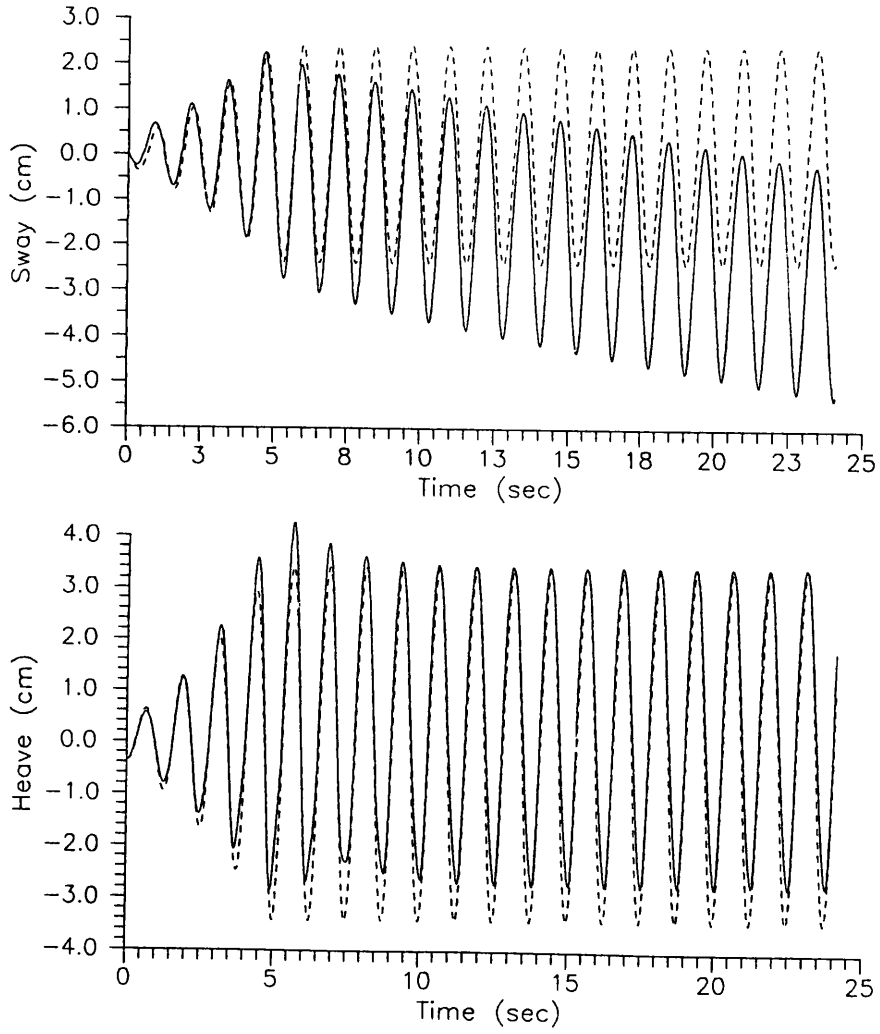

Fig. 6.69, 6.70 Numerical results, sway and heave time histories,
$\zeta^* = 3.4$ cm, $\omega_n = 5.03$ rad / s

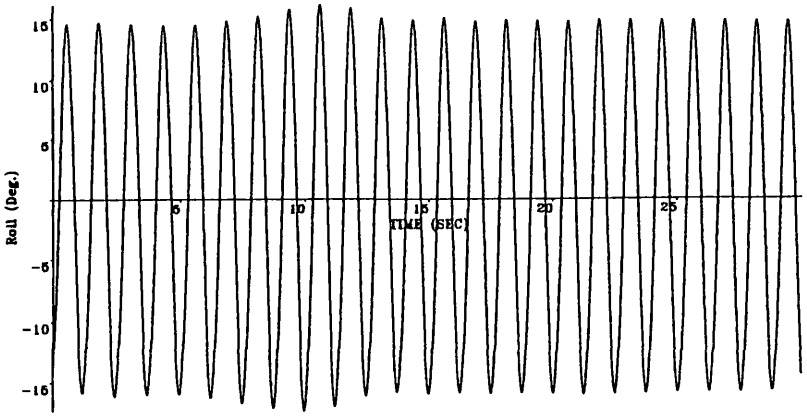

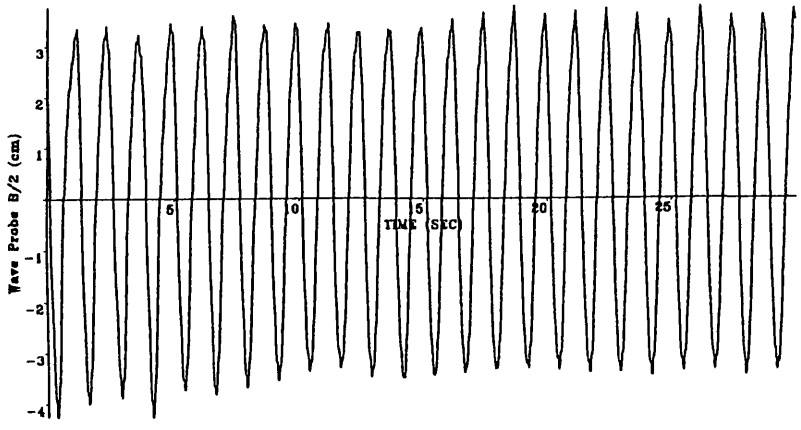

Fig. 6.71 Experimental result, roll time history,
$\zeta_a = 3.4$ cm, $\omega_e = 5.03$ rad / s

Fig. 6.72 Experimental result, free surface elevation

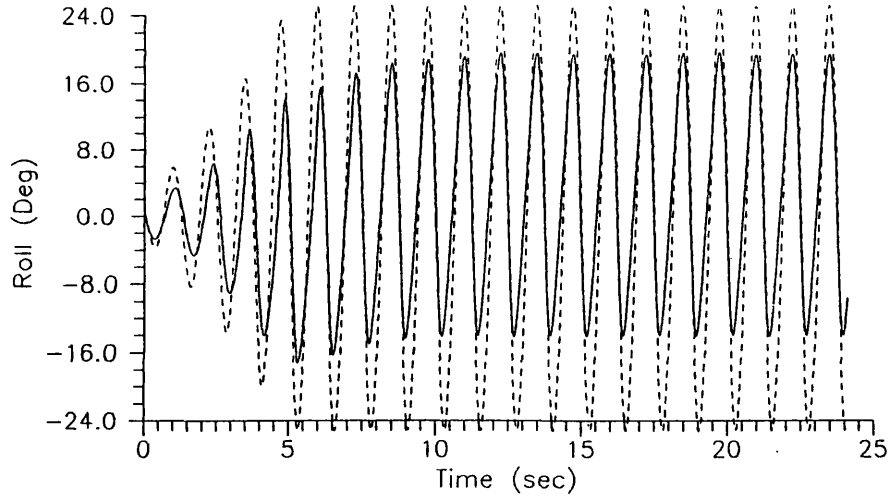

Fig. 6.73 Numerical results, roll time history,
$\zeta_a = 3.4$ cm, $\omega_e = 5.03$ rad / s

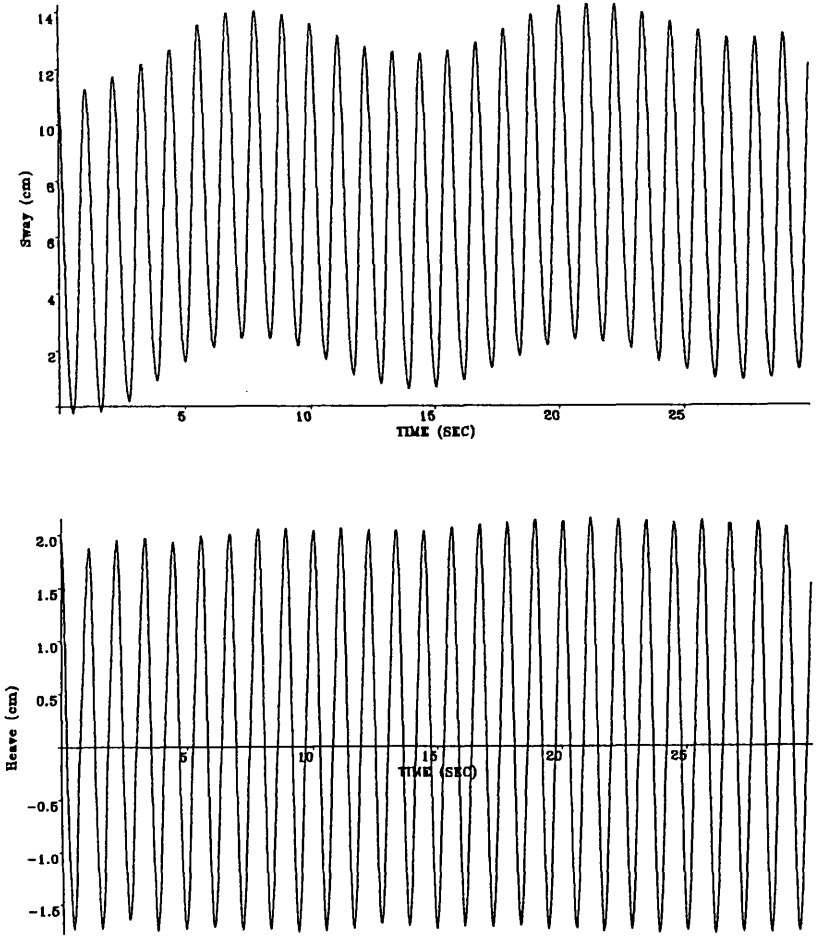

Fig. 6.74, 6.75 Experimental results, sway and heave time histories,
ζ_a = 2.0 cm, ω_n = 5.65 rad / s

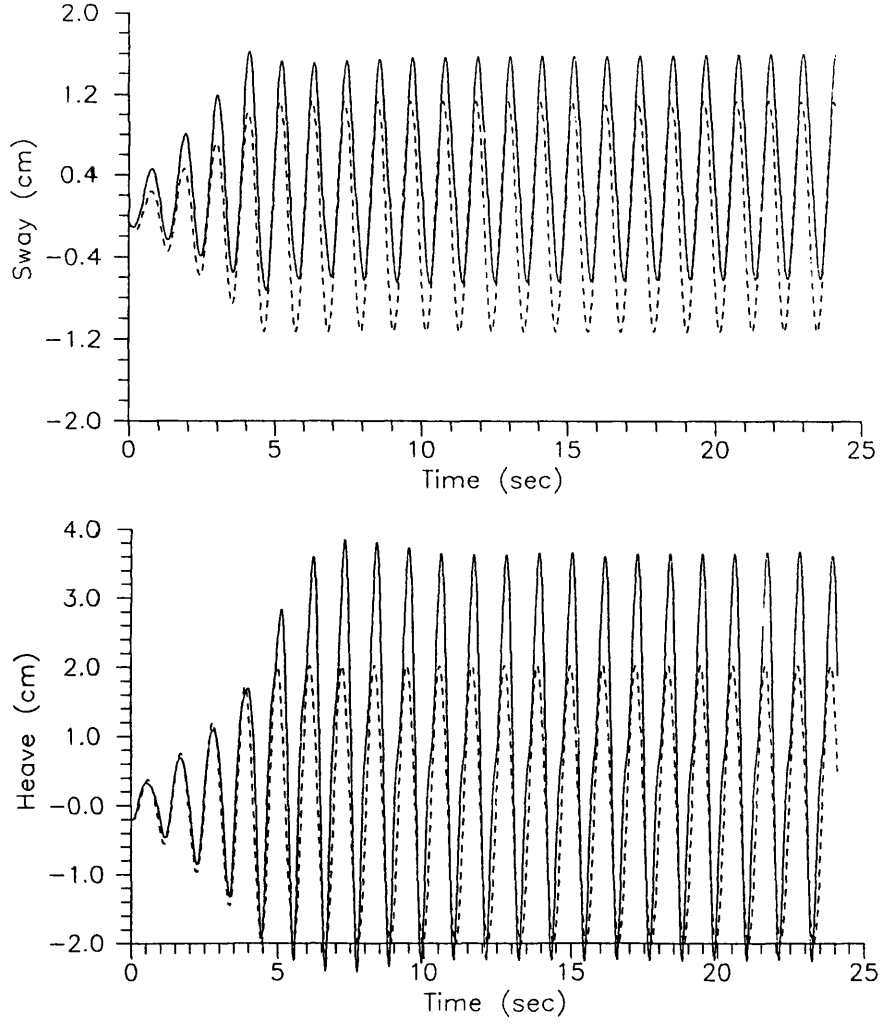

Fig. 6.76, 6.77 Numerical results, sway and heave time histories,
ζ_a = 2.0 cm, ω_n = 5.65 rad / s

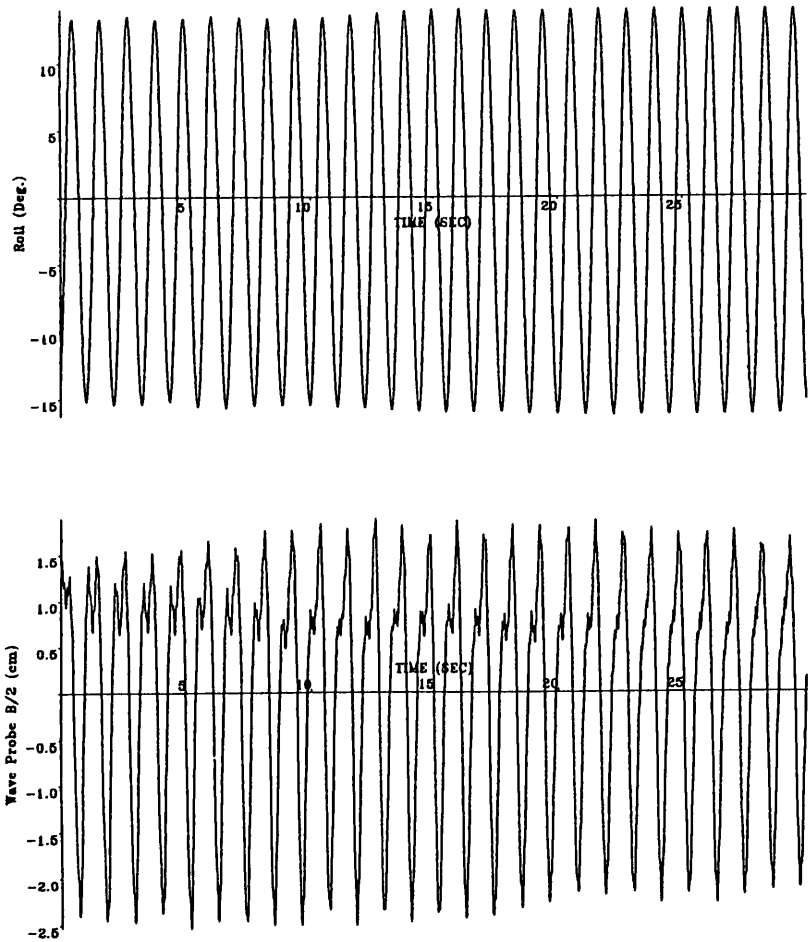

Fig. 6.78 Experimental result, roll time history,
ζ_a = 2.0 cm, ω_e = 5.65 rad / s

Fig. 6.79 Experimental result, free surface elevation

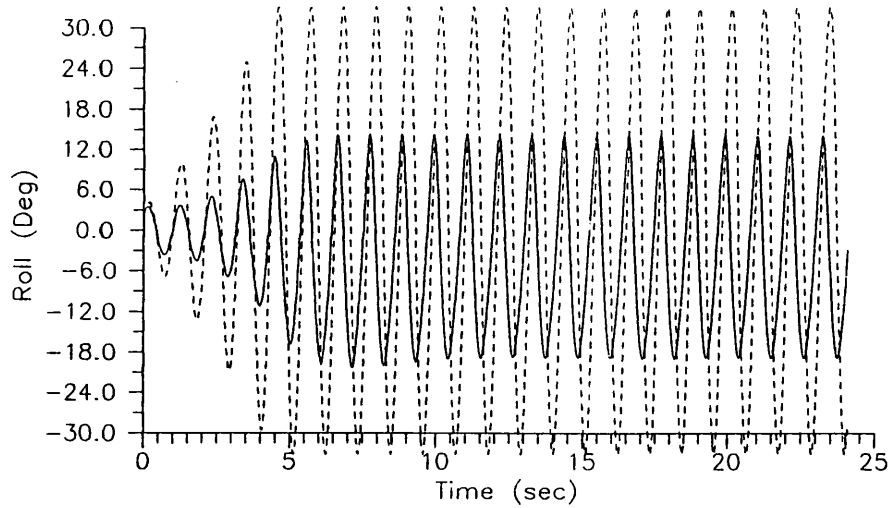

Fig. 6.80 Numerical results, roll time history,
ζ_a = 2.0 cm, ω_e = 5.65 rad / s

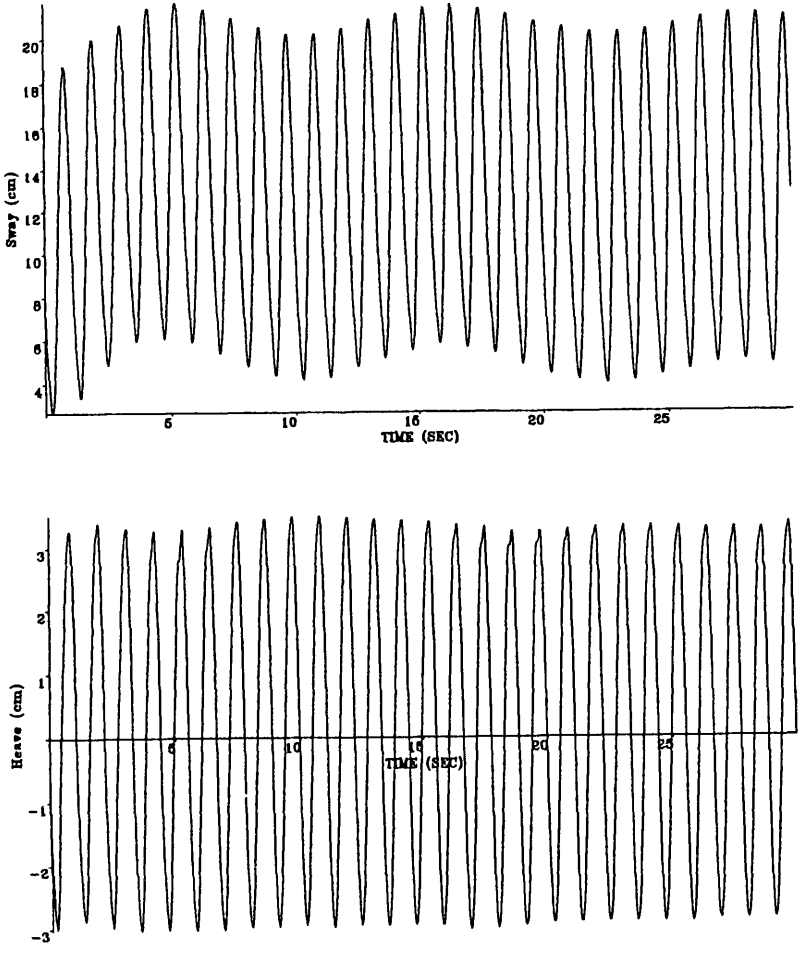

Fig. 6.81, 6.82 Experimental results, sway and heave time histories,
$\zeta^* = 3.0$ cm, $\omega_n = 5.65$ rad / s

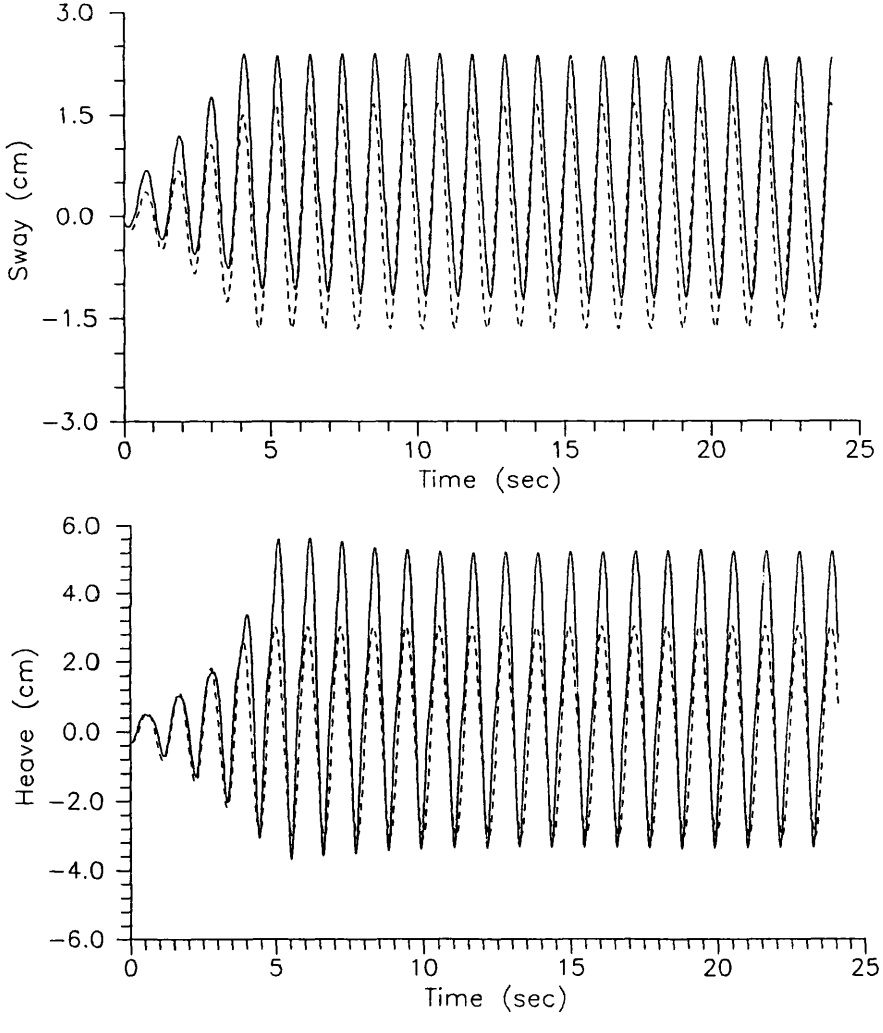

Fig. 6.83, 6.84 Numerical results, sway and heave time histories,
$\zeta^* = 3.0$ cm, $\omega_n = 5.65$ rad / s

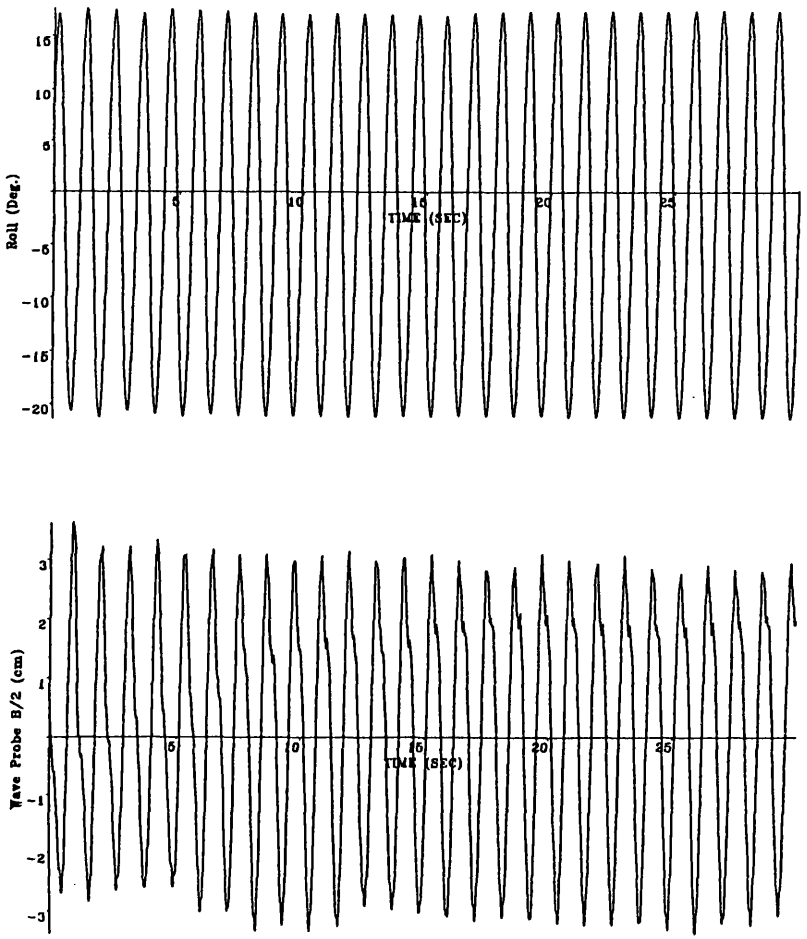

Fig. 6.85 Experimental result, roll time history,
$\zeta^* = 3.0$ cm, $\omega_n = 5.65$ rad / s

Fig. 6.86 Experimental result, free surface elevation

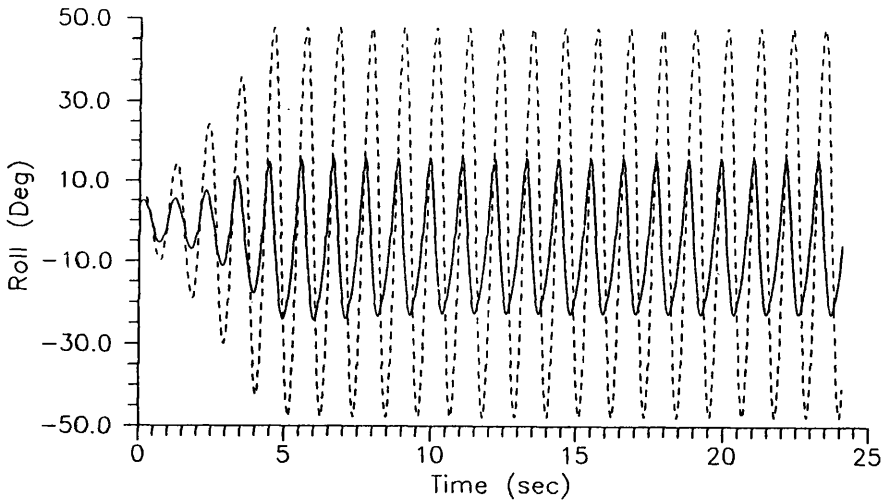

Fig. 6.87 Numerical results, roll time history,
$\zeta^* = 3.0$ cm, $\omega_n = 5.65$ rad / s

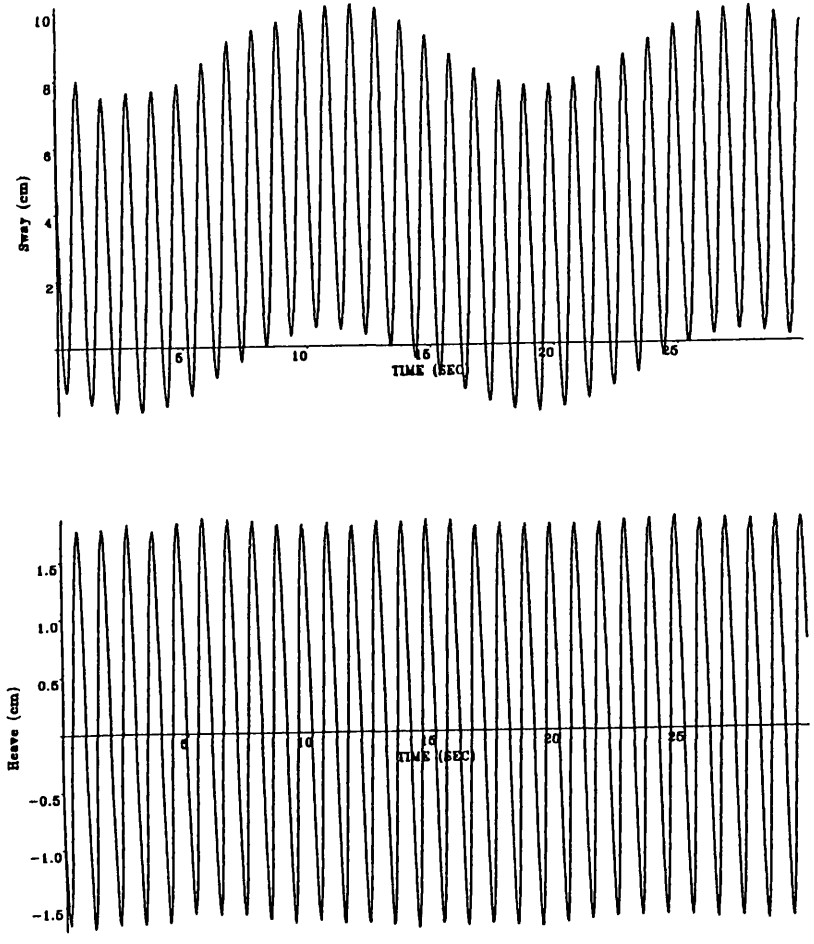

Fig. 6.88, 6.89 Experimental results, sway and heave time histories,
$\zeta^* = 2.0$ cm, $\omega_n = 6.28$ rad / s

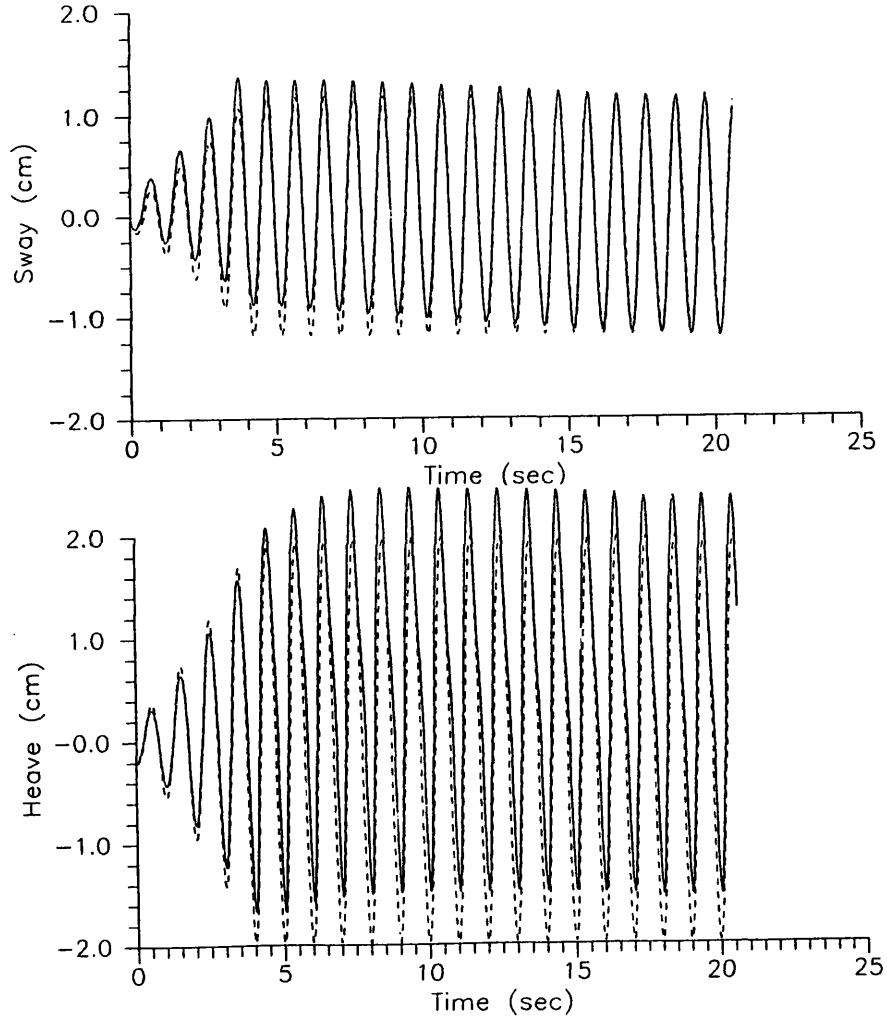

Fig. 6.90, 6.91 Numerical results, sway and heave time histories,
$\zeta^* = 2.0$ cm, $\omega_n = 6.28$ rad / s

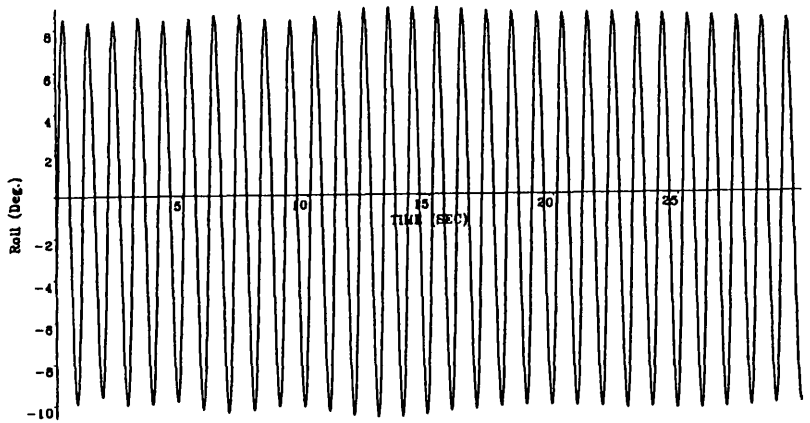

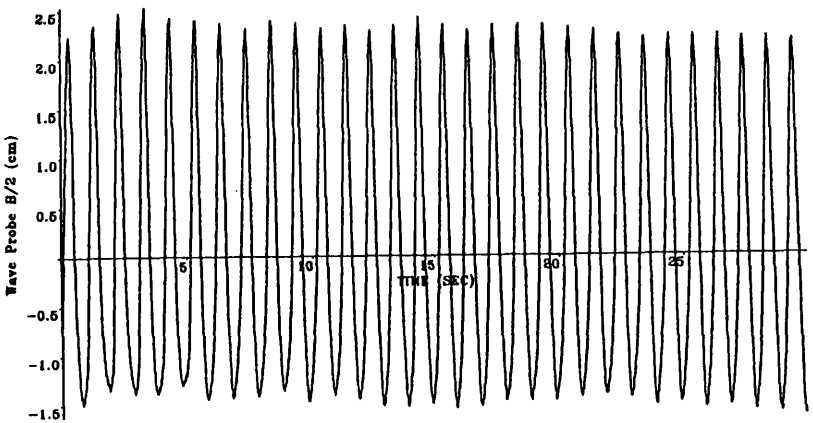

Fig. 6.92 Experimental result, roll time history,
$\zeta_a = 2.0$ cm, $\omega_0 = 6.28$ rad / s

Fig. 6.93 Experimental result, free surface elevation

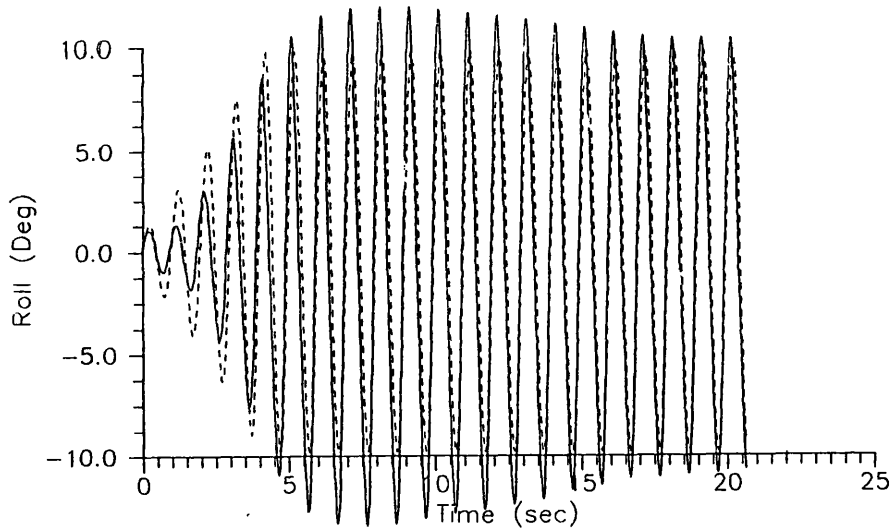

Fig. 6.94 Numerical results, roll time history,
$\zeta_a = 2.0$ cm, $\omega_0 = 6.28$ rad / s

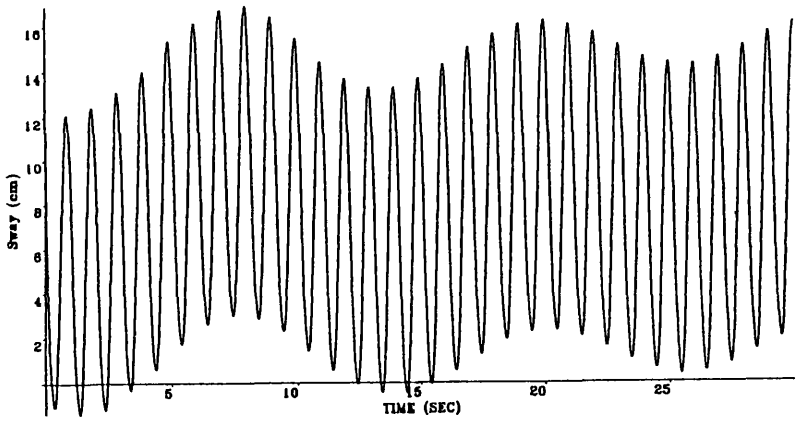

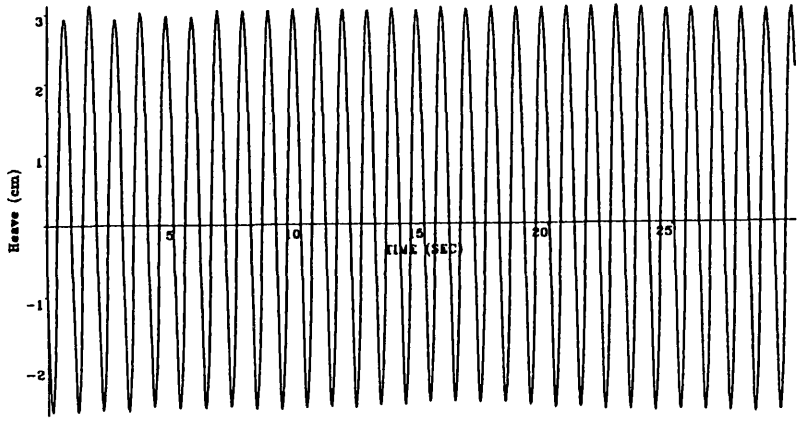

Fig. 6.95, 6.96 Experimental results, sway and heave time histories,
$\zeta^* = 3.0$ cm, $\omega_n = 6.28$ rad / s

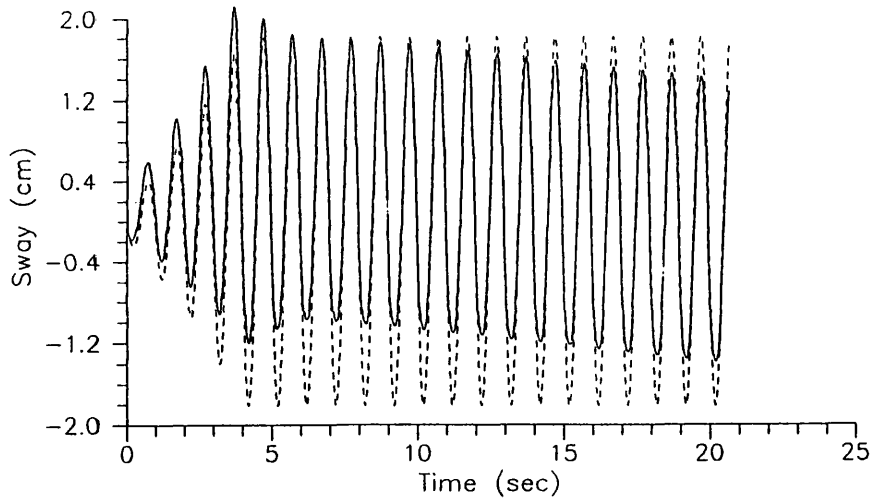

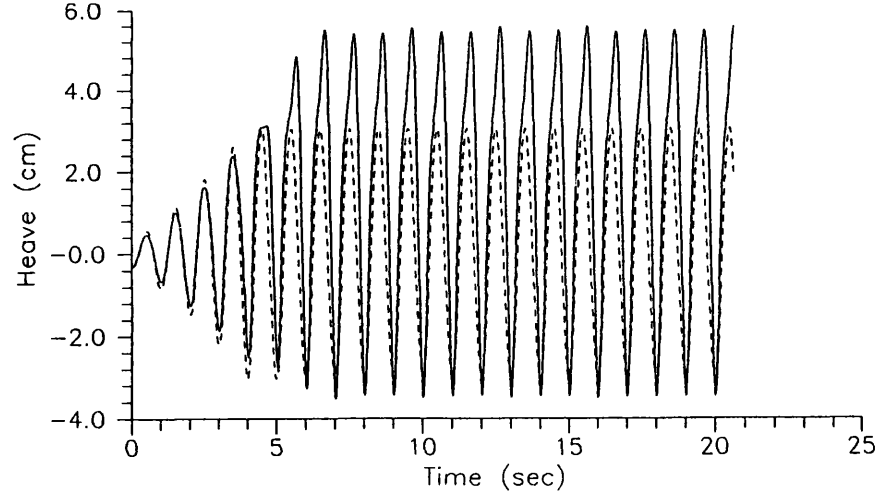

Fig. 6.97, 6.98 Numerical results, sway and heave time histories,
$\zeta^* = 3.0$ cm, $\omega_n = 6.28$ rad / s

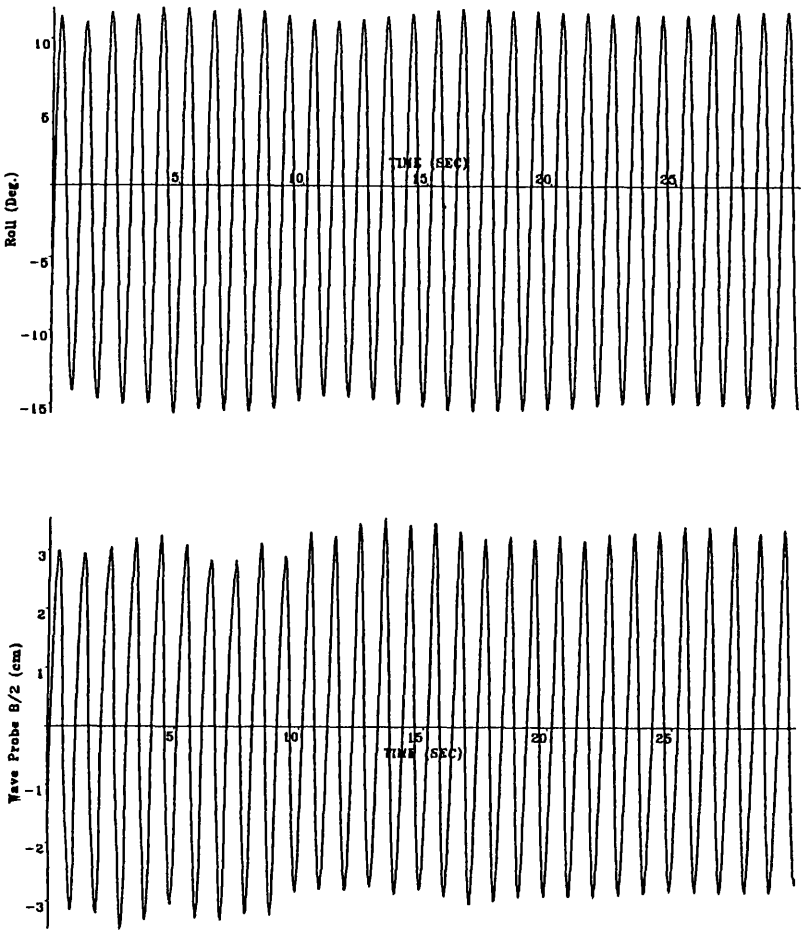

Fig. 6.99 Experimental result, roll time history,
ζ_a = 3.0 cm, ω_n = 6.28 rad / s

Fig. 6.100 Experimental result, free surface elevation

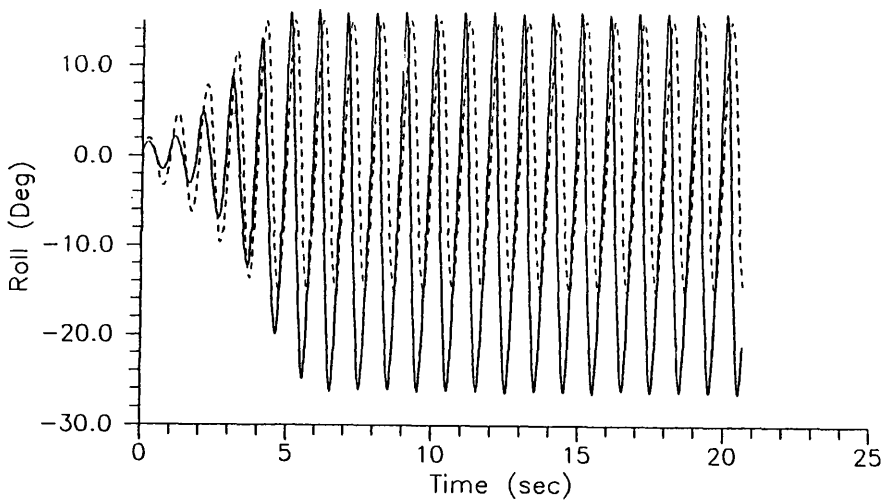

Fig. 6.101 Numerical results, roll time history,
ζ_a = 3.0 cm, ω_n = 6.28 rad / s

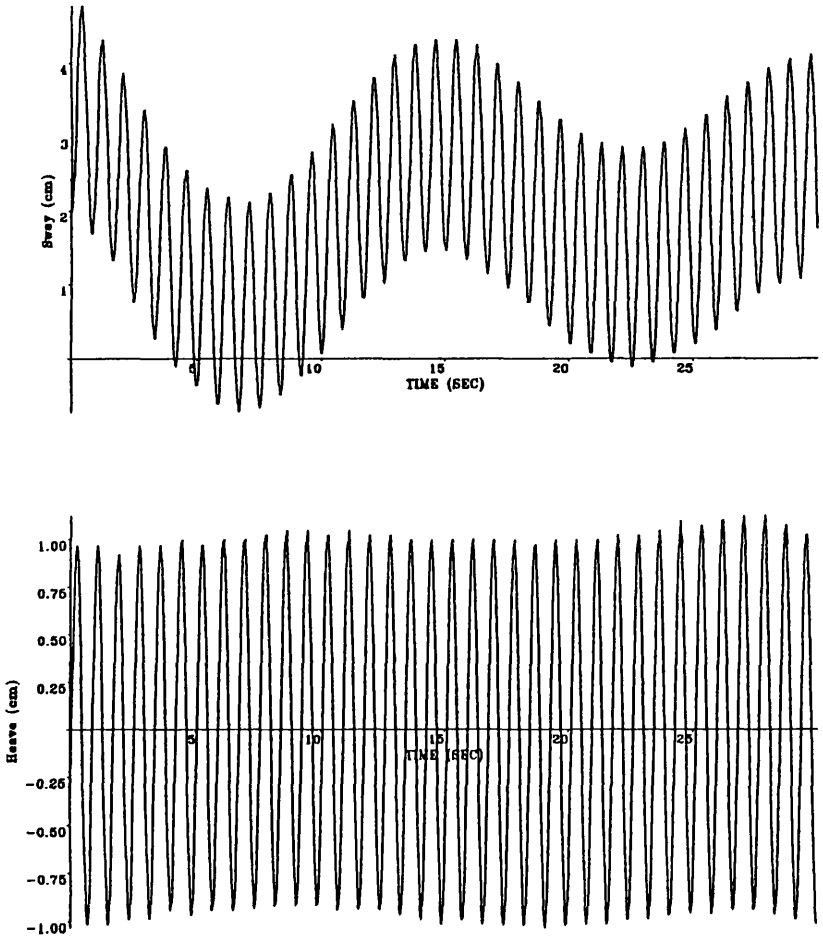

Fig. 6.102, 6.103 Experimental results, sway and heave time histories, $\zeta^* = 1.2$ cm, $\omega_n = 7.54$ rad / s

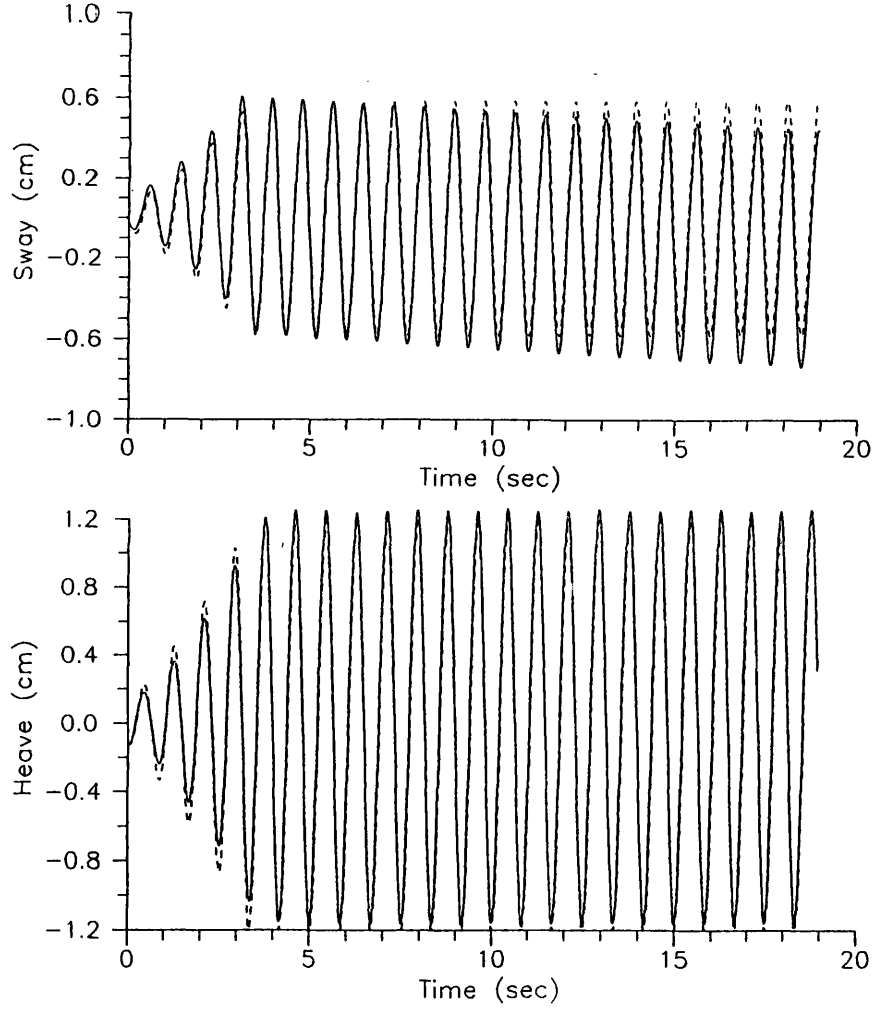

Fig. 6.104, 6.105 Numerical results, sway and heave time histories, $\zeta^* = 1.2$ cm, $\omega_n = 7.54$ rad / s

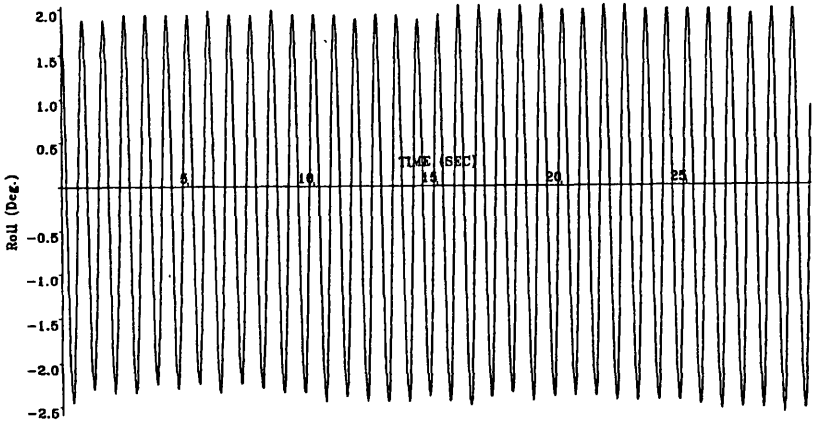

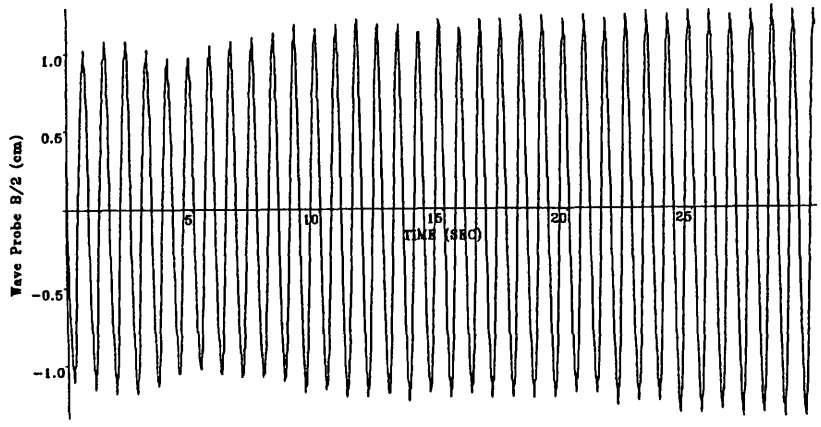

Fig. 6.106 Experimental result, roll time history,
$\zeta^* = 1.2$ cm, $\omega_n = 7.54$ rad / s

Fig. 6.107 Experimental result, free surface elevation

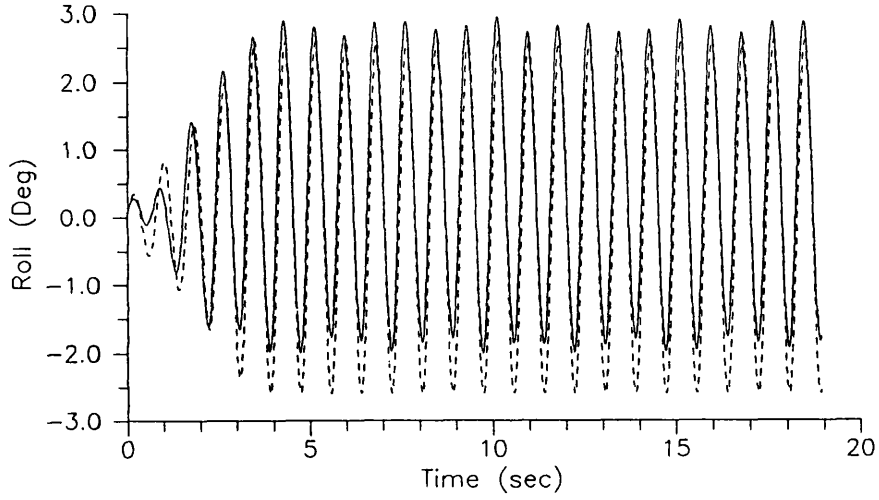

Fig. 6.108 Numerical results, roll time history,
$\zeta^* = 1.2$ cm, $\omega_n = 7.54$ rad / s

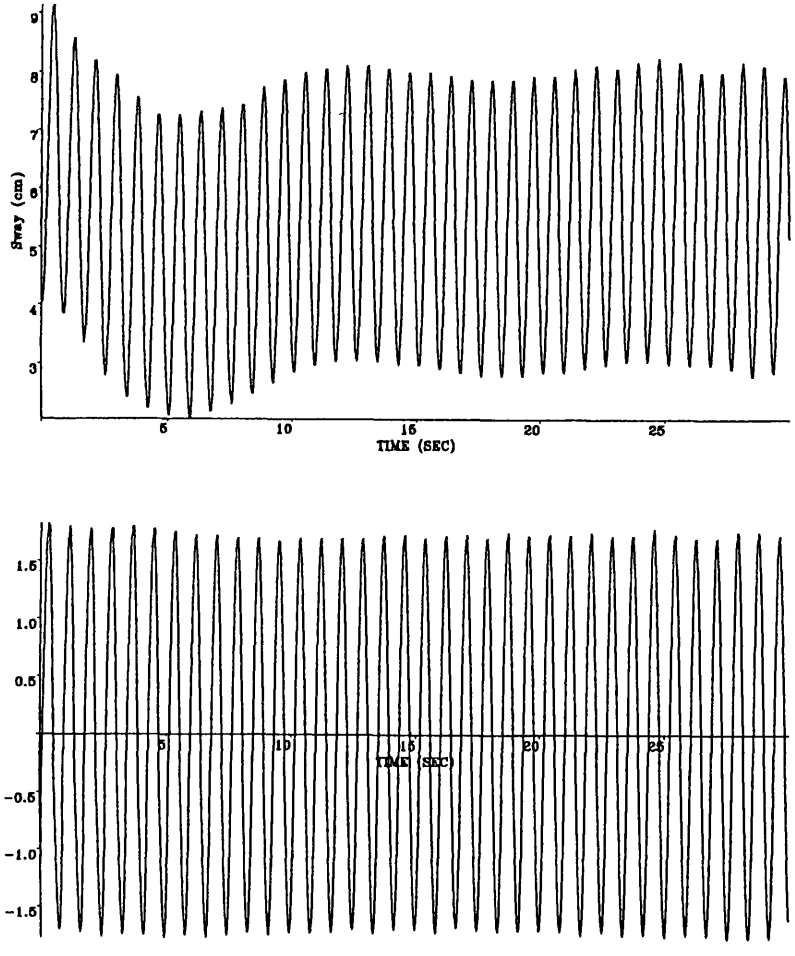

Fig. 6.109, 6.110 Experimental results, sway and heave time histories,
$\zeta^* = 1.8$ cm, $\omega_0 = 7.54$ rad / s

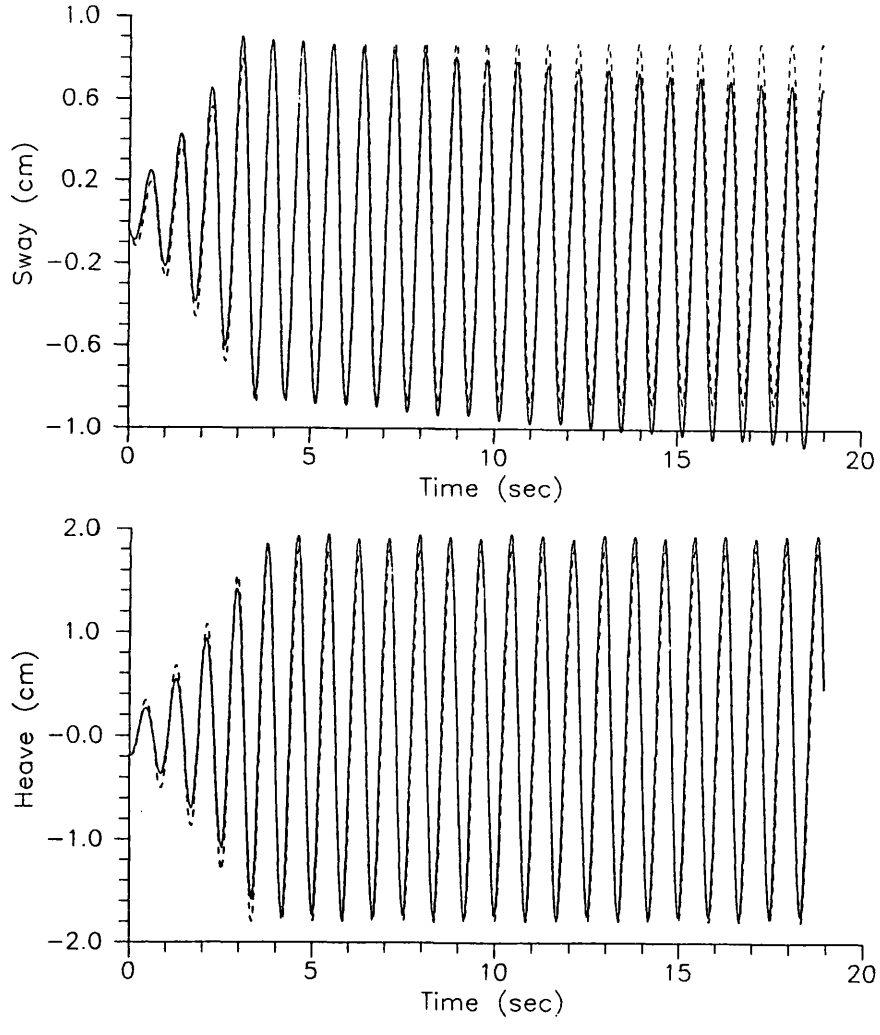

Fig. 6.111, 6.112 Numerical results, sway and heave time histories,
$\zeta^* = 1.8$ cm, $\omega_0 = 7.54$ rad / s

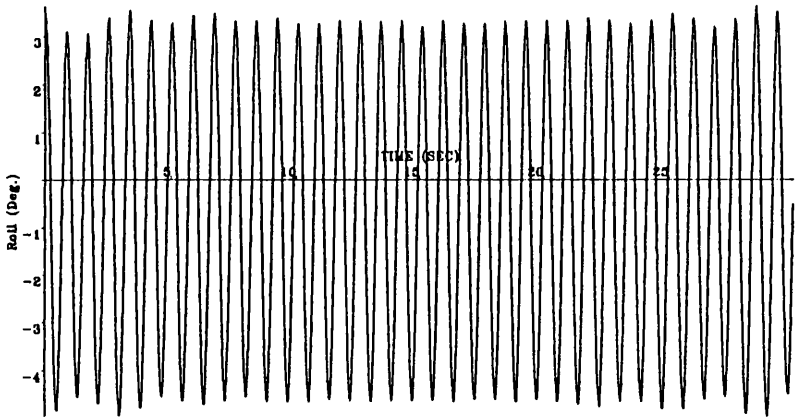

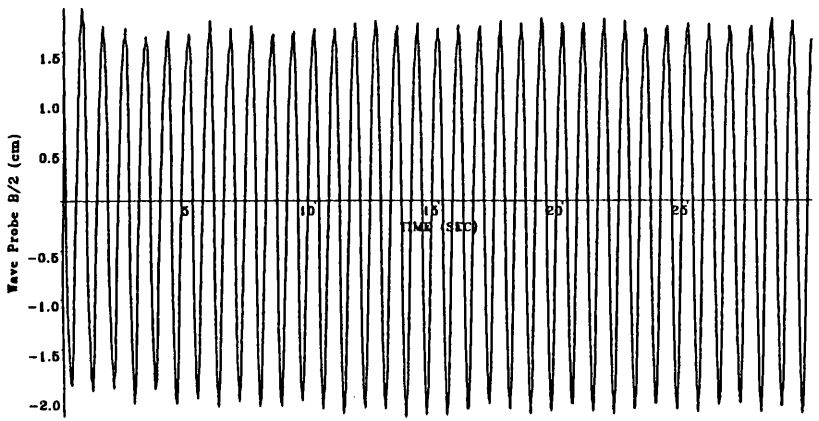

Fig. 6.113 Experimental result, roll time history,
$\zeta^* = 1.8$ cm, $\omega_n = 7.54$ rad / s

Fig. 6.114 Experimental result, free surface elevation

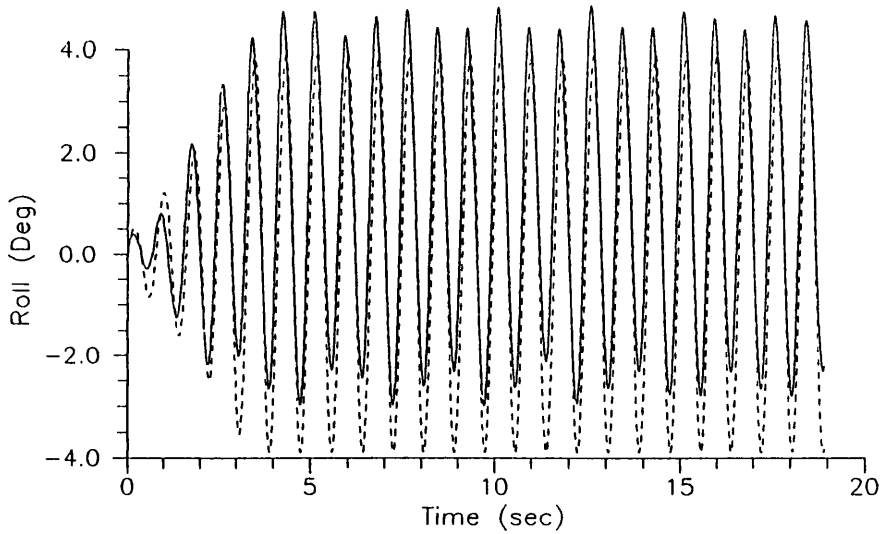

Fig. 6.115 Numerical results, roll time history,
$\zeta^* = 1.8$ cm, $\omega_n = 7.54$ rad / s

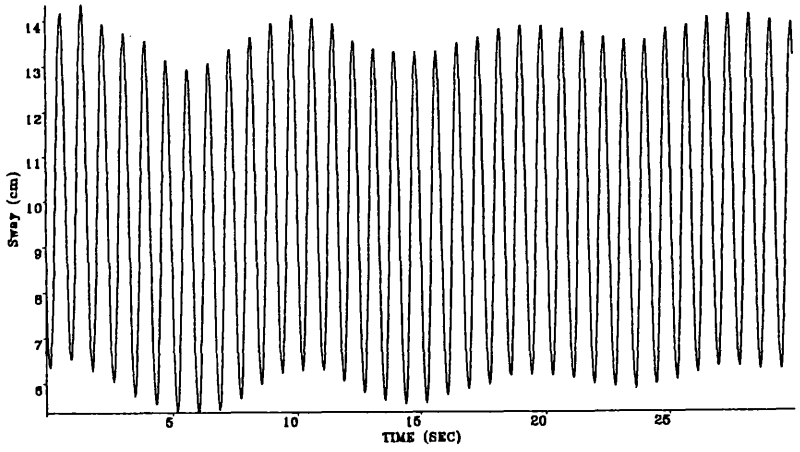

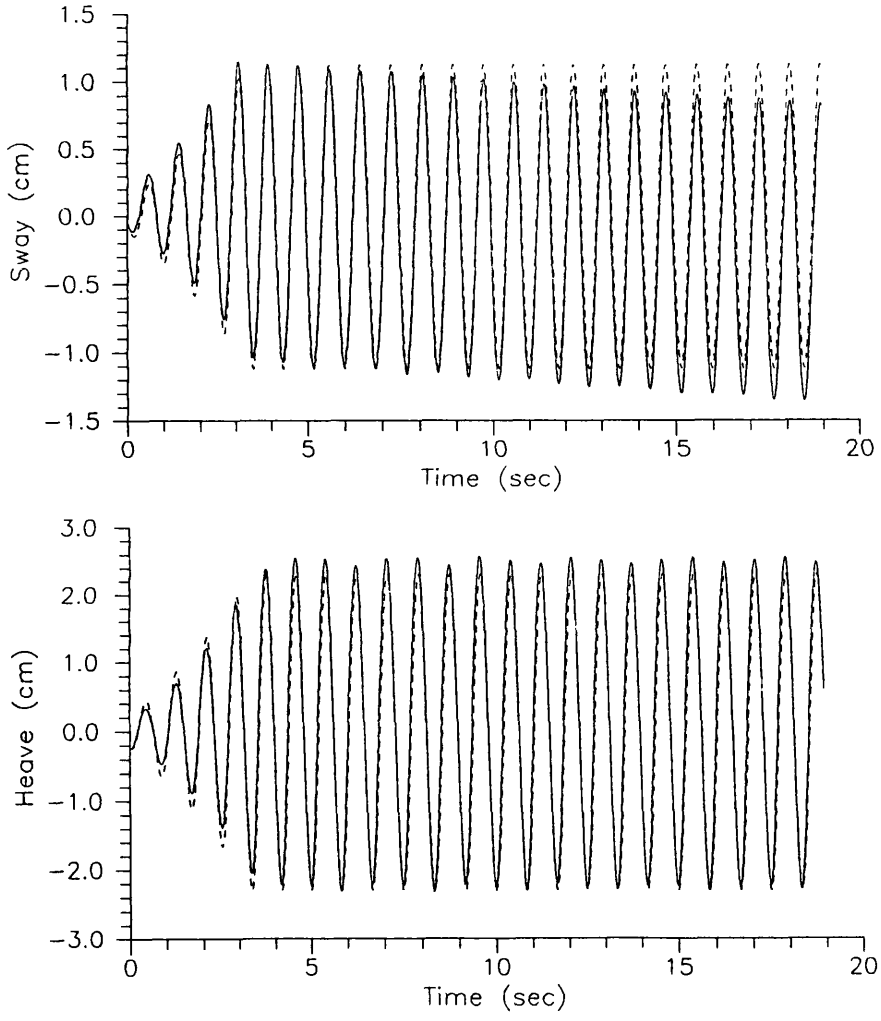

Fig. 6.116, 6.117 Experimental results, sway and heave time histories, $\zeta^* = 2.3$ cm, $\omega_n = 7.54$ rad / s

Fig. 6.118, 6.119 Numerical results, sway and heave time histories, $\zeta^* = 2.3$ cm, $\omega_n = 7.54$ rad / s

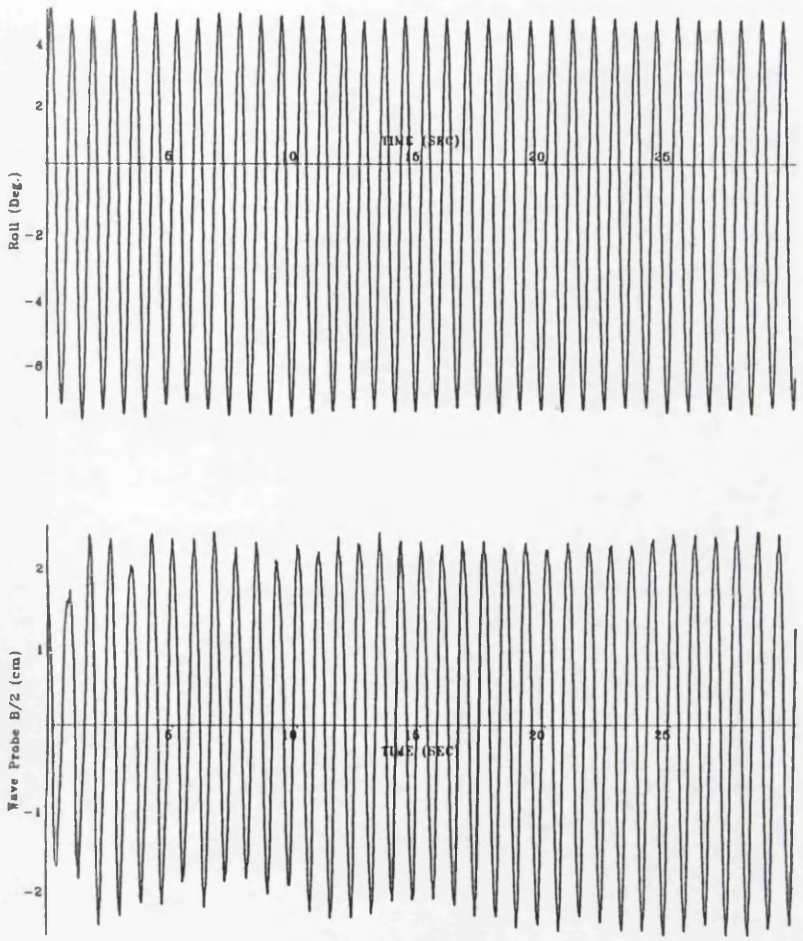

Fig. 6.120 Experimental result, roll time history,
$\zeta^* = 2.3$ cm, $\omega_n = 7.54$ rad / s

Fig. 6.121 Experimental result, free surface elevation

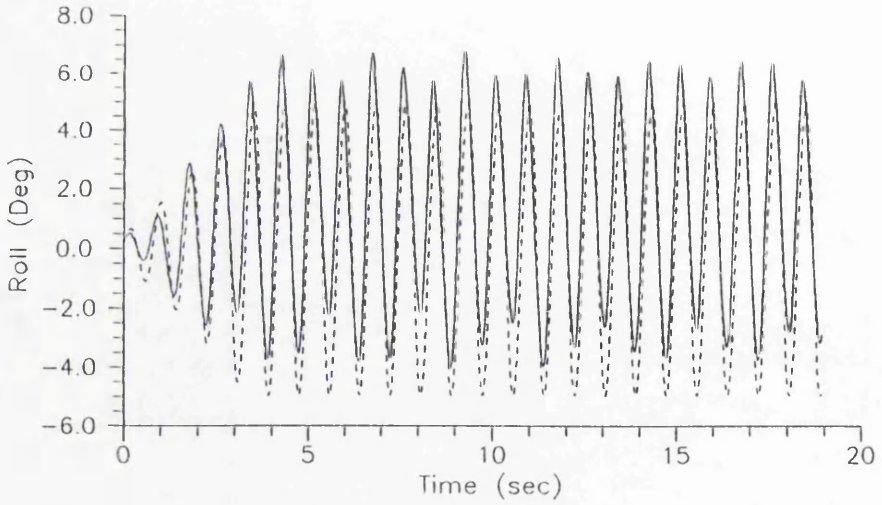

Fig. 6.122 Numerical results, roll time history,
$\zeta^* = 2.3$ cm, $\omega_n = 7.54$ rad / s

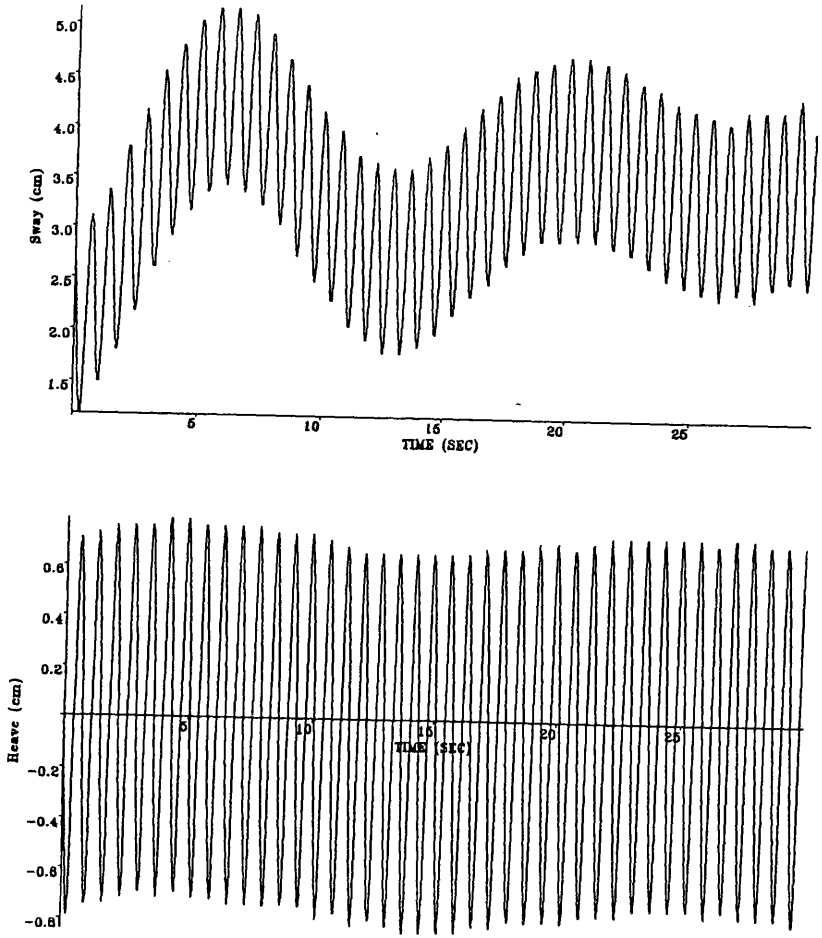

Fig. 6.123, 6.124 Experimental results, sway and heave time histories, $\zeta^* = 1.1$ cm, $\omega_n = 8.80$ rad / s

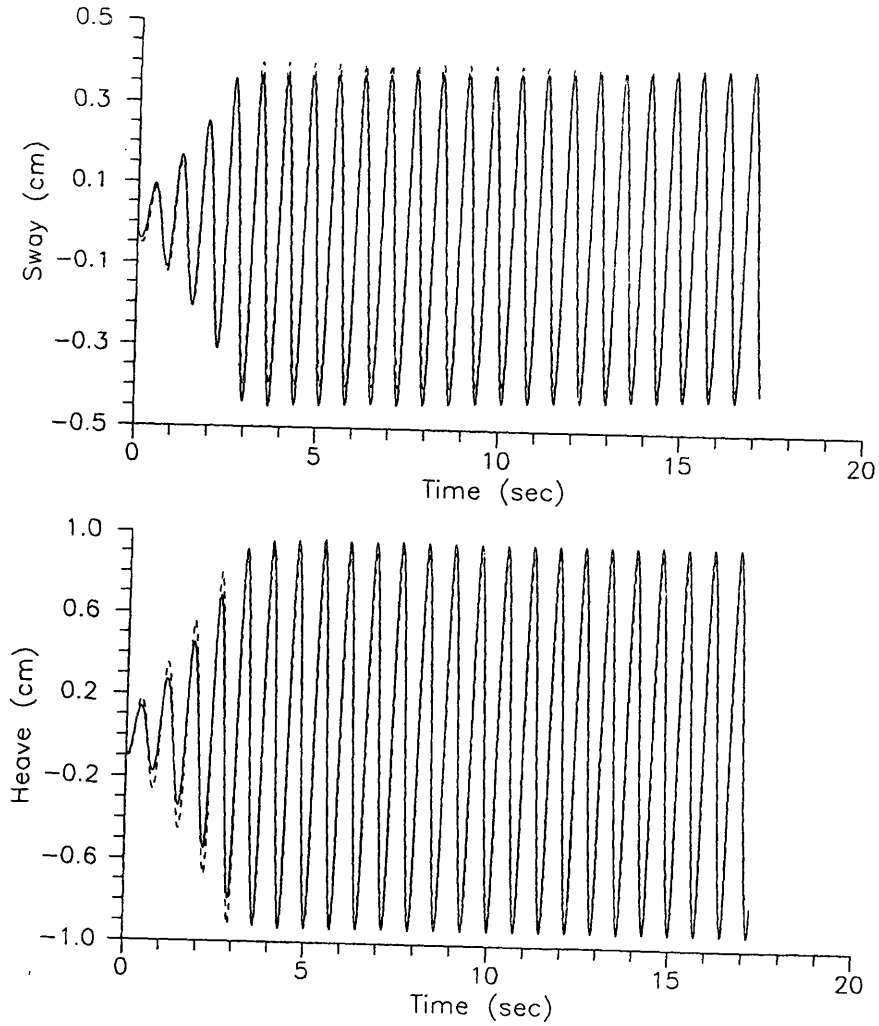

Fig. 6.125, 6.126 Numerical results, sway and heave time histories, $\zeta^* = 1.1$ cm, $\omega_n = 8.80$ rad / s

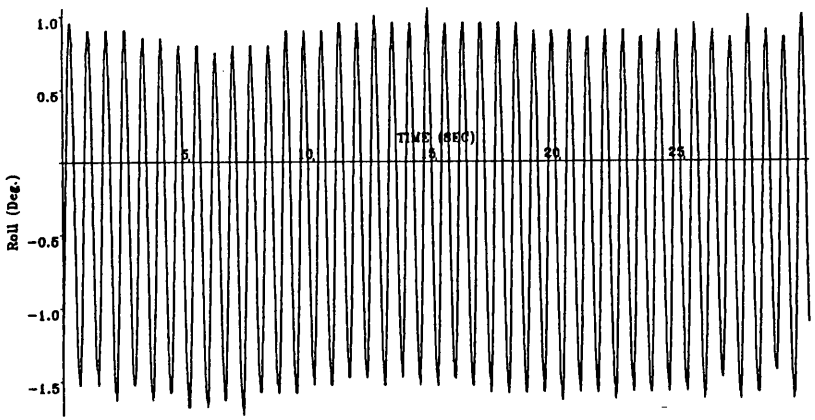

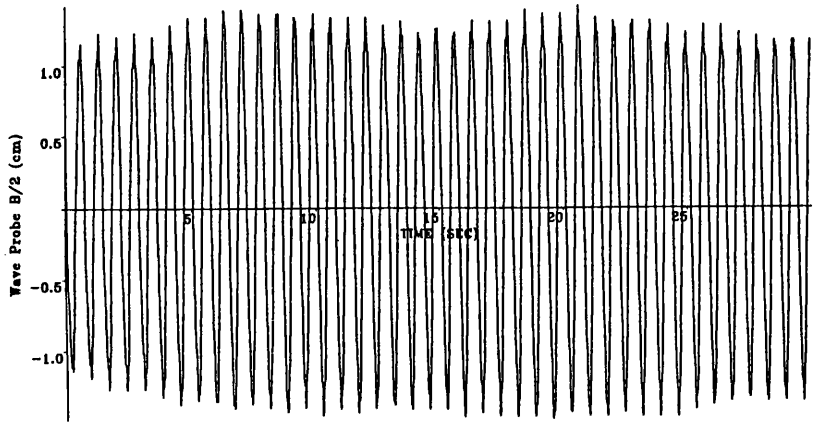

Fig. 6.127 Experimental result, roll time history,
$\zeta^a = 1.1$ cm, $\omega_e = 8.80$ rad / s

Fig. 6.128 Experimental result, free surface elevation

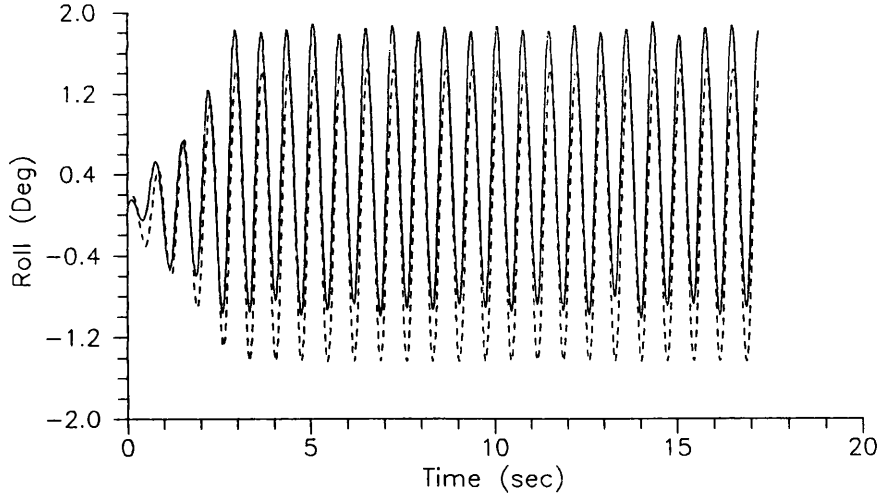

Fig. 6.129 Numerical results, roll time history,
$\zeta^a = 1.1$ cm, $\omega_e = 8.80$ rad / s

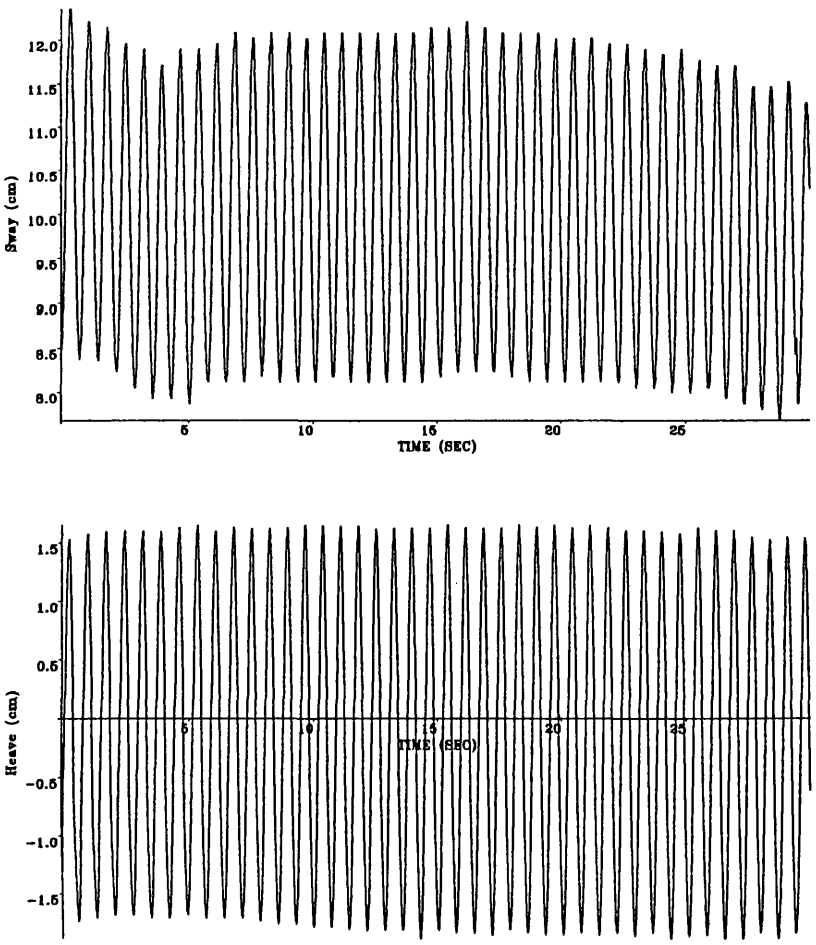

Fig. 6.130, 6.131 Experimental results, sway and heave time histories, $\zeta^* = 1.5$ cm, $\omega_n = 8.80$ rad / s

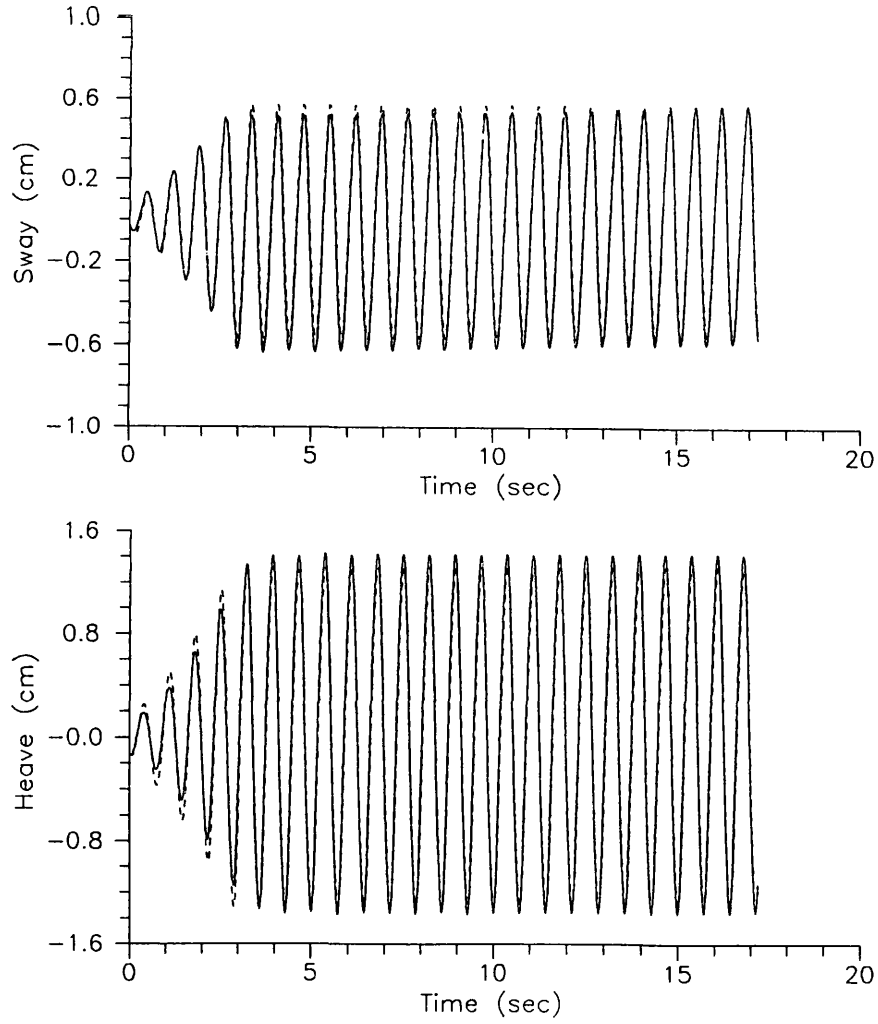

Fig. 6.132, 6.133 Numerical results, sway and heave time histories, $\zeta^* = 1.5$ cm, $\omega_n = 8.80$ rad / s

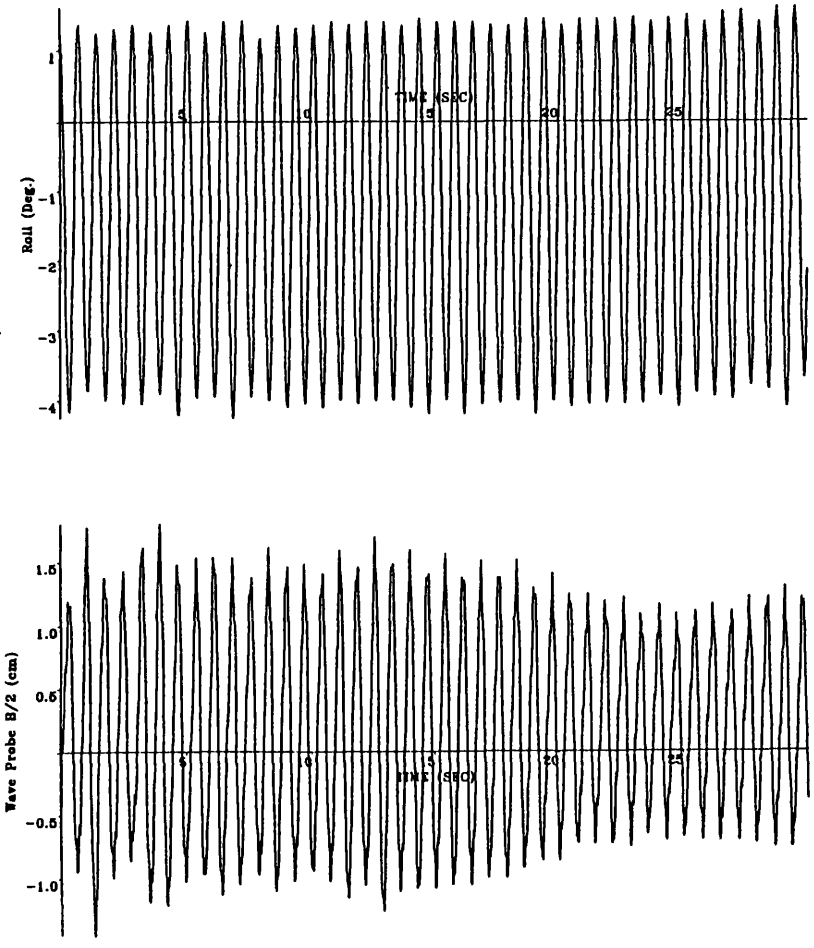

Fig. 6.134 Experimental result, roll time history,
ζ_a = 1.5 cm, ω_n = 8.80 rad / s

Fig. 6.135 Experimental result, free surface elevation

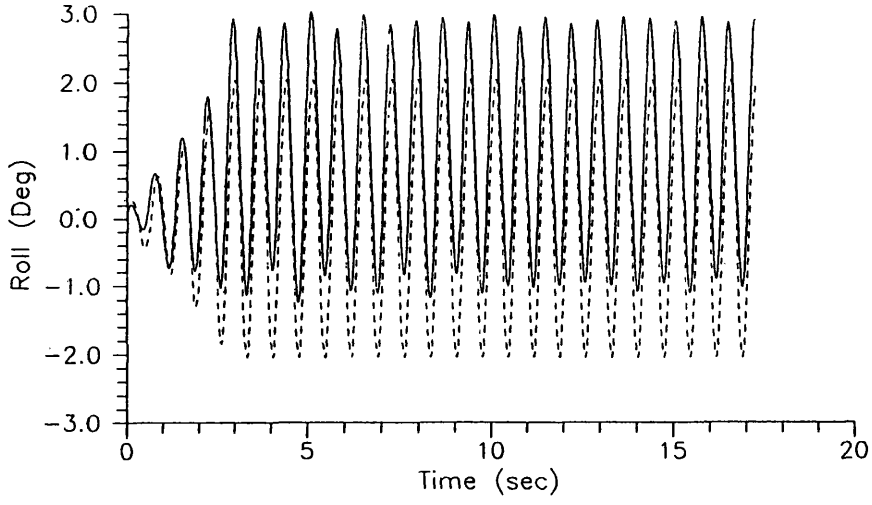

Fig. 6.136 Numerical results, roll time history,
ζ_a = 1.5 cm, ω_n = 8.80 rad / s

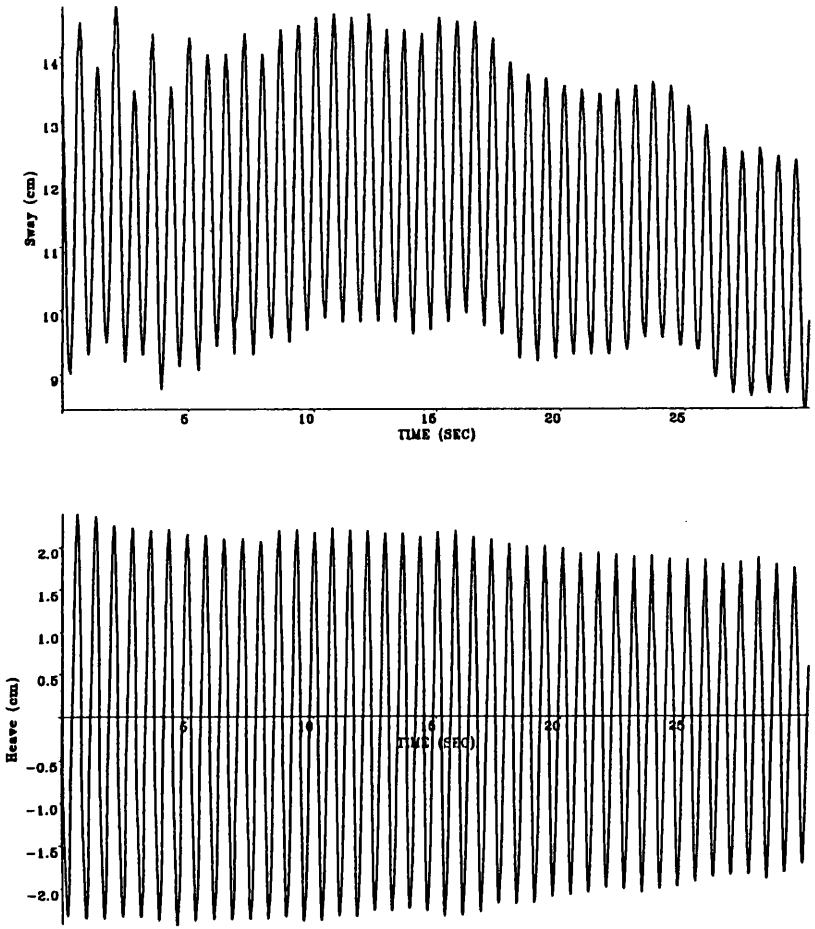

Fig. 6.137, 6.138 Experimental results, sway and heave time histories, $\zeta^* = 2.5$ cm, $\omega_n = 8.80$ rad / s

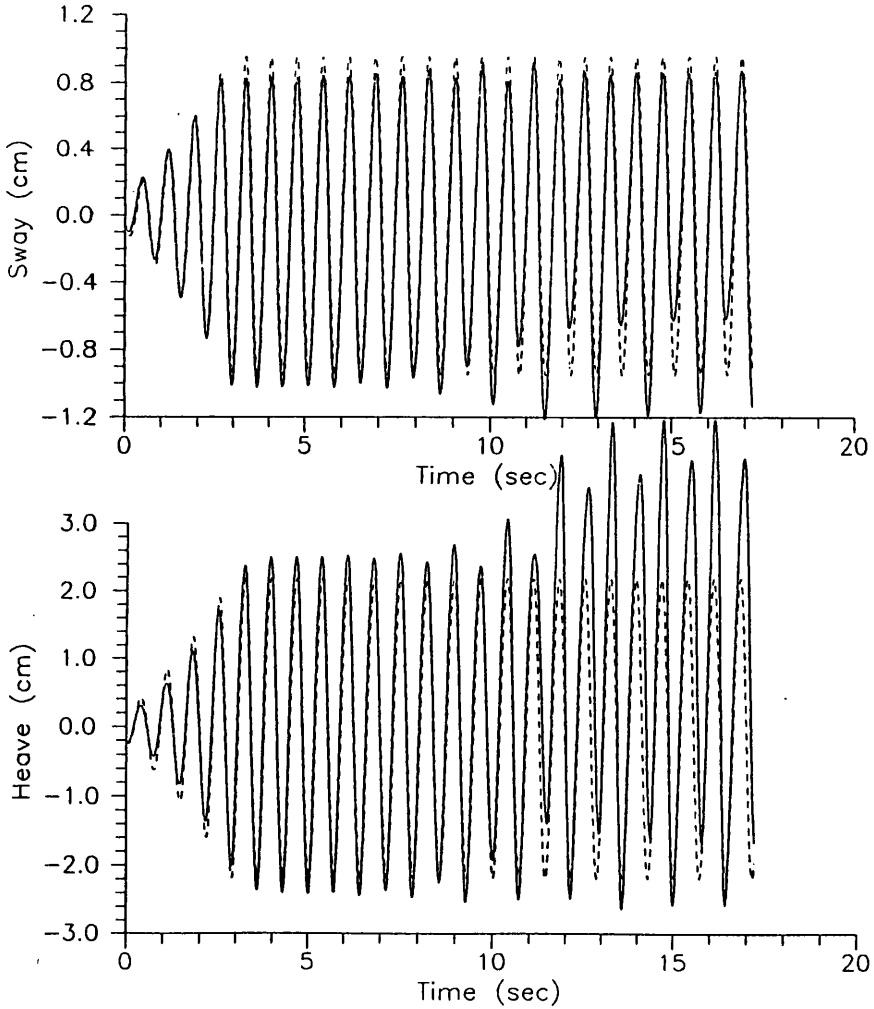

Fig. 6.139, 6.140 Numerical results, sway and heave time histories, $\zeta^* = 2.5$ cm, $\omega_n = 8.80$ rad / s

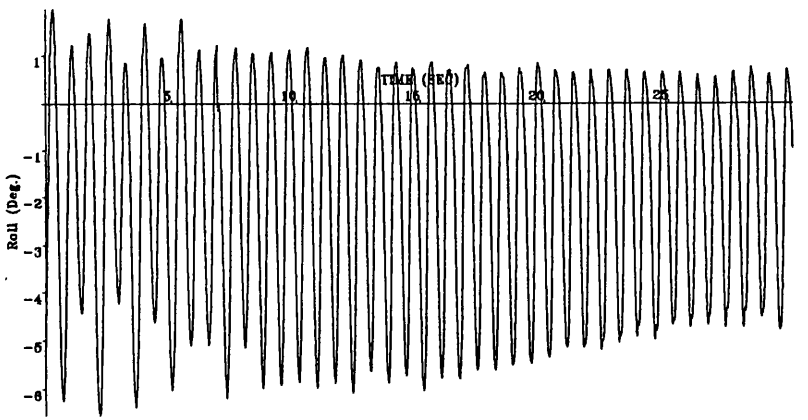

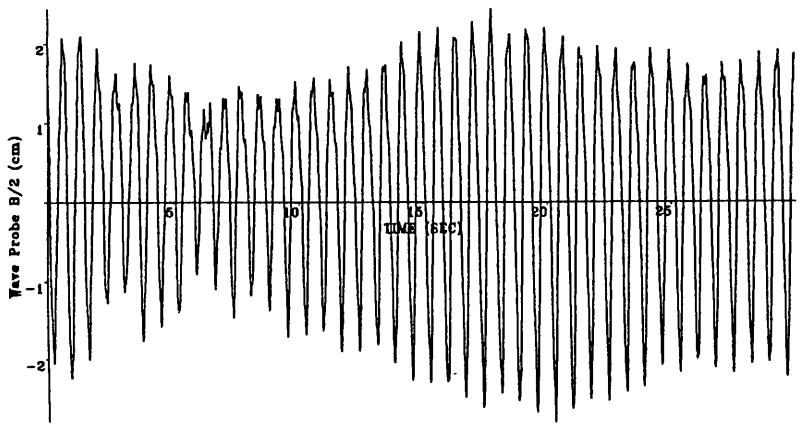

Fig. 6.141 Experimental result, roll time history,
$\zeta^* = 2.5$ cm, $\omega_n = 8.80$ rad / s

Fig. 6.142 Experimental result, free surface elevation

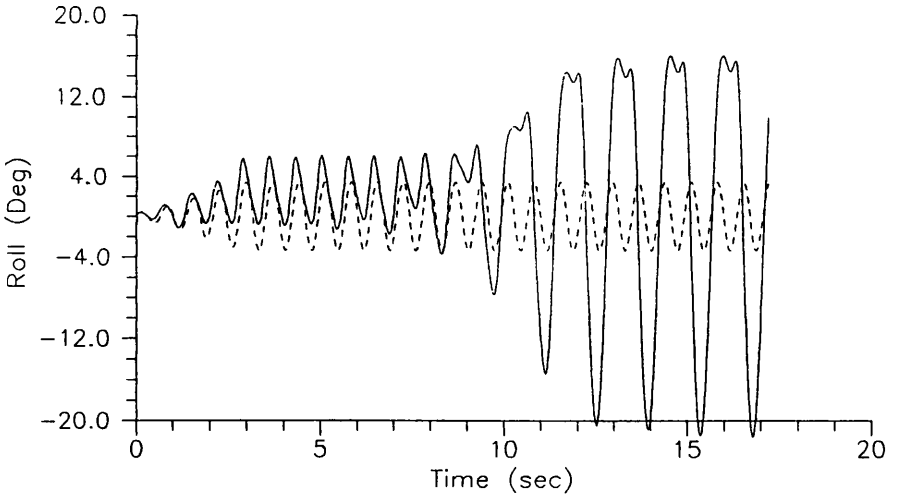

Fig. 6.143 Numerical results, roll time history,
$\zeta^* = 2.5$ cm, $\omega_n = 8.80$ rad / s

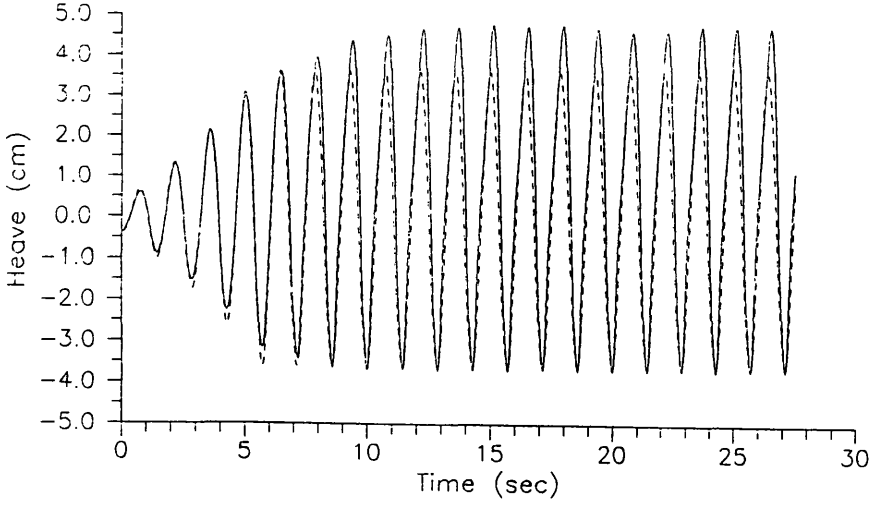

Fig. 6.56 Heave time-domain solution
$\zeta^* = 3.6$ cm, $\omega_0 = 4.40$ rad / s

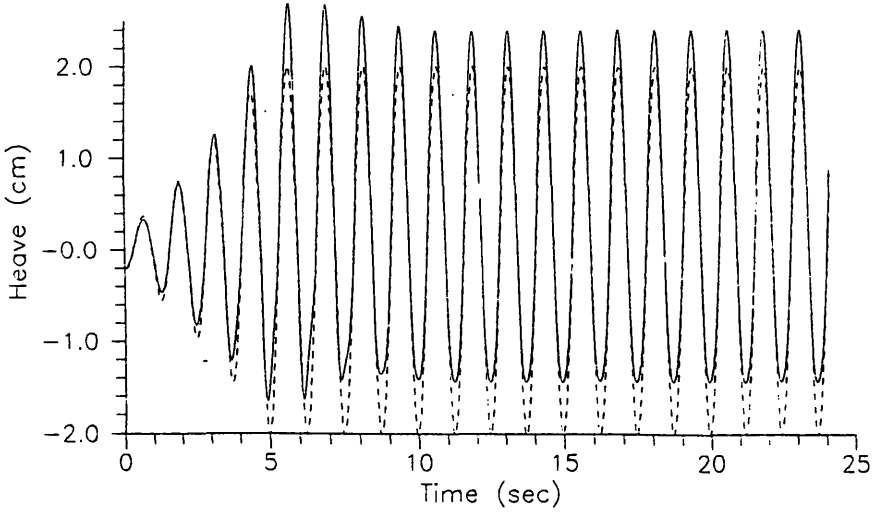

Fig. 6.77 Heave time-domain solution
$\zeta^* = 2.0$ cm, $\omega_0 = 5.03$ rad / s

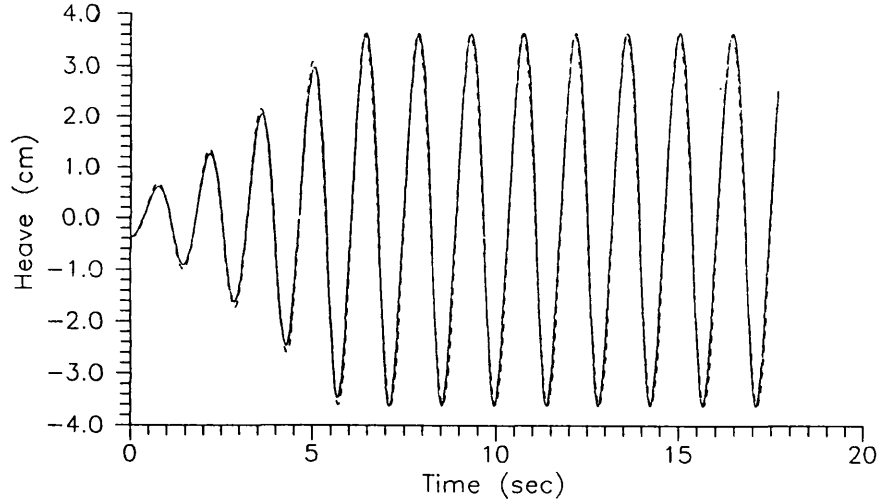

Fig. 6.144 Heave time-domain solution neglecting the coupling with the roll, $\zeta^* = 3.6$ cm, $\omega_0 = 4.40$ rad / s

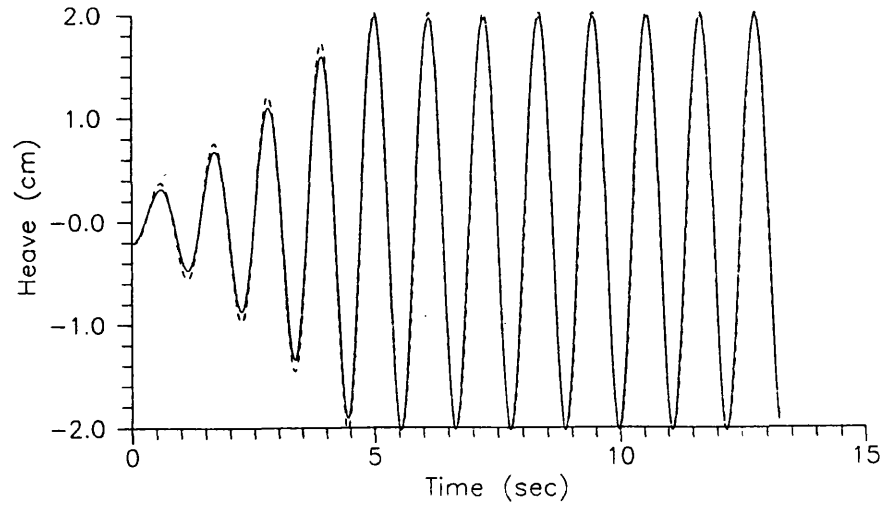

Fig. 6.145 Heave time-domain solution neglecting the coupling with the roll, $\zeta^* = 2.0$ cm, $\omega_0 = 5.03$ rad / s

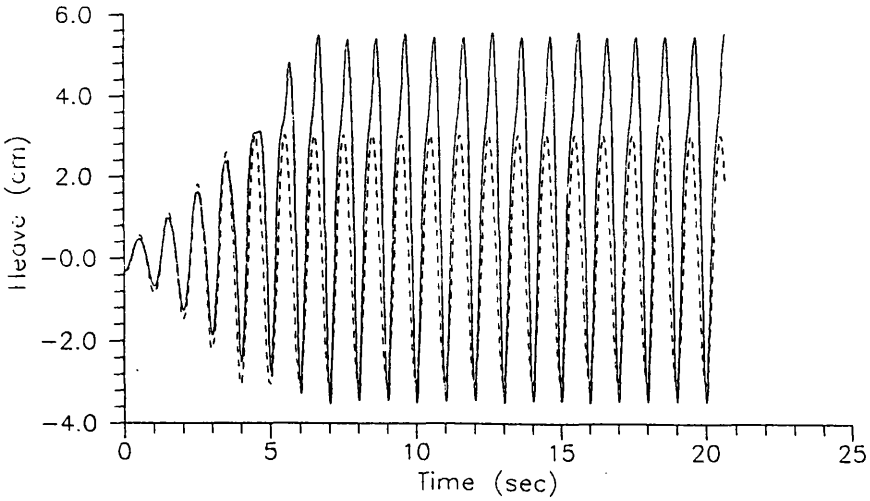

Fig. 6.98 Heave time-domain solution
$\zeta^a = 3.0$ cm, $\omega_a = 6.28$ rad / s

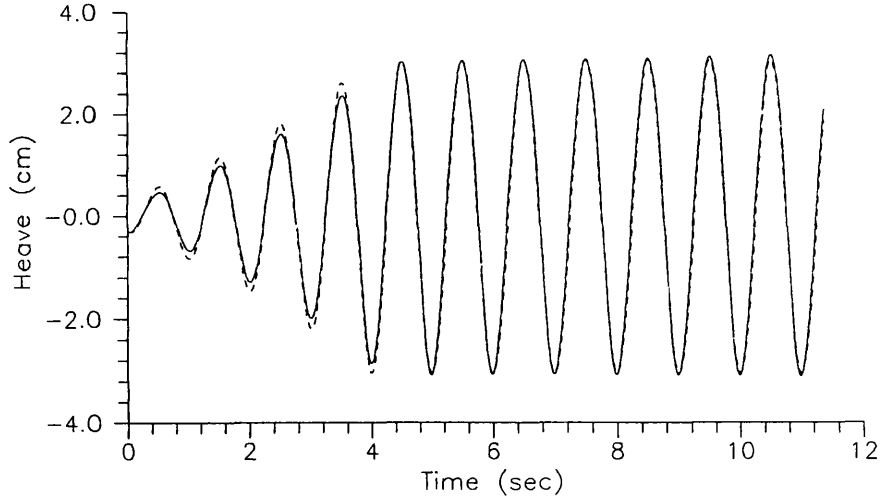

Fig. 6.146 Heave time-domain solution neglecting the coupling with the roll, $\zeta^a = 3.0$ cm, $\omega_a = 6.28$ rad / s

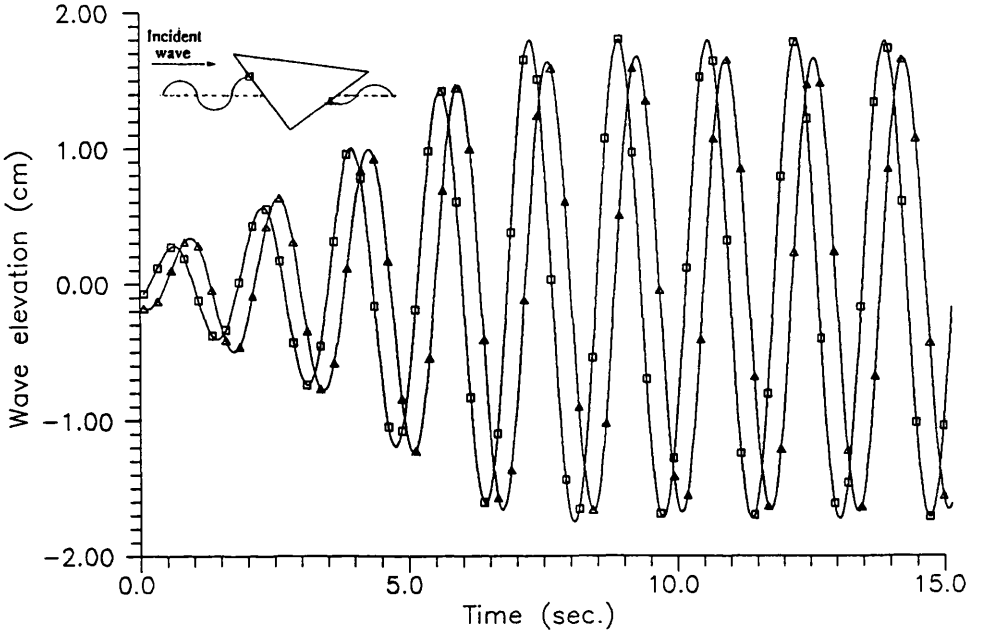

Fig. 6.147 Calculated free surface elevation on both sides of the cylinder, $\zeta^a = 2.0$ cm, $\omega_0 = 3.77$ rad / s

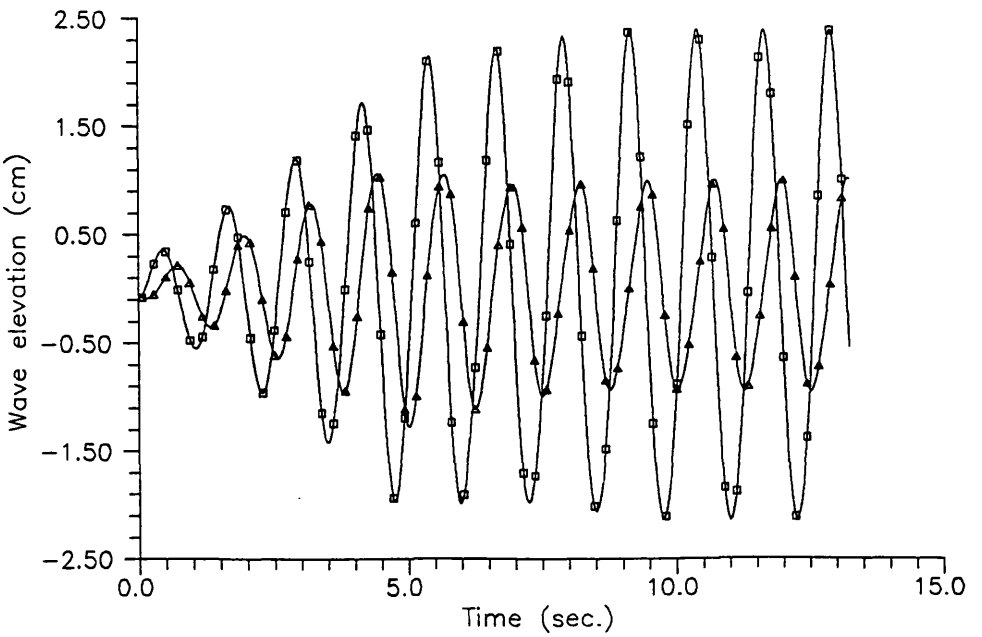

Fig. 6.148 Calculated free surface elevation on both sides of the cylinder, $\zeta^a = 2.0$ cm, $\omega_0 = 5.03$ rad / s

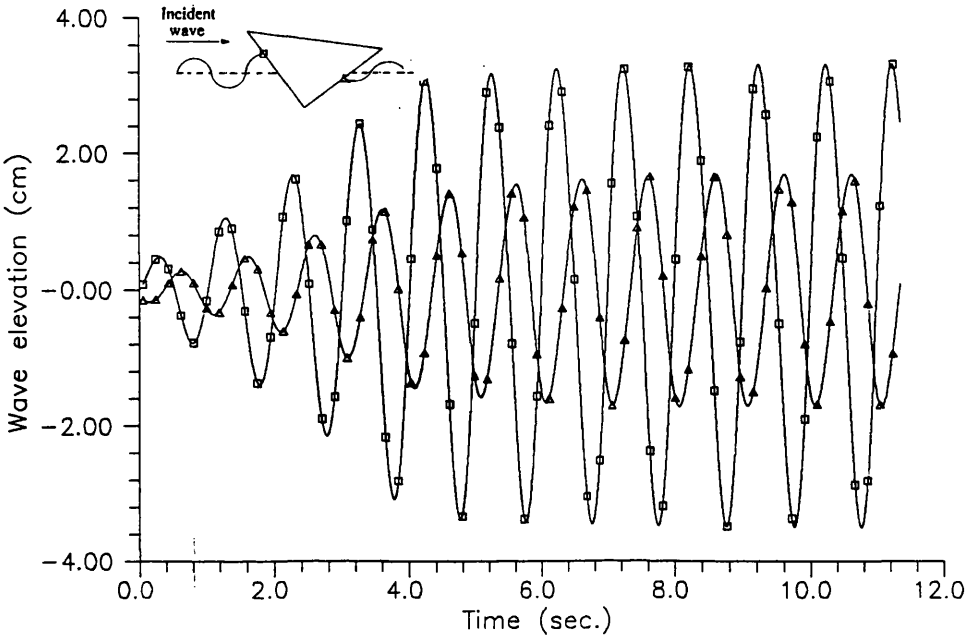

Fig. 6.149 Calculated free surface elevation on both sides of the cylinder, $\zeta^a = 2.0$ cm, $\omega_0 = 6.28$ rad / s

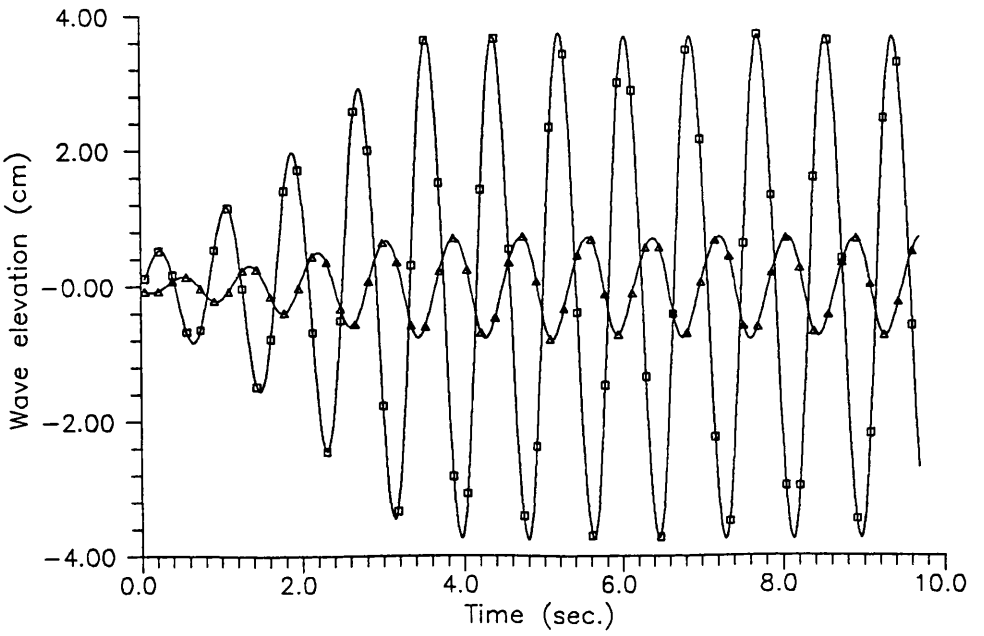

Fig. 6.150 Calculated free surface elevation on both sides of the cylinder, $\zeta^a = 2.0$ cm, $\omega_0 = 7.54$ rad / s

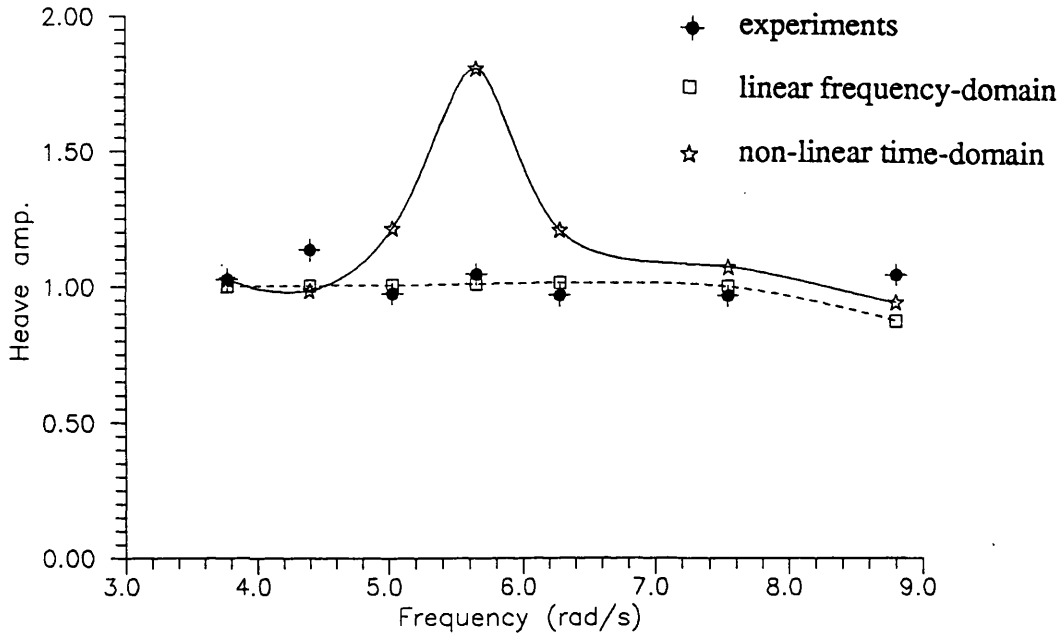

Fig. 6.151 ξ_3^{a+}/ζ^a, heave transfer function considering the positive amplitudes, for $\zeta^a \cong 2.0$ cm

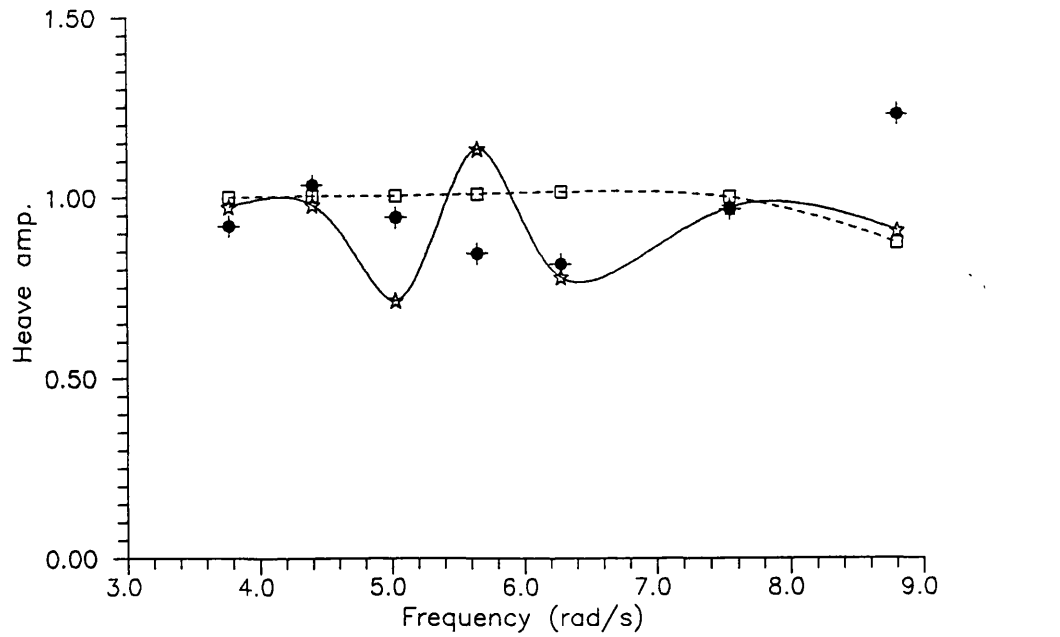

Fig. 6.152 $\left|\xi_3^{a-}\right|/\zeta^a$, heave transfer function considering the negative amplitudes, for $\zeta^a \cong 2.0$ cm

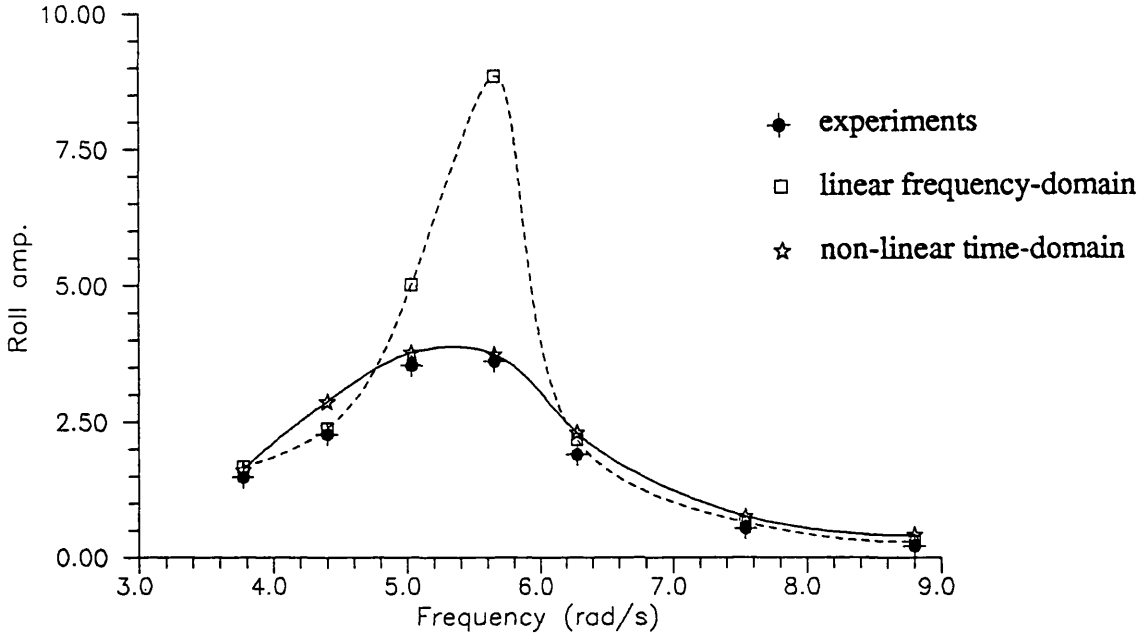

Fig. 6.153 $\xi_4^{a-} / k_0\zeta^a$, roll transfer function considering the positive amplitudes, for $\zeta^a \cong 2.0$ cm

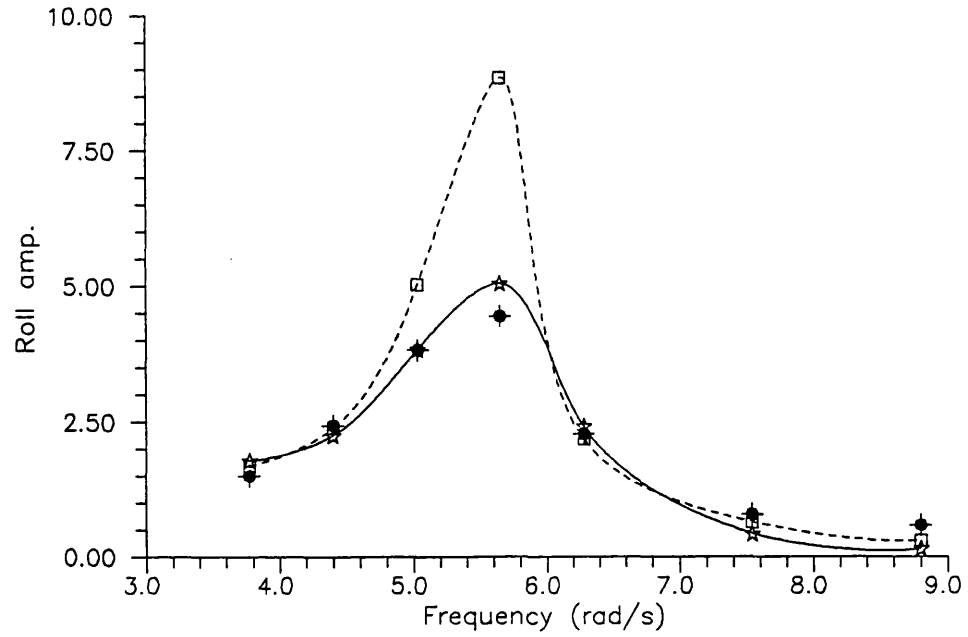

Fig. 6.154 $\left|\xi_4^{a-}\right| / k_0\zeta^a$, roll transfer function considering the negative amplitudes, for $\zeta^a \cong 2.0$ cm

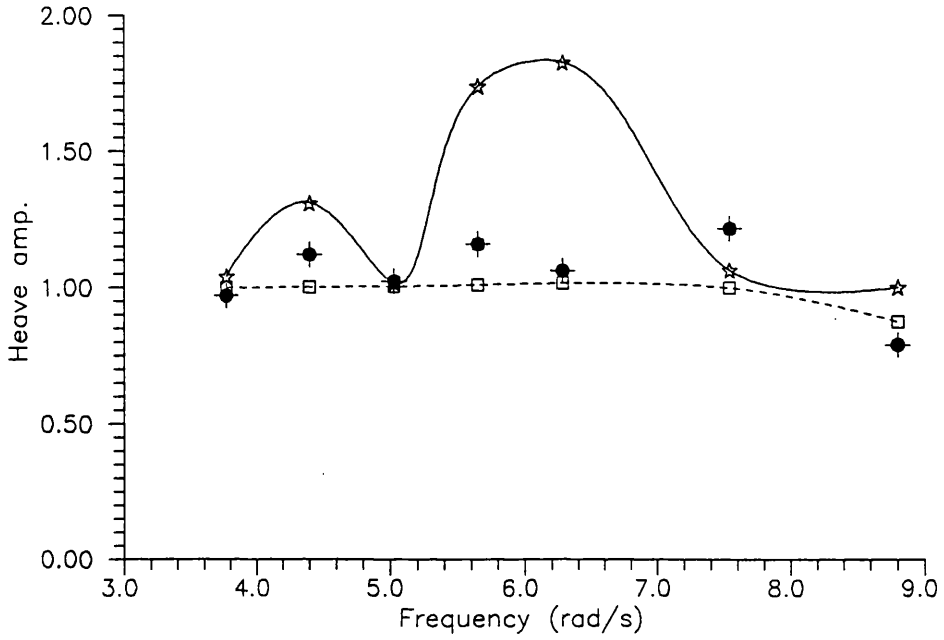

Fig. 6.155 ξ_3^{a+}/ζ^a, heave transfer function considering the positive amplitudes, for $\zeta^a \cong 3.0$ cm

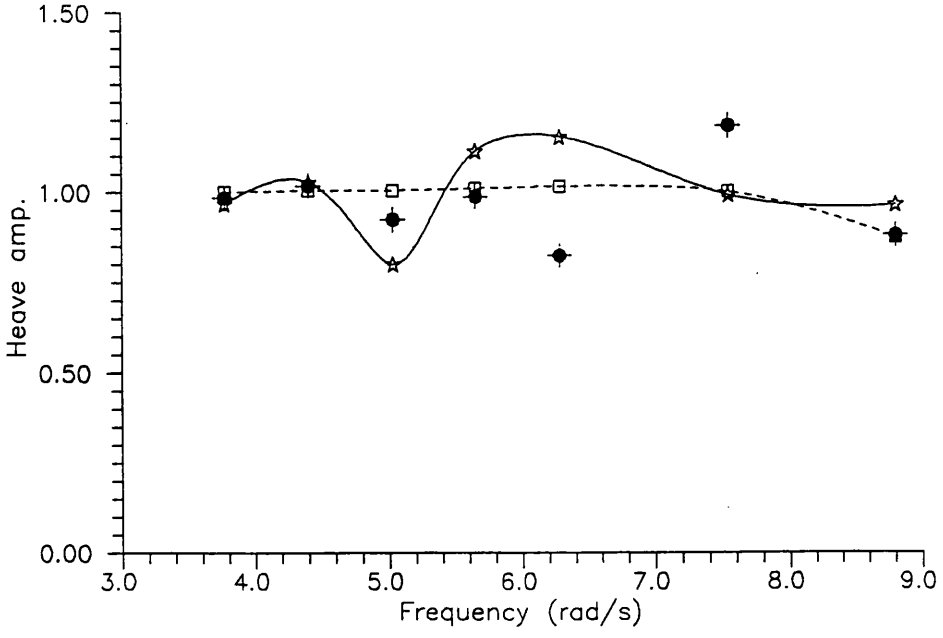

Fig. 6.156 $\left|\xi_3^{a-}\right|/\zeta^a$, heave transfer function considering the negative amplitudes, for $\zeta^a \cong 3.0$ cm

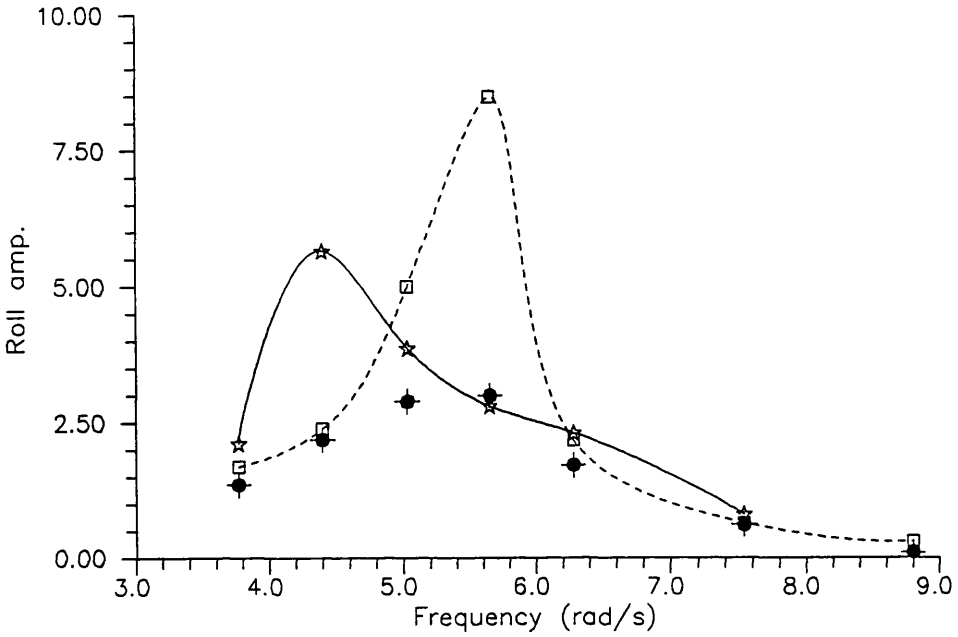

Fig. 6.157 $\xi_4^{a+} / k_0\zeta^a$, roll transfer function considering the positive amplitudes, for $\zeta^a \cong 3.0$ cm

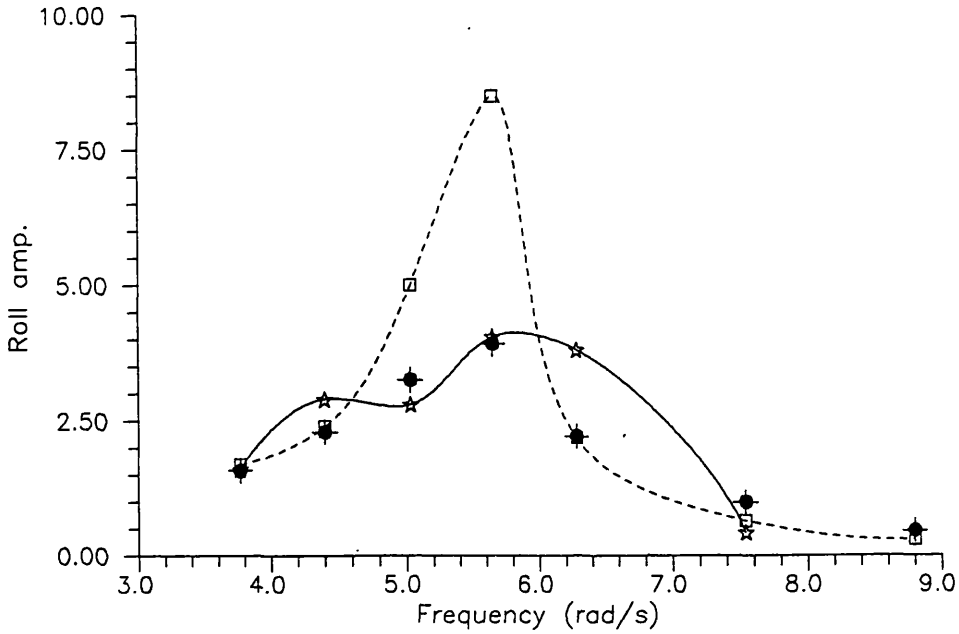

Fig. 6.158 $\left|\xi_4^{a-}\right| / k_0\zeta^a$, roll transfer function considering the negative amplitudes, for $\zeta^a \cong 3.0$ cm

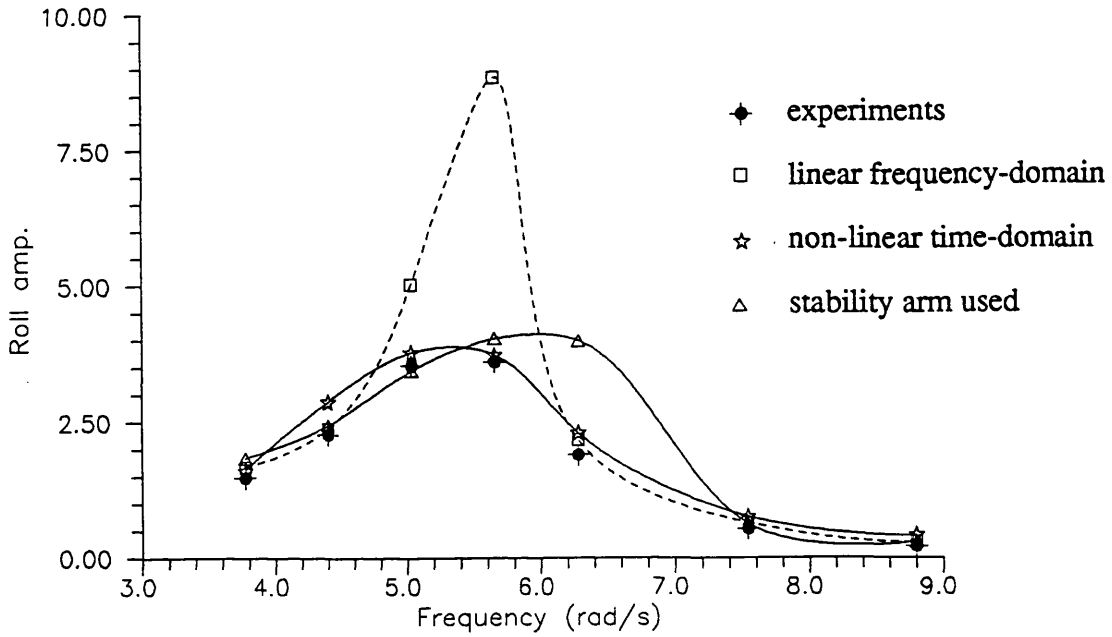

Fig. 6.159 $\xi_4^{a+} / k_0\zeta^a$, positive amp. roll transfer function for $\zeta^a \cong 2.0$ cm, hydrostatic moment computed assuming $\xi_3(t) = 0$ and $\zeta(t) = 0$

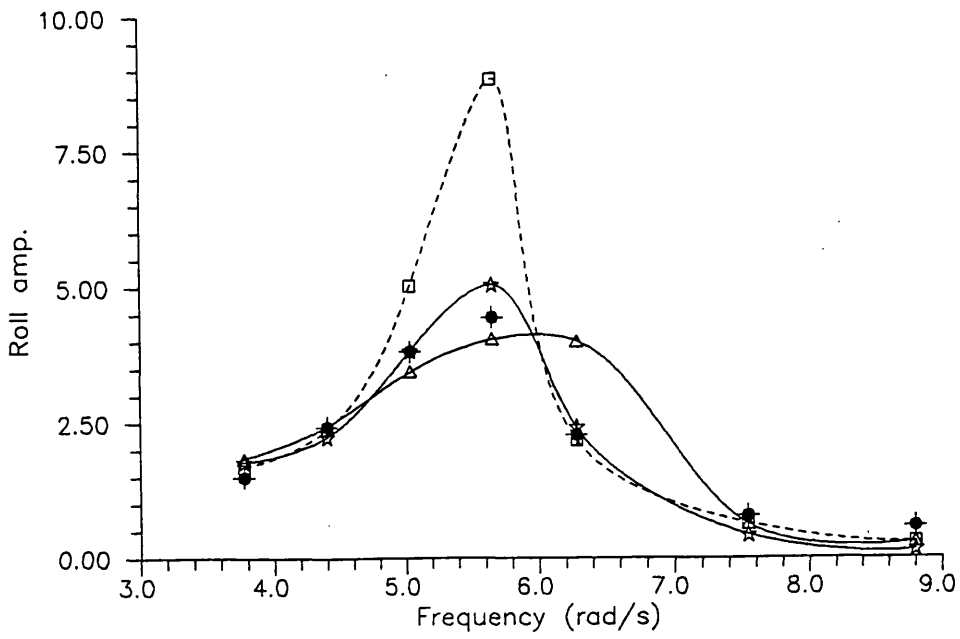

Fig. 6.160 $\left|\xi_4^{a-}\right| / k_0\zeta^a$, negative amp. roll transfer function for $\zeta^a \cong 2.0$ cm, hydrostatic moment computed assuming $\xi_3(t) = 0$ and $\zeta(t) = 0$

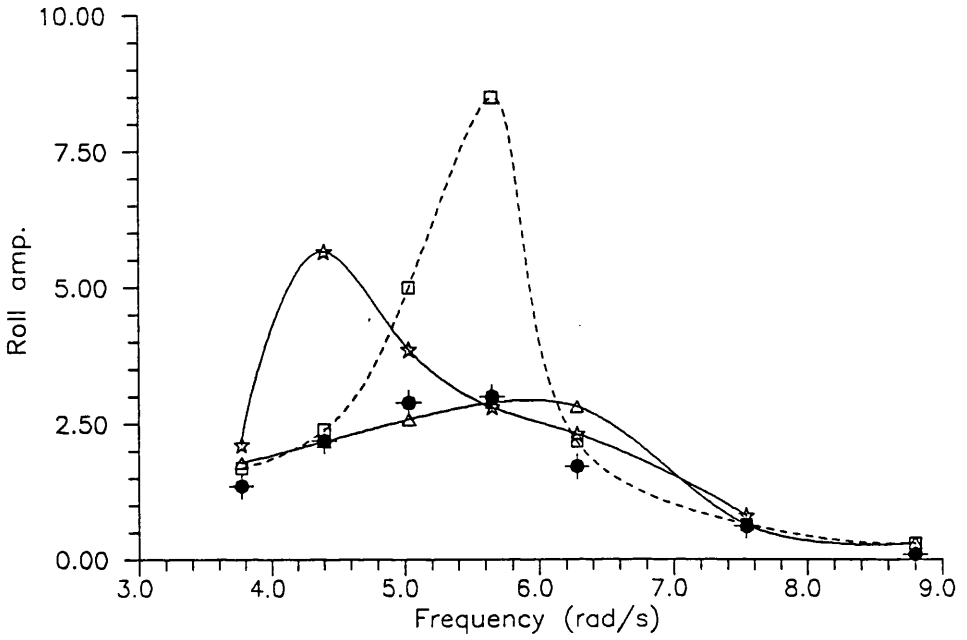

Fig. 6.161 $\xi_4^{a+} / k_0\zeta^a$, positive amp. roll transfer function for $\zeta^a \cong 3.0$ cm, hydrostatic moment computed assuming $\xi_3(t) = 0$ and $\zeta(t) = 0$

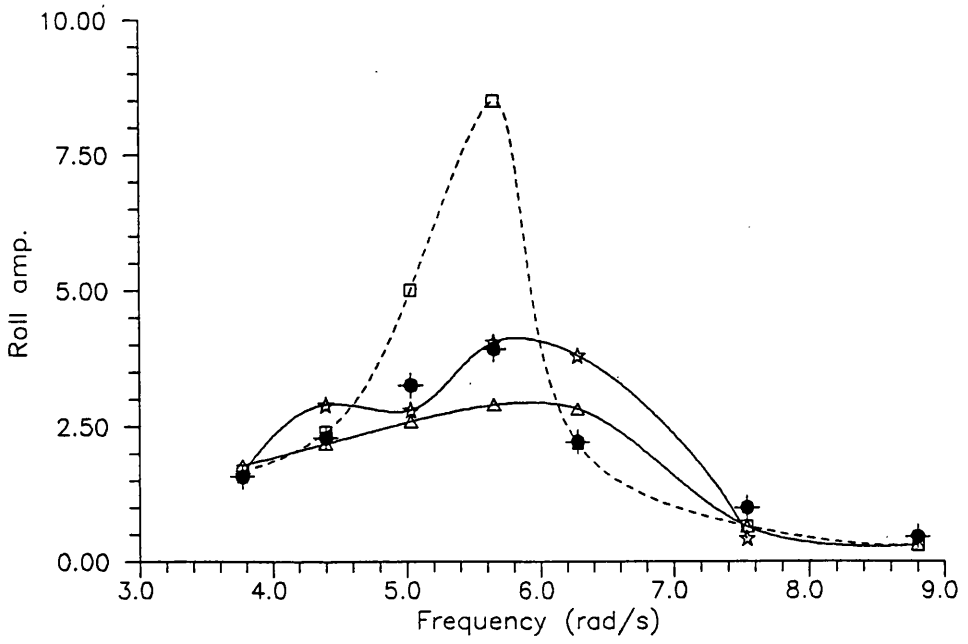

Fig. 6.162 $\left|\xi_4^{a-}\right| / k_0\zeta^a$, negative amp. roll transfer function for $\zeta^a \cong 3.0$ cm, hydrostatic moment computed assuming $\xi_3(t) = 0$ and $\zeta(t) = 0$

7. Frequency-Domain Solution of the Ship Motion Problem

7.1 - Introduction

In this Chapter general linearized problem presented in Section 3-1 will be restricted to sinusoidal excitations and to linear and harmonic responses of the ship. The mathematical model represents inertial, damping and restoring forces which are linearly proportional respectively to amplitudes of the ship oscillatory acceleration, velocity and displacement. In addition all these forces are linearly proportional to the amplitude of motions. A more practical consequence of the linearity of the system can be stated as follows; if the ship were subject to a sum of two excitations, both sinusoidal at the same frequency, the total response would be the sum of the separate responses. This seems to be a severe limitation of the model to represent real ship motions, but the experience proves that under certain conditions (of practical interest in many cases) the model is valid.

The exciting forces and the motions are now given by;

$$F_k^E(t) = \mathrm{Re}\left[F_k^E e^{i\omega t}\right] \quad , \quad k = 1...6 \tag{7.1.1}$$

$$\xi_j(t) = \mathrm{Re}\left(\xi_j^A\right)e^{i\omega t} \quad , \quad j = 1...6 \tag{7.1.2}$$

Where 'F_k^E' are the complex amplitudes of the exciting forces, and 'ξ_j^A' are the complex amplitudes of the sinusoidal motions. (The real part is to be taken in all terms involving $e^{i\omega t}$.)

The co-ordinate system where the motions and exciting forces are represented, $X = (x, y, z)$, has been defined in Section-3.1.

In order to obtain several terms of the motion equations (3.1.34) it will be necessary to solve the linearized boundary value problem and evaluate the integrals for the forces, as stated in Section 3-1.

In order to evaluate the added mass and damping coefficients of the ship, the strip theory from Salvesen, Tuck, and Faltinsen (1970) will be used, together with the two-dimensional results obtained from the "Frank close fit method". The strip-theory derivations will not be presented here in detail, as they are very well explained in the paper, however the major steps will be highlighted since

this is important to understand well the advantages and principally the limitations of the strip-theory developed by Salvesen et al..

The exciting forces will be evaluated using also a strip theory method. The basic idea follows the method presented by Kim (1980).

Basically in the "strip methods" the ship is divided, or discretized, in a number of cylinders along the length, so in an approximat way the form of the ship is kept. The hydrodynamic coefficients and the exciting forces on each section are obtained from two-dimensional results of the cylinder problem, where the cylinder has the same cross section and the same oscillatory motion as that of the corresponding section of the ship. So it is assumed that the flow passing through a section of the ship does not affect the flow passing adjacent sections. This assumption is more valid as the ship gets thinner. The three-dimensional effects arise from the steady fluid velocity passing the ship. The way of using the two-dimensional results to evaluate the hydrodynamic coefficients, and the way of dealing with the three-dimensional effects distinguish the different strip theories. Hydrodynamic coefficients and exciting forces are then integrated over the length of the ship in the final step to obtain the motion equations.

7.2 - Radiation Forces

Analogy with linear mass damping system

As explained in Section-3.1, under certain assumptions, the linearized radiation force problem can be treated as an independent problem, neglecting the effects interference with the exciting force. This way the problem consists of evaluating the forces, other than hydrostatic forces, associated with oscillatory motion of the ship in otherwise calm water.

The equation derived in Section-3.1, for the radiation force acting on a ship when it is subjected to general (although small) oscillatory motions is;

$$F^R = -\rho \iint_{S_0} \left(\frac{\partial \Phi^R}{\partial t} \tilde{n} - \Phi^R U \tilde{m} \right) ds \qquad (3.1.32)$$

As the unsteady motion is assumed sinusoidal the time derivative of the unsteady potential is now;

$$\frac{\partial \Phi^R}{\partial t} = i\omega \Phi^R \qquad (7.2.1)$$

As the unsteady potential is equal to the linear superposition of its different components, the radiation force in each principal direction is;

$$F_k^R = -\rho \iint_{S_0} \Phi^R (i\omega n_k - U m_k) ds \quad , \quad k = 1,\ldots,6 \qquad (7.2.2)$$

$$F_k^R = -\rho \iint_{S_0} \sum_{j=1}^{6} \xi_j \hat{\Phi}_j^R (i\omega n_k - U m_k) ds \quad , \quad k = 1,\ldots,6 \qquad (7.2.3)$$

Where $\hat{\Phi}_j^R$ is the radiation potential due to an unit oscillatory motion in the j-mode.

In a more compact form the equation can be expressed as;

$$F_k^R = \sum_{j=1}^{6} \hat{F}_{kj}^R \xi_j \qquad , \quad k=1...6 \tag{7.2.4}$$

The term '$\hat{F}_{kj}^R$' represents the radiation force in the 'k' direction due to an unit imposed motion in the j-mode;

$$\hat{F}_{kj}^R = -\rho \iint_{S_0} \hat{\Phi}_j^R (i\omega n_k - Um_k) ds \qquad , \quad k,j = 1,...,6 \tag{7.2.5}$$

This force can be divided into real and imaginary parts;

$$\mathrm{Re}\left(\hat{F}_{kj}^R\right) = -\rho\, \mathrm{Re} \iint_{S_0} \hat{\Phi}_j^R (i\omega n_k - Um_k) ds \qquad , \quad k,j = 1,...,6 \tag{7.2.6}$$

$$\mathrm{Im}\left(\hat{F}_{kj}^R\right) = -\rho\, \mathrm{Im} \iint_{S_0} \hat{\Phi}_j^R (i\omega n_k - Um_k) ds \qquad , \quad k,j = 1,...,6 \tag{7.2.7}$$

If we define now the following constants;

$$A_{kj} = \frac{\rho}{\omega^2} \mathrm{Re} \iint_{S_0} \hat{\Phi}_j^R (i\omega n_k - Um_k) ds \qquad , \quad k,j = 1,...,6 \tag{7.2.8}$$

$$B_{kj} = -\frac{\rho}{\omega} \mathrm{Im} \iint_{S_0} \hat{\Phi}_j^R (i\omega n_k - Um_k) ds \qquad , \quad k,j = 1,...,6 \tag{7.2.9}$$

The equation (7.2.5) can be written as;

$$\hat{F}_{kj}^R = -\omega^2 A_{kj} + i\omega B_{kj} \tag{7.2.10}$$

The radiation force in the 'k' direction due to an sinusoidal motion of arbitrary amplitude becomes;

$$F_{kj}^R = \xi_j \left(-\omega^2 A_{kj} + i\omega B_{kj}\right) \tag{7.2.11}$$

We have now a formula similarly to the motion equation of general linear dynamic systems modelled with mass and damping;

$$F_{kj}^{R} = A_{kj}\ddot{\xi} + B_{kj}\dot{\xi} \qquad (7.2.12)$$

This equation indicates that the radiation force has two components. The first is in phase with the acceleration of the motion and it is called the added inertia of the ship for the translational modes of motion, and added moment of inertia for angular modes of motion. This is a mathematical finding, and the physical interpretation of the result is that certain quantity of mass of fluid is accelerated when the ship oscillates. This equivalent mass of fluid is given by the coefficient 'A_{kj}' and named 'added mass'. The second term in equation (7.2.12) is in phase with the velocity of motion and is called the damping force. This term appears because the unsteady motion of the body occurs near the free-surface and thus waves are created and radiated away. The ship loses some energy generating these waves, which is transmitted on the form of damping forces. It is interesting to note that the damping forces exist because of the free-surface, and if an object oscilates in an unbounded fluid the damping forces will not arise. The coefficient 'B_{kj}' is the damping coefficient. The added mass and the damping coefficient are not characteristics of the ship shape alone since they depend also on the oscillatory frequency.

Hydrodynamic coefficients

Equation (7.2.2) permits the evaluation of the radiation forces which a ship with a slender hull is subjected to when it is travelling with a constant forward speed in sinusoidal waves. Now the strip theory approach must be used to simplify this general equation.

The derivation will start by rewriting the conditions given in Section-3.1. These conditions must be satisfied by the radiation potential.

$$\text{(L)} \quad \Phi_{xx}^{R} + \Phi_{yy}^{R} + \Phi_{zz}^{R} = 0 \qquad (7.2.12)$$

$$\text{(F)} \quad \Phi_{tt}^{R} - 2U\Phi_{xt}^{R} + U^{2}\Phi_{xx}^{R} + g\Phi_{z}^{R} = 0 \quad , \quad \text{on } z = 0 \qquad (7.2.13)$$

$$(K) \quad \frac{\partial \Phi_j^R}{\partial n} = i\omega n_j + U m_j \qquad , \; j = 1,...,6 \; , \; \text{on} \; S_0 \tag{7.2.14}$$

$$(B) \quad \nabla \Phi^R \rightarrow 0 \qquad , \; \text{on} \; z \rightarrow -\infty \tag{7.2.15}$$

$$(R) \quad \frac{\partial \Phi^R}{\partial r} - i\frac{\omega^2}{g}\Phi^R = 0 \quad \text{as} \quad |r| \rightarrow \infty \tag{7.2.16}$$

where $r = \sqrt{(x^2 + y^2)}$ is the distance from the body.

The next step is to further simplify the kinematic body boundary condition (7.2.14). The steady potential due to the forward speed of the ship is given by;

$$\Phi_0 = -Ux + \Phi^S \tag{3.1.8}$$

If it is assumed that the ship is very thin, the steady potential, 'Φ^S', may be neglected which will result in the following simplification for the 'm' vector;

$$\begin{aligned} m_j &= 0 \qquad \text{for} \quad j = 1,2,3,4 \\ m_5 &= n_3 \\ m_6 &= -n_2 \end{aligned} \tag{7.2.17}$$

This assumption is common in other consistent ship motion theories, like for example the "Three-Dimensional Panel Methods". However the "rational strip-theory" from Ogilvie and Tuck (1969), make use of a better representation of the steady potentials effects.

From now on we will work with the radiation potentials due to unit amplitude motions in each mode, $\hat{\Phi}_j^R$.

In view of the body boundary condition (7.2.14) we can divide the radiation potential into two components, first being the speed independent;

$$\hat{\Phi}_j^R = \hat{\Phi}_j^0 + \frac{U}{i\omega}\hat{\Phi}_j^U \tag{7.2.18}$$

This results in two kinematic body boundary conditions;

$$\frac{\partial \hat{\Phi}_j^0}{\partial n} = i\omega n_j$$
$$\frac{\partial \hat{\Phi}_j^U}{\partial n} = i\omega m_j \qquad \text{on} \quad S_0 \qquad (7.2.19)$$

Simultaneously the potentials must satisfy all the other conditions stated in the beginning of this sub-section, so it follows from the kinematic conditions (7.2.19) and the new definitions for the 'm' vector (7.2.17) that;

$$\hat{\Phi}_j^U = 0 \qquad \text{for } j = 1,2,3,4$$
$$\hat{\Phi}_5^U = \hat{\Phi}_3^0 \qquad (7.2.20)$$
$$\hat{\Phi}_6^U = -\hat{\Phi}_2^0$$

This way the oscillatory components of the radiation potentials can be expressed in terms of the speed independent parts;

$$\hat{\Phi}_j^R = \hat{\Phi}_j^0 \qquad , \quad \text{for } j = 1,2,3,4$$
$$\hat{\Phi}_5^R = \hat{\Phi}_5^0 + \frac{U}{i\omega}\hat{\Phi}_3^0 \qquad (7.2.21)$$
$$\hat{\Phi}_6^R = \hat{\Phi}_6^0 - \frac{U}{i\omega}\hat{\Phi}_2^0$$

These speed independent radiation potentials must satisfy the kinematic body condition;

$$\frac{\partial \hat{\Phi}_j^0}{\partial n} = i\omega n_j \qquad , \quad \text{on} \quad S_0 \qquad (7.2.22)$$

The linearized free-surface boundary condition;

$$\left(\hat{\Phi}_j^0\right)_{tt} - 2U\left(\hat{\Phi}_j^0\right)_{xt} + U^2\left(\hat{\Phi}_j^0\right)_{xx} + \left(\hat{\Phi}_j^0\right)_z = 0 \qquad , \quad \text{on} \quad z = 0 \qquad (7.2.23)$$

Where the subscript 'j' represents the motion mode, and the subscripts outside of the parenthesis means partial differentiation with respect to these variables.

In addition, these potentials must satisfy the three-dimensional Laplace equation, and the appropriate conditions at infinity.

We can now return to the equation (7.2.5) that gives the radiation force in the 'k' direction due to an unit oscillatory motion in the j-mode.

$$\hat{F}_{kj}^{R} = -\rho \iint_{S_0} \hat{\Phi}_j^{R} (i\omega n_k - U m_k) ds \qquad , \quad k, j = 1, \ldots, 6 \tag{7.2.5}$$

Now we are not going to use the variation of the Stokes theorem derived by Ogilvie and Tuck (1969), as Salvesen et al. did on their formulation. The reason is that the equation we have for the radiation forces, Eq. (7.2.5) was derived in the earlier stage using the Stokes theorem, hence we do not have derivatives of the potential.

Finally the radiation forces due to rigid-body motions with a unit amplitude become;

$$\hat{F}_{kj}^{R} = -\rho i\omega \iint_{S_0} \left(n_k \hat{\Phi}_j^{R} \right) ds + U\rho \iint_{S_0} \left(m_k \hat{\Phi}_j^{R} \right) ds \tag{7.2.24}$$

In the formulation of Salvesen et al. there is one additional term in this equation, whose necessity as Newman (1978) stated "is questionable". The term is a line integral of the potential multiplied by the normal vector and evaluated over the contour of the aftermost cross section. In any case this term can only exists for ships with transom stern under the waterline, and even in these cases its value is very small. Furthermore the potential theory assumes that the ship do not have a wide transom stern under the waterline, otherwise important viscous effects will be present in the flow near the stern. Finally, it noted be referred that in the present formulation the end term was "lost" when the variation of the Stokes theorem was used to remove the derivative of the potential from the unsteady forces (see Section-3.1).

The next steps will be described briefly since they are very well explained in the paper by Salvesen et al..

- A set of equations for the radiation forces '$\hat{F}_{kj}^{R}$', in terms of the speed independent potentials '$\hat{\Phi}_{j}^{0}$', can be obtained by applying Eqs. (7.2.21) to each component of the radiation potential. It should be noted that until this point no strip-theory assumptions have been made, and in fact the results to this point are exact, within the linear potential theory for bluff bodies at zero forward speed.

The next two steps are used to simplify further the speed independent terms obtained just before, to a form suitable for computations.

- By assuming that the beam and the draft of a ship are much smaller then its length it can be concluded that;

  -The integration variable in the integrals over the mean wetted surface is $ds = d\ell d\varsigma$, where 'ds' is a surface element, '$d\ell$' is over the length of the ship, and '$d\varsigma$' is over the cross section contour 'C_x'. With this relation it is possible to evaluate the surface integrals for the radiation forces over the length of the ship in a very practical way.

  -For the same reason the unit vector normal to the hull surface, 'n', has one component on the x-direction which is much smaller than the normal components in the in the y and z directions, thus the unit normal vector can be redefined as;

$$\begin{aligned} n_1 &= 0 \\ n_2, n_3, n_4 &= N_2, N_3, N_4 \\ n_5 &= -xN_3 \\ n_6 &= xN_2 \end{aligned} \qquad (7.2.25)$$

  Where N_2, N_3, N_4 are the components of the two-dimensional unit normal vector in the y-z plane (This vector is the same as the $\tilde{n} = (n_2, n_3, n_4)$ used in Chapters 4 and 5, however with another notation here to be easily distinguished form the three-dimensional normal vector, n).

- The free-surface condition (7.2.23) applied to the speed independent potentials can take the alternative form;

$$\left(i\omega - U\frac{\partial}{\partial x}\right)^2 \hat{\Phi}_j^0 + g\frac{\partial}{\partial z}\hat{\Phi}_j^0 = 0 \qquad , \quad \text{on} \quad z=0 \tag{7.2.26}$$

Now if it is assumed that the frequency of encounter is high such that;

$$\omega \rangle\rangle U\frac{\partial}{\partial x} \tag{7.2.27}$$

The free-surface condition can be reduced to a more suitable form;

$$-\omega^2\hat{\Phi}_j^0 + g\frac{\partial}{\partial z}\hat{\Phi}_j^0 = 0 \qquad , \quad \text{on} \quad z=0 \tag{7.2.28}$$

This assumption requires the wave length to be relatively small compared to the ship length, which seems a very severe restriction, however for the heave and pitch motions in the low-frequency range the restoring forces are dominant, so an exact prediction of the radiation forces are not so important. In fact the strip theory predicts the heave and pitch motions well in this frequency range.

Under the former assumptions the conditions to be satisfied by the speed independent radiation potentials, $\hat{\Phi}_j^0$, for j=2,3,4 , will be summarised here;

(L) Two-dimensional Laplace equation

$$\left(\hat{\Phi}_j^0\right)_{yy} + \left(\hat{\Phi}_j^0\right)_{zz} = 0 \tag{7.2.29}$$

(F) Two-dimensional linearized free-surface boundary condition

$$-\omega^2\hat{\Phi}_j^0 + g\frac{\partial}{\partial z}\hat{\Phi}_j^0 = 0 \qquad , \quad \text{on} \quad z=0 \tag{7.2.28}$$

(B) Two-dimensional linearized body boundary condition

$$\frac{\partial\hat{\Phi}_j^0}{\partial N} = i\omega N_j \qquad , \quad \text{on} \quad C_x \tag{7.2.30}$$

(B) The bottom condition

$$\nabla\hat{\Phi}_j^0 \to 0 \quad , \text{ on } z \to -\infty \tag{7.2.31}$$

(R) The radiation condition at infinity

$$\frac{\partial\hat{\Phi}_j^0}{\partial r} - i\frac{\omega^2}{g}\hat{\Phi}_j^0 = 0 \quad \text{as} \quad |r| \to \infty \tag{7.2.32}$$

Above we have the two-dimensional problem of a cylinder, with cross section C_x oscillating in the free-surface with no forward speed. This problem have already been solved in Chapter-4, and the corresponding radiation forces were calculated and represented in terms of hydrodynamic coefficients.

In addition the speed independent potentials $\hat{\Phi}_5^0$ and $\hat{\Phi}_6^0$ can be related with the two-dimensional potentials using the relations (7.2.25), while the potential $\hat{\Phi}_1^0$ can be neglected since $n_1 = 0$.

In the numerical solution the integrals over the length of the ship, for the radiation forces, are descritized in such a way that the ship will be represented by a set of two-dimensional cylinders. The total radiation force acting upon the ship will be the sum of the forces acting upon each cylinder. The most important conclusion is that the three-dimensional radiation forces on the ship can be calculated using the two-dimensional radiation results of cylinders simple oscillating on the free-surface and with no forward speed, and however some three-dimensional effects due the forward speed are consistently retained.

Recalling that the radiation forces due to unit oscillatory motions are given by;

$$\hat{F}_{kj}^R = -\omega^2 A_{kj} + i\omega B_{kj} \tag{7.2.10}$$

The vector of the radiation forces, where each component is related with one direction, is;

$$\{F_k^R\} = -\omega^2[A_{kj}]\{\xi_j\} + i\omega[B_{kj}]\{\xi_j\} \quad , \quad k,j = 1,\ldots,6 \tag{7.2.33}$$

$$\{F_k^R\} = [A_{kj}]\{\ddot{\xi}_j\} + [B_{kj}]\{\dot{\xi}_j\} \quad , \quad k,j = 1,\ldots,6 \tag{7.2.34}$$

Similarly the two-dimensional cylinder radiation forces due to unit oscillatory motions are given by;

$$\hat{f}_{kj}^{R} = -\omega^2 a_{kj} + i\omega b_{kj} \qquad (7.2.35)$$

Where 'a_{kj}' and 'b_{kj}' are the sectional added mass and damping coefficient.

Assuming the ship to have lateral symmetry the non-zero added mass and damping coefficients of the ship, A_{kj} and B_{kj}, in terms of the sectional added mass and damping coefficients integrated over the length of the ship are (the terms related with the integrals over the aftermost cross section that appear in the results of Salvesen et al. do not exist here, all the other terms are the same);

$$A_{33} = \int a_{33} d\ell \qquad (7.2.36)$$

$$B_{33} = \int b_{33} d\ell \qquad (7.2.37)$$

$$A_{35} = -\int \ell a_{33} d\ell - \frac{U}{\omega^2} B_{33}^0 \qquad (7.2.38)$$

$$B_{35} = -\int \ell b_{33} d\ell + U A_{33}^0 \qquad (7.2.39)$$

$$A_{53} = -\int \ell a_{33} d\ell + \frac{U}{\omega^2} B_{33}^0 \qquad (7.2.40)$$

$$B_{53} = -\int \ell b_{33} d\ell - U A_{33}^0 \qquad (7.2.41)$$

$$A_{55} = \int \ell^2 a_{33} d\ell + \frac{U^2}{\omega^2} A_{33}^0 \qquad (7.2.42)$$

$$B_{55} = \int \ell^2 b_{33} d\ell + \frac{U^2}{\omega^2} B_{33}^0 \qquad (7.2.43)$$

Where the integrals are over the length of the ship, 'A_{33}^0' and 'B_{33}^0' refer to the speed independent part of 'A_{33}' and 'B_{33}'.

Here only the added masses and damping coefficients corresponding to the heave and pitch motions are presented, since in this work only these motions will be studied and they are decoupled from the roll, sway, and yaw. Furthermore as the ship is long and slender the hydrodynamic forces associated with the surge motions are small, so the surge forces are not included. Both these aspects will be referred further ahead.

The speed effects on the hydrodynamic coefficients satisfy the Timman-Newman (1962) symmetry relations. These authors proved that for slender ships with pointed ends A_{35} and A_{53} must have the same forward speed terms but opposite sign. Ordinary strip-theories do not satisfy this requirement.

It is important now to review and comment on the simplifications of this strip-theory. Basically some assumptions were made in order to obtain a model in which the oscillatory flow in every transverse section is two-dimensional;

- In order to simplify the body boundary condition, the effects of the steady perturbation due to the presence of the ship in the steady incoming flow were neglected. In other words, there is no coupling between the steady perturbation field and the unsteady field. Being mathematically consistent this means that the relation B/L, and/or the ship forward speed are approaching asymptotically zero. The former assumption is especially critical near the ends of the ship (bow and stern) where the deflection on the steady incident flow is greater. In practice we find that these restrictions are not so severe, specially if the exciting wave frequency is high

- In order to evaluate the surface integrals in terms of integrals over the cross sections and integrals over the length of the ship, and to reduce the three-dimensional surface unit normal vectors in each section to two-dimensional vectors, it was necessary to assume that the hull surface almost do not change in the longitudinal direction. So the ship must be very thin.

- Finally in order to reduce the three-dimensional free-surface boundary condition to a two-dimensional form in each section, the frequency was assumed high. This means that the wave length must be of the same order as the beam. Again in practice we find that this restriction is not so severe, and good results can be obtained even for low frequency range.

These assumptions will be used in the exciting force problem of the next Section.

7.3 - Exiting Forces

Following the derivations and assumptions made in Section-3.1, the linearized exciting force problem is treated as an independent problem by neglecting the interferences with motion induced forces. These forces are evaluated assuming the ship fixed at its static equilibrium position, and the waves passing through it.

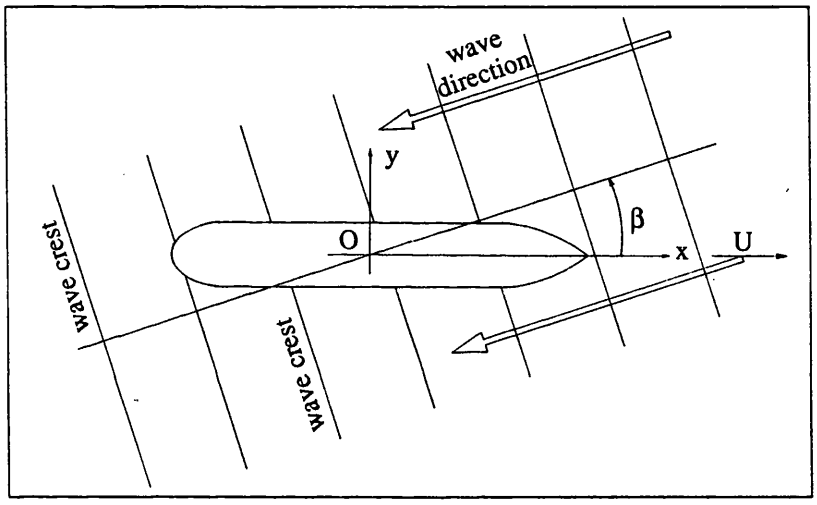

Figure 7.1 Definition of heading angle

The equation for the exciting force of ships advancing in sinusoidal waves was derived in the Section-3.1;

$$F^E = -\rho \iint_{S_0} \left(\frac{\partial(\Phi^I + \Phi^D)}{\partial t} \tilde{n} - (\Phi^I + \Phi^D) U \tilde{m} \right) ds \qquad (3.1.31)$$

Where 'Φ^I' is the incident wave potential, and in accordance with the linear gravity-wave theory is given by;

$$\Phi^I(x,y,z,t) = \frac{ig\zeta^a}{\omega_0} \left(e^{ik_0(x\cos\beta + y\sin\beta)} \right) \left(e^{k_0 z} \right) \left(e^{i\omega t} \right) \qquad (7.3.1)$$

Where 'ζ^a' is the wave amplitude, 'k_0' is the wave number, 'β' is the heading angle (β=0 for head waves), and 'ω_0' is the wave frequency which is related with the encounter frequency 'ω' by;

$$\omega_0 = \omega - k_0 U \cos\beta \tag{7.3.2}$$

$$k_0 = \frac{\omega_0^2}{g} \tag{7.3.3}$$

In figure 7.1 is represented the convention used for the heading angle.

In equation (3.1.31) 'Φ^D' represents the diffracted potential which appears as a perturbation on the incident potential because of the presence of the ship. The incident wave potential and the diffracted potential must satisfy;

(L) The Laplace equation

$$\Phi^I_{xx} + \Phi^I_{yy} + \Phi^I_{zz} = 0 \tag{7.3.4}$$

$$\Phi^D_{xx} + \Phi^D_{yy} + \Phi^D_{zz} = 0 \tag{7.3.5}$$

(B) The body boundary condition on the hull at mean position

$$\frac{\partial \Phi^D}{\partial n} = -\frac{\partial \Phi^I}{\partial n} \quad , \text{ on } S_0 \tag{3.1.10}$$

(F) The free-surface boundary condition in accordance with (3.1.9)

$$\left(i\omega - U\frac{\partial}{\partial x}\right)^2 \Phi^I + g\frac{\partial}{\partial z}\Phi^I = 0 \quad , \text{ on } z = 0 \tag{7.3.6}$$

$$\left(i\omega - U\frac{\partial}{\partial x}\right)^2 \Phi^D + g\frac{\partial}{\partial z}\Phi^D = 0 \quad , \text{ on } z = 0 \tag{7.3.7}$$

(B) The bottom condition

$$\nabla\Phi^I \to 0 \quad , \text{ on } z \to -\infty \tag{7.3.8}$$

$$\nabla\Phi^D \to 0 \quad , \text{ on } z \to -\infty \tag{7.3.9}$$

(R) The diffraction potential must satisfy the radiation condition at infinity

$$\frac{\partial \Phi^D}{\partial r} - i\frac{\omega^2}{g}\Phi^D = 0 \quad \text{as} \quad |r| \to \infty \tag{7.3.10}$$

The incident potential of the linear gravity wave satisfies the Laplace equation, the free-surface condition, and the bottom condition.

Under the assumption of linearity and as incident wave is sinusoidal, the incident and diffracted potentials are sinusoidal in time, so equation (3.1.31) can be writen as;

$$F^E = -\rho \iint_{S_0} (i\omega\tilde{n} - U\tilde{m})(\Phi^I + \Phi^D) ds \tag{7.3.11}$$

Like the radiation potential, these potentials can be assumed equal to the linear superposition of the contributions in each direction, so the exciting force in k-direction is;

$$F_k^E = -\rho \iint_{S_0} (i\omega n_k - U m_k)(\Phi^I + \Phi^D) ds \quad , \quad k = 1...6 \tag{7.3.12}$$

It will be convenient now to separate the exciting force in two parts, the incident wave part, and the diffraction part;

$$F_K^I = -\rho \iint_{S_0} (i\omega n_k - U m_k)\Phi^I ds \quad , \quad k = 1...6 \tag{7.3.13}$$

$$F_k^D = -\rho \iint_{S_0} (i\omega n_k - U m_k)\Phi^D ds \quad , \quad k = 1...6 \tag{7.3.14}$$

In the evaluation of the incident part of the exciting forces it is assumed that the pressure distribution in waves is not affected by the presence of the ship, thus the forces are determined from the knowledge of the pressure associated with the incident wave.

Obviously the presence of the ship generates a perturbation on the incident wave field near the hull. This perturbation is accounted by the diffraction potential,

which represents the wave scattering due to the presence of the ship. The diffraction force is associated with the diffraction potential.

Incident wave part of the exciting force

Given the assumption made for the steady potential ($\Phi_0 = -Ux$), equation (7.3.13) may have the alternative form;

$$F_k^I = -\iint_{S_0}\left(i\omega - U\frac{\partial}{\partial x}\right)\Phi^I n_k ds \quad , \quad k = 1...6 \tag{7.3.15}$$

Introducing the expression for the wave incident potential in the former equation results;

$$F_k^I = -\rho i\omega_0 \iint_{S_0}(n_k \Phi^I)ds \quad , \quad k = 1...6 \tag{7.3.16}$$

This is the well known Froude-Krilov force.

The incident wave potential (7.3.1) can be expressed as;

$$\Phi^I(x,y,z,t) = \varphi^I(y,z)e^{ik_0 x\cos\beta}e^{i\omega t} \tag{7.3.17}$$

$$\varphi^I(y,z) = \zeta^a \hat{\varphi}^I(y,z) \tag{7.3.18}$$

$$\hat{\varphi}^I(y,z) = \frac{ig}{\omega_0}e^{k_0 z}e^{ik_0 y\sin\beta} \tag{7.3.19}$$

where 'φ^I' is the complex amplitude of the incident wave potential, acting on each cross section of the ship. '$\hat{\varphi}^I$' is the complex amplitude of the potential corresponding to an unit amplitude wave.

Thus equation (7.3.13) can be rewritten as;

$$F_k^I = -\rho i\omega_0 \zeta^a \iint_{S_0}\{e^{ik_0 x\cos\beta}\hat{\varphi}(y,z)n_k\}ds \quad , \quad k = 1...6 \tag{7.3.20}$$

As the ship is slender, the three-dimensional unit vector normal to the hull surface, 'n', can be reduced to a two-dimensional vector, since the normal component in the x-direction is much smaller than the normal components in the y and z directions, thus finally the forces can be evaluated over the ship length in terms of cross section characteristics;

$$F_1^I = 0 \tag{7.3.21}$$

$$F_K^I = -i\rho\omega_0\zeta^a \int_L e^{ik_0\ell\cos\beta} \int_{C_x} \{\hat{\varphi}^I(y,z)N_k\} d\varsigma d\ell \quad , \quad k = 2,3,4 \tag{7.3.22}$$

$$F_5^I = i\rho\omega_0\zeta^a \int_L e^{ik_0\ell\cos\beta} \ell \int_{C_x} \{\hat{\varphi}^I(y,z)N_3\} d\varsigma d\ell \tag{7.3.23}$$

$$F_6^I = -i\rho\omega_0\zeta^a \int_L e^{ik_0\ell\cos\beta} \ell \int_{C_x} \{\hat{\varphi}^I(y,z)N_2\} d\varsigma d\ell \tag{7.3.24}$$

The former equations may be represented in a more compact form;

$$F_k^I = \zeta^a \int_L \left(e^{ik_0\ell\cos\beta}\hat{f}_k^I\right) d\ell \quad , \quad k = 2,3,4 \tag{7.3.25}$$

$$F_5^I = -\zeta^a \int_L \left(e^{ik_0\ell\cos\beta}\ell\hat{f}_3^I\right) d\ell \tag{7.3.26}$$

$$F_6^I = \zeta^a \int_L \left(e^{ik_0\ell\cos\beta}\ell\hat{f}_2^I\right) d\ell \tag{7.3.27}$$

where '$\hat{f}_k^I$' is;

$$\hat{f}_k^I = -i\omega_0\rho \int_{C_x} \{\hat{\varphi}^I(y,z)N_k\} d\varsigma \quad , \quad k = 2,3,4 \tag{7.3.28}$$

which represents the sectional Froude-Krilov force due to waves of unit amplitude. A procedure to solve this two-dimensional problem was presented in

Section-4.3, where it is necessary only to incorporate the term '$\sin\beta$' in the expression for the incident wave potential. It is interesting to find that the Froude-Krilov force is speed independent.

Diffraction part of the exciting force

. (a) Direct Approach

Following Kim (1980) the three-dimensional diffraction forces will be represented in terms of assumed two-dimensional diffraction forces acting on every cross section of the ship.

The diffraction part of the exciting force was obtained in the initial part of this Section, and is given by;

$$F_k^D = -\rho \iint_{S_0} (i\omega n_k - U m_k)\Phi^D ds \quad , \; k = 1,\ldots,6 \tag{7.3.14}$$

The three-dimensional diffraction potential, Φ^D, can be represented as;

$$\Phi^D(x,y,z,t) = \varphi^D(x,y,z)\left(e^{ikx\cos\beta}\right)\left(e^{i\omega t}\right) \tag{7.3.29}$$

where 'φ^D' is the complex amplitude of the three-dimensional diffraction potential acting on the cross sections of the ship.

Strip theory assumptions:

The same strip theory simplifications used to evaluate the radiation forces, are used here.

. First the surface integrals are simplified assuming that the ship is slender. Thus $ds \cong d\ell d\varsigma$, where '$d\ell$' is over the length of the ship, and '$d\varsigma$' is over the cross section contour 'C_x'. Equation (7.3.14) becomes;

$$F_k^D = -\rho \int_L e^{ik\ell\cos\beta} \int_{C_x} \{(i\omega n_k - U m_k)\varphi^D(x,y,z)\} d\varsigma d\ell \quad , \; k = 1,\ldots,6 \tag{7.3.30}$$

- As the ship is slender, the three-dimensional unit vector normal to the hull surface, 'n', can be reduced to a two-dimensional vector.

- Also because the ship is slender, thus its surface is almost parallel to the x-axis, the sectional three-dimensional diffraction potential, $\varphi^D(x,y,z)$, can be reduced to a two-dimensional potential '$\varphi^D(y,z)$'. (It should be noted that the slenderness assumptions tend to fail near the ends of the ship, however these are small areas compared with the remainder part of the hull.)

- If the encounter frequency is assumed high, the free-surface condition (7.3.7) can be reduced to;

$$-\omega^2\Phi^D + g\frac{\partial}{\partial z}\Phi^D = 0 \quad , \text{ on } z=0 \tag{7.3.31}$$

With these strip theory simplifications, the complex amplitudes of the diffraction forces in the k-direction are;

$$F_1^D = 0 \tag{7.3.32}$$

$$F_k^D = -\rho\int_L e^{ik_0\ell\cos\beta}\int_{C_x}\{i\omega N_k\varphi^D(y,z)\}d\varsigma d\ell \quad , \ k=2,3,4 \tag{7.3.33}$$

$$\begin{aligned} F_5^D = {} & \rho\int_L e^{ik_0\ell\cos\beta}\ell\int_{C_x}\{i\omega N_3\varphi^D(y,z)\}d\varsigma d\ell \\ & + U\rho\int_L e^{ik_0\ell\cos\beta}\int_{C_x}\{\varphi^D(y,z)N_3\}d\varsigma d\ell \end{aligned} \tag{7.3.34}$$

$$\begin{aligned} F_6^D = {} & -\rho\int_L e^{ik_0\ell\cos\beta}\ell\int_{C_x}\{i\omega N_2\varphi^D(y,z)\}d\varsigma d\ell \\ & - U\rho\int_L e^{ik_0\ell\cos\beta}\int_{C_x}\{\varphi^D(y,z)N_2\}d\varsigma d\ell \end{aligned} \tag{7.3.35}$$

After the strip theory assumptions, the diffraction boundary value problem stated in the beginning of this Section is simplified. The conditions which the new diffraction potential, $\varphi^D(y,z)$, must now satisfy are;

(L) The 2-D Laplace equation

$$\varphi^D_{yy} + \varphi^D_{zz} = 0 \tag{7.3.36}$$

(B) The body boundary condition on the hull at mean position

$$\frac{\partial \varphi^D}{\partial N} = -\frac{\partial \varphi^I}{\partial N} \quad , \text{ on each cross section, } C_x, \text{ of } S_0 \tag{7.3.37}$$

(F) The free-surface boundary condition

$$-\omega^2 \varphi^D + g\frac{\partial}{\partial z}\varphi^D = 0 \quad , \text{ on } z = 0 \tag{7.3.38}$$

(B) The bottom condition

$$\nabla\varphi^D \to 0 \quad , \text{ on } z \to -\infty \tag{7.3.39}$$

(R) The diffraction potential must satisfy the radiation condition at infinity

$$\frac{\partial \varphi^D}{\partial y} - i\frac{\omega^2}{g}\varphi^D = 0 \quad \text{as} \quad |y| \to \infty \tag{7.3.40}$$

This is clearly the two-dimensional problem solved in Section-4.3. However the present two-dimensional problem have one difference, which is the ship cross sections are not in general subjected to beam waves, but to waves of arbitrary direction (in Section-4.3 the solution is restricted to beam waves). This must be taken into account in the body boundary condition which becomes now;

$$\frac{\partial \varphi^D(y,z)}{\partial n} = -\frac{\partial \varphi^I(y,z)}{\partial n} = \omega_0 \zeta^a e^{kz} \begin{Bmatrix} [n_3 \sin(k_0 y \sin\beta) + n_2 \sin\beta \cos(k_0 y \sin\beta)] \\ +i[n_3 \cos(k_0 y \sin\beta) - n_2 \sin\beta \sin(k_0 y \sin\beta)] \end{Bmatrix}$$

In the Section-4.3 a procedure was described to evaluate the sectional diffraction potential and forces. The equations defining these forces in terms of the diffraction potential resultant from an incident wave of unit amplitude are;

$$f^D_k = \zeta^a \hat{f}^D_k = -i\omega\rho\zeta^a \int_{C_x} \hat{\varphi}^D N_k d\varsigma \quad , \quad k = 2,3,4 \tag{7.3.41}$$

where '$\hat{f}_k^D$' is the diffraction force due to unit amplitude incident wave, and 'ζ^a' is the incident wave amplitude.

Concluding, the three-dimensional diffraction forces can be represented in terms of the two-dimensional diffraction forces acting on all the cross sections over the ship's length. Equations (7.3.30) to (7.3.33), can have the more compact form;

$$F_1^D = 0 \tag{7.3.41}$$

$$F_k^D = \zeta^a \int_L \left(e^{ik_0 \ell \cos\beta} \hat{f}_k^D \right) d\ell \quad , \quad k = 2,3,4 \tag{7.3.42}$$

$$F_5^D = -\zeta^a \int_L \left\{ e^{ik_0 \ell \cos\beta} \left(\ell \hat{f}_3^D + \frac{U}{i\omega} \hat{f}_3^D \right) \right\} d\ell \tag{7.3.43}$$

$$F_6^D = \zeta^a \int_L \left\{ e^{ik_0 \ell \cos\beta} \left(\ell \hat{f}_2^D + \frac{U}{i\omega} \hat{f}_2^D \right) \right\} d\ell \tag{7.3.44}$$

These final expressions are similar to those obtained by Salvesen (1970) and Kim (1980), in spite of the fact that the way chosen for the deduction is different from the presented by the first author, and also somewhat different from the one presented by Kim. Salvesen used the Haskind Newman relations (see Newman (1965)) to obtain the diffraction forces in terms of the ship motion induced potentials. The method presented here follows the initial idea from Kim of using the two-dimensional sectional diffraction forces to evaluate the ship diffraction force, however the formulation is different.

The results obtained here do not contain the end terms, similarly to the afore mentioned references, for the same reason already presented in Section-7.2 in deriving the hydrodynamic coefficients. It should be remembered that these end terms exist only if the underwater hull has one or both of the ends (bow and stern) with non-zero area of the cross section. Even in that case, for a slender ship, the end term will be a very small quantity compared with the remaining forces.

. (b) Haskind's relations.

An alternative method to compute the ship diffraction forces was studied and applied in order to confirm the results. This makes use of the Haskind's relations, which means that instead of solving directly the diffraction problem the motion induced potentials are used to evaluate the diffraction forces. Newman (1962),(1965) has studied the Haskind's relations for zero and forward speed cases.

The equation which gives the diffraction part of the exciting force is;

$$F_k^D = -\rho \iint_{S_0} (i\omega n_k - U m_k)\Phi^D ds \quad , \quad k = 1...6 \tag{7.3.14}$$

Use can be made of the body boundary condition from the radiation problem given by equation (7.2.19);

$$F_k^D = -\iint_{S_0} \frac{\partial}{\partial n}\left(\Phi_k^0 - \frac{U}{i\omega}\Phi_k^U\right)\Phi^D ds \quad , \quad k = 1...6 \tag{7.3.45}$$

Now in order to relate the diffraction potential with the incident wave potential Green's theorem is used.

Theorem

If 'ϕ' and 'φ' are two solutions of Laplace equation in a certain volume of fluid bounded by a closed surface 'S_T', these potentials are related in the following way;

$$\iint_{S_T}\left[\phi\frac{\partial\varphi}{\partial n} - \varphi\frac{\partial\phi}{\partial n}\right] = 0$$

where 'n' is the outward normal vector of the surface.

In the present problem we set;

$$\phi = \Phi_k^0 - \frac{U}{i\omega}\Phi_k^U$$

$$\varphi = \Phi^D$$

These potentials must satisfy the same Laplace equation, free-surface condition, body condition, radiation condition at infinity, and bottom condition. Applying Green's theorem to the surface '$S_T = S_0 + S_F + S_\infty$' (see figure 7.2), and using the former relations, finally the diffraction force is represented in terms of the known radiation potential and wave incident potential:

$$F_k^D = \rho \iint_{S_0} \left(\Phi_k^0 - \frac{U}{i\omega} \Phi_k^U \right) \frac{\partial \Phi^I}{\partial n} ds \quad , \quad k = 1...6 \tag{7.3.46}$$

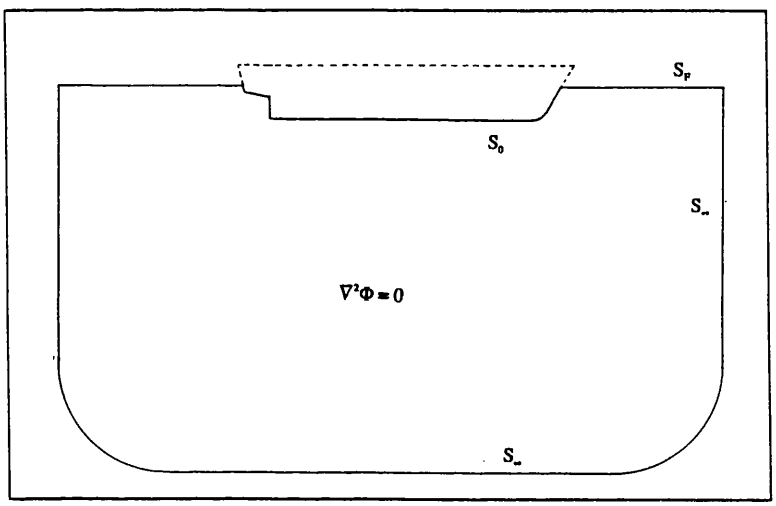

Figure 7.2 Control surfaces used for the application of Green's theorem

Now the same steps followed on the solution of the radiation problem can be done to obtain the three-dimensional radiation potentials in terms of the sectional two-dimensional potentials, and the same strip theory assumptions can be used to obtain the forces in terms of the sectional two-dimensional diffraction forces. These steps are very well presented in the paper by Salvesen et al. (1970), thus they will be omitted here.

The final equations for the ship diffraction forces are:

$$F_1^D = 0 \tag{7.3.47}$$

$$F_k^D = \zeta^a \int_L \left(e^{ik_0 \ell \cos\beta} \hat{f}_k^D \right) d\ell \quad , \quad k = 2,3,4 \tag{7.3.48}$$

$$F_5^D = -\zeta^a \int_L \left\{ e^{ik_0 \ell \cos\beta} \left(\ell \hat{f}_3^D + \frac{U}{i\omega} \hat{f}_3^D \right) \right\} d\ell \tag{7.3.49}$$

$$F_6^D = \zeta^a \int_L \left\{ e^{ik_0 \ell \cos\beta} \left(\ell \hat{f}_2^D + \frac{U}{i\omega} \hat{f}_2^D \right) \right\} d\ell \tag{7.3.50}$$

where the sectional diffraction forces per unit incident wave amplitude, $\hat{f}_k^D$, are:

$$\hat{f}_k^D = \omega_0 \rho \int_{C_x} \{ (iN_3 - N_2 \sin\beta) e^{ik_0 y \sin\beta} e^{k_0 z} \Psi_k \} ds \qquad k = 2,3,4 \tag{7.3.51}$$

N_2, N_3 are the components of the two-dimensional unit normal vector to the cross section, and Ψ_k are the two dimensional radiation potentials. A procedure to evaluate these potentials was presented in Section 4.2.

This method has the advantage that only one boundary value problem is solved when computing the overall ship hydrodynamic force. However the Haskind's relations provide only the force values, not the associated fluid pressure distributions.

Total Exciting Force

The total exciting force is equal to the sum of the incident wave part and the diffraction part ;

$$F_k^E(t) = F_k^I(t) + F_k^D(t) \quad , \quad k = 1,\ldots,6 \tag{7.3.52}$$

Both parts are sinusoidal in time with the same frequency, thus the total exciting force is sinusoidal in time, with frequency ω, and can be represented in each direction as;

$$F_k^E(t) = \mathrm{Re}\left[F_k^E e^{i\omega t} \right] \quad , \quad k = 1,\ldots,6 \tag{7.3.52}$$

or with the understanding that the real part is to be taken;

$$F_k^E(t) = F_k^E e^{i\omega t} \qquad (7.3.53)$$

Here F_k^E is the amplitude of the total exciting force, and it represents a complex number which have the information about the absolute value of the force, and the corresponding phase angle. 'ω' is the encounter frequency.

Alternatively (7.3.53) can be written as;

$$F_k^E(t) = \left(F_k^E\right)^C \cos\omega t + \left(F_k^E\right)^S \sin\omega t \quad , \quad k = 1,\ldots,6 \qquad (7.3.54)$$

Here we have the exciting force divided in a cosine part and a sine part.

7.4 - Restoring Forces

Restoring forces are obtained by combining the hydrostatic forces with the weight forces. The hydrostatic forces are dependent only of the vertical position of every point of the wetted surface and can be given as:

$$F_k^H = -\rho g \iint_S (z n_k) ds \quad , \quad k = 1...6 \tag{3.1.33}$$

Assuming small angular displacements and neglecting higher order terms, the z-co-ordinate of a point on the wetted surface is;

$$z = z' + \xi_3 + y'\xi_4 - x'\xi_5 \tag{7.4.1}$$

where x', y', z' are the co-ordinates of the same point represented on the reference system fixed on the ship. Introducing this expression in equation (3.1.33) results;

$$F_k^H = -\rho g \iint_S (z' + \xi_3 + y'\xi_4 - x'\xi_5) n_k ds \quad , \quad k = 1...6 \tag{7.4.2}$$

Now several assumptions are made in order to obtain hydrostatic forces linearly proportional to the ship's displacements, namely, the pressure is evaluated up to the still water line level, the angular displacements are assumed small, and the sides of the ship are assumed vertical near the water line. Using these assumptions the surface integral in equation (7.4.2) can be developed and finally the only non-zero hydrostatic forces for a vessel with a longitudinal plane of symmetry become;

$$F_3^H = \rho g V_0 - \rho g A_{wl} \xi_3 + \left\{ \rho g \iint_{A_{wl}} x ds \right\} \xi_5 \tag{7.4.3}$$

$$F_4^H = \rho g V_0 y_{B_0} - \rho g \left\{ V_0 (z_{B_0} - z_G) + \iint_{A_{wl}} y^2 ds \right\} \xi_4 \tag{7.4.4}$$

$$F_5^H = -\rho g V_0 x_{B_0} + \left\{ \rho g \iint_{A_{wl}} x ds \right\} \xi_3 - \rho g \left\{ V_0 \left(z_{B_0} - z_G \right) + \iint_{A_{wl}} x^2 ds \right\} \xi_5 \qquad (7.4.5)$$

where, only in the present Section, V_0 is the body's volume under the water line in static condition, and $x_{B_0}, y_{B_0}, z_{B_0}$ are the co-ordinates of the centre of this volume. In addition x_{B_0}, y_{B_0} are equal to the correspondent co-ordinates of the gravity centre, x_G, y_G, if the ship is in the same static condition.

The ship's weight forces are;

$$F_3^W = -\rho g V_0 \qquad (7.4.6)$$

$$F_4^W = -\rho V_0 g y_G \qquad (7.4.7)$$

$$F_5^W = \rho V_0 g x_G \qquad (7.4.8)$$

Combining the weight forces with the hydrostatic forces results on the restoring forces;

$$F_1^B = F_2^B = F_6^B = 0 \qquad (7.4.9)$$

$$F_3^B = -C_{33}\xi_3 - C_{35}\xi_5 \qquad (7.4.10)$$

$$F_4^B = -C_{44}\xi_4 \qquad (7.4.11)$$

$$F_5^B = -C_{53}\xi_3 - C_{55}\xi_5 \qquad (7.4.12)$$

the restoring coefficients, C_{kj}, are given by;

$$C_{33} = \rho g A_{wl} \qquad (7.4.13)$$

$$C_{35} = C_{53} = -\rho g \iint_{A_{wl}} x ds \qquad (7.4.14)$$

$$C_{44} = \rho g V_0 \overline{GM}_T \qquad (7.4.15)$$

$$C_{55} = \rho g V_0 \overline{GM}_L \qquad (7.4.16)$$

$\overline{GM_T}$ and $\overline{GM_L}$ are respectively the transverse metacentric height and longitudinal metacentric height.

7.5 - Body-Mass Force

Newton's second law states that a force (or moment) occurs when the velocity of a body changes. This is the inertial force associated with the inertia of the body mass.

Being more formal, if 'ρ_B' is the mass density of the body, which depends of the position, the inertial force associated with this mass is given by the rate of change of linear momentum;

$$F^M = \frac{\partial}{\partial t}\iiint_{V_B} \rho_B\left(\dot{\eta} + \dot{\Omega}' \times r\right)dV \tag{7.5.1}$$

And the inertial moment is given by the rate of change of angular momentum;

$$M^M = \frac{\partial}{\partial t}\iiint_{V_B} \rho_B r \times \left(\dot{\eta} + \dot{\Omega}' \times r\right)dV \tag{7.5.2}$$

Where, in this case, according to Section-3.1;

$$v = \dot{\eta} + \dot{\Omega}' \times r \tag{7.5.3}$$

is the velocity of each element of the ship in the reference system advancing with its forward speed and fixed in the mean position. '$\dot{\eta}(t)$' is the translatory unsteady velocity, represented in the reference system fixed in the mean position of the ship, $X = (x, y, z)$, and '$\dot{\Omega}'(t)$' is the angular velocity, represented in the reference system fixed in the ship, $X' = (x', y', z')$. '$r = (x', y', z')$' is the vector position of the body volume elements in the reference system fixed in the ship. The integration is over the body volume 'V_B'.

If we define the six component velocity vector 'u' as follows;

$$u = \left(\dot{\eta}_1, \dot{\eta}_2, \dot{\eta}_3, \dot{\Omega}'_1, \dot{\Omega}'_2, \dot{\Omega}'_3\right) \tag{7.5.4}$$

The integrand of (7.5.1) can be expressed as;

$$\dot{\eta}+\dot{\Omega}\times r=\begin{Bmatrix}u_1\\u_2\\u_3\end{Bmatrix}+\begin{Bmatrix}u_4\\u_5\\u_6\end{Bmatrix}\times\begin{Bmatrix}x'\\y'\\z'\end{Bmatrix} \tag{7.5.5}$$

Or defining $'(e_x,e_y,e_z)'$ as the unit vectors parallel to (x,y,z);

$$\begin{aligned}\dot{\eta}+\dot{\Omega}'\times r=&(u_1+u_5z'-u_6y')e_x+\\&(u_2-u_4z'+u_6x')e_y+\\&(u_3+u_4y'-u_5x')e_z\end{aligned} \tag{7.5.6}$$

The integrand of (7.5.2) can be calculated as;

$$\begin{aligned}r\times\left(\dot{\eta}+\dot{\Omega}'\times r\right)=&\left(-u_2z'+u_3y'+u_4y'^2+u_4z'^2-u_5x'y'-u_6x'z'\right)e_x+\\&\left(u_1z'-u_3x'-u_4x'y'+u_5x'^2+u_5z'^2-u_6y'z'\right)e_y+\\&\left(-u_1y'+u_2x'-u_4x'z'-u_5y'z'+u_6x'^2+u_6y'^2\right)e_z\end{aligned} \tag{7.5.7}$$

Introducing the relations (7.5.6) and (7.5.7) into (7.5.1) and (7.5.2) we obtain the total vector inertial force and vector inertial moment. As the body mass is constant in time the volume integral can be taken out of the derivative. Furthermore the force and moment can be decomposed into six components along the six directions defined. As an example the inertial moment in the 4th-direction (moment about x-axis) is given by;

$$\begin{aligned}F_4^M=&\frac{\partial u_2}{\partial t}\iiint_{V_B}(-\rho_B z')dv+\frac{\partial u_3}{\partial t}\iiint_{V_B}(\rho_B y')dv+\frac{\partial u_4}{\partial t}\iiint_{V_B}\rho_B\left(y'^2+z'^2\right)dv+\\&\frac{\partial u_5}{\partial t}\iiint_{V_B}(-\rho_B x'y')dv+\frac{\partial u_6}{\partial t}\iiint_{V_B}(-\rho_B x'z')dv\end{aligned} \tag{7.5.8}$$

Where the body mass is given by;

$$m = \iiint_{V_B} \rho_B dv \tag{7.5.9}$$

And the co-ordinates of the centre of gravity are;

$$x'_G = \frac{1}{m}\iiint_{V_B}(\rho_B x')dv$$

$$y'_G = \frac{1}{m}\iiint_{V_B}(\rho_B y')dv \tag{7.5.10}$$

$$z'_G = \frac{1}{m}\iiint_{V_B}(\rho_B z')dv$$

According to Section-3.1, if we assume small unsteady motions of the ship, they can be decomposed as;

$$\begin{cases} \eta(t) = (\xi_1(t), \xi_2(t), \xi_3(t)) \\ \Omega(t) = (\xi_4(t), \xi_5(t), \xi_6(t)) \end{cases} \tag{3.1.11)}$$

Where we have; surge, sway, heave translations, and roll, pitch, yaw rotations. All the components are now represented on the reference system fixed at the mean position of the ship.

Now the equation (7.5.8) can be written in a more usual way;

$$F_4^M = -mz'_G \ddot{\xi}_2 + my'_G \ddot{\xi}_3 + I_{44}\ddot{\xi}_4 + I_{45}\ddot{\xi}_5 + I_{46}\ddot{\xi}_6 \tag{7.5.11}$$

Here the I_{kj} , $k, j = 4,5,6$ coefficients are normally named moments of inertia.

One can see that the inertial moment is proportional to the accelerations and depend on the mass, mass distribution of the body, and location of gravity centre. Furthermore one can conclude that the inertial moment in one direction depends not only on the characteristics of the inertia and the motion in that direction but also on a contribution from other motions. Therefore we can conclude that there are inertial coupling between the motions.

The derivation given for the 4th-direction can be carried out for all other directions, and finally the vector of inertial forces (and moments) may be presented as follows;

$$\{F_k^M\} = [M_{kj}]\{\ddot{\xi}_j\} \qquad , \quad k,j = 1,\ldots,6 \tag{7.5.12}$$

In the equation the terms '$M_{kj}\ddot{\xi}_j$' represent the inertial force in k-direction due to the acceleration in j-direction. The matrix of the body-inertia coefficients is;

$$[M_{kj}] = \begin{bmatrix} m & 0 & 0 & 0 & mz'_G & -mz'_G \\ 0 & m & 0 & -mz'_G & 0 & mz'_G \\ 0 & 0 & m & my'_G & -mx'_G & 0 \\ 0 & -mz'_G & my'_G & I_{44} & -I_{45} & -I_{46} \\ mz'_G & 0 & -mx'_G & -I_{54} & I_{55} & -I_{56} \\ -my'_G & mx'_G & 0 & -I_{64} & -I_{65} & I_{66} \end{bmatrix} \tag{7.5.13}$$

Where the moments of inertia are defined as;

$$I_{44} = \iiint_{V_B} \rho_B (y'^2 + z'^2) dv \qquad I_{45} = I_{54} = \iiint_{V_B} \rho_B (x'y') dv$$

$$I_{55} = \iiint_{V_B} \rho_B (x'^2 + z'^2) dv \qquad I_{46} = I_{64} = \iiint_{V_B} \rho_B (x'z') dv \tag{7.5.14}$$

$$I_{66} = \iiint_{V_B} \rho_B (x'^2 + y'^2) dv \qquad I_{56} = I_{65} = \iiint_{V_B} \rho_B (y'z') dv$$

If it is assumed that the ship has lateral symmetry (symmetry about the x'-z' plane) and that the centre of gravity is located at $(0,0,z'_G)$, then the mass matrix is given by; (this is the normal case when the co-ordinate system used is the one shown is fig 3.1)

$$\left[M_{kj}\right]=\begin{bmatrix} m & 0 & 0 & 0 & mz'_G & 0 \\ 0 & m & 0 & -mz'_G & 0 & 0 \\ 0 & 0 & m & 0 & 0 & 0 \\ 0 & -mz'_G & 0 & I_{44} & 0 & -I_{46} \\ mz'_G & 0 & 0 & 0 & I_{55} & 0 \\ 0 & 0 & 0 & -I_{64} & 0 & I_{66} \end{bmatrix} \qquad (7.5.15)$$

7.6 - Equations of Motion and Solution

Equations of Motion

In the previous Sections of this Chapter the several components of the total pressure force, as well as the forces due to the mass of the ship have been discussed. We are now ready to derive the equations of motion for free oscillations of the ship in waves by equating the external pressure forces acting upon the hull to the internal forces due to gravity and internal forces associated with acceleration of the body mass. The ship will be assumed as a rigid body, unrestrained, and in state of equilibrium when in calm water.

Remembering the six component vectors representing the various forces in each direction are;

F_k^E , $k = 1,\ldots,6$ For the sinusoidal exciting forces due to waves

$$F_k^M = \sum_{j=1}^{6}\left(M_{kj}\ddot{\xi}_j\right) \quad , \quad k = 1,\ldots,6 \quad \text{For the body-mass inertial forces}$$

$$F_k^R = \sum_{j=1}^{6}\left(A_{kj}\ddot{\xi}_j + B_{kj}\dot{\xi}_j\right) \quad , \quad k = 1,\ldots,6 \quad \text{For the radiation forces}$$

$$F_k^B = \sum_{j=1}^{6} C_{kj}\xi_j \quad , \quad k = 1,\ldots,6 \quad \text{For the restoring forces}$$

Substituting the above terms in Newton's equation we finally obtain the equations of motion;

$$\sum_{j=1}^{6}\left\{\left(M_{kj} + A_{kj}\right)\ddot{\xi}_j + B_{kj}\dot{\xi}_j + C_{kj}\xi_j\right\} = F_k^E \quad , \quad k = 1,\ldots,6 \qquad (7.6.1)$$

Where the coefficients in the equations are sequentially; the body-inertia coefficients, the added mass coefficients, the damping coefficients and the restoring coefficients.

The generalised body-inertia matrix for ships with symmetry about the x',y' plane, and with the centre of gravity located at $(0,0,z'_G)$ is given by (7.5.15).

For ships with lateral symmetry it also follows that the added mass and damping coefficients matrices are;

$$\left[A_{kj}(\omega)\right]=\begin{bmatrix} A_{11} & 0 & A_{13} & 0 & A_{15} & 0 \\ 0 & A_{22} & 0 & A_{24} & 0 & A_{26} \\ A_{31} & 0 & A_{33} & 0 & A_{35} & 0 \\ 0 & A_{42} & 0 & A_{44} & 0 & A_{46} \\ A_{51} & 0 & A_{53} & 0 & A_{55} & 0 \\ 0 & A_{62} & 0 & A_{64} & 0 & A_{66} \end{bmatrix} \tag{7.6.2}$$

$$\left[A_{kj}(\omega)\right]=\begin{bmatrix} B_{11} & 0 & B_{13} & 0 & B_{15} & 0 \\ 0 & B_{22} & 0 & B_{24} & 0 & B_{26} \\ B_{31} & 0 & B_{33} & 0 & B_{35} & 0 \\ 0 & B_{42} & 0 & B_{44} & 0 & B_{46} \\ B_{51} & 0 & B_{53} & 0 & B_{55} & 0 \\ 0 & B_{62} & 0 & B_{64} & 0 & B_{66} \end{bmatrix} \tag{7.6.3}$$

These added-mass and damping coefficients are dependent of the encounter frequency, ship's hull shape, and forward speed. The corresponding hydrodynamic forces are dependent of the same parameters and also of the unsteady motion amplitudes.

For a ship with lateral symmetry oscillating in the free-surface, the only non-zero linear restoring coefficients are;

$$C_{33}, C_{44}, C_{55}, C_{35}, \text{ and } C_{53} \qquad (7.6.4)$$

It should be noted that the corresponding restoring forces are linearly proportional to the displacements.

Substituting the mass matrix (7.5.15), the added mass and damping coefficients (7.6.2) and (7.6.3), and the restoring coefficients (7.6.4) into the equations of motion (7.6.1), we find that for the ship with lateral symmetry the six coupled equations of motion reduce to two sets of equations. One set of three coupled equations for the surge, heave and pitch motions, and another set for the roll, sway, and yaw motions. So for this linearized mathematical model the surge, heave, and pitch are independent from the roll, sway, and yaw, in case of ships with lateral symmetry.

As shown in Section-7.2 and Section-7.3, if the ship in addition to lateral symmetry has a slender hull shape, the radiation and exciting forces associated with the surge motions are much smaller than the others associated with other modes, and so the surge motion is not included.

It was already mentioned that we are interested only in the heave and pitch motions of the ship. Developing the equation (7.6.1) for these motions, and using relations (7.5.15), (7.6.2), (7.6.3), (7.6.4), results in the equations of motion necessary for heave and pitch calculations;

$$\begin{cases} (M + A_{33})\ddot{\xi}_3 + B_{33}\dot{\xi}_3 + C_{33}\xi_3 + A_{35}\ddot{\xi}_5 + B_{35}\dot{\xi}_5 + C_{35}\xi_5 = F_3^E(t) \\ A_{53}\ddot{\xi}_3 + B_{53}\dot{\xi}_3 + C_{53}\xi_3 + (I_{55} + A_{55})\ddot{\xi}_5 + B_{55}\dot{\xi}_5 + C_{55}\xi_5 = F_5^E(t) \end{cases} \qquad (7.6.5)$$

The relationships for the added mass and damping coefficients, A_{kj} and B_{kj}, are given in Section-7.2, the restoring coefficients, C_{kj}, are derived in Section-7.4, the moment of inertia, I_5, is derived in Section-7.5, and the exciting forces, $F_k^E(t)$, are given in Section-7.4.

Solution of the Motion Equations

We have build a mathematical model which will permites to solve the motion equations easily. As a result of the sinusoidal exciting forces, and the fact that

all other forces are linearly proportional respectively to the accelerations, velocities, and displacements, the responses will be sinusoidal in time. So we can write;

$$F_k^E(t) = F_k^E e^{i\omega t} \quad , \quad k = 2,\ldots,6 \tag{7.3.36}$$

$$\xi_j(t) = \xi_j^A e^{i\omega t} \quad , \quad j = 2,\ldots,6 \tag{7.6.6}$$

$$\dot{\xi}_j(t) = i\omega\xi_j^A e^{i\omega t} \quad , \quad j = 2,\ldots,6 \tag{7.6.7}$$

$$\ddot{\xi}_j(t) = -\omega^2\xi_j^A e^{i\omega t} \quad , \quad j = 2,\ldots,6 \tag{7.6.8}$$

Where F_k^E is the complex amplitude of the exciting force in the k-direction, and ξ_j^A is the complex amplitude of the motion in j-mode.

Introducing these relations in the equations of motion (7.6.1) it follows;

$$\sum_{j=2}^{6}\left[-\omega^2\left(M_{kj}+A_{kj}\right)+i\omega B_{kj}+C_{kj}\right]\xi_j^A = F_k^E \quad , \quad k = 2,\ldots,6 \tag{7.6.9}$$

Once all the coefficients have been derived on the previous Sections, these equations have an easy algebraic solution. If only the heave and pitch motions are considered equation (7.6.5) becomes;

$$\begin{cases} \left[-\omega^2\left(m+A_{33}\right)+i\omega B_{33}+C_{33}\right]\xi_3^A + \\ \qquad \left[-\omega^2 A_{35}+i\omega B_{35}+C_{35}\right]\xi_5^A = F_3^E \\ \left[-\omega^2 A_{53}+i\omega B_{53}+C_{53}\right]\xi_3^A + \\ \qquad \left[-\omega^2\left(I_{55}+A_{55}\right)+i\omega B_{55}+C_{55}\right]\xi_5^A = F_5^E \end{cases} \tag{7.6.10}$$

It will be more convenient to make the program code with real variables than imaginary variables, thus the equivalent relations are introduced;

$$F_k^E(t) = \left(F_k^E\right)^C \cos\omega t + \left(F_k^E\right)^S \sin\omega t \quad , \quad k = 2,\ldots,6 \tag{7.3.37}$$

$$\xi_j(t) = \xi_j^C \cos\omega t + \xi_j^S \sin\omega t \qquad , \quad j = 2,\ldots,6 \tag{7.6.11}$$

$$\dot{\xi}_j(t) = -\omega\xi_j^C \sin\omega t + \omega\xi_j^S \cos\omega t \qquad , \quad j = 2,\ldots,6 \tag{7.6.12}$$

$$\ddot{\xi}_j(t) = -\omega^2\xi_j^C \cos\omega t - \omega^2\xi_j^S \sin\omega t \qquad , \quad j = 2,\ldots,6 \tag{7.6.13}$$

Where $\left(F_k^E\right)^C$ and ξ_j^C are respectively the amplitudes of the cosine parts of the exciting force in k-direction and motion in j-mode. The same follows for the sine parts.

Introducing these relations in the equations for the heave and pitch motions (7.6.5), and separating the sine and cosine terms it results;

Heave Motion

$$\begin{cases} -\omega^2\xi_3^C(m + A_{33}) + \omega\xi_3^S B_{33} + \xi_3^C C_{33} \\ \qquad -\omega^2\xi_5^C A_{35} + \omega\xi_5^S B_{35} + \xi_5^C C_{35} = \left(F_3^E\right)^C \\ -\omega^2\xi_3^S(m + A_{33}) - \omega\xi_3^S B_{33} + \xi_3^S C_{33} \\ \qquad -\omega^2\xi_5^S A_{35} - \omega\xi_5^C B_{35} + \xi_5^S C_{35} = \left(F_3^E\right)^S \end{cases} \tag{7.6.14}$$

Pitch Motion

$$\begin{cases} -\omega^2\xi_3^C A_{53} + \omega\xi_3^S B_{53} + \xi_3^C C_{53} \\ \qquad -\omega^2\xi_5^C(I_{55} + A_{55}) + \omega\xi_5^S B_{55} + \xi_5^C C_{33} = \left(F_5^E\right)^C \\ -\omega^2\xi_3^S A_{53} - \omega\xi_3^S B_{53} + \xi_3^S C_{53} \\ \qquad -\omega^2\xi_5^S(I_{55} + A_{55}) - \omega\xi_5^C B_{55} + \xi_5^S C_{33} = \left(F_5^E\right)^S \end{cases} \tag{7.6.15}$$

Solving these two sets of two coupled very simple equations we obtain the cosine and sine amplitudes, ξ_j^C and ξ_j^S , $j = 3,5$. Then the real amplitudes of the motions, ξ_j^a, and the corresponding phase angles, 'θ_j', are;

$$\xi_j^a = \sqrt{\left(\xi_j^C\right)^2 + \left(\xi_j^S\right)^2} \quad , \quad j = 3,5 \tag{7.6.16}$$

$$\theta_j = tg^{-1}\left(\frac{\xi_j^S}{\xi_j^C}\right) \quad , \quad j = 3,5 \tag{7.6.17}$$

Finally the motions are given either by;

$$\xi_j(t) = \xi_j^C \cos\omega t + \xi_j^S \sin\omega t \quad , \quad j = 3,5 \tag{7.6.11}$$

Or by;

$$\xi_j(t) = \xi_j^a \sin\left(\omega t + \theta_j\right) \quad , \quad j = 3,5 \tag{7.6.18}$$

The mathematical model have reached a very convenient form which enables us to use the frequency dependent hydrodynamic coefficients, and to derive differential equations of motion easy to solve. However there are some restrictions imposed on the reality in order to obtain these useful model, and it is important to recognise them now. Beside the simplifications associated with the linear potential theory of ship motions, and the strip theory approximations, this frequency-domain solution is based on the following assumptions:

- The exciting forces must be sinusoidal in time, so the sea state must be composed of unidirectional sinusoidal waves. It is known that the waves are in most cases irregular, as can easily be observed. Furthermore other external forces due for example to gusts of wind, slamming, water on deck, etc, can not be introduced in the equations of motion since generally they are not sinusoidal in time.

- The hydrodynamic coefficients are frequency dependent, so the unsteady motions are restricted to one frequency of oscillation. Once again this is not generally the real case.

- The restoring forces are linearly proportional to the displacements, which means that; the water plane area do not change when the ship is moved from its static equilibrium position, or in other words, the ship sides are assumed to be vertical. Also the roll and pitch angular motions are supposed to occur at constant immersion, since the displacement is assumed always equal to the

ship's weight. Finally in order to apply the linear mentacentric theory the roll and pitch motions are assumed small. The validity of this assumptions depends on the hull shape of the ship, and of course on the motions amplitude.

It should be referred that the inability of this model to make predictions in irregular seas is overcome, by the hypothesis first suggested by St. Denis and Pierson (1953) and later proved (see Ogilvie (1964)) which states that an irregular sea state can be decomposed in a number of sinusoidal components, and the response of the ship to the irregular sea is the sum of its response to the various components. Dalzell (1962a,b) conducted a series of experiments in which the limits of validity of the superposition principle were tested. The results were surprisingly good, since the effects of non-linearities were found not important even for severe sea states, for instants the comparisons between the linear mathematical model results, and experimental results for a destroyer model at moderate speed ($F_n = 0.18$) for the high-7 sea state were rather good. This has also been observed by Ochi (1964). As Ogilvie commented, it appears that non-linearities make themselves felt more easily in regular waves than in irregular waves.

8. TIME-DOMAIN SOLUTION OF THE SHIP MOTION PROBLEM

8.1 - Introduction

In Chapter-7 the ship motion problem was for a ship hull travelling with constant forward speed and heading angle in relation to sinusoidal sea waves. The exciting forces were sinusoidal in time, and the radiation forces were proportional to frequency dependent coefficients, thus the model is appropriate only if the motions are strictly sinusoidal in time. Golovato (1959) gave direct experimental proof that the classical second order equations with frequency dependent coefficients, cannot be used to describe non-sinusoidal motions, and Ursell (1954) reached the same conclusion analytically.

In this Chapter a method will be presented which is valid whatever is the nature of the exciting force (as long as it result in small unsteady motions of the ship), and where some non-linearities can be introduced. Furthermore the ship forward speed and heading angle do not need to be constant.

The ship motion problem will be solved in the time-domain, which means that the differential equations of motion instead of being solved analytically, are solved numerically with a time-integration procedure and the solution is built time step by time step.

In order to implement this method all the forces in the motion equations must be represented in the time-domain. This brings no major difficulties in the evaluation of the exciting and restoring forces, since these forces do not have the time dependency of the previous history of the fluid motion. However the radiation forces behave in a different manner. The existence of radiated waves implies a complicated time dependence of the fluid motion and hence the pressure forces. Waves generated by the body at time 't' will persist, in principle, for an infinite time thereafter, as well as the associated pressure force on the body surface. This situation is analogous to the case of a stone falling in still water, where we can observe waves moving away from the incident point for a very long time. If the fluid were not viscous, the waves would appear forever. This problem can be described mathematically by a convolution integral, with the fluid motion and pressure force at a given time being dependent on the previous history of the motion.

The total hydrodynamic forces acting upon the hull will be evaluated using a Strip-Theory approach, which means that instead of solving a three-dimensional boundary value problem, we will use the results from a set of two-dimensional boundary value problems.

The time-domain method presented here is specially developed to calculate directly the motion response of a ship subjected to non-sinusoidal exciting forces. In addition the method is able to work with the non-linear restoring forces which appear when the sides of the ship are non-vertical and the angular motion amplitudes are larger than 8-12 degrees. Other non-linearities can also be introduced.

8.2 - Radiation Forces

In Section-5.2 the radiation forces associated with the unsteady motions of two-dimensional bodies were studied, however all the formulations are valid for three-dimensional bodies oscillating with zero forward speed, if only the Laplace equation and the free-surface boundary condition are substituted by the correspondent three-dimensional conditions. All the other equations remain without changes since the boundary value problem is not solved in Section-5.2.

In the present Section a ship travelling with a forward speed and undergoing oscillatory motions in otherwise calm water is studied. This is a continuation of the study carried out in Section-5.2 and the approach used is the same. Cummins (1962) studied this problem also, but we will follow closely the formulation presented by Ogilvie (1964) since it seems to be more explicit. However, the final forms of the equation of motions are similar in both cases.

The co-ordinate systems have been defined in Section-3.1.

The total velocity potential for this problem is given by (see eqn. (3.1.8)):

$$\Phi^t(x,y,z,t) = -Ux + \Phi_S(x,y,z) + \Phi^R(x,y,z,t) \qquad (8.2.6)$$

Where the first two terms represent the potential for the steady flow past the ship fixed in its undisturbed position.

The conditions which the velocity potential for this problem must satisfy have been presented in Section-3.1, and are;

(L) $$\Phi^R_{xx} + \Phi^R_{yy} + \Phi^R_{zz} = 0 \qquad (8.2.1)$$

(F) $$\Phi^R_{tt} - 2U\Phi^R_{xt} + U^2\Phi^R_{xx} + g\Phi^R_z = 0 \quad , \text{ on } z = 0 \qquad (8.2.2)$$

(K) $$\frac{\partial \Phi^R_j}{\partial n} = \dot{\xi}_j n_j + \xi_j U m_j \quad , \; j = 1,...,6 \; , \text{ on } S_0 \qquad (8.2.3)$$

(B) $$\nabla\Phi^R \to 0 \quad , \text{ on } z \to -\infty \qquad (8.2.4)$$

$$(R) \quad \nabla\Phi^R \to 0 \quad , \text{ on } (x^2+y^2) \to \infty \tag{8.2.5}$$

The total velocity potential for this problem is given by (see eqn. (3.1.8)):

$$\Phi^t(x,y,z,t) = -Ux + \Phi_S(x,y,z) + \Phi^R(x,y,z,t) \tag{8.2.6}$$

Where the first two terms represent the potential for the steady flow past the ship fixed in its undisturbed position.

Now we state that the solution can be written in a form similar to equation (5.2.21), however two new functions are introduced so that the potential can satisfy the additional term in the body boundary condition (8.2.3). Thus the radiation potential is assumed to be;

$$\begin{aligned}\Phi_j^R(t) &= \dot{\xi}_j(t)\vartheta_{1j} + \xi_j(t)\vartheta_{2j} \\ &+ \int_{-\infty}^{t} \chi_{1j}(t-\tau)\dot{\xi}_j(\tau)d\tau + \int_{-\infty}^{t} \chi_{2j}(t-\tau)\xi_j(\tau)d\tau\end{aligned} \tag{8.2.7}$$

where the unknown functions, $\vartheta_{mj}, \chi_{mj}$, $m=1,2$, $j=1,...6$, satisfy the following conditions;

- Condition necessary for the radiation potential to satisfy the free-surface boundary condition (see equation (5.2.22)).

$$\vartheta_{mj} = 0 \quad , \text{ on } z=0 \tag{8.2.8}$$

- The kinematic body boundary condition to be satisfied by the potential proportional to the impulsive displacements.

$$\frac{\partial\vartheta_{1j}}{\partial n} = n_j \quad , \text{ on } S_0 \tag{8.2.9}$$

$$\frac{\partial\vartheta_{2j}}{\partial n} = Um_j \quad , \text{ on } S_0 \tag{8.2.10}$$

- The kinematic body boundary condition, and the free-surface boundary condition to be satisfied by the potential representing the perturbations that remain in the fluid after the impulsive displacements have finished.

$$\frac{\partial \chi_{mj}}{\partial n} = 0 \quad , \text{ on } S_0 \tag{8.2.11}$$

$$\frac{\partial^2 \chi_{mj}}{\partial t^2} - 2U\frac{\partial^2 \chi_{mj}}{\partial t \partial x} + U^2\frac{\partial^2 \chi_{mj}}{\partial x^2} + g\frac{\partial \chi_{mj}}{\partial z} = 0 \quad , \text{ on } z = 0 \tag{8.2.12}$$

- The conditions that the potentials must be zero at the first instant of the impulsive displacements. The second condition states that there exists continuity on the free-surface elevation at this instant.

$$\chi_{mj} = 0 \quad , \text{ for } t = 0 \tag{8.2.13}$$

$$\frac{\partial \chi_{mj}}{\partial t} = -g\frac{\partial \vartheta_{mj}}{\partial z} \tag{8.2.14}$$

Following the same procedure as in Section-5.2 it can be proved that this solution satisfies the free-surface and body boundary conditions, (8.2.2) and (8.2.3). In addition the solution is assumed to satisfy the conditions at infinity.

This solution is similar to the zero-speed solution presented in Section-5.2, and in fact if U=0 it becomes identical to the zero speed solution.

The pressure at any point in the fluid is given by the linearized Bernoulli's equation as given in Section-3.1. The time dependent part of the pressure is;

$$\frac{p - p_a}{\rho} = -\left(\frac{\partial \Phi^R}{\partial t} + \nabla\Phi_0 \cdot \nabla\Phi^R + zg\right) \tag{8.2.15}$$

where the steady potential is given by;

$$\Phi_0 = -Ux + \Phi_S$$

Substituting this potential in equation (8.2.15) the oscillatory pressure becomes;

$$\frac{p-p_a}{\rho} = -\left(\frac{\partial \Phi^R}{\partial t} + \nabla\Phi_S \cdot \nabla\Phi^R - U\frac{\partial \Phi^R}{\partial x} + zg\right) \qquad (8.2.16)$$

If the radiation velocity potential (8.2.7) is substituted into equation (8.2.16), the unsteady linearized pressure can be represented in terms of the solution potentials;

$$\frac{p-p_a}{\rho} = -gz$$

$$-\sum_{j=1}^{6} \ddot{\xi}_j(t)\vartheta_{1j}(x,y,z)$$

$$-\sum_{j=1}^{6} \dot{\xi}_j(t)\left[\vartheta_{2j}(x,y,z) + \left(-U\frac{\partial}{\partial x} + \nabla\Phi_S \cdot \nabla\right)\vartheta_{1j}(x,y,z)\right]$$

$$-\sum_{j=1}^{6} \xi_j(t)\left[\left(-U\frac{\partial}{\partial x} + \nabla\Phi_S \cdot \nabla\right)\vartheta_{2j}(x,y,z)\right]$$

$$-\sum_{j=1}^{6} \int_{-\infty}^{t} \dot{\xi}_j(\tau)\left[\frac{\partial}{\partial t} + \left(-U\frac{\partial}{\partial x} + \nabla\Phi_S \cdot \nabla\right)\right]\chi_{1j}(x,y,z,t-\tau)d\tau$$

$$-\sum_{j=1}^{6} \int_{-\infty}^{t} \xi_j(\tau)\left[\frac{\partial}{\partial t} + \left(-U\frac{\partial}{\partial x} + \nabla\Phi_S \cdot \nabla\right)\right]\chi_{2j}(x,y,z,t-\tau)d\tau \qquad (8.2.17)$$

The first term on the right-hand side represents the hydrostatic pressure, and it will be removed from the equations hereafter since in this Section we are dealing only with the effects due to the body motions. The second, third, and fourth terms represent pressures linearly proportional respectively to the instantaneous acceleration, velocity, and displacement of the body. The last two terms are convolution integrals which represent the whole past history of the velocity and displacement of the body.

Integrating the pressure over the mean wetted surface (the hydrostatic term is removed), we obtain the radiation forces associated with the oscillatory motion

of the ship travelling with forward speed. The radiation force in k-direction due to a motion in j-mode is given by;

$$F_{kj}^{R}(t) = -\ddot{\xi}_j(t)A_{kj}^{\infty} - B_{kj}^{t}\dot{\xi}_k(t) - C_{kj}^{t}\xi(t) - \int_{-\infty}^{t}\left\{K_{kj}(t-\tau)\dot{\xi}_j(t)\right\}d\tau \quad , \; k,j = 1,\ldots,6 \tag{8.2.18}$$

A full description of the radiation forces in terms of the unknown potentials ($\vartheta_{mj}, \chi_{mj}$, $m = 1,2$) is given by Ogilvie (1969), however we are not going to rewrite them since, beside ϑ_{1j}, the other potentials will not be evaluated in this study.

The several terms present in the equation are:

- The coefficient 'A_{kj}^{∞}', as was found in Section-5.2, is;

$$A_{kj}^{\infty} = \rho\iint_{S_0}\left\{\vartheta_{1j}n_k\right\}ds \quad , \; k,j = 1,\ldots,6 \tag{8.2.19}$$

  In accordance with (8.2.8) and the definition of added mass given in Section-4.2.2, A_{kj}^{∞} represents the infinite frequency added mass coefficient, contributing to the forces in k-direction due to unsteady motion in j-mode. This constant is dependent only on the ship geometry.

- The coefficient 'B_{kj}^{t}' is a constant which depends on ship geometry and forward speed. It was proven by King (1987) that B_{kj}^{t} is zero.

- The coefficient 'C_{kj}^{t}' is also a constant which depends on ship geometry and forward speed. The force proportional to this coefficient is a "radiation restoring force", and it represents a correction to the hydrodynamic steady forces acting on the ship due to the steady flow. The correction arises because this steady force is evaluated assuming the ship in the equilibrium position, and in fact the ship's position changes with time. In many forward speed formulations this term does not appears, at least explicitly. King (1987)

derived a set of equations in order to calculate the coefficients C^t_{kj}. In Appendix-B the these equations are presented.

. The function '$K_{kj}(t)$', named retardation function, is dependent on time, geometry, and forward speed. This quantity contains all the memory of the fluid response. It is interesting to note that $K_{kj}(t)$ is equivalent to the impulse response function of any stable linear system. As in Chapter-5 the retardation function will be related to the frequency dependent damping coefficients for the entire range of oscillatory frequencies.

The last term in equation (8.2.18) is a convolution integral obtained from the two integrals given in equation (8.2.17) by means of an integration by parts. It involves the effects of the whole past history of the motion, so the memory effects due to the radiated waves are represented here.

It is important to stress that none of the quantities described above (A^∞_{kj}, B^t_{kj}, C^t_{kj}, and $K_{kj}(t)$) is dependent of the past history of the unsteady motions. This means that they need only to be calculated once for a given vessel, and then the radiation forces can be evaluated for any arbitrary motion using (8.2.18).

The B^t_{kj} is zero, thus the radiation force in k-direction due to a motion in j-mode is;

$$F^R_{kj}(t) = -\ddot{\xi}_j(t)A^\infty_{kj} - C^t_{kj}\xi(t) - \int_{-\infty}^{t}\left\{K_{kj}(t-\tau)\dot{\xi}_j(\tau)\right\}d\tau \quad , \; k,j = 1,\ldots,6 \qquad (8.2.20)$$

Finally the radiation force in k-direction is given by;

$$F^R_k(t) = \sum_{j=1}^{6} F^R_{kj}(t) \quad , \; k = 1,\ldots,6 \qquad (8.2.21)$$

The relations we have obtained for the radiation forces do not have coefficients dependent on the frequency, thus they are valid to evaluate the radiation forces associated with non-sinusoidal motions, for example irregular motions. The only condition necessary to apply this method is the linearity of the radiation forces, and this means that the unsteady motions must be of small amplitude. So far no

procedure has been divised to evaluate the velocity potentials, ϑ_{2j} and χ_{mj}, since instead of evaluating them directly in time-domain, we are going to relate the radiation forces in time-domain to the radiation forces of all of the frequency-domain range. This will be described in Section-8.6.

8.3 - Exciting Forces

Exciting Forces in Sinusoidal Waves

As explained in Section-3.1, under certain assumptions, the linearized exciting potential problem can be treated as an independent problem, neglecting the interferences with the radiation potential. Furthermore in this linearized model the exciting forces are not affected by the previous history of the fluid motion. Thus the frequency-domain formulation derived in Section-7.3 can be used to evaluate the time-domain exciting forces, when a ship travelling with constant forward speed and arbitrary heading angle is subjected to sinusoidal waves.

The time-domain sinusoidal wave exciting forces are obtained from;

$$F_k^E(t) = \left(F_k^E\right)^C \cos\omega t + \left(F_k^E\right)^S \sin\omega t \quad , \; k = 1,\ldots,6 \qquad (7.3.48)$$

Exciting Forces in Irregular Waves

The linear exciting forces due to sinusoidal waves are linearly proportional to the wave amplitude. Thus the superposition principle can be applied to obtain the exciting forces arising from irregular waves. A procedure to calculate the exciting forces when a cylinder is subjected to irregular waves as they pass it, was presented in Section-4.3. The same procedure can be used to calculate the wave exciting forces acting on a ship travelling in irregular seas.

8.4 - Restoring Forces

The total restoring forces can be formulated by combining the effects of the hydrostatic forces, the weight of the ship, and the hydrodynamic restoring forces.

Hydrostatic Forces

The hydrostatic forces are the result of hydrostatic pressure action upon the hull. The expression to evaluate these forces has been given in Chapter-3, and is;

$$F^H = \iint_S (p_h \tilde{n}) ds \qquad (8.4.1)$$

It was assumed that the unit normal vector to the body surface is positive outwards. Since the pressure force acts towards the body the sign of the hydrostatic force must be changed. Separating the forces from the moments we redefine;

$$F^H = -\iint_S (p_h n) ds \qquad (8.4.2)$$

$$M^H = -\iint_S p_h (r \times n) ds \qquad (8.4.3)$$

where 'S' is the instantaneous wetted surface, '$p_h = -\rho g z$' is the hydrostatic pressure, '$\tilde{n}$' is the six component normal vector as defined in Section-3.1, 'n' is the unit vector normal to S, and 'r' is the vector position of any point on the body surface defined in the reference system advancing with the ship's forward speed but fixed on the undisturbed position of the ship, X=(x,y,z). (see figures 3.1 and 3.2.)

In order to evaluate the surface integral in (8.4.1) the Divergence theorem of Gauss will be used:

Gauss Theorem

Let V be a closed bounded region in space whose boundary is a piecewise smooth orientable surface Σ. Let f(x,y,z) be a vector function which is continuous and has continuous first partial derivatives in some domain containing Σ. Then;

$$\iint_{\Sigma}(f \cdot n)ds = \iiint_{V}(\nabla f)dv$$

and

$$\iint_{\Sigma}(f \times n)ds = \iiint_{V}(\nabla \times f)dv$$

where 'n' is the outer unit normal vector of Σ.

We state that our surface Σ is equal to the ship's wetted surface plus the water plane surface, $\Sigma = S + S_{wl}$, as drawn in figure 8.1. This surface is a smooth orientable surface. The hydrostatic pressure is a vector function which satisfies the conditions imposed by the theorem, thus the Gauss theorem can be applied to the hydrostatic problem.

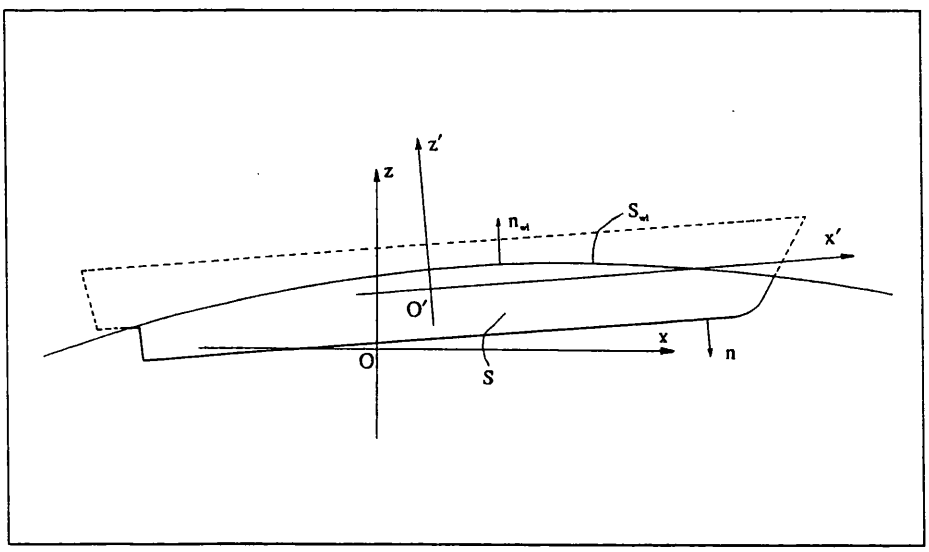

Figure 8.1 Application of the Gauss Theorem

. **Forces**

Applying the first relation of the Gauss theorem over the defined region results;

$$-\iint_{S}(p\cdot n)ds-\iint_{S_{wl}}(p\cdot n^{wl})ds=-\iiint_{V_{wl}}(\nabla p)dv \qquad (8.4.4)$$

where 'V_{wl}' is the instantaneous immersed volume of the ship, and 'n^{wl}' is the outward unit normal vector at the intersection of the free surface with the body volume, 'S_{wl}'.

Noting that $\nabla p=-\rho g\nabla z=-\rho g e_z$, e_x, e_y, e_z being the unit vectors parallel respectively to x, y, and z, the hydrostatic force becomes;

$$F^H=\rho g e_z\iiint_{V}dv-\rho g\iint_{S_{wl}}(z\cdot n^{wl})ds \qquad (8.4.5)$$

The expression can be further simplified by substituting the volume integral with the immersed volume of the body;

$$F^H=\rho g V_{wl}(t)e_z-\rho g\iint_{S_{wl}}(z\cdot n^{wl})ds \qquad (8.4.6)$$

The surface integral is to be evaluated over the intersection of the free-surface with the floating body volume.

The hydrostatic forces in each direction of the reference system can be evaluated using a strip theory geometric assumption, which implies that the unit normal vector at the intersection of the free surface with each cross section of the ship is assumed to have components only in the y and z directions, $n^{wl}=(0,N_2^{wl},N_3^{wl})$. This way the surface integrals can be simplified and finally the hydrostatic forces become;

$$F_1^H=-\rho g\int_{L}\int_{C_x}(zN_1^{wl})d\varsigma d\ell=0 \qquad (8.4.7)$$

The contribution of the hydrostatic force in the x-direction should be included in an extended theory when the surge motions are to be considered.

$$F_2^H = -\rho g \int_L \int_{C_x} (zN_2^{wl}) d\varsigma d\ell \tag{8.4.8}$$

$$F_3^H(t) = \rho g V_{wl}(t) - \rho g \int_L \int_{C_x} (zN_3^{wl}) d\varsigma d\ell \tag{8.4.9}$$

- **Moments**

Applying the second relation of the Gauss theorem over the defined region results;

$$-\iint_S p(r \times n) ds - \iint_{S_{wl}} p(r \times n^{wl}) ds = -\iiint_{V_{wl}} (r \times \nabla p) dv \tag{8.4.10}$$

Thus the hydrostatic moment becomes;

$$M^H = \rho g \iiint_{V_{wl}} (r \times \nabla z) dv - \iint_{S_{wl}} p(r \times n^{wl}) ds \tag{8.4.11}$$

The vectors in the volume integral are, $r = (x, y, z)$ and $\nabla z = (0, 0, e_z)$. Applying the products the hydrostatic moments about the three axes of the reference system, x, y, z, are respectively;

$$M_1^H = F_4^H = \rho g \iiint_{V_{wl}} y dv - \rho g \iint_{S_{wl}} z(yn_3^{wl} - zn_2^{wl}) ds \tag{8.4.12}$$

$$M_2^H = F_5^H = -\rho g \iiint_{V_{wl}} x dv - \rho g \iint_{S_{wl}} z(zn_1^{wl} - xn_3^{wl}) ds \tag{8.4.13}$$

$$M_3^H = F_6^H = -\rho g \iint_{S_{wl}} z(xn_2^{wl} - yn_1^{wl}) ds \tag{8.4.14}$$

The volume under the water line, and the co-ordinates of the centre of this volume are;

$$V_{wl} = \iiint_{V_{wl}} dv \tag{8.4.15}$$

$$x_B = \frac{1}{V_{wl}} \iiint_{V_{wl}} x dv, \quad y_B = \frac{1}{V_{wl}} \iiint_{V_{wl}} y dv, \quad z_B = \frac{1}{V_{wl}} \iiint_{V_{wl}} z dv \tag{8.4.16}$$

In terms of the former variables, and using again the strip theory assumption the hydrostatic moments become;

$$M_1^H = F_4^H = \rho g V_{wl}(t) y_B - \rho g \int_L \int_{C_x} z\left(yN_3^{wl} - zN_2^{wl}\right) d\varsigma d\ell \tag{8.4.17}$$

$$M_2^H = F_5^H = -\rho g V_{wl}(t) x_B + \rho g \int_L \int_{C_x} z\left(xN_3^{wl}\right) d\varsigma d\ell \tag{8.4.18}$$

$$M_3^H = F_6^H = -\rho g \int_L \int_{C_x} z\left(xN_2^{wl}\right) d\varsigma d\ell \tag{8.4.19}$$

In conclusion, in order to evaluate the hydrostatic forces the immersed volume, as well as the co-ordinates of the centre of this volume, must be calculated at each time instant. In addition the intersection of the exact free-surface with the body volume must also be computed. It is interesting to discover that using the expression obtained from Bernoulli's equation, with no simplifications, there are hydrostatic forces in all of the six principal directions defined. Namely, there are hydrostatic forces associated with the surge and sway motions, and hydrostatic moment associated the yaw motion, which can not be predicted by the linear theory.

Restoring Forces

The restoring forces and moments are obtained by combining the hydrostatic forces and moments respectively with the weight of the ship and the moment of

the weight about the origin of the reference system. In addition it is logical to introduce in the restoring force term the hydrodynamic restoring force, $\xi_j(t)C^t_{kj}$, presented in Section-8.2, the result is;

$$F_1^B(t) = \sum_{j=1}^{6} \xi_j C^t_{1j} \tag{8.4.20}$$

$$F_2^B(t) = -\rho g \int_L \int_{C_x} (zN_2^{wl}) d\varsigma d\ell + \sum_{j=1}^{6} \xi_j C^t_{2j} \tag{8.4.21}$$

$$F_3^B(t) = \rho g V_{wl} - \rho g \int_L \int_{C_x} (zN_3^{wl}) d\varsigma d\ell + \sum_{j=1}^{6} \xi_j C^t_{3j} - Mg \tag{8.4.22}$$

$$F_4^B(t) = \rho g V_{wl} y_B - \rho g \int_L \int_{C_x} z(yN_3^{wl} - zN_2^{wl}) d\varsigma d\ell + \sum_{j=1}^{6} \xi_j C^t_{4j} - y_G Mg \tag{8.4.23}$$

$$F_5^B(t) = -\rho g V_{wl} x_B + \rho g \int_L \int_{C_x} z(xN_3^{wl}) d\varsigma d\ell + \sum_{j=1}^{6} \xi_j C^t_{5j} + x_G Mg \tag{8.4.24}$$

$$F_6^B(t) = -\rho g \int_L \int_{C_x} z(xN_2^{wl}) d\varsigma d\ell + \sum_{j=1}^{6} \xi_j C^t_{6j} \tag{8.4.25}$$

where 'M' is the ship's mass, and 'x_G, y_G' are the x and y co-ordinates of the gravity centre in the reference system (x,y,z). All the variables are to be evaluated at each time instant.

Free-Surface Elevation Intersection with the Hull

As stated above the intersection of the free-surface with the ship's hull must be calculated at each time instant. To do so, both the co-ordinates of every point of the hull surface, and the free-surface elevation must be defined in the reference system fixed at the mean position of the ship, X=(x,y,z). Assuming small

angular motions, the transformation between the co-ordinates in the ship fixed reference system, $X' = (x', y', z')$, and $X = (x, y, z)$ is given by;

$$x = x' + \xi_1 + \xi_5 z' - \xi_6 y'$$

$$y = y' + \xi_2 + \xi_6 x' - \xi_4 z' \qquad (8.4.26)$$

$$z = z' + \xi_3 + \xi_4 y' - \xi_5 x'$$

Certainly, in some particular conditions, the assumption of small angular motions is not accurate. For example roll motions should be formulated using large amplitude motions. This problem is not studied in this thesis.

The true free-surface elevation in the neighbourhood of the ship's hull is obtained adding together several contributions due to the incident wave, the diffracted wave, the radiated waves associated with each of the six ship unsteady motions, and to the steady wave associated with the ship forward speed. In addition there are interferences between all these components. This is a very complex problem, however in the case of a ship, in the frequency range of interest, the incident wave contribution to the free-surface elevation is by far the largest and in practice can be assumed as the only one. The last step is to obtain the incident wave elevation associated with the incident wave potential used in Section-7.3 to evaluate the exciting forces.

In Section-3.1 Bernoulli's equation, defined in a reference system advancing with the ship's forward speed, was presented;

$$\frac{p - p_a}{\rho} = -\frac{\partial \Phi}{\partial t} - \frac{1}{2}|\nabla \Phi|^2 - zg + \frac{1}{2}U^2 \qquad (3.1.25)$$

Bernoulli's equation evaluated at the free-surface of the fluid results in;

$$\zeta = -\frac{1}{g}\left(\frac{\partial \Phi}{\partial t} + \frac{1}{2}\nabla\Phi \cdot \nabla\Phi - \frac{1}{2}U^2\right) \quad , \text{ on } z = \zeta \qquad (8.4.27)$$

since at the free-surface, $(z = \zeta)$, the fluid pressure is the atmospheric.

If the fluid velocity potential is expanded about the mean free-surface elevation, z=0, and the result substituted in equation (8.4.27), we obtain the free-surface

elevation in terms of the potential evaluated at the mean level (z=0). The higher order terms resulting from the expansion are neglected. The resulting equation has two kinds of terms, the steady terms, which are related to the ship wave resistance problem and are neglected in this work, and the unsteady terms which are of interest to the present work. The linearized free-surface elevation due to the unsteady potential is;

$$\zeta(x,y,t) = -\frac{1}{g}\left(\frac{\partial \Phi_1}{\partial t} + \nabla\Phi_0 \nabla\Phi_1\right) \quad , \text{ on } z=0 \tag{8.4.28}$$

where Φ_0 and Φ_1 are respectively the steady and unsteady velocity potentials.

It was assumed in Section-3.1 that the unsteady potential can be linearly decomposed, and that the steady potential is given by $\Phi_0 = -Ux$. Using these assumptions the free-surface elevation due to the incident potential is;

$$\zeta^I(x,y,t) = -\frac{1}{g}\left(\frac{\partial \Phi^I}{\partial t} - U\frac{\partial}{\partial x}\Phi^I\right) \quad , \text{ on } z=0 \tag{8.4.29}$$

or for a sinusoidal incident potential;

$$\zeta^I(x,y,t) = -\frac{1}{g}\left(i\omega - U\frac{\partial}{\partial x}\right)\Phi^I \quad , \text{ on } z=0 \tag{8.4.30}$$

The incident wave potential, in accordance with the linear gravity wave theory, is given by;

$$\Phi^I = \frac{ig\zeta^a}{\omega_0} e^{k_0 z} e^{ik_0(x\cos\beta + y\sin\beta)} e^{i\omega t} \tag{7.3.1}$$

Substituting the incident wave potential into equation (8.4.30) the free-surface elevation due to the linear incident wave potential is obtained;

$$\zeta^I(x,y,t) = -\zeta^a e^{ik_0(x\cos\beta + y\sin\beta)} e^{i\omega t} \tag{8.4.31}$$

and taking the real part;

$$\zeta^I(x,y,t) = \zeta^a \cos\{k_0(x\cos\beta + y\sin\beta)\}\cos(\omega t) - \zeta^a \sin\{k_0(x\cos\beta + y\sin\beta)\}\sin(\omega t) \tag{8.4.32}$$

which is the expression to be used in the numerical computations.

With the knowledge of the positions in space of the ship's surface and the fluid free-surface the intersection between both surfaces can be determined. It is assumed that this intersection is given by a plane, which is very near to reality for the incident wave frequency range of interest.

To evaluate the ship hydrostatic forces the strip theory approach is used again, thus the hydrostatic forces are computed for every cross section and then integrated over the ship's length.

8.5 - Body-Mass Forces

All derivations of the inertial forces have been given in Section-7.5, and here only the final results are presented.

The inertial force in k-direction due to an acceleration in j-mode is given by;

$$F_{kj}^{M} = M_{kj}\ddot{\xi}_j \quad , \quad k,j = 1,\ldots,6 \tag{8.5.1}$$

and the total inertial force in k-direction is;

$$F_{k}^{M} = \sum_{j=1}^{6} M_{kj}\ddot{\xi}_j \quad , \quad k = 1,\ldots,6 \tag{8.5.2}$$

where 'M_{kj}' are the coefficients of the mass matrix, which, for ship forms with lateral symmetry and the centre of gravity located at $(0,0,z'_G)$, are given by;

$$\left[M_{kj}\right] = \begin{bmatrix} M & 0 & 0 & 0 & Mz'_G & 0 \\ 0 & M & 0 & -Mz'_G & 0 & 0 \\ 0 & 0 & m & 0 & 0 & 0 \\ 0 & -Mz'_G & 0 & I_{44} & 0 & -I_{46} \\ Mz'_G & 0 & 0 & 0 & I_{55} & 0 \\ 0 & 0 & 0 & -I_{64} & 0 & I_{66} \end{bmatrix} \tag{8.5.3}$$

The moments of inertia, 'I_{kj}' coefficients are calculated using the following formulas;

$$I_{44} = \iiint_{V_B} \rho_B\left(y'^2 + z'^2\right)dv \qquad I_{55} = \iiint_{V_B} \rho_B\left(x'^2 + z'^2\right)dv$$

$$I_{66} = \iiint_{V_B} \rho_B\left(x'^2 + y'^2\right)dv \qquad I_{46} = I_{64} = \iiint_{V_B} \rho_B\left(x'z'\right)dv \tag{8.5.4}$$

8.6 - Equations of Motion and Solution

In the former Sections of this Chapter all the components of the total fluid forces acting on the ship have been evaluated, as well as the inertia and weight forces associated with the ship's mass. We can now combine these forces in order to obtain the motion equations for the free oscillations of the ship as a rigid body, subjected to sinusoidal or irregular waves.

The six component vectors representing the forces in each direction are;

$F_k^E(t)$, $k = 1,\ldots,6$ for exciting forces of arbitrary form

$$F_k^M(t) = \sum_{j=1}^{6} M_{kj}\ddot{\xi}_j(t) \quad , \quad k = 1,\ldots,6 \quad \text{for the body-mass inertial forces}$$

$$F_k^R(t) = \sum_{j=1}^{6}\left\{\ddot{\xi}_j(t)A_{kj}^{\infty} + \int_{-\infty}^{t}\left[K_{kj}(t-\tau)\dot{\xi}_j(\tau)\right]d\tau\right\} \quad , \quad k = 1,\ldots,6 \quad \text{for the radiation forces}$$

$$F_k^B(t) = F_k^H(t) + F_k^W(t) + \sum_{j=1}^{6}\xi(t)C_{kj}^t \quad , \quad k = 1,\ldots,6 \quad \text{for the restoring forces}$$

Combining the above equations in a proper way the time-domain motion equations become;

$$\sum_{j=1}^{6}\left\{\left(M_{kj} + A_{kj}^{\infty}\right)\ddot{\xi}_j(t) + \int_{-\infty}^{t}\left[K_{kj}(t-\tau)\dot{\xi}_j(\tau)\right]d\tau + C_{kj}^t\xi_j(t)\right\} + \\ + F_k^H(t) + F_k^W(t) = F_k^E(t) \quad , \quad k = 1,\ldots,6 \qquad (8.6.1)$$

Following the procedure adopted in Section-5.6, the frequency-domain and time-domain models will be related using the Fourier analysis. Calculating the Fourier transforms of the time-domain equations (8.6.1), we find the result equivalent to the frequency-domain equations of motion (7.6.1). If the imaginary parts are made equal it results;

$$B_{kj}(\omega) = \int_0^{\infty} \{K_{kj}(t)\cos\omega t\}dt \qquad (8.6.2)$$

where '$B_{kj}(\omega)$' is the frequency-domain damping coefficient of the ship.

The inverse of the cosine transform is given by;

$$K_{kj}(t) = \frac{2}{\pi}\int_0^{\infty} \{B_{kj}(\omega)\cos\omega t\}d\omega\}d\omega \qquad (8.6.3)$$

Thus the retardation functions, $K_{kj}(t)$, can be obtained from the frequency domain damping coefficients, $B_{kj}(\omega)$, covering the whole range of frequencies.

In Section-7.6, where the frequency-domain solution for the ship motion problem was studied, we found that for the ship with lateral symmetry the six coupled equations of motion would reduce to two sets of equations. One set of three coupled equations for the surge, heave and pitch motions, and another set for the roll, sway, and yaw motions. So for that linearized mathematical model the surge, heave, and pitch were independent from the roll, sway, and yaw, in case of ships with lateral symmetry. In the time-domain model developed here one non-linearity is taken into account, which arises from the fact that the hydrostatic forces are evaluated in terms of the "exact" immersed volume under the water line. This will induce a coupling between the heave displacement and the roll and pitch hydrostatic moments, since these moments depend on the immersed volume (see equations (8.4.20) and (8.4.21)). On the other hand, the frequency domain approach to this problem assumes that the roll displacements occur at a constant mean draft (see Section-7.4), so there is no hydrostatic coupling between the heave and roll motions.

As shown in Section-7.2 and Section-7.3, if the ship in addition to lateral symmetry has slender hull shape, the radiation and exciting forces associated with the surge motions are much smaller than the forces associated with other modes and can be neglected. In addition, all other forces being studied here have zero value in the surge direction, so the surge motion is not included.

Finally we can conclude that in the time-domain model the five motion modes are coupled (sway, heave, roll, pitch, and yaw). However we are interested only

in the particular case of a ship travelling with finite forward speed, and encountering head waves. The ship will experience heave and pitch motions, and the equations describing these motions are obtained from (8.6.1);

Heave Motion

$$\begin{aligned}&(M+A_{33}^{\infty})\ddot{\xi}_3(t)+\int_{-\infty}^{t}\left[K_{33}(t-\tau)\dot{\xi}_3(\tau)\right]d\tau+C_{33}^{l}\xi_3(t)\\&+A_{35}^{\infty}\ddot{\xi}_3(t)+\int_{-\infty}^{t}\left[K_{35}(t-\tau)\dot{\xi}_5(\tau)\right]d\tau+C_{35}^{l}\xi_5(t)+F_3^{H}(t)-Mg=F_3^{E}(t)\end{aligned}\qquad(8.6.4)$$

Pitch Motion

$$\begin{aligned}&(I_{55}+A_{55}^{\infty})\ddot{\xi}_5(t)+\int_{-\infty}^{t}\left[K_{55}(t-\tau)\dot{\xi}_5(\tau)\right]d\tau+C_{55}^{l}\xi_5(t)\\&+A_{53}^{\infty}\ddot{\xi}_3(t)+\int_{-\infty}^{t}\left[K_{53}(t-\tau)\dot{\xi}_3(\tau)\right]d\tau+C_{53}^{l}\xi_3(t)\\&+F_5^{H}(t)-x_G(t)Mg=F_5^{E}(t)\end{aligned}\qquad(8.6.5)$$

These equations are solved in the time-domain using the fourth-order Runge-Kutta method, which means that the time history of the motions is built time step by time step from the initial instant t=0.

Final Remarks

The final equations of motion do not have frequency dependent coefficients, and in fact this formulation is valid whatever the nature of the exciting forces or the ship response, once it results in permissible amplitudes of the motions. Thus the method presented here is specially formulated to calculate directly the motion response of a ship subjected to non-sinusoidal exciting forces. In addition the method is able to work with the non-linear restoring forces which appear when the sides of the ship are non-vertical, and the angular motion amplitudes are larger than 8-12 degrees.

Also other non-linearities, which have not been studied in this work, can be introduced like for example: slamming forces, water on deck, the steering forces in following seas or when the ship changes course suddenly, etc (this aspects will be discussed latter on).

The major advantage of this method in relation to other non-linear strip-theory methods where the motion equations are solved numerically in the time-domain is found when responses in irregular seas are needed. Here the radiation forces are evaluated in a consistent manner. In other words these are really time-domain radiation forces. The existing time-domain strip theory methods make use of frequency dependent coefficients, and the question which normally arise is "which frequency should the coefficients correspond when the exciting frequency is not well defined?". There are several compromise answers to this question (see Oliver (1985) and Petersen (1992)), however this is an attempt to solve a problem which is basically wrong.

It is also author's opinion that this method has a real advantage in relation to the time-domain panel methods, which solve the radiation problem in the time-domain (see Liapis (1985), King (1988), and Beck (1991)). This has to do with the computational effort necessary to run the numerical models. The time-domain panel methods have to solve at each time-step a system of integral differential equations, in number equal to the number of panels used to represent the ship. Furthermore each equation has a complicated time-domain Green's function also to be evaluated. Powerful computers must be used, and long time-runs are normal.

On the other hand, the method presented here can be used on a PC computer with acceptable run-times. The retardation function, the infinite frequency added masses, and the hydrodynamic restoring coefficients must be calculated only once for a given vessel, and after that many runs, using different kinds of exciting forces, can be executed.

It is true that the applicability of the panel methods is wider than the strip theory methods. The strip theory method implies thinner ships, and in principle is intended for high frequencies.

About the first restriction, it is accepted from the results and comparisons made in the last three decades, that the usual ship forms are valid for application of the

strip theory. The limits of applicability of the strip theory are discussed by Kim (1980) for the case of barges at zero forward speed. In the paper good agreement between the theory and experiments is shown for a barge with L/B=4.0, and the text referred to good results being found even for L/B as low as 2.5.

The radiation, and diffraction forces in the strip theory are formulated under the assumption that the frequency is high, and in fact the results for high frequencies are good, specially for the heave and pitch motions. However at low frequencies the external forces acting upon the ship are dominated by the Froude-Krylov and hydrostatic forces, thus a poor prediction of the other forces does not significantly affect the results. Comparisons between the numerical results and experiments confirm this fact.

9. NUMERICAL RESULTS

9.1 - Computer Programs

The objective of the ship motions study in this thesis work is to compare the predictions of the heave and pitch of ships by two different methods. The first is the well known linear frequency domain strip theory. This method is recognised as giveing reliable predictions in a wide variety of conditions, and in fact has been the most used for practical purposes during the last two decades. The theory behind the strip method used is described in Chapter-7. The second method is a time domain strip theory, were the radiation forces are evaluated in the time domain, and one non-linearity is introduced in the restoring force term. All the theory used is explained in Chapters 7 and 8.

Two computer programs were developed in order to obtain numerical results for both theories, and will be briefly explained in this Section.

Frequency-Domain Program

The frequency domain equations which must be solved to obtain the heave and pitch motions of the ship were derived in Section-7.6 and are;

Heave and Pitch Motions

$$\begin{cases} -\omega^2\xi_3^C(m+A_{33})+\omega\xi_3^S B_{33}+\xi_3^C C_{33}-\omega^2\xi_5^C A_{35}+\omega\xi_5^S B_{35}+\xi_5^C C_{35}=\left(F_3^E\right)^C \\ -\omega^2\xi_3^S(m+A_{33})-\omega\xi_3^S B_{33}+\xi_3^S C_{33}-\omega^2\xi_5^S A_{35}-\omega\xi_5^C B_{35}+\xi_5^S C_{35}=\left(F_3^E\right)^S \\ -\omega^2\xi_3^C A_{53}+\omega\xi_3^S B_{53}+\xi_3^C C_{53}-\omega^2\xi_5^C(I_{55}+A_{55})+\omega\xi_5^S B_{55}+\xi_5^C C_{55}=\left(F_5^E\right)^C \\ -\omega^2\xi_3^S A_{53}-\omega\xi_3^C B_{53}+\xi_3^S C_{53}-\omega^2\xi_5^S(I_{55}+A_{55})-\omega\xi_5^C B_{55}+\xi_5^S C_{55}=\left(F_5^E\right)^S \end{cases}$$

These four coupled equations are simple algebraic equations and once all coefficients are determined the solutions (ξ_j^C, ξ_j^S) are readily obtained.

1. The added mass and damping coefficients, A_{kj}, B_{kj}, are computed using the expressions (7.2.36) to (7.2.43). The sectional added mass and damping coefficients, a_{kj}, b_{kj}, are computed using the "Frank Close Fit Method" described in Section-4.2.

2. The sinusoidal exciting forces, $F_k^E(t)$, are computed using the strip theory approach explained in Section-7.3.

- Expressions (7.3.25) and (7.3.26) give the ship Froude-Krylov forces in terms of the sectional Froude-Krylov forces expressed by equation (7.3.28). A procedure to evaluate the sectional parts is described in Section-4.3, and the modifications explained in Section-7.3 should be added. If the exciting forces due to irregular sea states are to be calculated, the procedure explained in Section-4.3, with the small modifications explained in Section-8.3 to be adapted to ship problems, is to be used.

- The ship diffraction forces are calculated by equations (7.3.42), and (7.3.43) in terms of the sectional diffraction forces. To compute the sectional diffraction forces two different methods were implemented in the computer program. The first solves the diffraction problem directly, and the method to evaluate the sectional diffraction forces is basically the "Frank Close Fit Method" described in Section-4.3, with the modifications explained in Section-7.3. The second method uses Haskind's relations and is derived in Section-7.3. The sectional diffraction forces are computed using equations (7.3.51).

3. The restoring and inertia coefficients are computed using the expressions presented in Section-7.4 and Section-7.5.

4. Finally the equations are solved by the Gauss-Jordan method.

The frequency domain program written calculates only the heave and pitch motions for any heading of the ship with forward speed. However it was written is prepared to be easily extended to solve the other modes of motion since the corresponding sectional exciting forces were already computed.

Time Domain Program

The time domain equations of motion were derived in Chapter-8, and are;

Heave Motion

$$(M+A_{33}^{\infty})\ddot{\xi}_3(t)+\int_{-\infty}^{t}\left[K_{33}(t-\tau)\dot{\xi}_3(\tau)\right]d\tau+C_{33}^{t}\xi_3(t)$$
$$+A_{35}^{\infty}\ddot{\xi}_3(t)+\int_{-\infty}^{t}\left[K_{35}(t-\tau)\dot{\xi}_5(\tau)\right]d\tau+C_{35}^{t}\xi_5(t)+F_3^{H}(t)-Mg=F_3^{E}(t)$$

Pitch Motion

$$(I_{55}+A_{55}^{\infty})\ddot{\xi}_5(t)+\int_{-\infty}^{t}\left[K_{55}(t-\tau)\dot{\xi}_5(\tau)\right]d\tau+C_{55}^{t}\xi_5(t)+A_{53}^{\infty}\ddot{\xi}_3(t)+$$
$$\int_{-\infty}^{t}\left[K_{53}(t-\tau)\dot{\xi}_3(\tau)\right]d\tau+C_{53}^{t}\xi_3(t)+F_5^{H}(t)-x_G(t)Mg=F_5^{E}(t)$$

These are integro-differential equations, with two non-linear terms both included in the restoring force term. Thus, given the nature of the equations, the solution must be numerical.

This is an initial value problem, since the characteristics of the motion are known at some starting point, t=0, and it is desired to find the same characteristics at some final point, or at some discrete list of points. The method chosen to solve the problem is the "fourth-order Runge-Kutta", which processes the integration of coupled first order ordinary differential equations, thus the first step is to reduce the second order differential equations presented above, to a set of equivalent first order differential equations;

$$\dot{y}_1=\frac{\partial\xi_3}{\partial t}=\dot{\xi}_3(t)$$

$$\dot{y}_2 = \frac{\partial \dot{y}_1}{\partial t} = \ddot{\xi}_3(t) = \frac{\left(I_5 + A_{55}^{\infty}\right)}{\left(M + A_{33}^{\infty}\right)\left(I_5 + A_{55}^{\infty}\right) - A_{35}^{\infty}A_{53}^{\infty}} \times$$

$$\left\{ F_3^E(t) - CV_{33}(t) - CV_{35}(t) - F_3^B(t) + A_{35}^{\infty} \frac{\left[CV_{55}(t) + CV_{53}(t) + F_5^B(t) - F_5^E(t)\right]}{\left(I_5 + A_{55}^{\infty}\right)} \right\}$$

$$\dot{y}_3 = \frac{\partial \xi_5}{\partial t} = \dot{\xi}_5(t)$$

$$\dot{y}_4 = \frac{\partial \dot{\xi}_5}{\partial t} = \ddot{\xi}_5(t) = \frac{\left[F_5^E(t) - A_{53}^{\infty}\ddot{\xi}_3(t) - CV_{55}(t) - CV_{53}(t) - F_5^B(t)\right]}{\left(I_{55} + |A_{55}^{\infty}\right)}$$

where the convolution integrals and restoring terms are given by;

$$CV_{kj}(t) = \int_{-\infty}^{t} \left\{ K_{kj}(t-\tau)\dot{\xi}_j(\tau) \right\} d\tau$$

$$F_3^B(t) = \rho g V_{wl}(t) - \rho g \int_L \int_{C_x} \left\{ z(t) N_3^{wl}(t) \right\} d\varsigma d\ell + \sum_{j=1}^{6} \xi_j(t) C_{3j}^t - Mg$$

$$F_5^B(t) = -\rho g V_{wl}(t) x_B(t) + \rho g \int_L \int_{C_x} z(t) \left\{ x(t) N_3^{wl}(t) \right\} d\varsigma d\ell + \sum_{j=1}^{6} \xi_j C_{5j}^t + x_G Mg$$

Basically the fourth-order Runge-Kutta method advances a solution from 't_n' to '$t_{n+1} = t_n + \Delta t$', using the derivative information at four points across the interval 'Δt'. Thus the method requires four evaluations per step of the right-hand side of the equations presented above. Then the derivative information is used to math a Taylor series expansion. The error obtained is of the order Δt^5.

The several terms on the equations of motion are evaluated as follows;

1. The ship's mass coefficients, M_{kj}, are obtained according to (8.5.3) and (8.5.4).

2. The infinite frequency added mass coefficients, A_{kj}^{∞}, are evaluated using the strip theory approach described in Section-7.2. The formulas to be used are the (7.2.36) to (7.2.43), which are expressed in terms of the sectional infinite frequency added mass coefficients, a_{kj}^{∞}. The former coefficients are evaluated using the particular case of the "Frank Close Fit Method" adapted to the infinite frequency problem, as described in Section-4.2.2

3. The convolution integrals, $CV_{kj}(t)$, are evaluated four times per time step at the instants required by the Runge-Kutta method. The same follows for all the time dependent terms. The retardation functions, $K_{kj}(t)$, are computed before the routine which solves the motions equations is called the first time. In fact these functions are computed by a different program since they are independent of the characteristics of the motion. This way, once we have got the retardation functions, several runs can be made with the motions program in different exciting conditions. The retardation functions are given by the cosine fourier transform of the damping coefficients correspondent to all the frequency domain range of frequencies;

$$K_{kj}(t) = \frac{2}{\pi}\int_0^{\infty}\{B_{kj}(\omega)\cos\omega t\}d\omega$$

$$K_{kj}(t) = \frac{2}{\pi}\int_0^{\infty}\{B_{kj}(\omega)\cos\omega t\}d\omega$$uted between the second '0' and the second '30', since for t>30 sec. the value of the functions is approximately zero, as is shown by the graphics in Section-9.2. In practical terms this means that '$-\infty = -30$ sec.' in the convolution integrals, or in other words that the history of the fluid motion which occurred 30 seconds before is not affecting the actual fluid motion at the actual instant. The frequency-domain damping coefficients, $B_{kj}(\omega)$, correspondent to all frequencies (from $\omega = 0$ to $\omega = \infty$) are calculated using the strip theory approach described in Section-7.2. The formulas to be used are the (7.2.36) to (7.2.43), which are expressed in terms of the sectional frequency dependent damping coefficients, $b_{kj}(\omega)$. The sectional damping coefficients are evaluated using the "Frank Close Fit Method" described in Section-4.2.

4. To compute the restoring forces several steps must be taken;

- The instantaneous free-surface elevation due the incident wave is calculated on both sides of every cross section of the ship, as well as the intersection of this surface with the cross sections at their exact position. The intersection is assumed to be a horizontal plane.

- The surface integrals over the former intersections are calculated and then integrated over the length of the ship.

- The exact immersed volume of every cross section is calculated, as well as the centre of these volumes. The results are then integrated over the length of the ship.

- Finally the buoyancy and weight moments about the origin are calculated.

- The hydrodynamic restoring forces are not evaluated, thus the program is working only for the zero speed condition.

5. The exciting forces due to sinusoidal waves are calculated by the same procedure as the one used in the frequency domain program.

The program initialises the motion at same negative time using the frequency domain solution corresponding to the incident wave imposed. At the instant t=0 the transition occurs and the time domain computation starts. At the present moment the program is working only for the zero speed condition, since the rather complex equation to be solved in order to obtain the speed dependent hydrodynamic restoring coefficients was not solved during the period of this thesis. The equation referred to is presented in Appendix-B. In addition only the heave and pitch equations are solved, however the program is prepared to be easily extended to the other modes of motion. It is important to note that all the modes of motion are coupled through the restoring force term, thus, in opposition to the frequency domain solution, the predictions of heave and pitch are valid only for head and following seas.

9.2 - Ship Characteristics

A container ship with a bulbous bow has been chosen to perform the computations by both numerical models. The container ship has been tested in the Seakeeping Laboratory of the Netherlands Ship Model Basin. The model was constructed to a scale of 1 to 55, and during the tests it was self-propelled and free in its motions, except it was kept on course by an auto-pilot controlling the rudder. The heave motion was measured by a vertical light-weight rod driving a potentiometer, while the pitch was recorded by a gyroscope. Model tests were conducted in a wide range of wave directions, and for the wave frequencies corresponding to the following wave length to ship length ratios; 0.35, 0.5, 0.6, 0.7, 0.9, 1.1, and 1.4. The wave height was kept constant at 1/60 the model length. Three ship speed were used, corresponding to the following Froude numbers, 0.220, 0.245, and 0.270.

A detailed description of the model, procedure, and experimental results can be found in the report by Gie (1972). Flokstra (1974) used these experimental results to compare three strip theories.

The main characteristics of the ship are listed, and a bodyplan is reproduced in figure 9.1.

Length between perpendiculars	270.0 m
Breadth	32.2 m
Draught even keel	10.85 m
Displacement volume	56.097 m^3
Block coefficient	0.598
Waterplane coefficient	0.757
Midship section coefficient	0.950
LCG aft of station 10	10.12 m
Centre of gravity above base	13.49 m
Metacentric height	1.15 m
Longitudinal gyradius in pitch direction	24.8 $\%L_{pp}$

Natural pitch period	8.6 sec.
Natural heave period	8.7 sec.

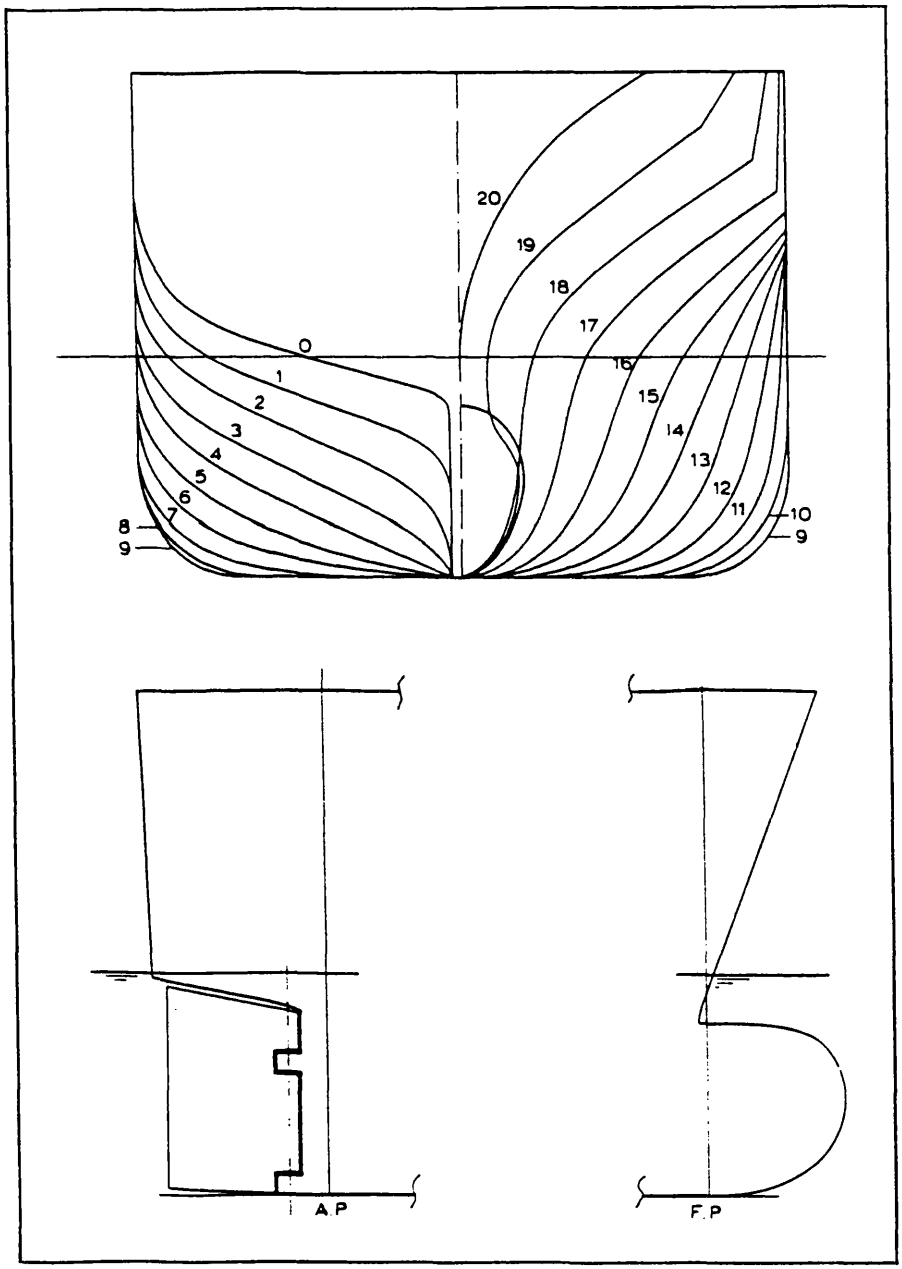

Fig. 9.1 Body plan, bow and stern outlines of container ship

9.3 - Frequency Domain Results

The first point to be stressed refers to the exciting forces, as mentioned the diffracted part of the exciting forces was computed by two different methods, one solves the diffracted problem directly and the other uses Haskind's relations. It was found that the results are very similar for the whole frequency range, which indicates that the computations are properly done.

In this Section results of the heave and pitch motions predicted by the frequency domain strip theory are compared with experimental results and the predictions from two other ship motion theories. These results bring nothing new since this kind of strip theory has been in use since 1970, however it is important to verify that the computations are done properly because in the next step the time domain strip theory will be compared with the present one. In addition some frequency domain results will be used by the time domain program, namely the exciting forces and the damping coefficients correspondent to all the frequency range.

The two other ship motion theories to be compared were developed by the German Classification Society (Germanischer-Loyds). One is a two dimensional theory , GL_{2D}, studied by Hochmann (1991), and the other is a three dimensional panel method, GL_{3D}, developed by Papanikolaou (1992).

The results are presented in the form of transfer functions, where the heave is non-dimensioned with respect to the wave amplitude and the pitch is non-dimensionalised with respect to the product wave amplitude-wave number. The experimental results are represented by the black symbols, the results from the theory used in these thesis by the stars, the GL_{2D} results by the triangles, and the GL_{3D} results by the squares. The transfer functions are shown in figures 9.2 to 9.9.

In general the numerical results compare well with the experiments, but there is a tendency to over-estimate the heave motion in head and bow waves at the lower wave frequencies. Comparing the two strip theories it can be observed that the thesis strip theory results are closer to the experiments than the GL_{2D}.

The GL_{3D} program gives very good results for the heave motion in head waves, however its results of the pitch are not better than the strip theory programs and it under-estimates both motions in quartering waves.

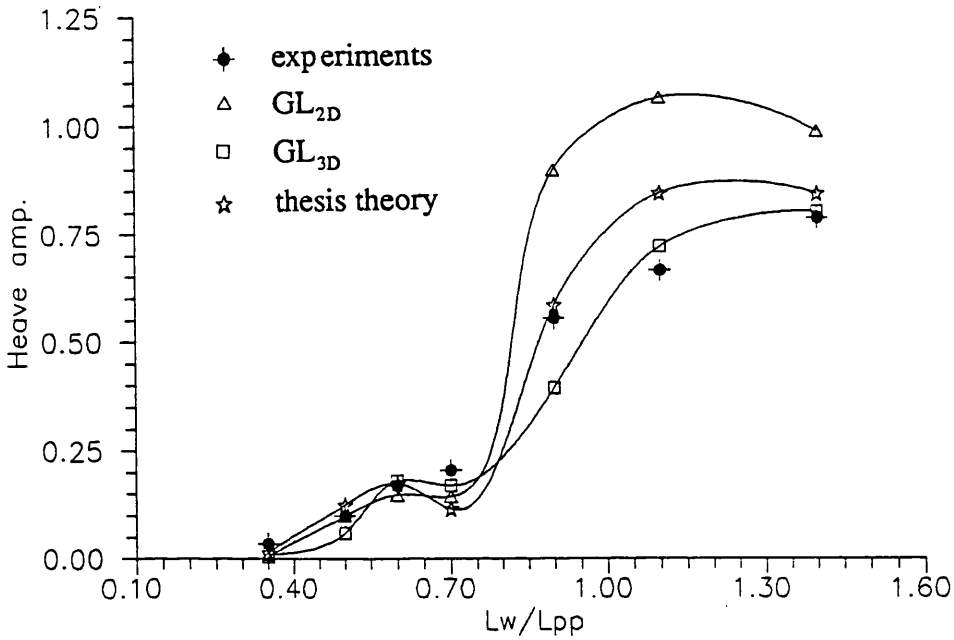

Fig. 9.2 ξ_3^a / ζ^a, heave transfer function in head waves
$\beta = 0°$, Fn = 0.220

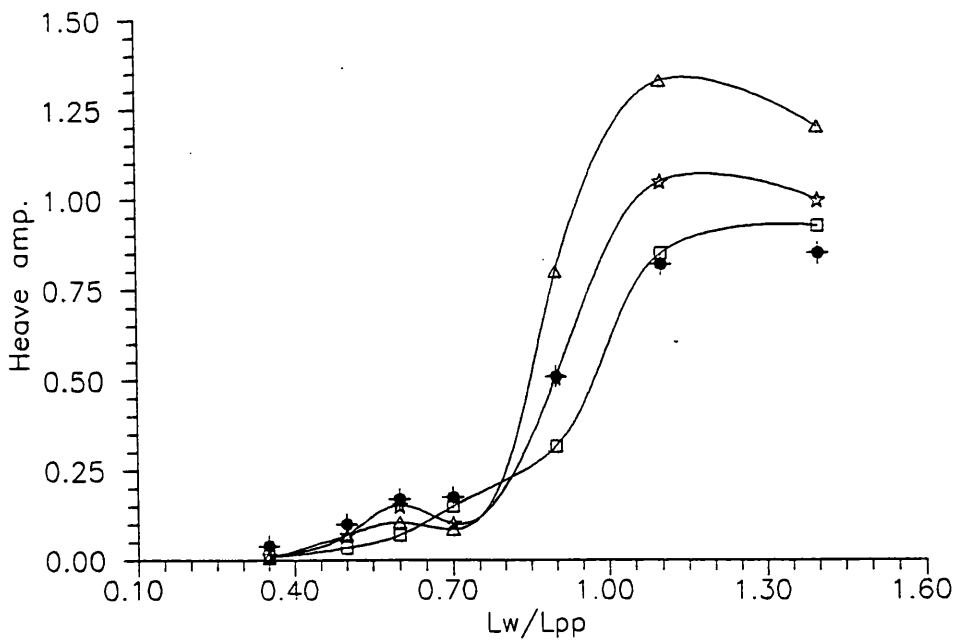

Fig. 9.3 ξ_3^a / ζ^a, heave transfer function in head waves
$\beta = 0°$, Fn = 0.270

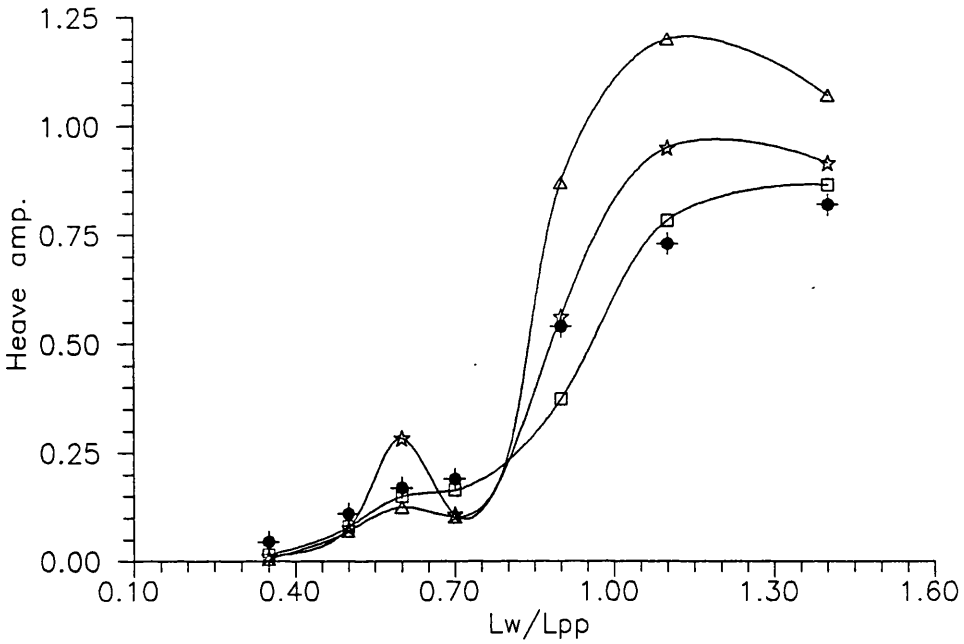

Fig. 9.4 ξ_3^a / ζ^a, heave transfer function in head waves
$\beta = 0°$, Fn = 0.245

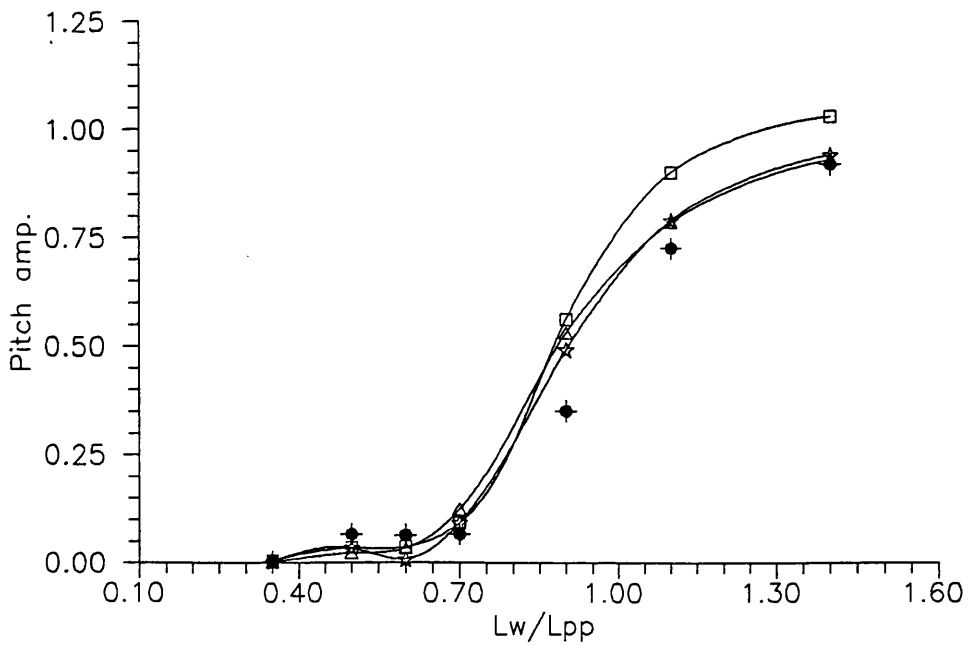

Fig. 9.5 $\xi_5^a / k_0\zeta^a$, pitch transfer function in head waves
$\beta = 0°$, Fn = 0.245

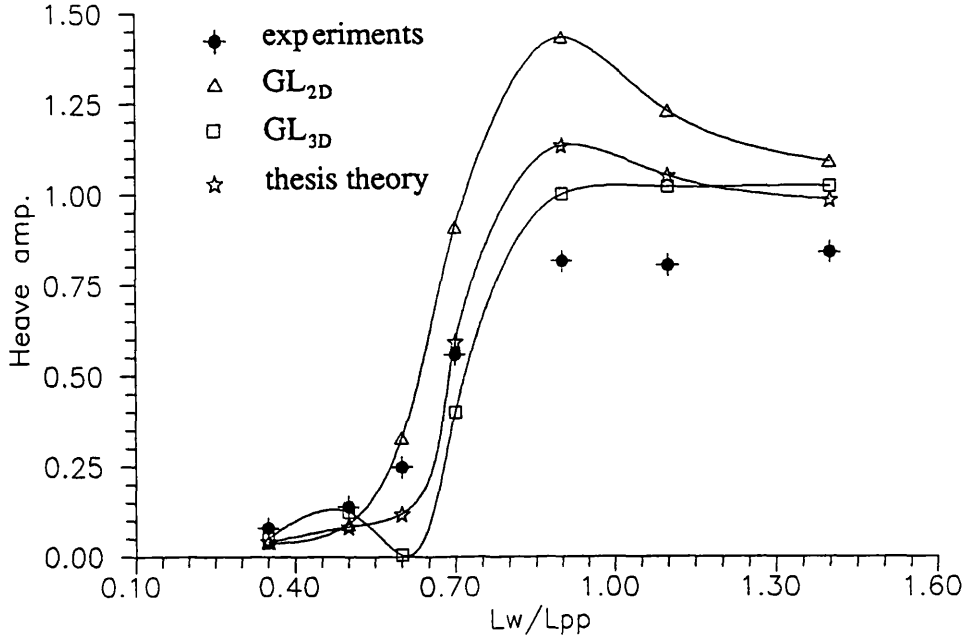

Fig. 9.6 ξ_3^a / ζ^a, heave transfer function in bow waves

$\beta = 45°$, $Fn = 0.245$

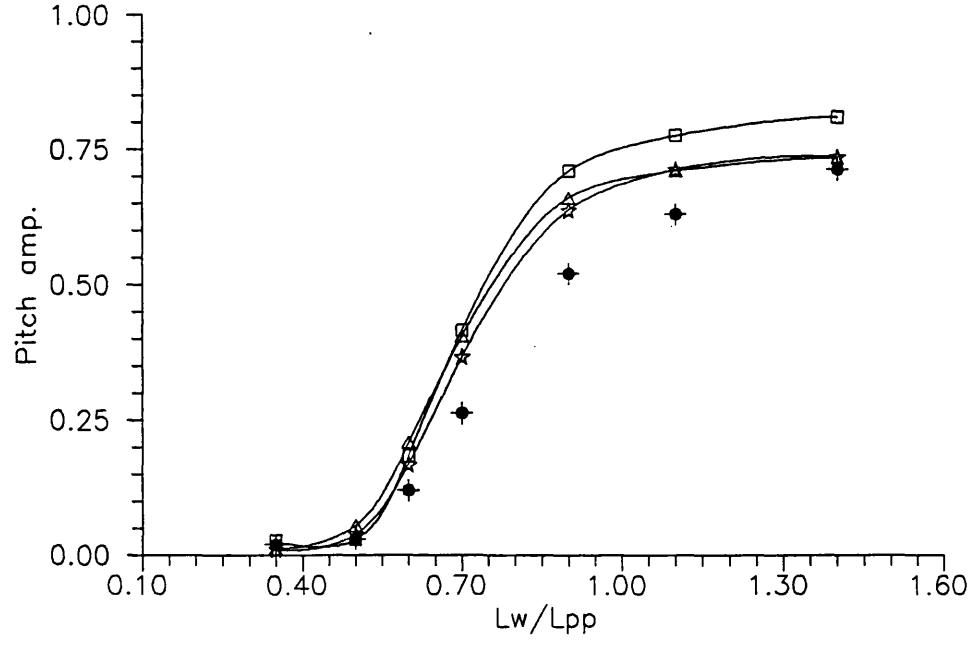

Fig. 9.7 $\xi_5^a / k_0\zeta^a$, pitch transfer function in bow waves

$\beta = 45°$, $Fn = 0.245$

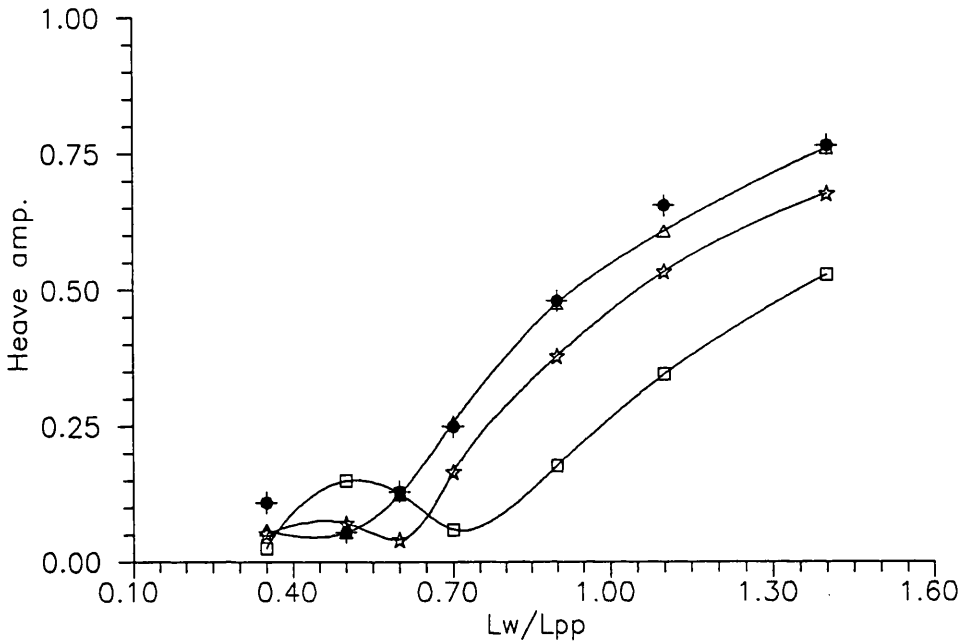

Fig. 9.8 ξ_3^a / ζ^a, heave transfer function in quartering waves
$\beta = 135°$, Fn = 0.245

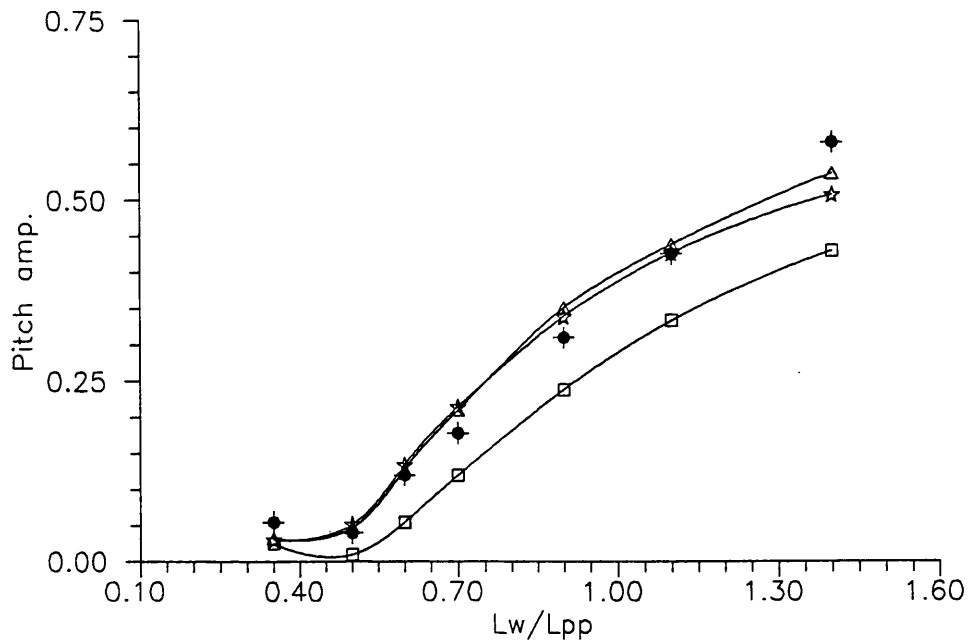

Fig. 9.9 $\xi_5^a / k_0\zeta^a$, pitch transfer function in quartering waves
$\beta = 135°$, Fn = 0.245

9.4 - Time Domain Results

In this Section the non-linear time domain solution will be compared with the corresponding linear frequency domain solution, for the condition head waves-zero forward speed.

Before the time histories of the motions are presented there are some intermediate results in the time domain solution which should be analysed. I am referring to the process of computing the radiation forces, where the first step to be done before the "Runge-Kutta" starts solving the motion equations is to determine the retardation functions, K_{kj}, which are given by;

$$K_{kj}(t) = \frac{2}{\pi}\int_{\wedge}^{\infty}\{B_{kj}(\omega)\cos\omega t\}d\omega$$

$$K_{kj}(t) = \frac{2}{\pi}\int_{0}^{\infty}\{B_{kj}(\omega)\cos\omega t\}d\omega$$

The damping coefficients, B_{kj}, corresponding to the whole frequency range (from $\omega = 0$ to $\omega = \infty$) are computed by the strip theory method. The non-dimensional results are presented in figures 9.10 to 9.11, where the non-dimensionalising factors for each damping coefficient are as follows;

$$B_{33} \rightarrow M\sqrt{\frac{g}{L_{pp}}}$$

$$B_{35}, B_{53} \rightarrow L_{pp}M\sqrt{\frac{g}{L_{pp}}}$$

$$B_{55} \rightarrow L_{pp}^2M\sqrt{\frac{g}{L_{pp}}}$$

where 'L_{pp}' is the length between perpendiculars and 'M' is the ship's mass.

For high frequencies the "Frank close fit method", used to compute the ship sectional damping coefficients, is very unstable, thus the end parts of the damping coefficients curves presented have been smoothed out.

The retardation functions, or impulse response functions, for the present time domain problem are presented in figures 9.13 to 9.15. They are non-dimensionalised with respect to the same factors presented above. These functions represent the influence of the past history of the fluid motion to the radiation forces acting on the ship at the actual instant. Observing the graphs two conclusions are immediate, the actual instant and the instants corresponding to a period of a few seconds before are those which contribute most to the forces, and the history of the motion which occurred more than 30 seconds before can be neglected.

The first numerical results presented are linear for both models, frequency-domain and time-domain, which means that the time-domain restoring forces are computed using the restoring coefficients given in Section-7.4. In this way all the terms in the time domain equations are linear, thus theoretically the predictions given by both models should be equal. Tests were carried out for a wide range of frequencies and amplitudes of the exciting forces, and the results were similar. The time histories of the heave and pitch motions are presented in figures 9.16 to 9.21 for three wave frequencies distributed over the frequency range. The wave frequencies correspond to the following wave length to ship length ratios, 2.0, 1.1, and 0.35. The frequency-domain results are represented by the dashed lines, while the time-domain results are represented by the solid lines. It can be observed that the predictions of the heave and roll motions by both methods are exactly the same for the two lower frequencies and are very similar for the higher frequency. Thus it can be concluded that the theory used in this thesis to evaluate the radiation forces in the time domain works, and also that the numerical procedure is properly programmed.

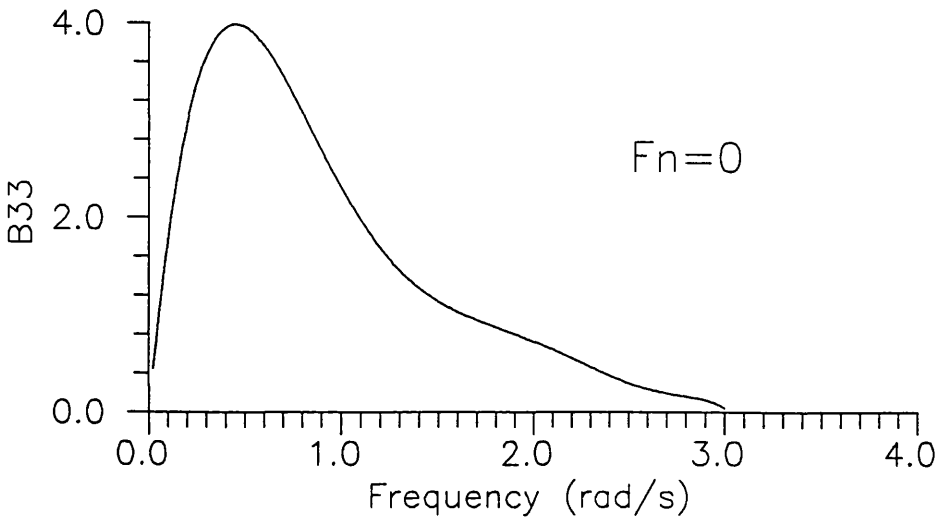

Fig. 9.10 Damping coefficient in heave

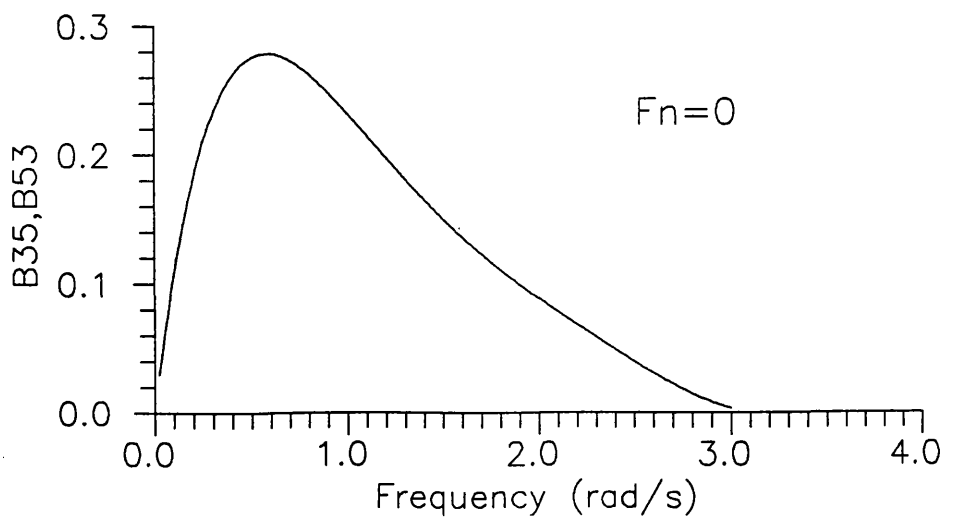

Fig. 9.11 Coupling coefficients of pitch into heave and heave into pitch

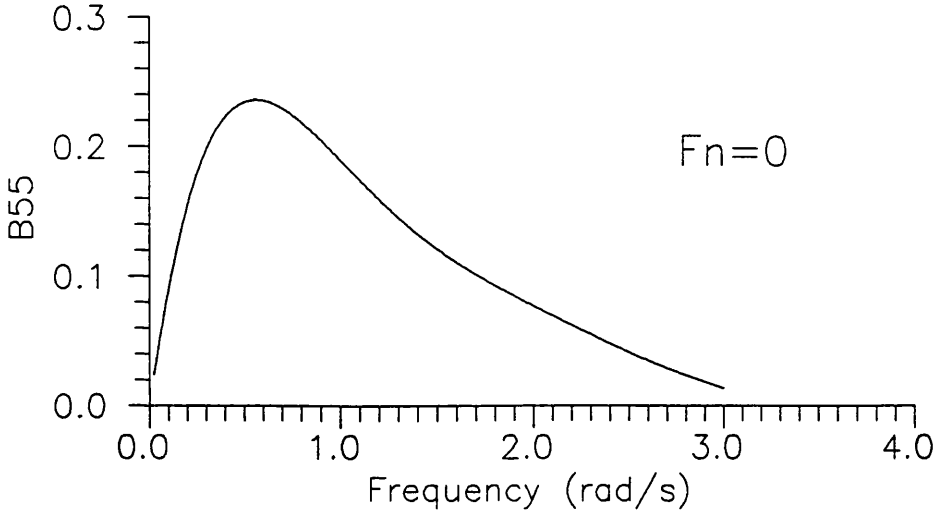

Fig. 9.12 Damping coefficient in pitch

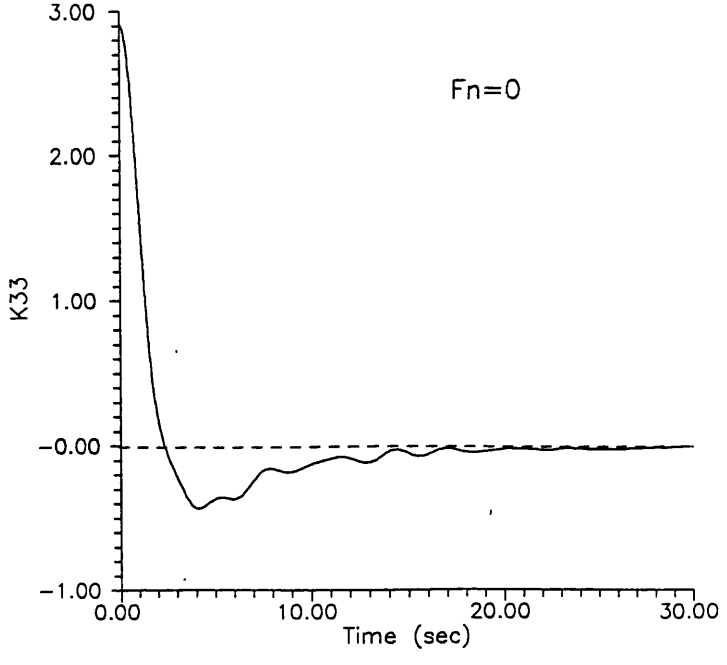

Fig. 9.13 Retardation function for heave

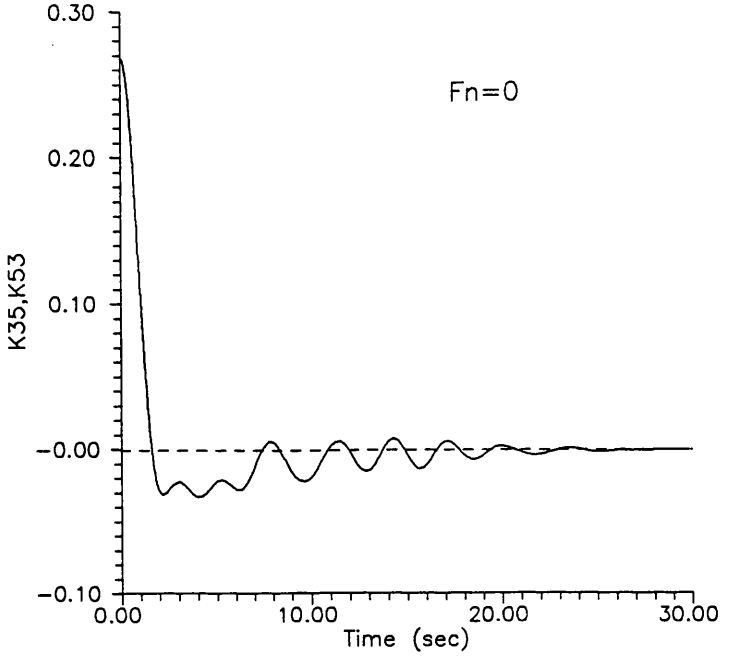

Fig. 9.14 Retardation function for pitch into heave and heave into pitch

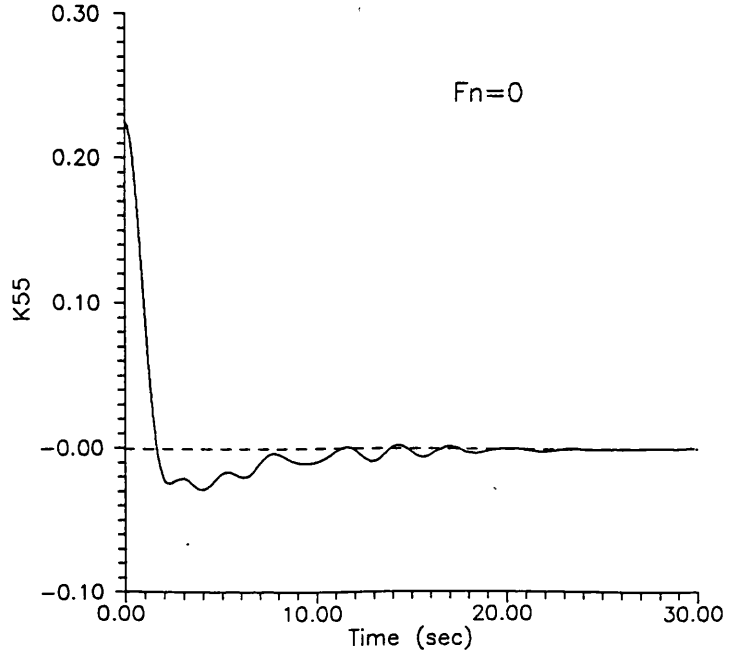

Fig. 9.15 Retardation function for pitch

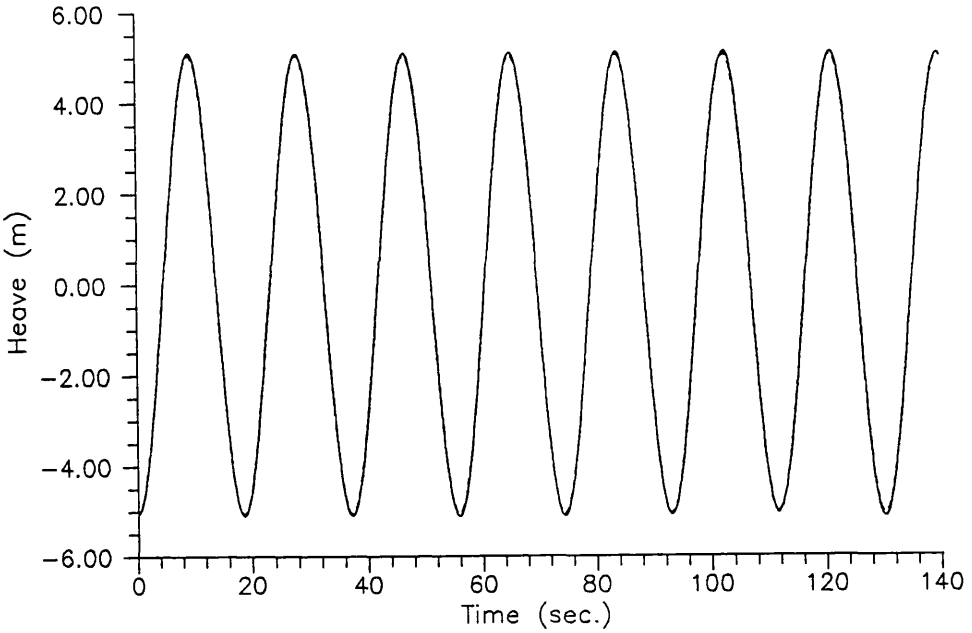

Fig. 9.16 Heave, linear time-domain and frequency-domain solutions

$$L_w / L_{pp} = 2.0, \quad L_w / 2\zeta^a = 40$$

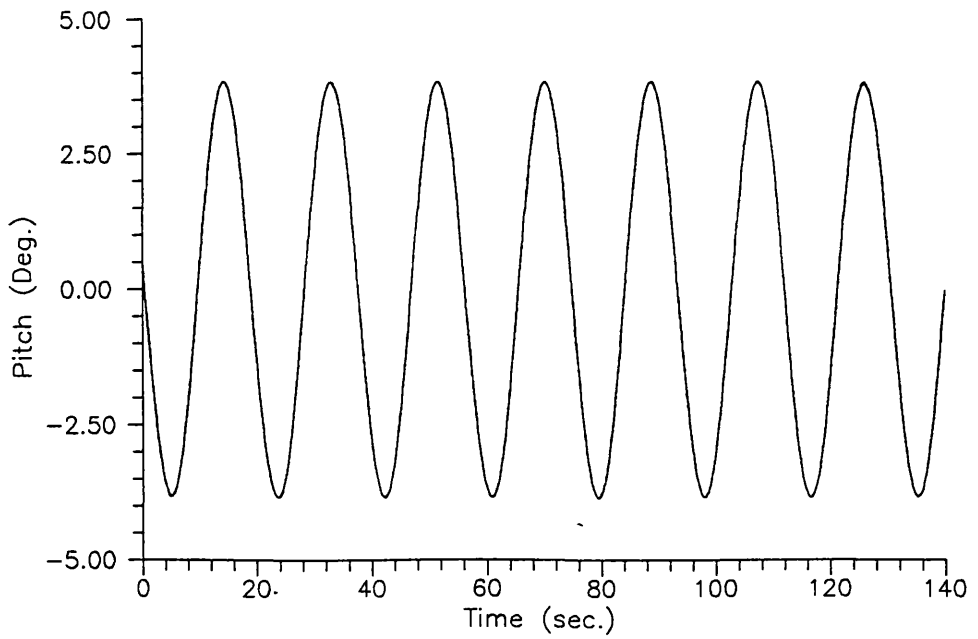

Fig. 9.17 Pitch, linear time-domain and frequency-domain solutions

$$L_w / L_{pp} = 2.0, \quad L_w / 2\zeta^a = 40$$

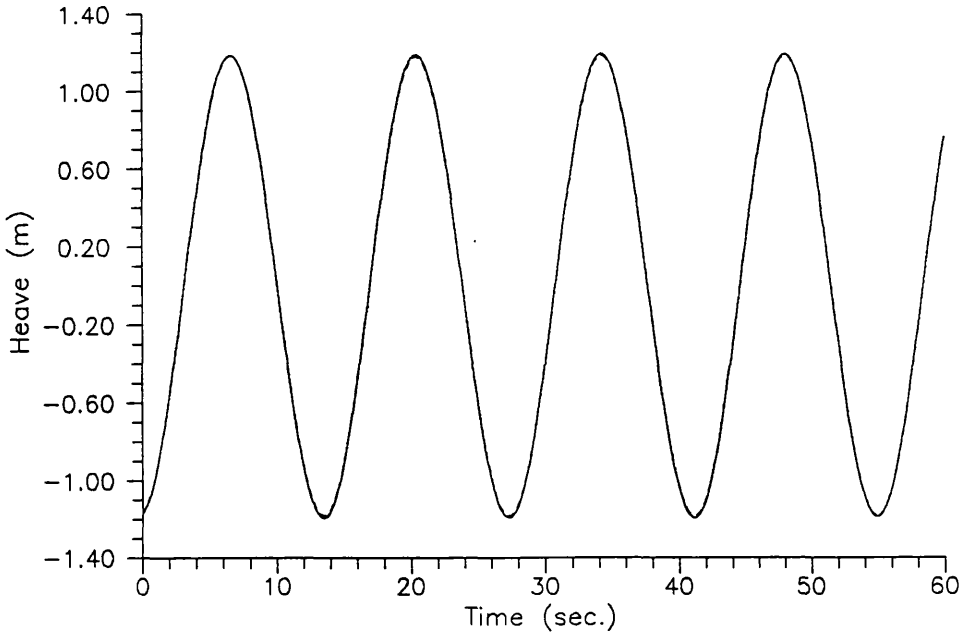

Fig. 9.18 Heave, linear time-domain and frequency-domain solutions

$L_w / L_{pp} = 1.1, \quad L_w / 2\zeta^a = 40$

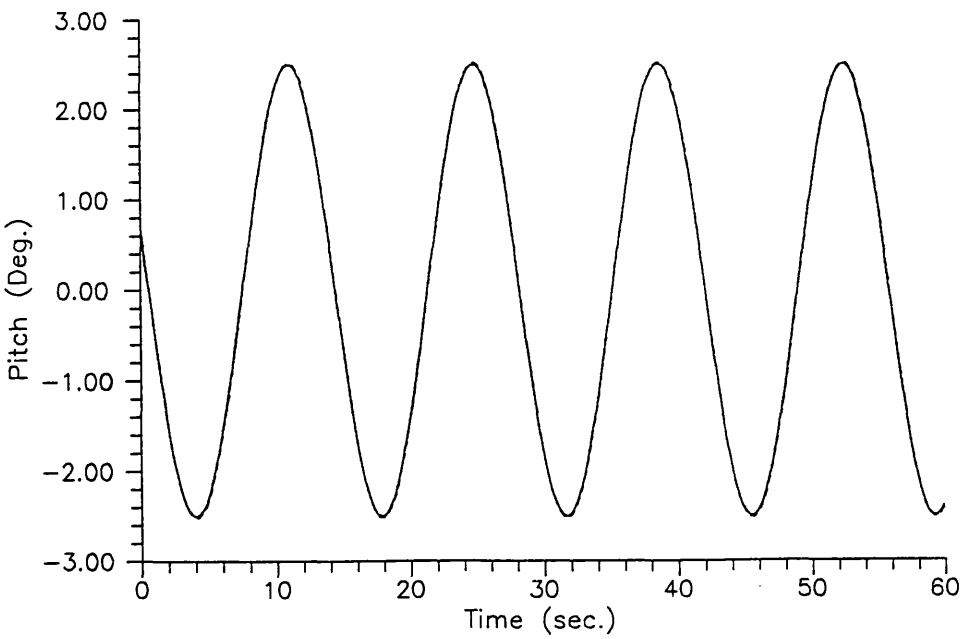

Fig. 9.19 Pitch, linear time-domain and frequency-domain solutions

$L_w / L_{pp} = 1.1, \quad L_w / 2\zeta^a = 40$

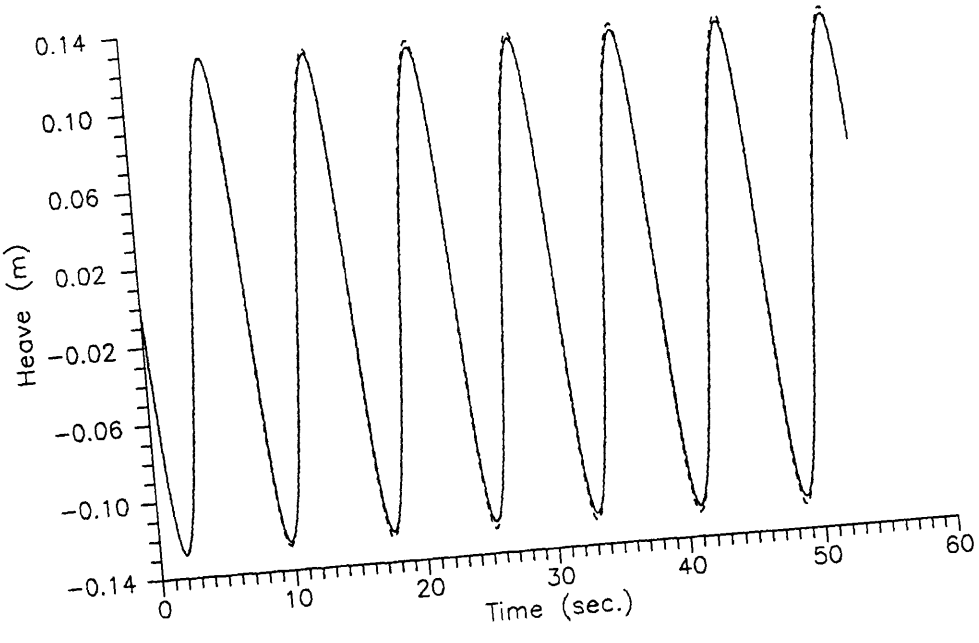

Fig. 9.20 Heave, linear time-domain and frequency-domain solutions

$L_w / L_{pp} = 0.35,\ L_w / 2\zeta^a = 40$

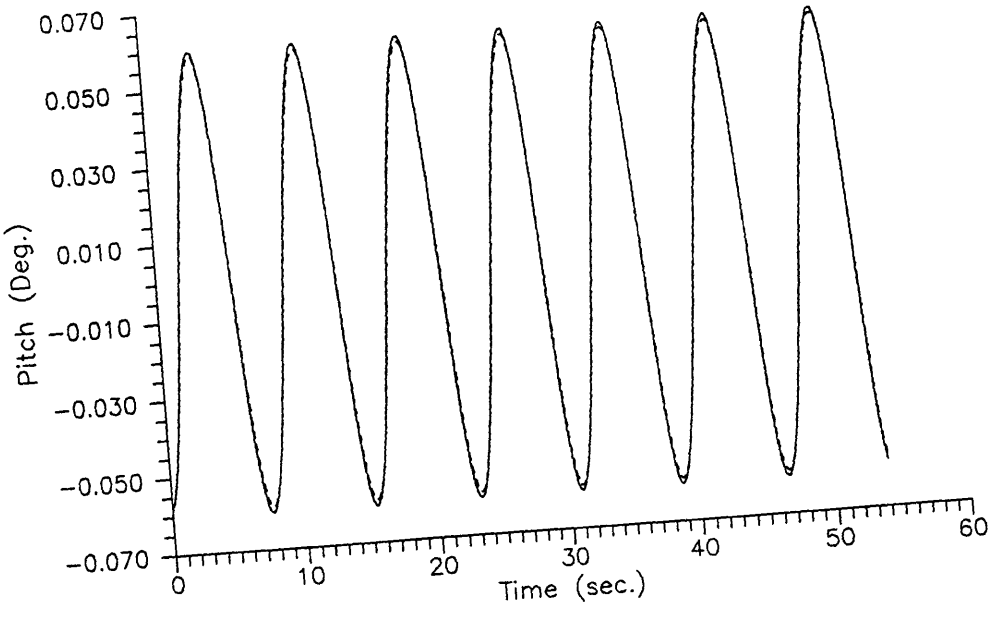

Fig. 9.21 Pitch, linear time-domain and frequency-domain solutions

$L_w / L_{pp} = 0.35,\ L_w / 2\zeta^a = 40$

Time histories of the heave and pitch obtained from the linear frequency domain model and non-linear time domain model are shown in figures 9.22 to 9.43. A wide range of wave lengths was tested, from Lw/Lpp equal to 2.6 to 0.35. The wave steepness, defined by the ratio wave length to wave height ($L_w / 2\zeta^a$), was kept constant at 40. This is believed to be a realistic value since it is calculated from the significant wave height and average wave length obtained from the statistical results of a fully developed sea state represented by the Pierson-Moskowitz wave spectrum correspondent to a range of wind velocities (see Neumann and Pierson (1966)).

Transfer functions of the former results are shown in figures 9.44 to 9.47, where again the linear solution is represented by the dashed line and the non-linear by the solid line. Because the time domain solution has different positive and negative amplitudes two transfer functions are used for each motion, one associated with the positive amplitude and the other with the negative.

For the heave motion the positive amplitudes are very similar for both models (fig. 9.44), however this is not the case with the negatives (fig. 9.45). Obviously the non-linear hydrostatic force is responsible for this behaviour, but to state why the motion is affected in this way is much more difficult. From the tests done it was found that in many cases the local characteristics of the motion can not explain a certain tendency, or difference from the linear solution, since there is a chain of interactions between several effects which keep affecting the dynamic system. For example the non-linear hydrostatic force may affect the velocity of the motion during a short time interval every period, then the inertia characteristics and the radiation forces at the end of the interval will be affected, and even if the local restoring force is similar to the linear model the resultant motion will be different.

Turning to the pitch transfer function the feature which stands out in the time domain solution is the difference from the linear model of the positive amplitudes for the larger wave lengths. This difference seems exaggerated and it is believed that the evaluation of the Froude-Krylov force over the exact wetted surface would change and improve the results. However it is also believed that this tendency has a physical meaning and exists in the real case, despite being less exaggerated. What happens is that the linear model over predicts the restoring moment. In fact a superficial analysis leads to the conclusion that in

the real case the restoring moment when the ship turns the bow down is higher than the linear prediction since there is a flare on the sides of the ship near the bow thus the buoyancy force increases more with the angle. However on the other half of the ship, on the stern side, the linear model assumes that the water plane area is kept constant with the pitch angle, thus it assumes that a huge volume is being lost when in fact this happens only during the first one or two degrees (see the bodyplan in figure 9.1 and the relative ship position in figure 9.48). Losing volume on the stern side means the restoring force is increased. The actual position of the ship and the free surface elevation at the instant when a maximum pitch occurs is reproduced in figure 9.48, together with the water plane area corresponding to the same instant (solid line) and the water plane are in static and still water condition (dashed line). As derived in Section 7.5 the linear pitch restoring moment is mainly given by the inertial moment of the water plane area about the y-axis (in the equilibrium static position), thus observing the water plane areas it can be concluded that the true restoring moment decreases as the ship turns the bow down.

Since the hydrostatic forces are computed taking into account the exact wetted surface the results are sensitive to the wave steepness. A set of runs were made in order to investigate the influence of the wave steepness keeping the wave length constant. The following ratios wave length to ship length were investigated, 2.0, 1.5, 1.0, 0.5. The linear and non-linear results are presented as transfer functions, in figures 9.49 to 9.64, with separate graphs to the positive and negative amplitudes. As expected the major differences are found for the higher waves and both solutions tend to be equal as the waves become smaller. Again these results are not expected to be accurate, specially for the higher waves, instead they are shown to make possible the analysis of the influence of a better prediction of the restoring forces in the final solution. In fact for the higher waves the linear results seem more reasonable than the non-linear, which indicates that the improvement of only one term in the motion equations do not necessarily means the solution becomes better.

The area of applicability where this method is believed to be especially useful is on the prediction of motion responses in irregular seas, if one or several non-linear effects need to be taken into account. In this case the superposition principle of frequency domain results can not be used since the motion responses to each frequency component must be linear. On the other hand the

known methods use frequency dependent hydrodynamic coefficients in the non-linear equations of motion, thus the user is faced with the problem of choosing a particular frequency to be associated with the coefficients when the nature of the response is irregular. The method used in this thesis solves non-linear time domain equations of motion where the radiation forces are evaluated in the time domain, thus they are frequency independent. In addition the computer program can be used in any PC computer with relatively small computational effort. Run tests were carried out in a 486 Dx33 PC computer, and the run time to compute the retardation functions correspondent to one heading one Froude number is about 5 minutes. Several runs can then be done with any exciting force. A time history of 300 seconds is obtained in about 3 minutes, however this run time can be much decreased by improving the routine which computes the convolution integrals. This will become important when simulations in irregular seas are performed since long time histories are needed to obtain statistical characteristics.

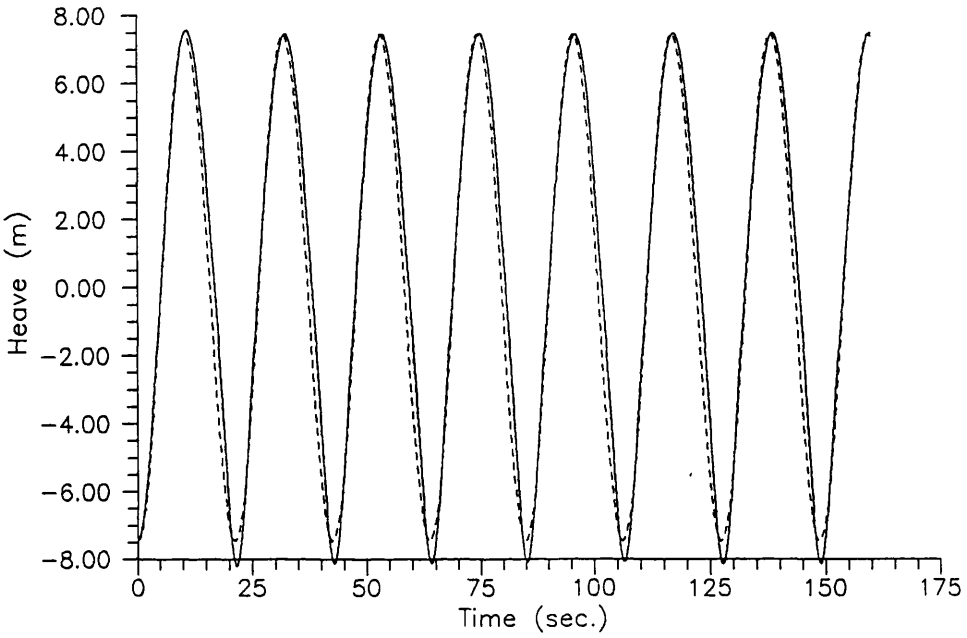

Fig. 9.22 Heave, time-domain and frequency-domain solutions

$L_w / L_{pp} = 2.6,\ L_w / 2\zeta^a = 40,\ \zeta^a = 8.79$ m

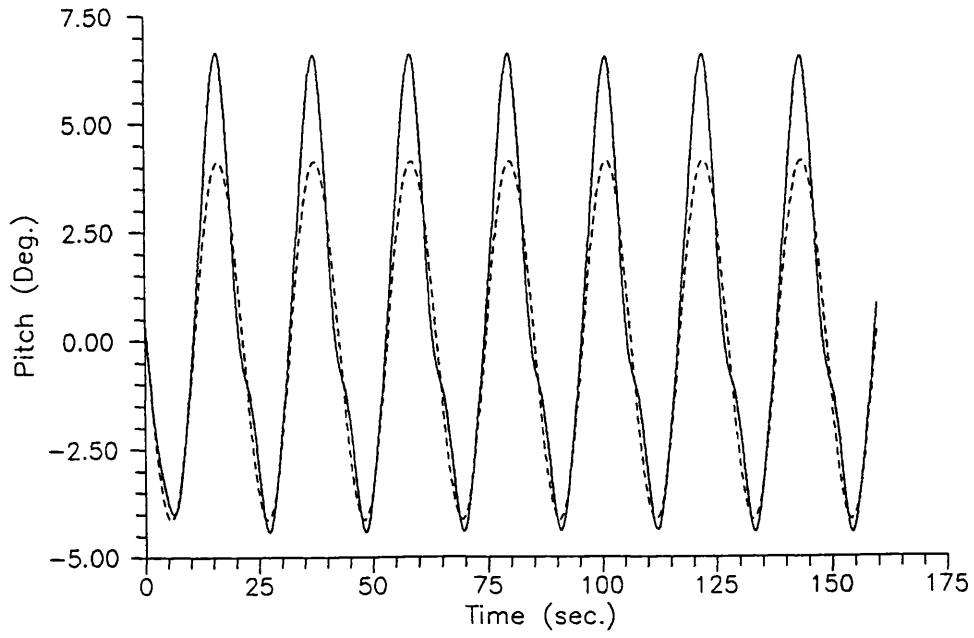

Fig. 9.23 Pitch, time-domain and frequency-domain solutions

$L_w / L_{pp} = 2.6,\ L_w / 2\zeta^a = 40,\ \zeta^a = 8.79$ m

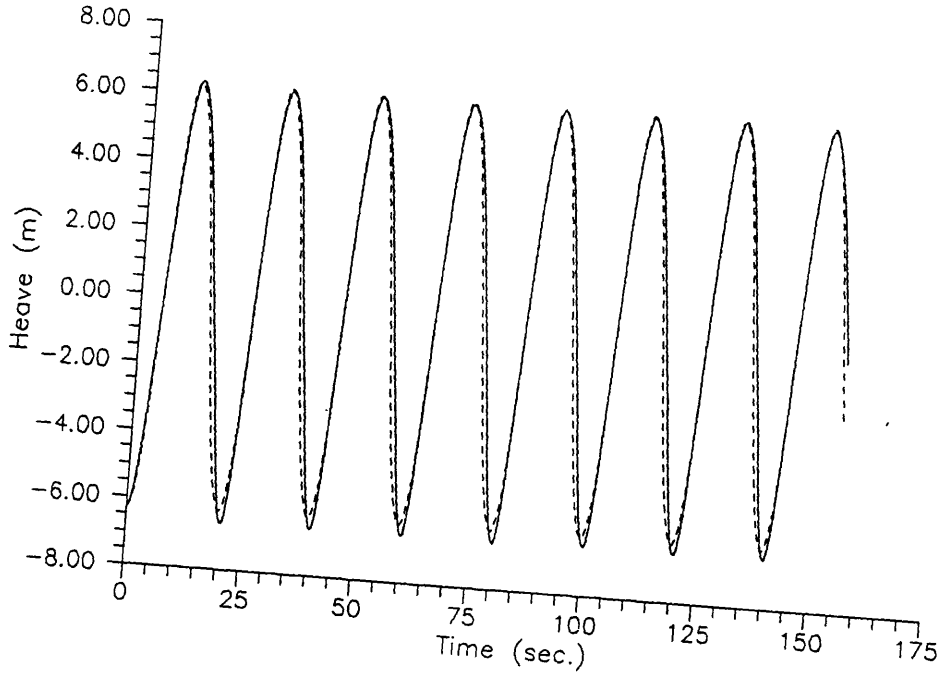

Fig. 9.24 Heave, time-domain and frequency-domain solutions

$L_w / L_{pp} = 2.3,\ L_w / 2\zeta^a = 40,\ \zeta^a = 7.76$ m

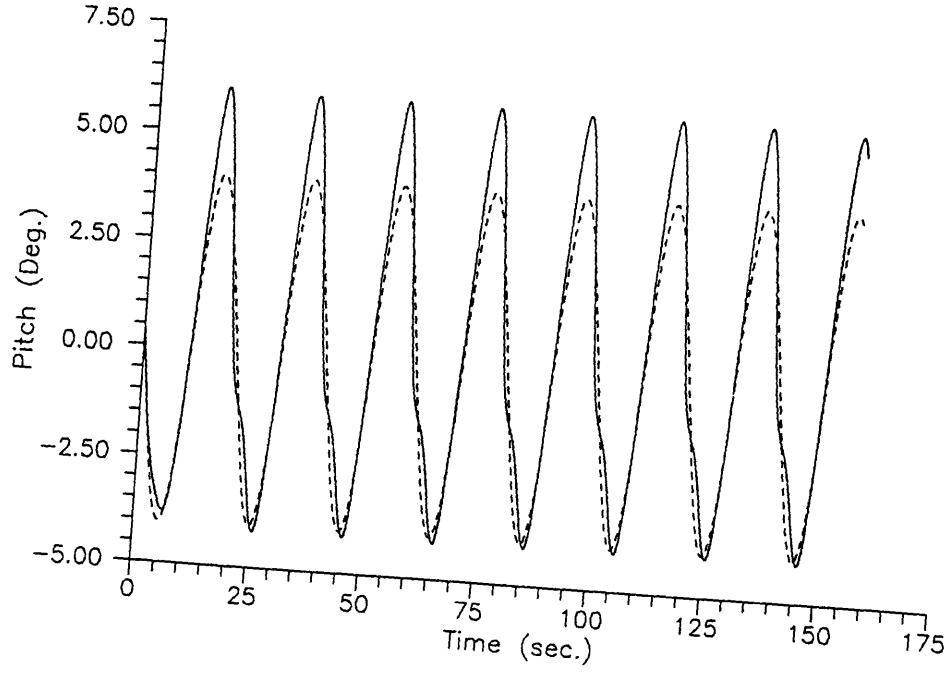

Fig. 9.25 Pitch, time-domain and frequency-domain solutions

$L_w / L_{pp} = 2.3,\ L_w / 2\zeta^a = 40,\ \zeta^a = 7.76$ m

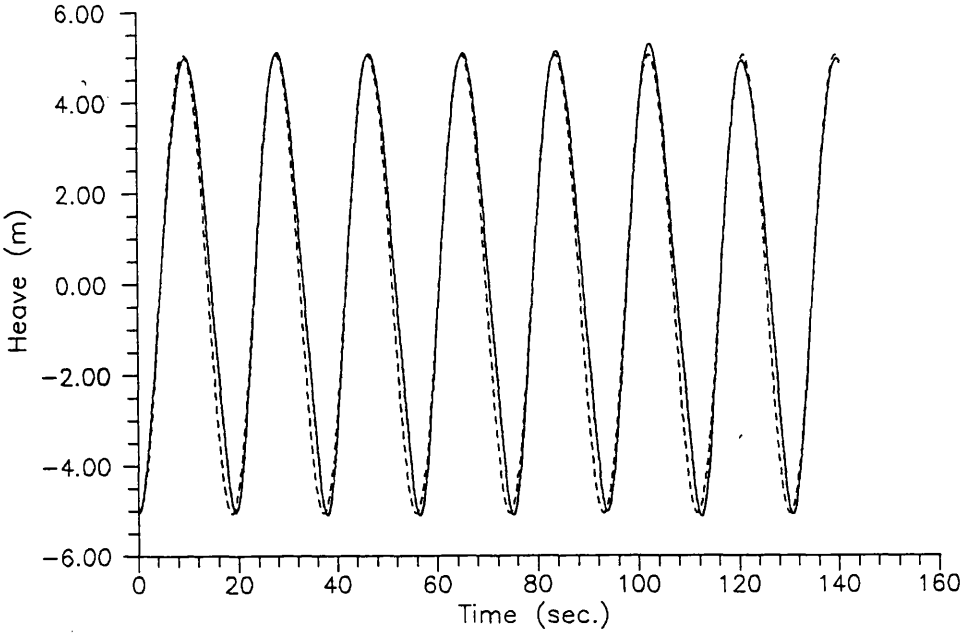

Fig. 9.26 Heave, time-domain and frequency-domain solutions

$L_w / L_{pp} = 2.0,\ L_w / 2\zeta^a = 40,\ \zeta^a = 6.75$ m

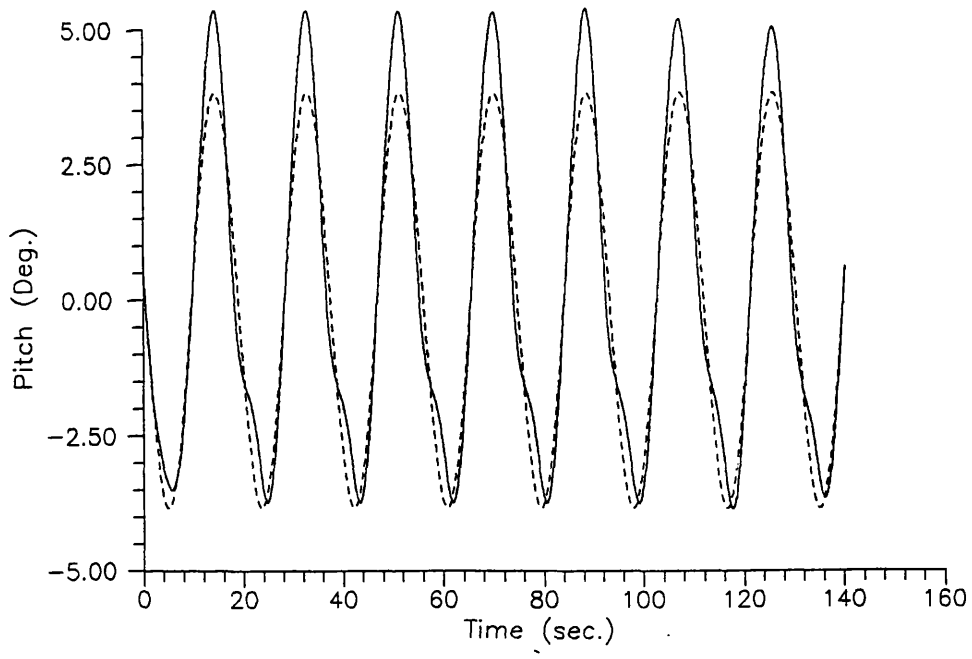

Fig. 9.27 Pitch, time-domain and frequency-domain solutions

$L_w / L_{pp} = 2.0,\ L_w / 2\zeta^a = 40,\ \zeta^a = 6.75$ m

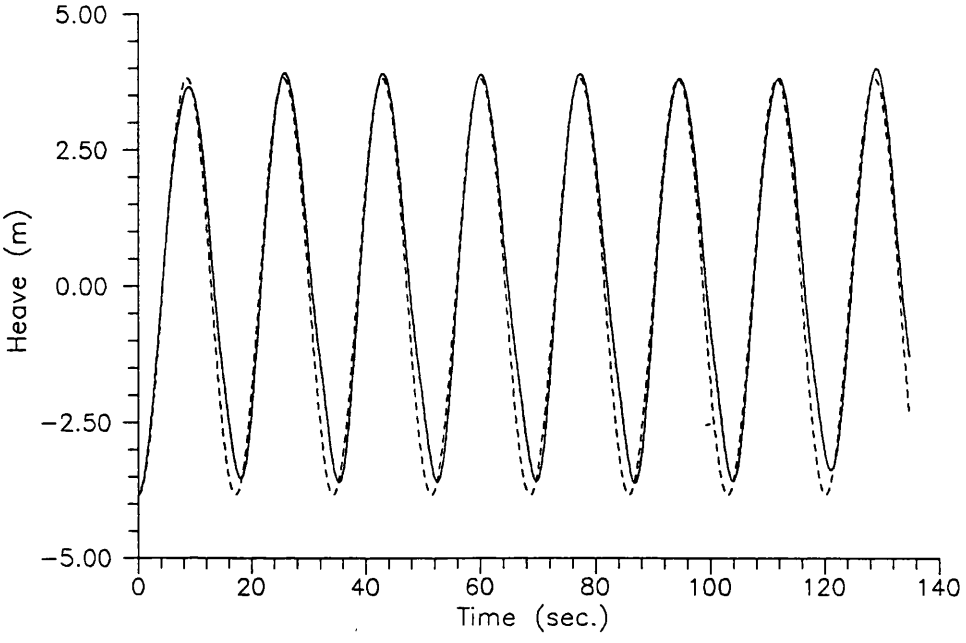

Fig. 9.28 Heave, time-domain and frequency-domain solutions

$L_w / L_{pp} = 1.7,\ L_w / 2\zeta^a = 40,\ \zeta^a = 5.75$ m

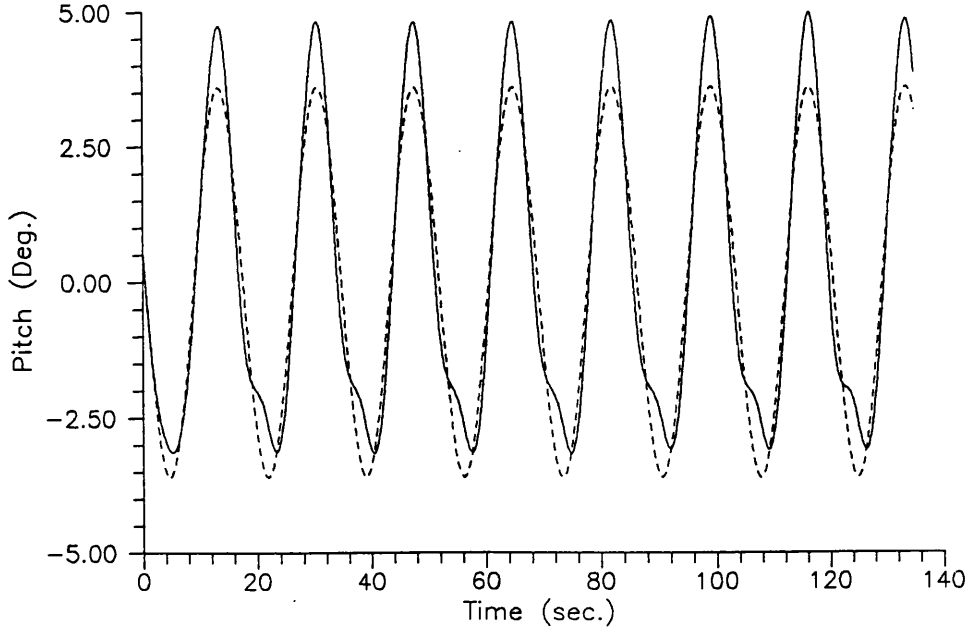

Fig. 9.29 Pitch, time-domain and frequency-domain solutions

$L_w / L_{pp} = 1.7,\ L_w / 2\zeta^a = 40,\ \zeta^a = 5.75$ m

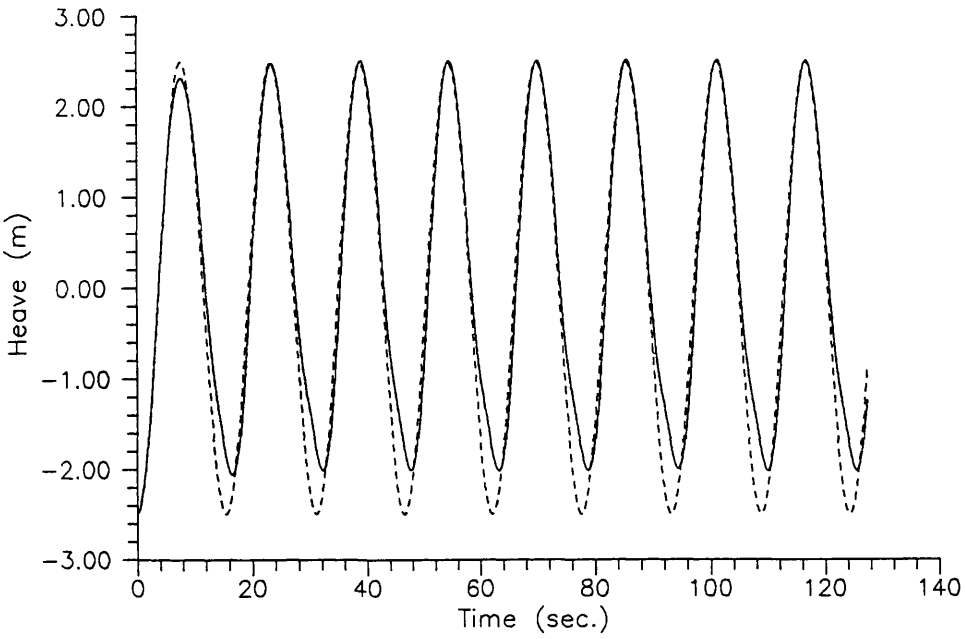

Fig. 9.30 Heave, time-domain and frequency-domain solutions

$L_w / L_{pp} = 1.4,\ L_w / 2\zeta^a = 40,\ \zeta^a = 4.73$ m

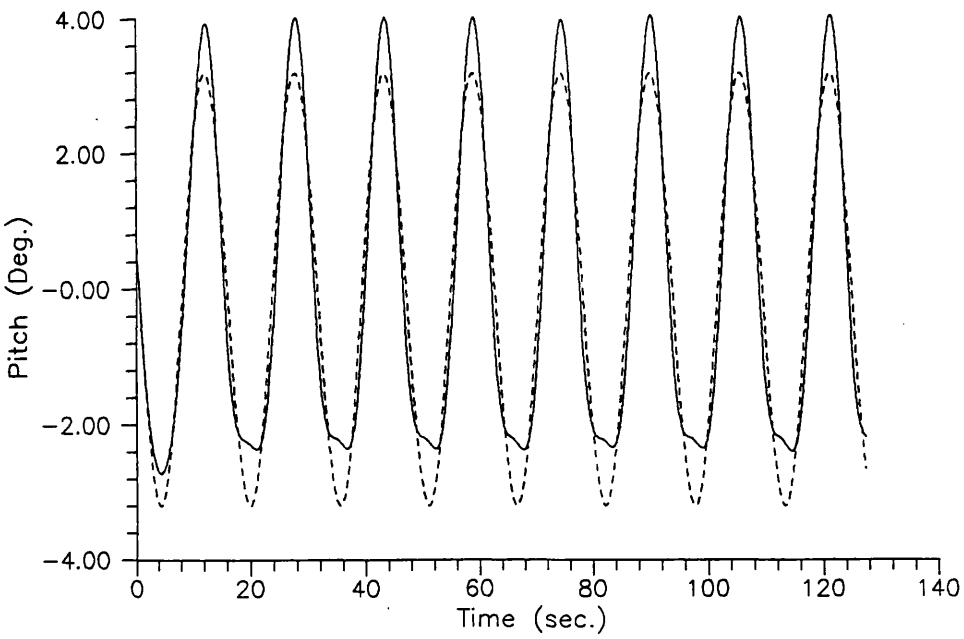

Fig. 9.31 Pitch, time-domain and frequency-domain solutions

$L_w / L_{pp} = 1.4,\ L_w / 2\zeta^a = 40,\ \zeta^a = 4.73$ m

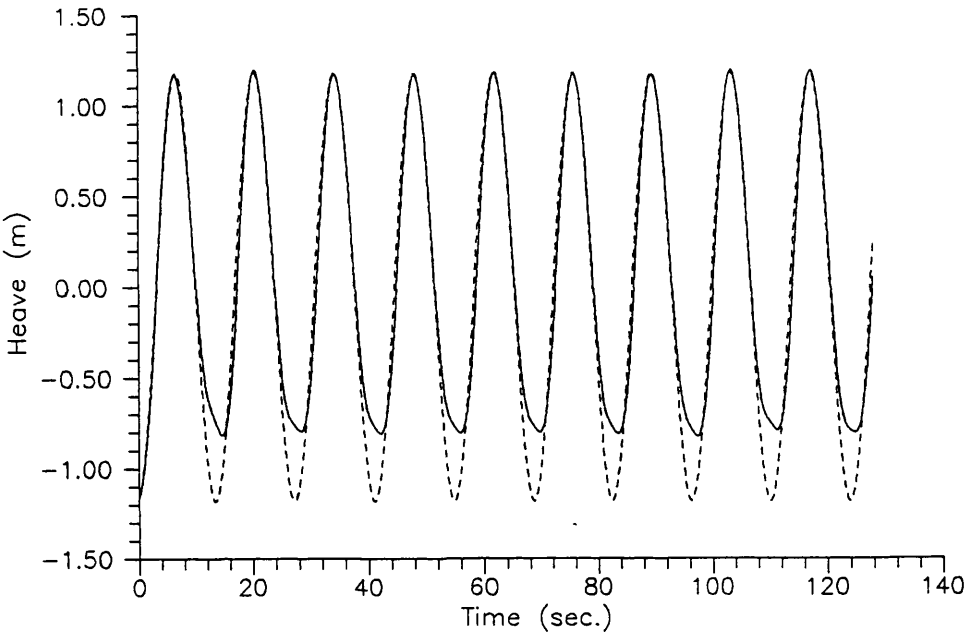

Fig. 9.32 Heave, time-domain and frequency-domain solutions

$L_w / L_{pp} = 1.1,\ L_w / 2\zeta^a = 40,\ \zeta^a = 3.72$ m

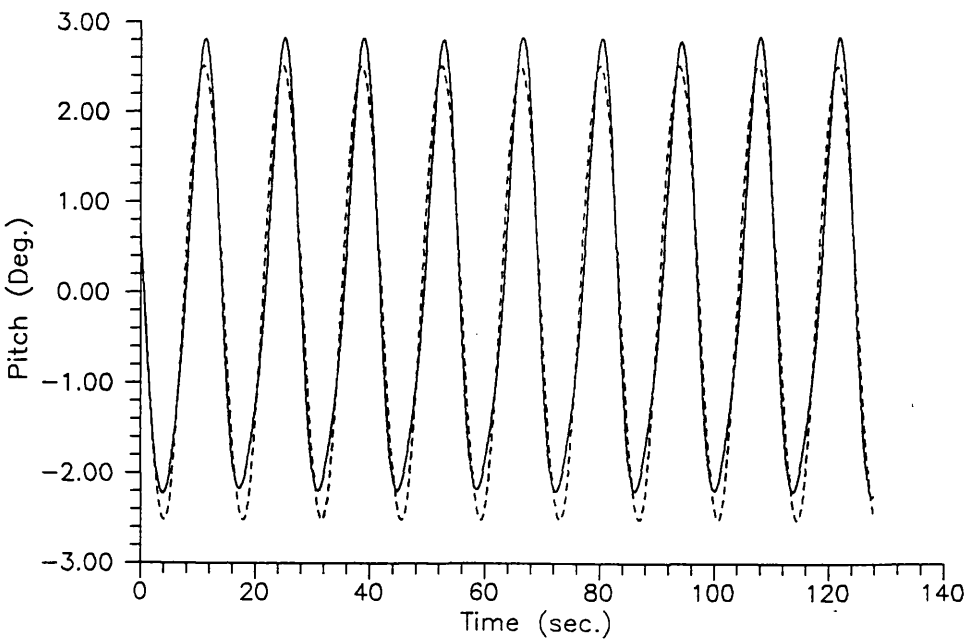

Fig. 9.33 Pitch, time-domain and frequency-domain solutions

$L_w / L_{pp} = 1.1,\ L_w / 2\zeta^a = 40,\ \zeta^a = 3.72$ m

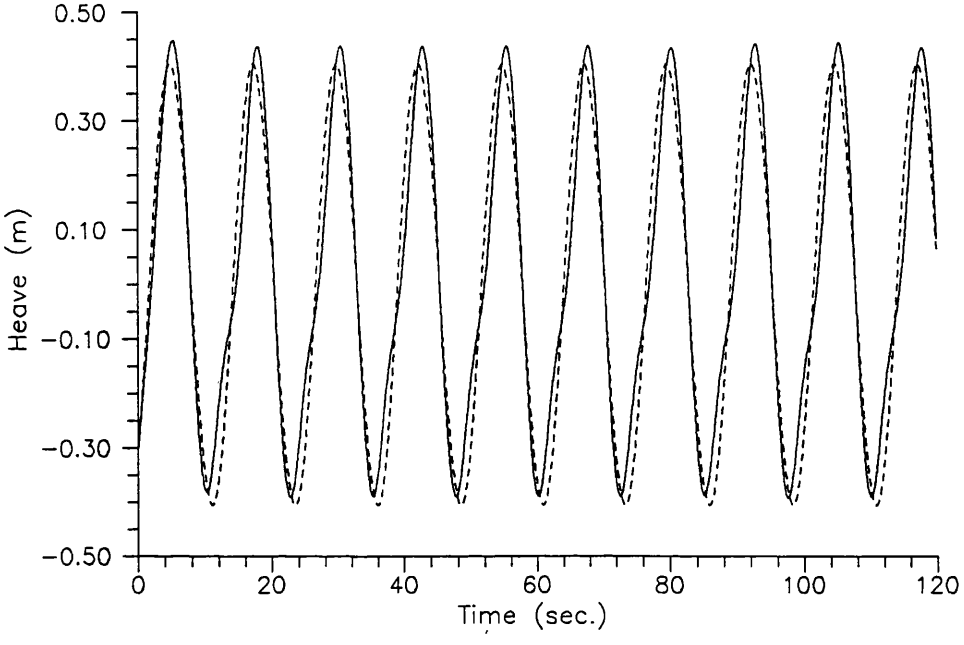

Fig. 9.34 Heave, time-domain and frequency-domain solutions

$L_w / L_{pp} = 0.90$, $L_w / 2\zeta^a = 40$, $\zeta^a = 3.03$ m

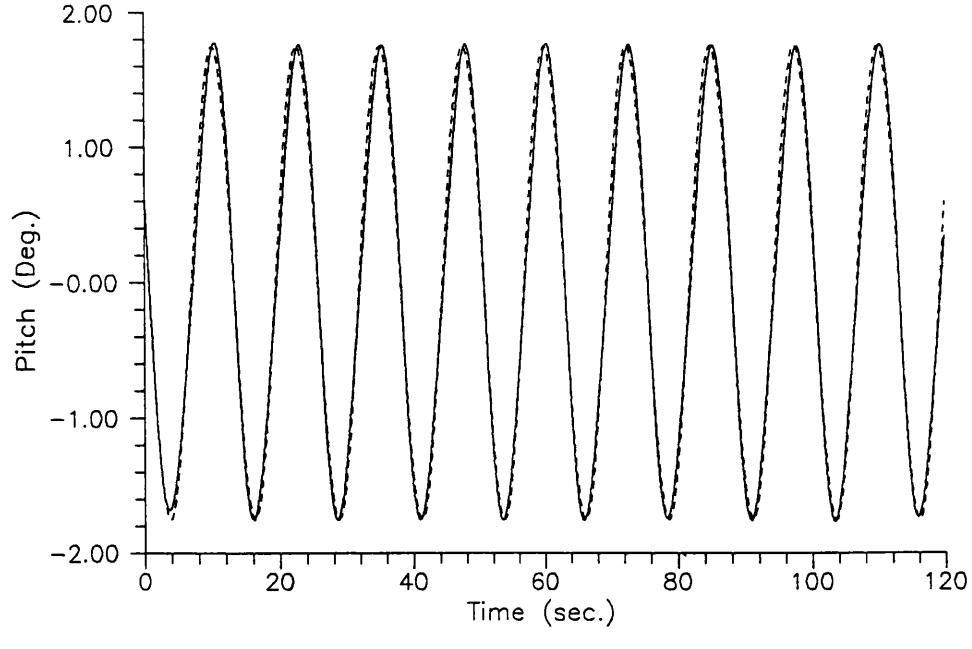

Fig. 9.35 Pitch, time-domain and frequency-domain solutions

$L_w / L_{pp} = 0.90$, $L_w / 2\zeta^a = 40$, $\zeta^a = 3.03$ m

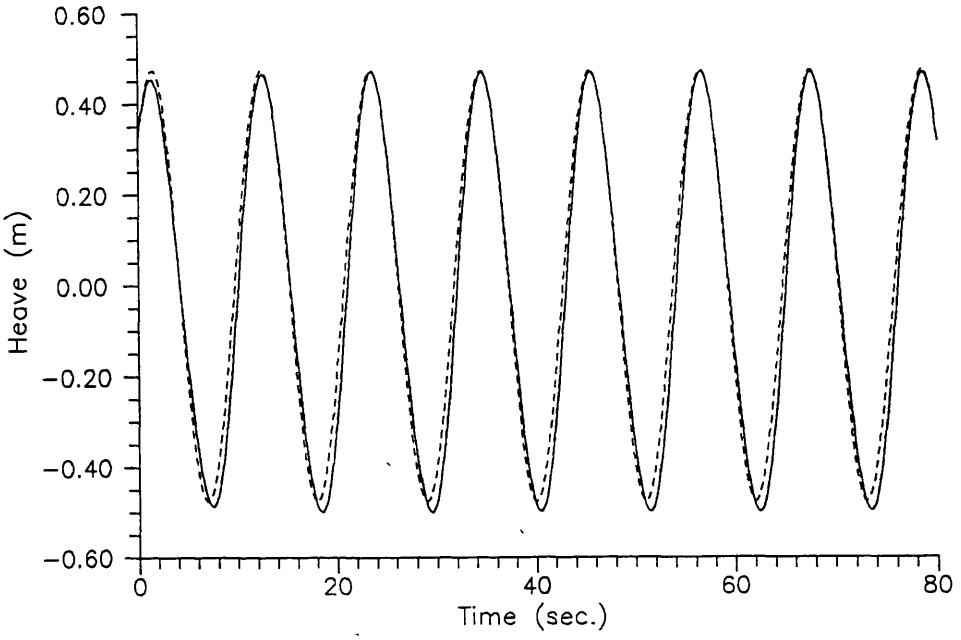

Fig. 9.36 Heave, time-domain and frequency-domain solutions

$L_w / L_{pp} = 0.70,\ L_w / 2\zeta^a = 40,\ \zeta^a = 2.36$ m

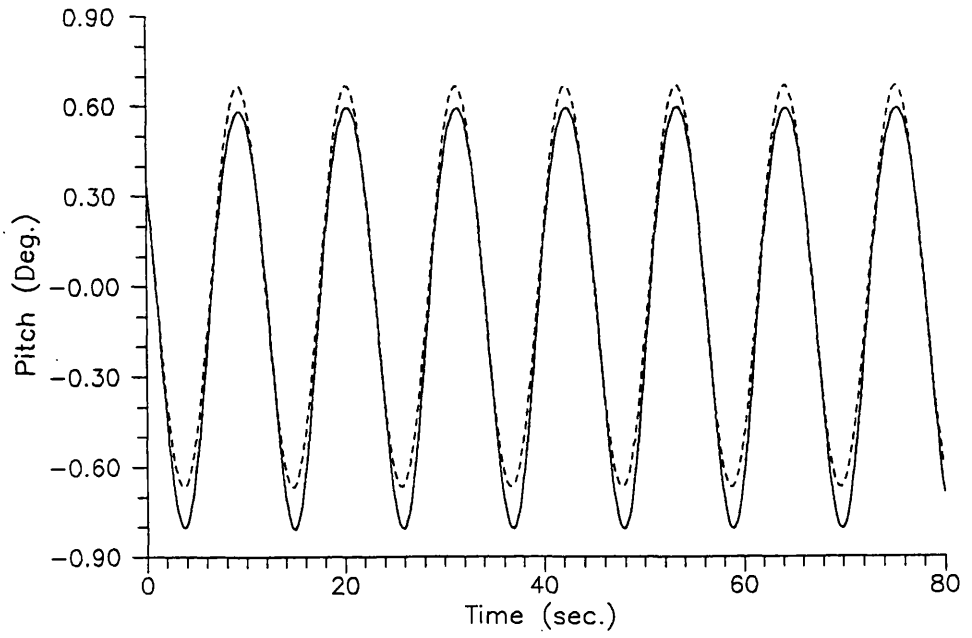

Fig. 9.37 Pitch, time-domain and frequency-domain solutions

$L_w / L_{pp} = 0.70,\ L_w / 2\zeta^a = 40,\ \zeta^a = 2.36$ m

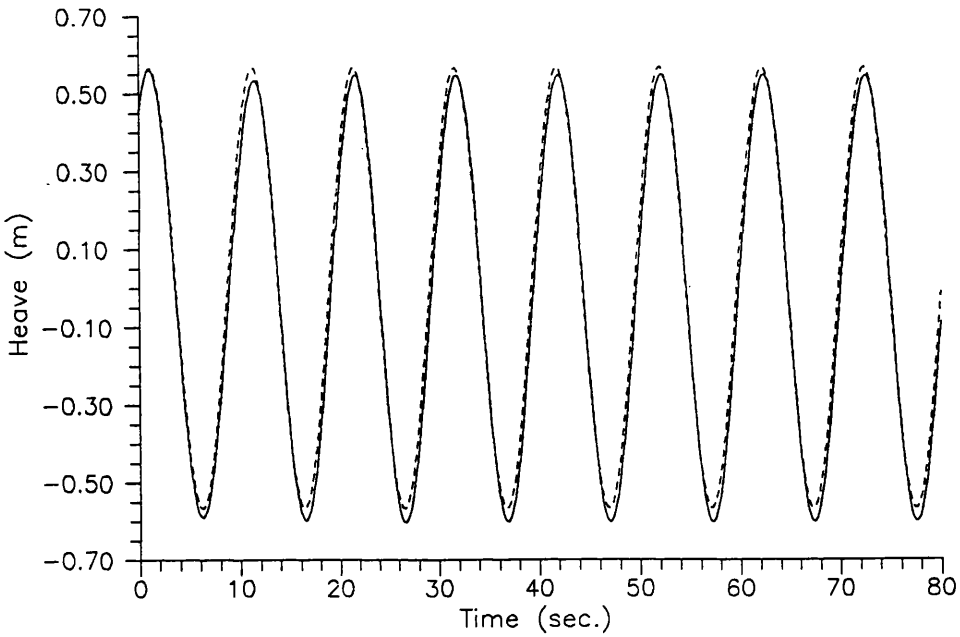

Fig. 9.38 Heave, time-domain and frequency-domain solutions

$L_w / L_{pp} = 0.60,\ L_w / 2\zeta^a = 40,\ \zeta^a = 2.02$ m

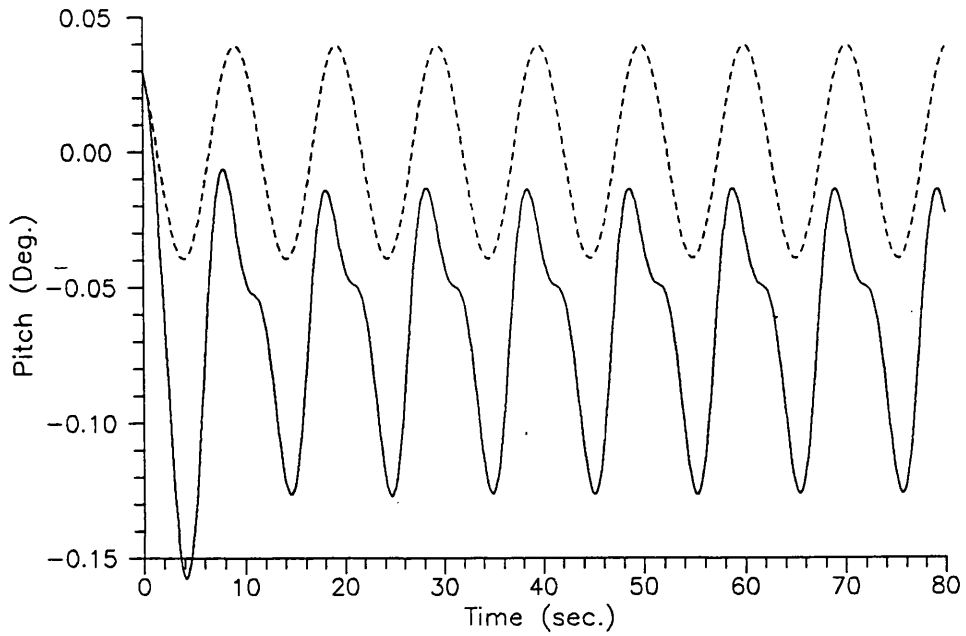

Fig. 9.39 Pitch, time-domain and frequency-domain solutions

$L_w / L_{pp} = 0.60,\ L_w / 2\zeta^a = 40,\ \zeta^a = 2.02$ m

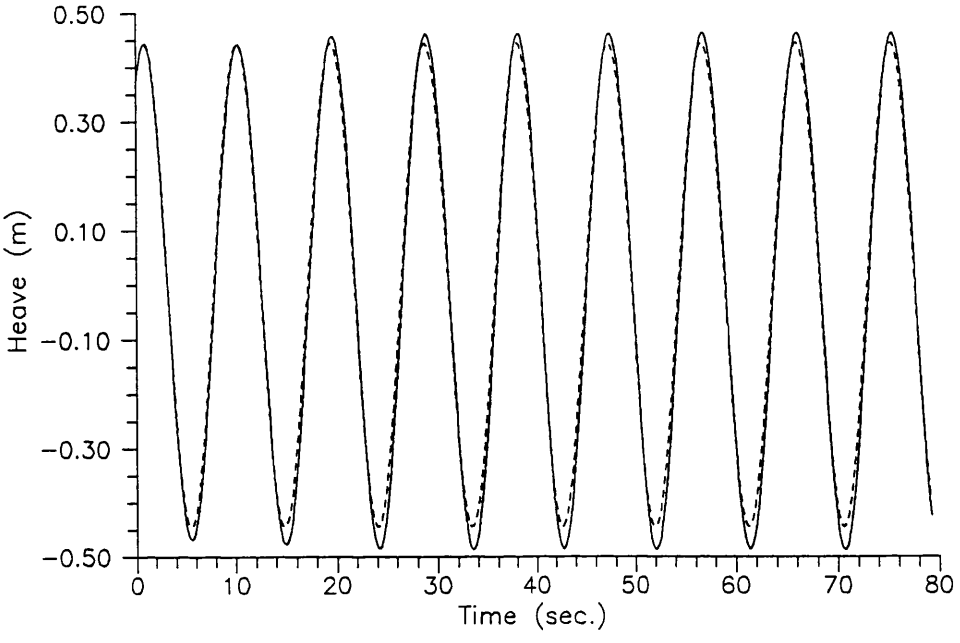

Fig. 9.40 Heave, time-domain and frequency-domain solutions

$L_w / L_{pp} = 0.50,\ L_w / 2\zeta^a = 40,\ \zeta^a = 1.69$ m

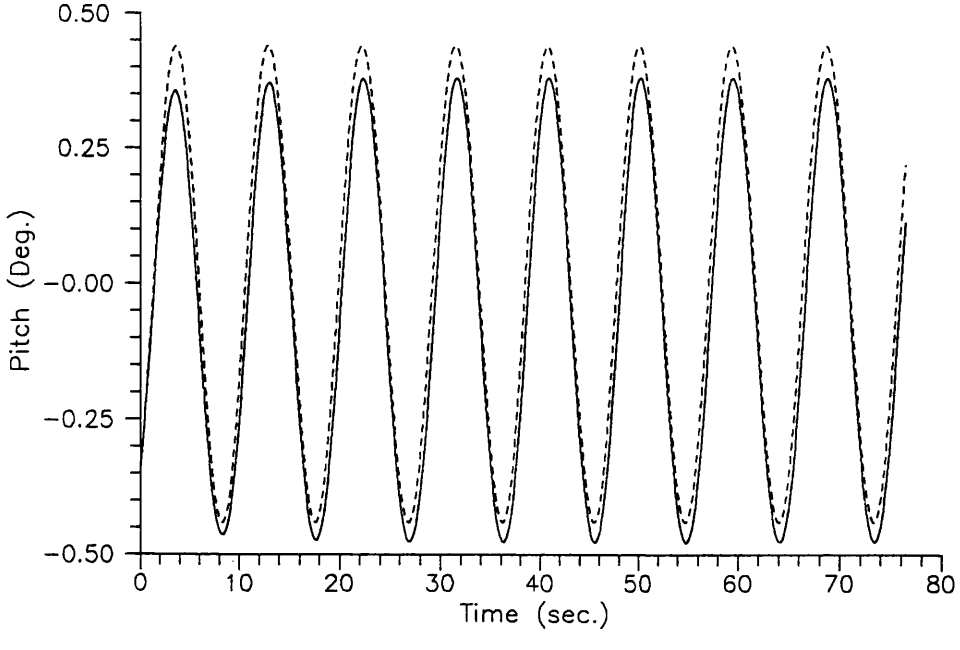

Fig. 9.41 Pitch, time-domain and frequency-domain solutions

$L_w / L_{pp} = 0.50,\ L_w / 2\zeta^a = 40,\ \zeta^a = 1.69$ m

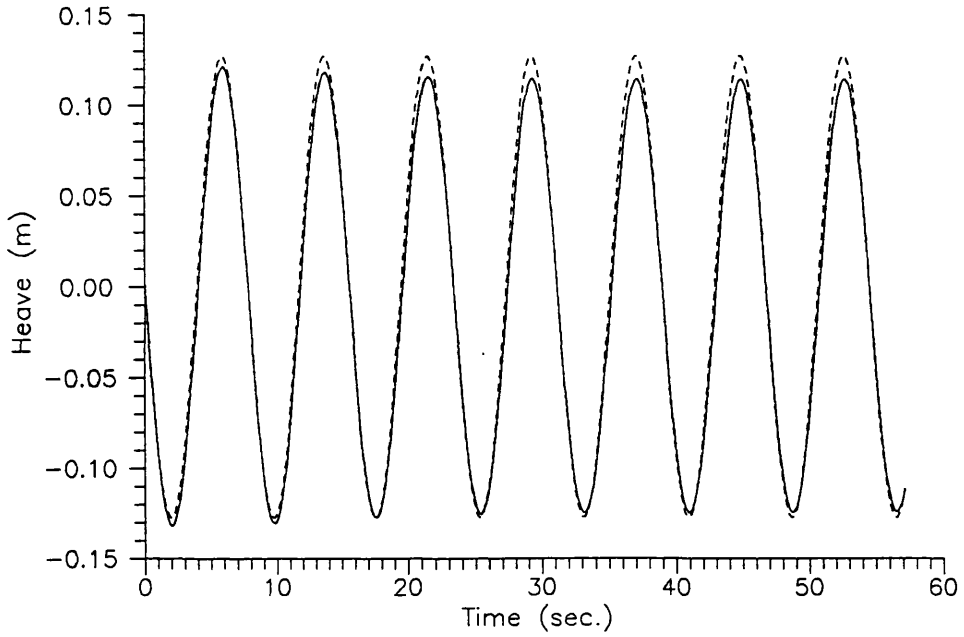

Fig. 9.42 Heave, time-domain and frequency-domain solutions

$L_w / L_{pp} = 0.35,\ L_w / 2\zeta^a = 40,\ \zeta^a = 1.18$ m

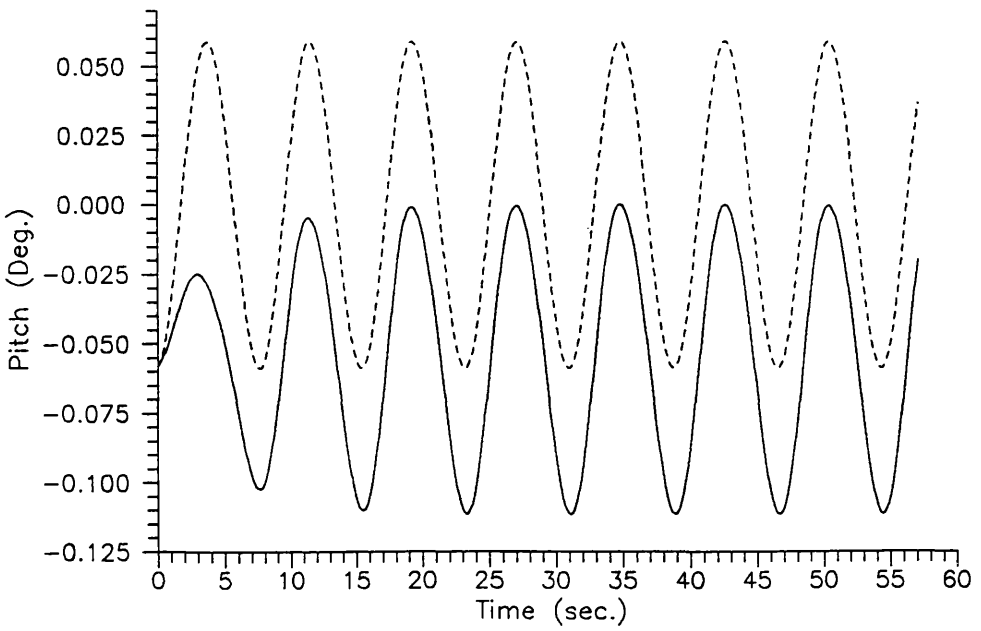

Fig. 9.43 Pitch, time-domain and frequency-domain solutions

$L_w / L_{pp} = 0.35,\ L_w / 2\zeta^a = 40,\ \zeta^a = 1.18$ m

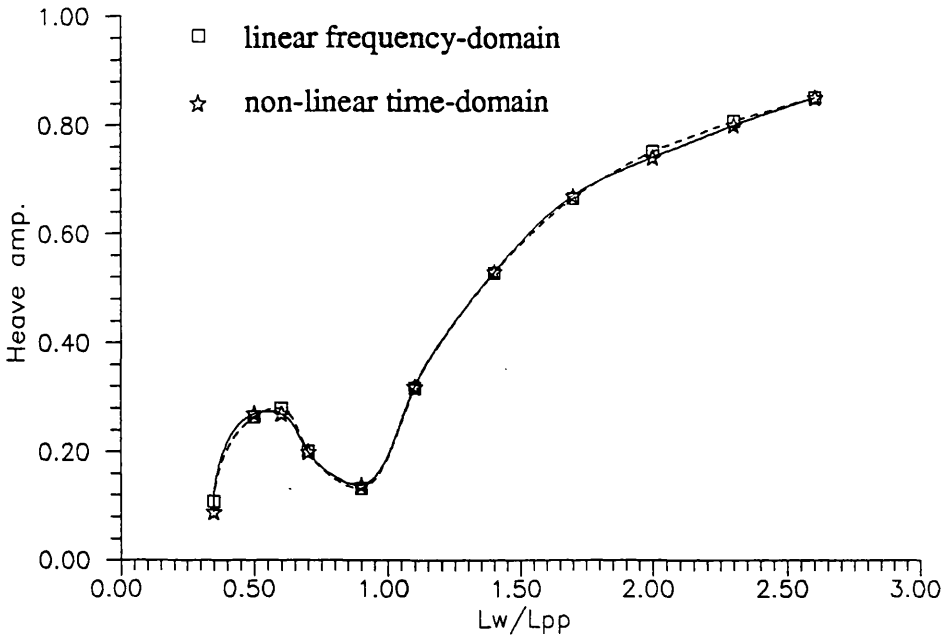

Fig. 9.44 ξ_3^{a+}/ζ^a, heave transfer function considering the positive amplitudes, $Fn = 0$, $\beta = 0°$, $L_w/2\zeta^a = 40$

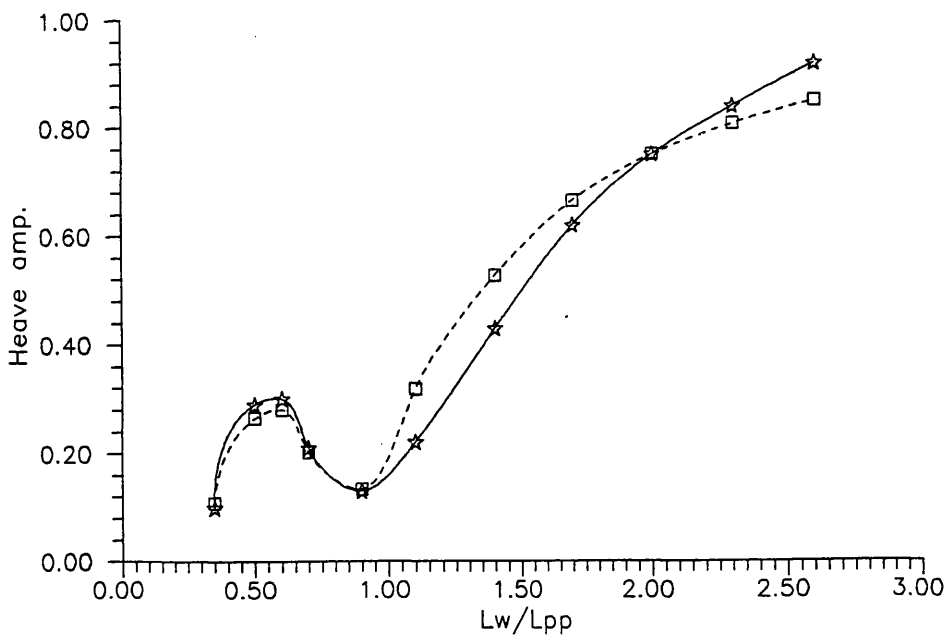

Fig. 9.45 $\left|\xi_3^{a-}\right|/\zeta^a$, heave transfer function considering the negative amplitudes, $Fn = 0$, $\beta = 0°$, $L_w/2\zeta^a = 40$

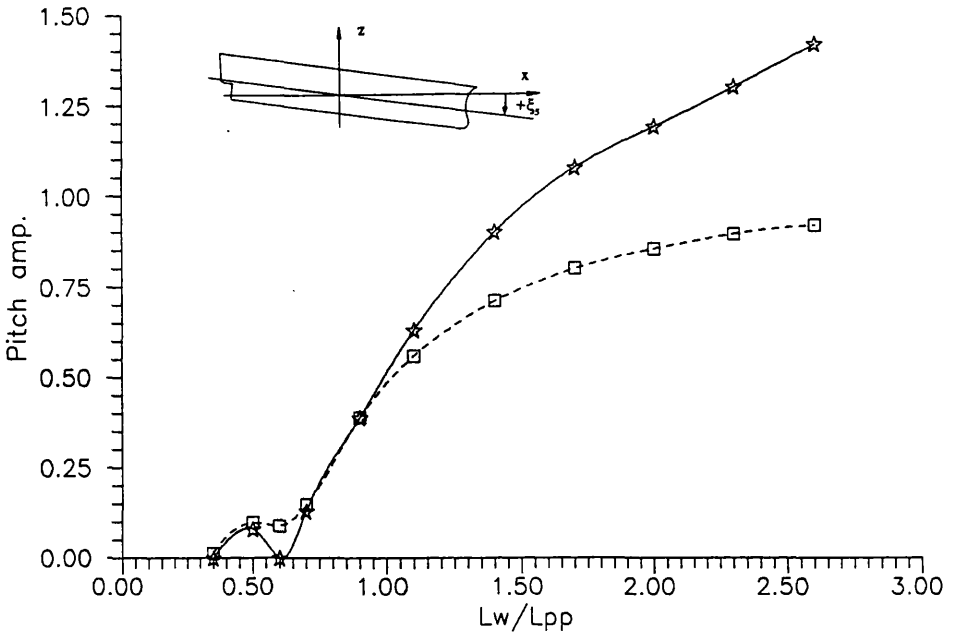

Fig. 9.46 $\xi_5^{a+} / k_0\zeta^a$, pitch transfer function considering the positive amplitudes, Fn = 0, $\beta = 0°$, $L_w / 2\zeta^a = 40$

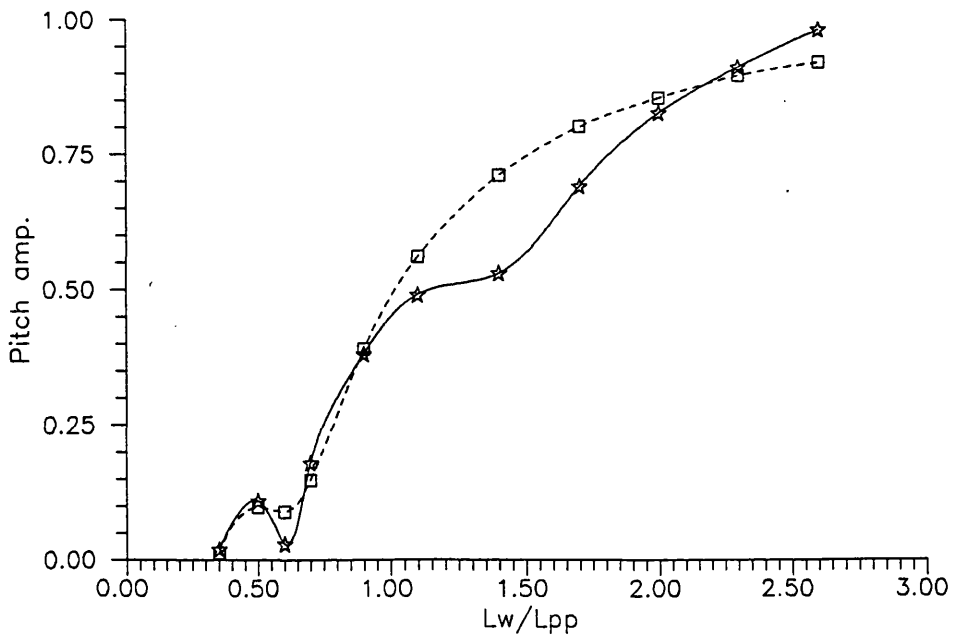

Fig. 9.47 $\left|\xi_5^{a-}\right| / k_0\zeta^a$, pitch transfer function considering the negative amplitudes, Fn = 0, $\beta = 0°$, $L_w / 2\zeta^a = 40$

Condition

$\zeta^a = 8.79$ m

$L_w / L_{pp} = 2.6$

Time = 79.75 sec.

$\xi_3(79.75) = 1.38$ m

$\xi_5(79.75) = 6.63°$

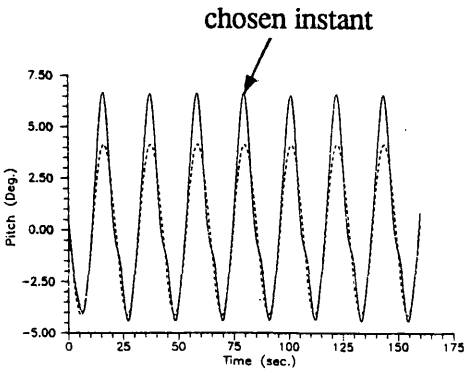

Figure 9.23

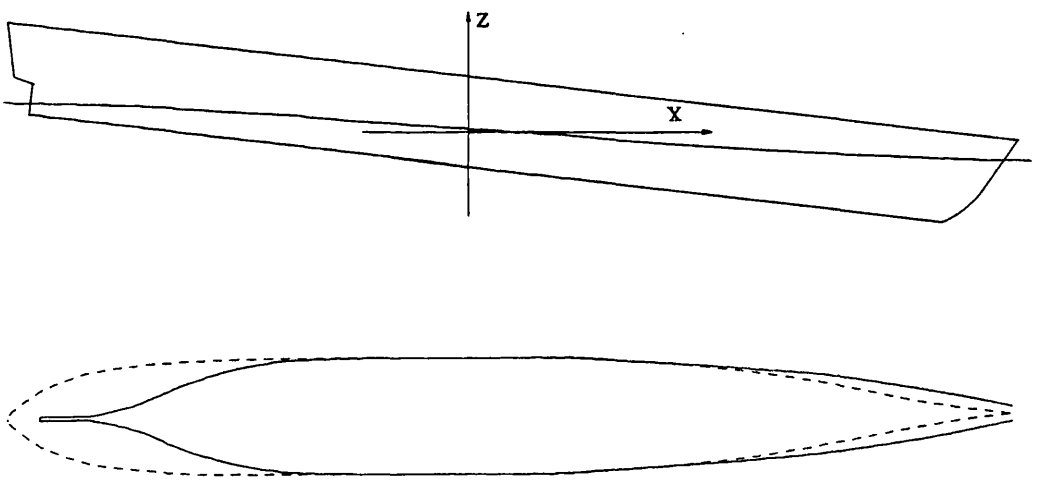

---------- static equilibrium condition in still water

_____ instantaneous profile

Computed values for the displacements given above:

Linear restoring moment $= C_{55}\xi_5 + C_{53}\xi_3 = 3.43 \times 10^{10}$ (Nm)

Non-linear restoring moment$= 2.88 \times 10^{10}$ (Nm)

Fig. 9.48 Position of the ship, free-surface elevation, and waterline

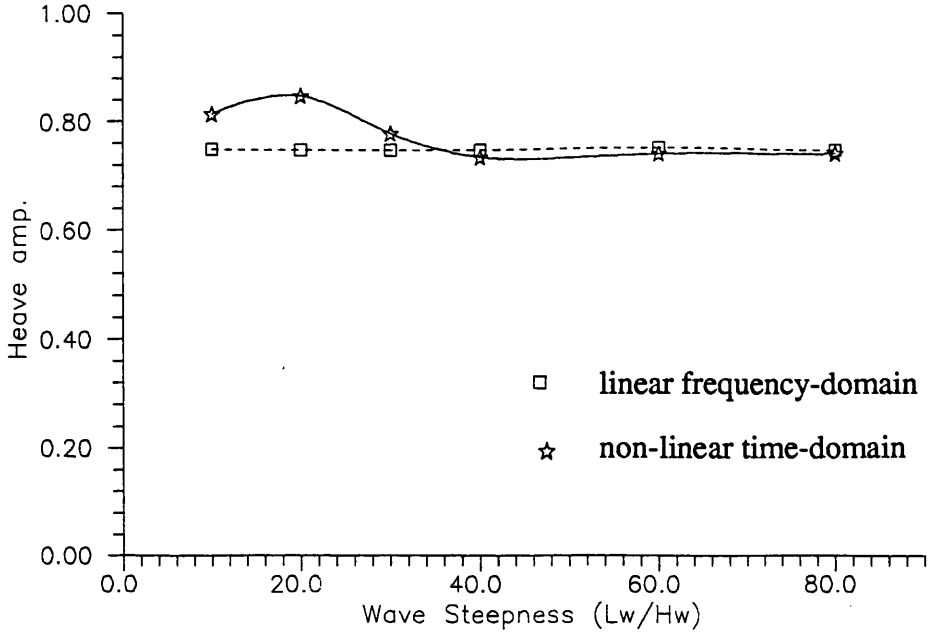

Fig. 9.49 ξ_3^{a+}/ζ^a, variation of the positive heave amplitude with the wave steepness for a constant wave length, $L_w/2\zeta^a = 2.0$

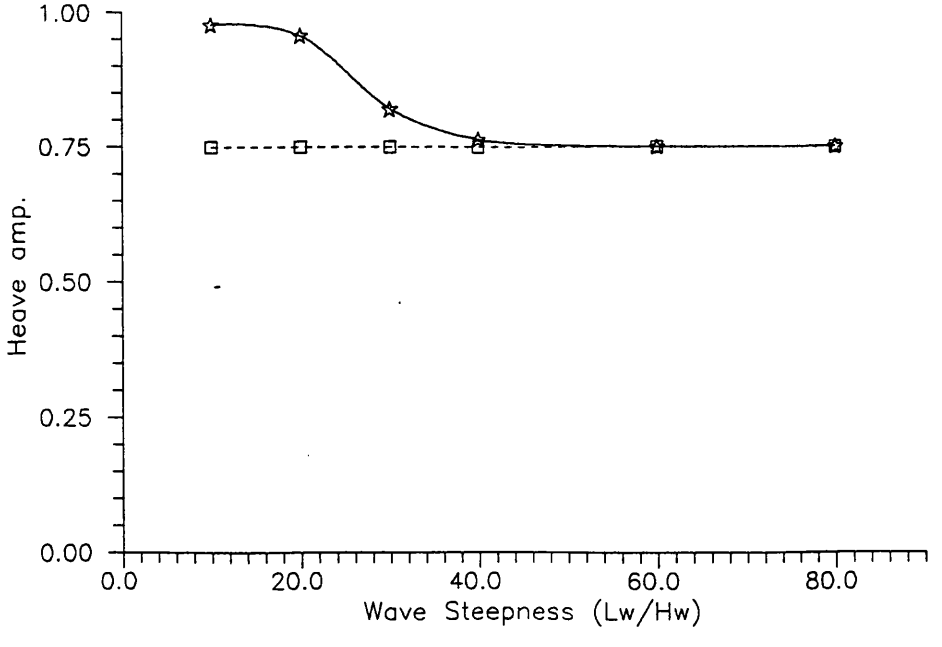

Fig. 9.50 $\left|\xi_3^{a-}\right|/\zeta^a$, variation of the negative heave amplitude with the wave steepness for a constant wave length, $L_w/2\zeta^a = 2.0$

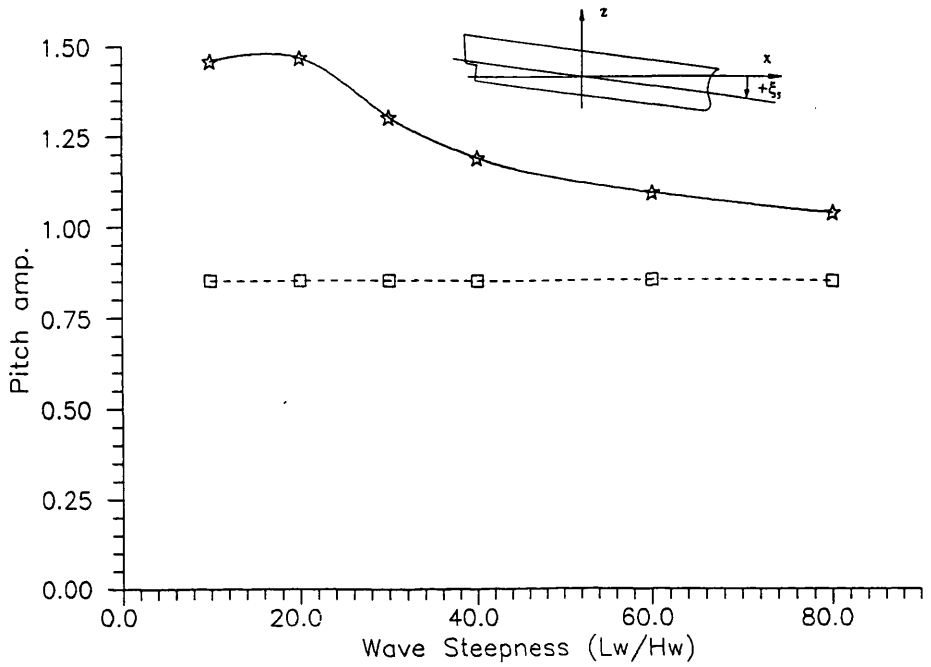

Fig. 9.51 $\xi_5^{a+} / k_0\zeta^a$, variation of the positive pitch amplitude with the wave steepness for a constant wave length, $L_w / 2\zeta^a = 2.0$

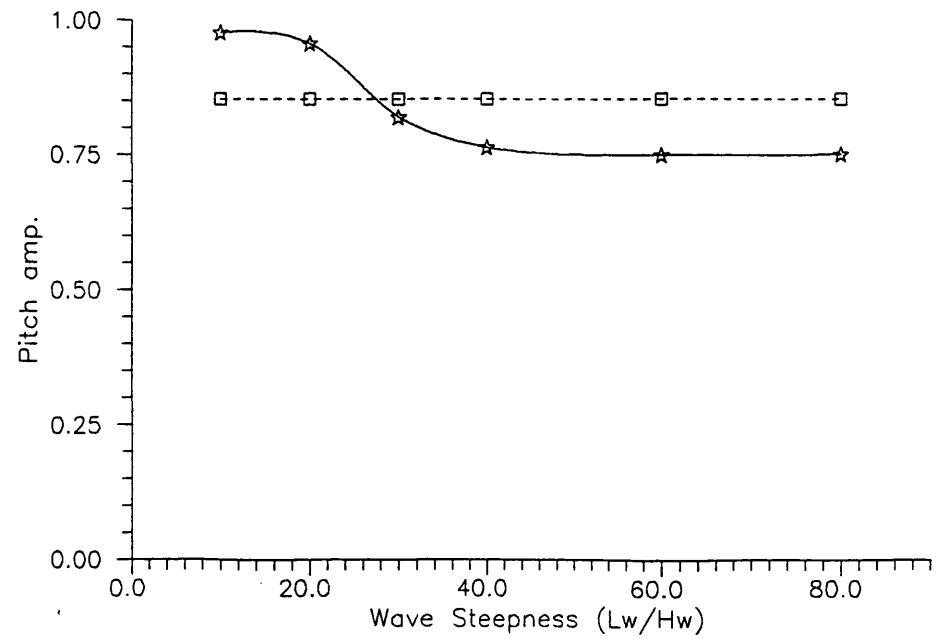

Fig. 9.52 $\left|\xi_5^{a-}\right| / k_0\zeta^a$, variation of the negative pitch amplitude with the wave steepness for a constant wave length, $L_w / 2\zeta^a = 2.0$

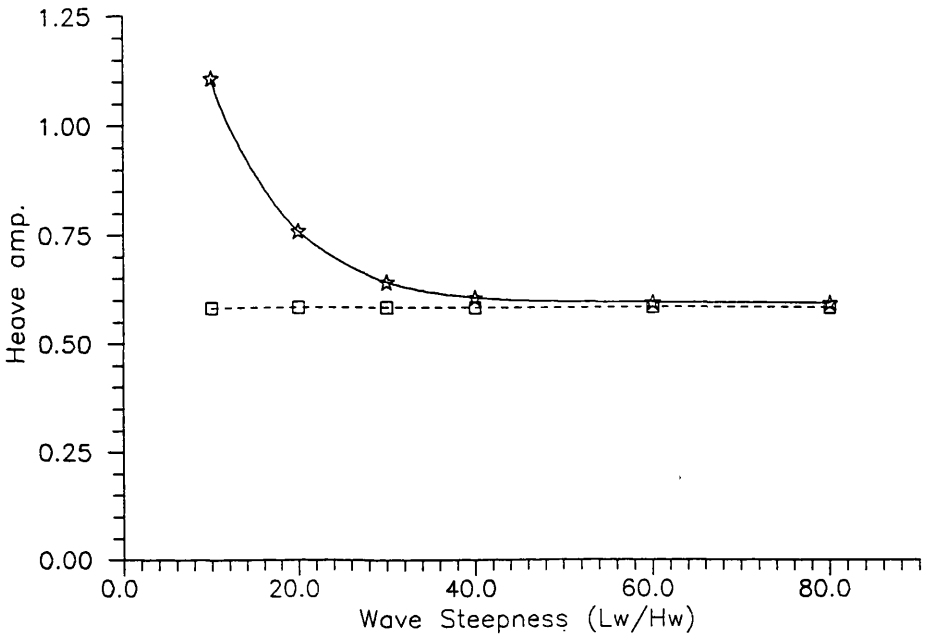

Fig. 9.53 ξ_3^{a+}/ζ^a, variation of the positive heave amplitude with the wave steepness for a constant wave length, $L_w / 2\zeta^a = 1.5$

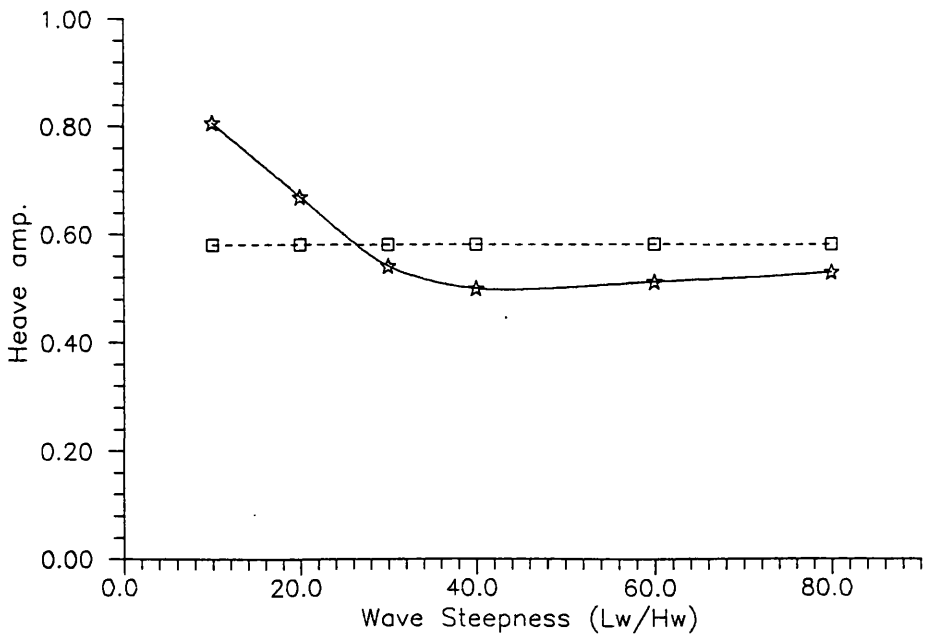

Fig. 9.54 $\left|\xi_3^{a-}\right|/\zeta^a$, variation of the negative heave amplitude with the wave steepness for a constant wave length, $L_w / 2\zeta^a = 1.5$

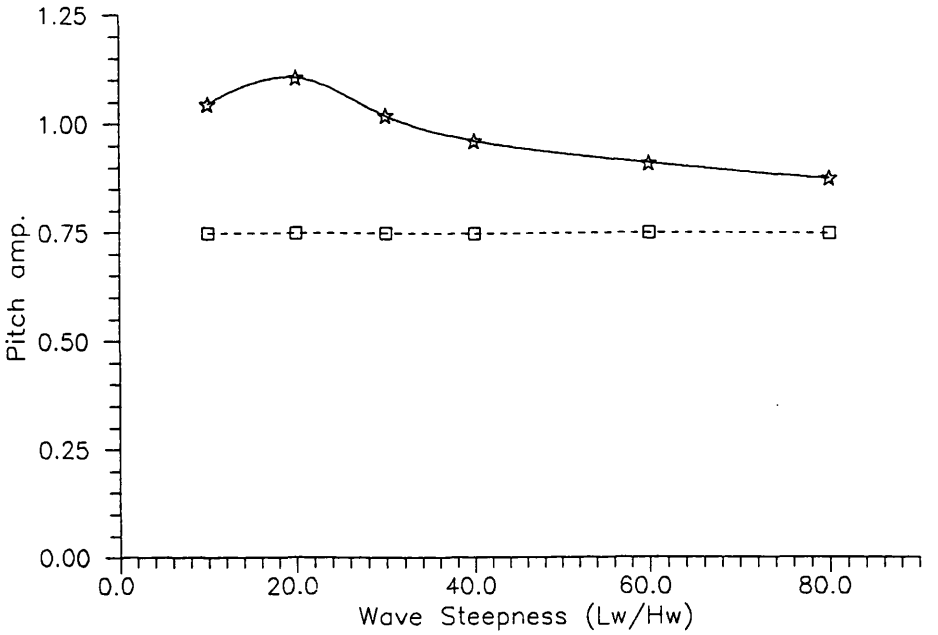

Fig. 9.55 $\xi_5^{a-} / k_0\zeta^a$, variation of the positive pitch amplitude with the wave steepness for a constant wave length, $L_w / 2\zeta^a = 1.5$

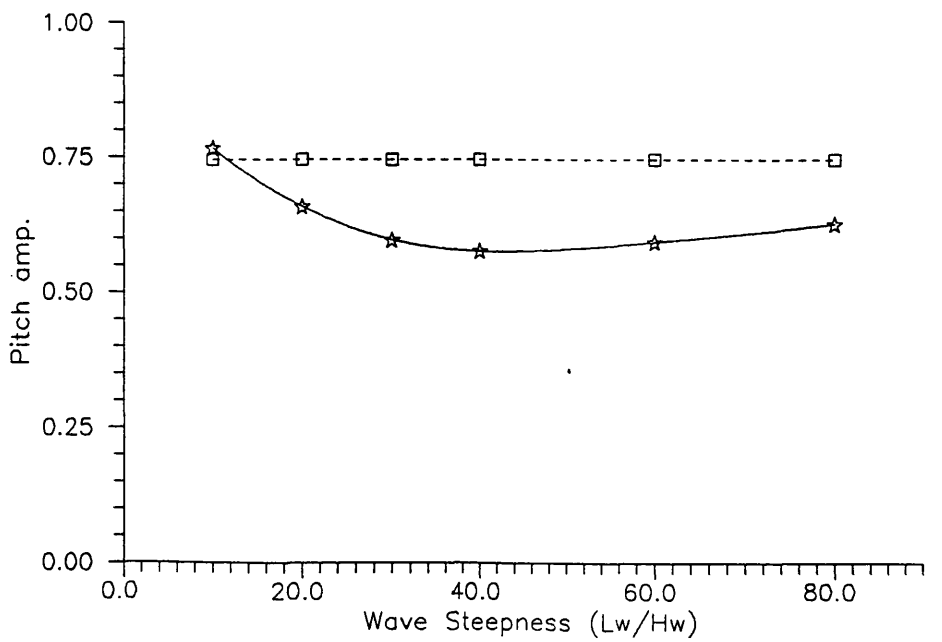

Fig. 9.56 $\left|\xi_5^{a-}\right| / k_0\zeta^a$, variation of the negative pitch amplitude with the wave steepness for a constant wave length, $L_w / 2\zeta^a = 1.5$

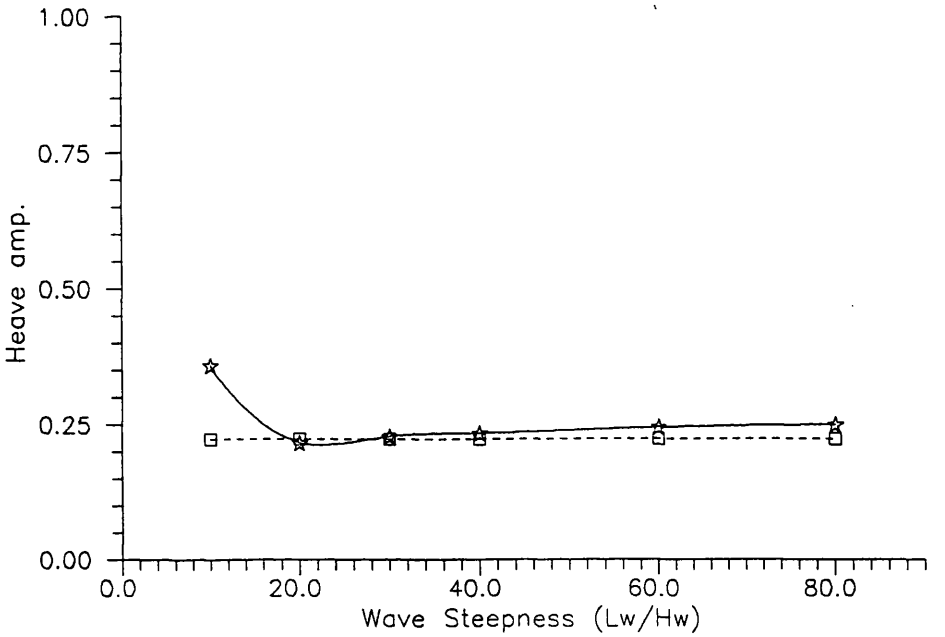

Fig. 9.57 ξ_3^{a-}/ζ^a, variation of the positive heave amplitude with the wave steepness for a constant wave length, $L_w / 2\zeta^a = 1.0$

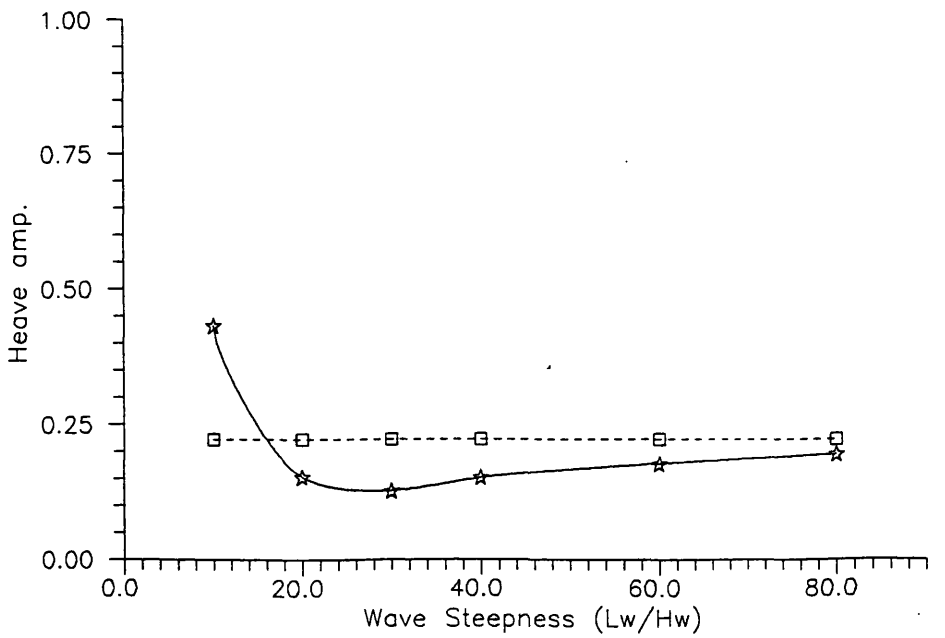

Fig. 9.58 $\left|\xi_3^{a-}\right|/\zeta^a$, variation of the negative heave amplitude with the wave steepness for a constant wave length, $L_w / 2\zeta^a = 1.0$

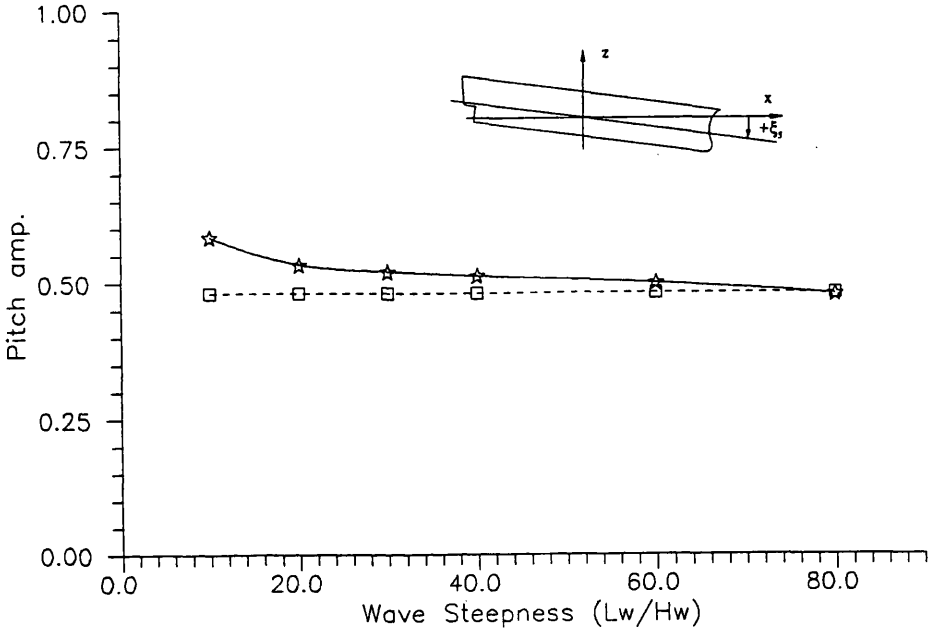

Fig. 9.59 $\xi_5^{a+} / k_0\zeta^a$, variation of the positive pitch amplitude with the wave steepness for a constant wave length, $L_w / 2\zeta^a = 1.0$

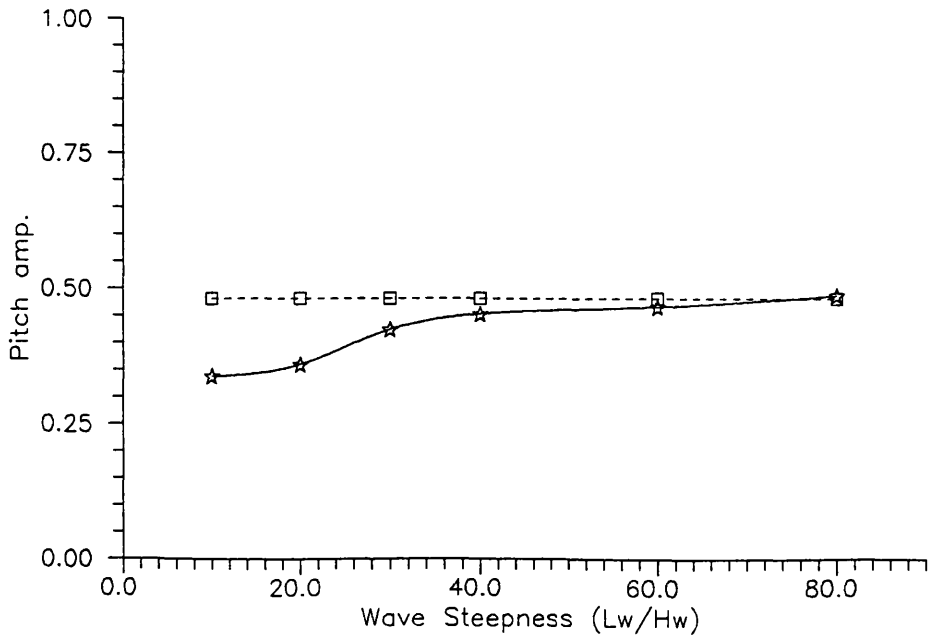

Fig. 9.60 $\left|\xi_5^{a-}\right| / k_0\zeta^a$, variation of the negative pitch amplitude with the wave steepness for a constant wave length, $L_w / 2\zeta^a = 1.0$

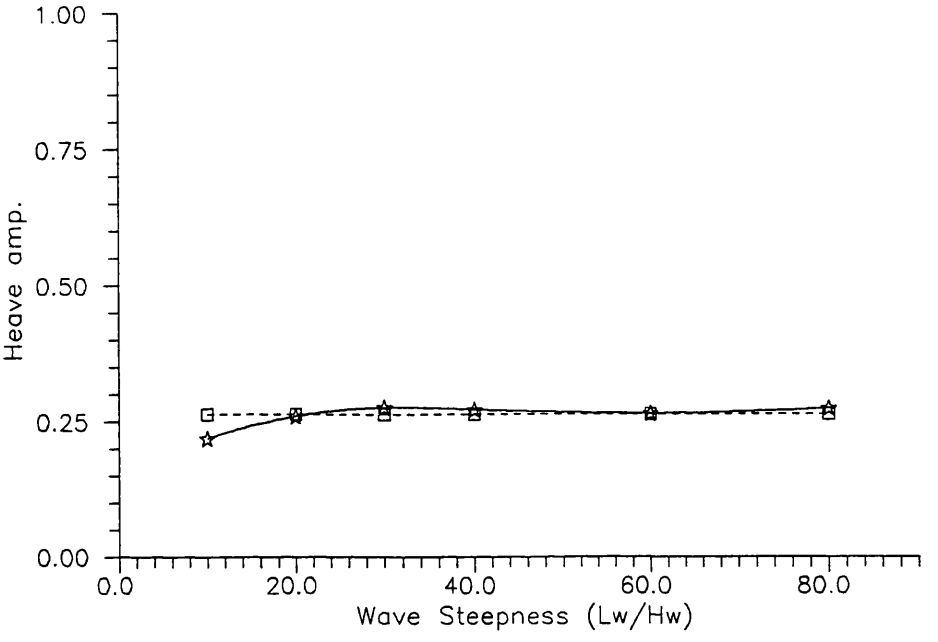

Fig. 9.61 ξ_3^{a-}/ζ^a, variation of the positive heave amplitude with the wave steepness for a constant wave length, $L_w / 2\zeta^a = 0.5$

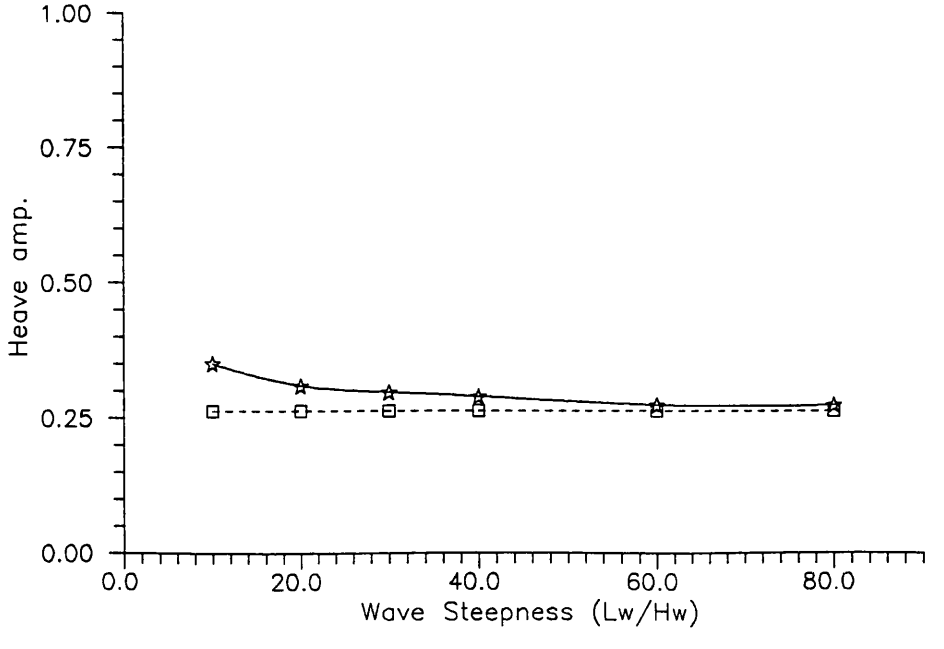

Fig. 9.62 $\left|\xi_3^{a-}\right|/\zeta^a$, variation of the negative heave amplitude with the wave steepness for a constant wave length, $L_w / 2\zeta^a = 0.5$

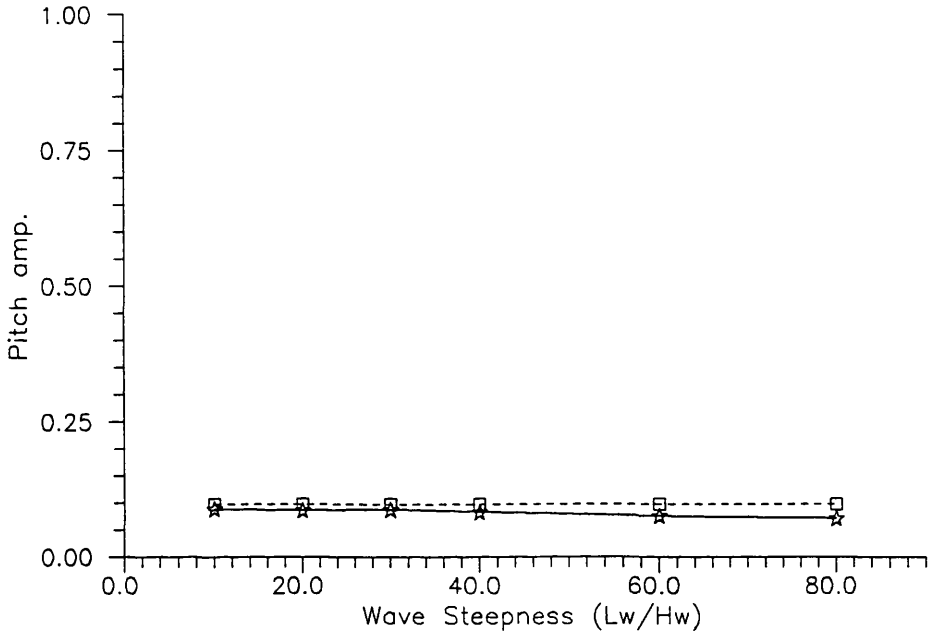

Fig. 9.63 $\xi_5^{a+} / k_0\zeta^a$, variation of the positive pitch amplitude with the wave steepness for a constant wave length, $L_w / 2\zeta^a = 0.5$

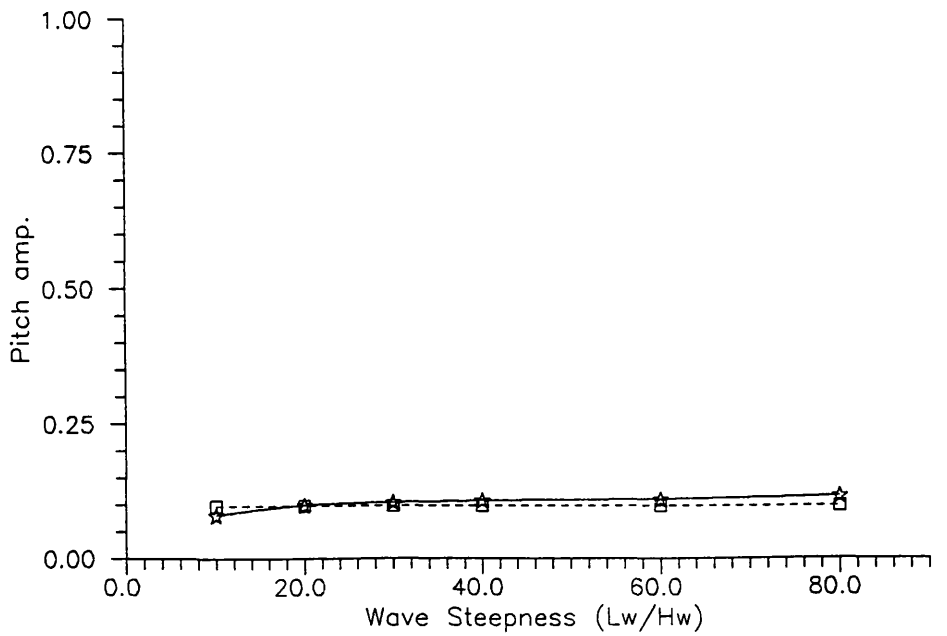

Fig. 9.64 $\left|\xi_5^{a-}\right| / k_0\zeta^a$, variation of the negative pitch amplitude with the wave steepness for a constant wave length, $L_w / 2\zeta^a = 0.5$

10. CONCLUSIONS

10.1 - General

The general aim of the study reported in this thesis was to develop a time domain method to predict non-linear motions of floating bodies subjected to waves. Two steps were followed, first, a time domain formulation for all the fluid forces was developed and applied, secondly, non-linear hydrostatic forces were formulated and introduced into the time domain motion equations. The non-linearities arise from the evaluation of the hydrostatic pressure over the instantaneous wetted surface, where the free surface elevation is taken into account. The well known linear frequency domain solution was also studied in detail and applied in order to compare and validate the non-linear time-domain results.

Two different problems were studied. In the first part of the thesis the two-dimensional motion of floating cylinders with arbitrary cross sections and subjected to beam waves was investigated. The motions are the sway, heave, and roll. Experiments using a cylinder with a particular cross section were conducted in order to obtain data to validate the mathematical models.

In the second part of the thesis the problem of ship forms travelling with forward speed and an arbitrary heading angle relative to linear incident waves was studied. Frequency domain results of the heave and pitch motions for several heading angles were compared with experimental data and with other theories. Numerical results presented for the non-linear model are restricted to the head waves condition and zero forward speed.

In order to apply the mathematical models several computer programs were developed which can be grouped into four main modules, two for the frequency domain solutions of the cylinder and ship motion problems, and two for the corresponding non-linear time domain solutions.

10.2 - Conclusions from the Cylinder Motion Solutions

The first important conclusion is that the only fluid forces which have dependency on the past history of the fluid motion, the radiation forces, can be properly calculated in the time domain by the method developed here, and in fact are different from the corresponding frequency domain forces when the motion is non-sinusoidal.

For the non-linear model the general conclusion is that although some results are very encouraging, at the present stage the model does not give reliable predictions since in some cases the solutions are wrong.

Beginning with the heave motion, in general the experimental data shows a small non-linearity because the absolute values of the positive amplitudes are higher than the negative. This is mainly due to the coupling with the roll. Since the sides of the cylinder are very steep the roll displacement is associated with an increase in the immersed volume, which creates an additional vertical hydrostatic force. The predictions given by the linear frequency domain model can not identify this tendency, but they compare well with the experiments in all cases. On the other hand the same non-linear characteristic is predicted by the time domain model, however in some cases it is very exaggerated. The radiation forces are properly computed, and the hydrostatic forces are believed to be also properly calculated, thus the cause of the disparate results must be the neglected effects on the linearization of the other fluid forces. One question arises: why in some cases the linear solution is good if all the forces were linearized, and on the other hand the time domain solution gives inaccurate results when one of the fluid force predictions was improved? In fact it seems that one great merit of the linear theory is that the several neglected effects tend to cancel each other out, and under a wide variety of conditions the final results are not much affected. As mentioned the linear heave results compare well with the experiments, and the small non-linearity arises not from the heave motion itself but from the coupling with the roll. However the body tested had a large ratio 'water plane area -- displacement', thus the relative motions were small. Certainly higher non-linearities are associated with heave motions itself where the relative motions are large, like for example the bow sections of ships.

The experimental data for the roll motion shows two non-linear effects. The first and the most obvious one, is related to the restoring moment which for large roll angles is higher than the linear theory prediction. Comparing the linear results with the experiments for the frequencies near the resonance one can see that the difference is very large. The time domain results are very encouraging for the smaller wave amplitudes, but for the higher waves there are some inaccurate estimations. The second non-linearity in the experimental data is found on the difference between the positive and negative roll amplitudes for the medium to high frequency range. The cylinder "turns down" more to the side receiving the waves. This tendency is predicted well by the time domain model for the frequencies near the resonance, and the non-linearity in the numerical results arise because of the different wave elevation amplitudes on both sides of the body used to compute the hydrostatic forces. However for the higher frequencies the tendency predicted is the opposite, probably because the neglected non-linear effects in the other forces, especially the diffracted forces, become more important. In addition time domain simulations were carried out using the exact stability arm of the cylinder in still water. Results show that the predicted resonance frequency is higher than the experiments, and the model tends to underestimate the roll amplitudes at the higher amplitude of waves. The poor correlation of the results with the experimental data indicates that the free surface elevation effects must be taken into account.

For the sway motion the linear and non-linear numerical results are similar, except that for the second case there is a small steady sway which arises from two effects: there is a sway hydrostatic force which in general is stronger for one of the directions due to the asymmetry of the free surface elevation on both sides of the body, and a small numerical error was found which induces a small steady sway velocity. Compared with the experimental data we find that for the lower frequencies the experimental amplitudes of the motion are smaller than the numerical results, but of the same order of magnitude. The smaller values can be explained by the fact that the mooring system, which restrains the motions, is not taken into account in the numerical models. However for the most of the cases the measured amplitudes are much higher than the predictions. No justification is found to for the inaccurate predictions of the forces associated with the sway motions since the same forces associated with the other modes of motion are nearly correct. One probable cause for these differences is error in the calibration of the Selspot system for the horizontal

displacements of the diodes, however the author is not able to state that this is the reason or one of the reasons. More research and more carefully conducted experiments are needed to validate the sway motion models.

10.3 - Conclusions from the Ship Motion Solutions

Starting with the frequency domain program it can be concluded that the procedure is validated by comparing the results with experimental data and two other ship motion theories.

The time domain model results show a strong a non-linear behaviour in the pitch motions. In general the ship tends to turn the bow down much more than the linear theory predicts, especially for the larger waves. It would be very useful to compare both the positive and negative amplitudes of the pitch motion with corresponding experimental data, but this data was not available. The predictions of positive pitch amplitudes are probably exaggerated, however it is believed that this tendency has a physical meaning and exists in the real case, despite being less exaggerated. What happens is that the linear model over-predicts the restoring moment. In fact a superficial analysis leads to the conclusion that in the real case the restoring moment when the ship turns the bow down is higher than the linear prediction since there is a flare on the sides of the ship near the bow thus the buoyancy force increases more with the angle. However if on the bow side the true water plane area is increasing as the ship rotates, on the stern side the true water plane area is decreasing much more, and the overall result is that the real restoring moment is smaller than the linear prediction. It is possible that the real mean amplitude of pitch (average between absolute positive and negative amplitudes) is very close to the linear predictions, as it is recognised that this kind of result is accurate. However the non-linearity described is believed to be very important since for large ships one degree of difference in the positive or negative amplitudes of the pitch may make the difference between the occurrence or not of strong slamming, deck wetness, or propeller emergence. The exaggerated predictions reported lead to the conclusion that improving the evaluation of only one term in the motion equation does not necessarily mean that the final result is improved.

The influence of the wave steepness was investigated by doing a set of simulations where the wave lengths were kept constant and several wave steepnesses were used. The bigger non-linearities are found for the higher waves and the time domain solution tends to be linear as the wave height becomes smaller.

10.4 - Recommendations for Future Work

For the time domain model to predict the cylinder motions some improvements can be made:

- The Froude-Krylov force can be computed in the time domain over the "exact" wetted surface, which would certainly improve the results in the low frequency range.

- The radiation forces and the diffracted part of the exciting forces could be calculated for several immersions and heel angles, and these values stored to be used by the time domain program which would choose the proper values at each time instant dependent on the immersed shape of the body.

- Finally the equation of roll motion could include the terms representing the large amplitude rotations of a rigid body in accordance with the Euler equations.

For the ship motion problem a considerable ammount of work can be perfomed extending the theory and program presented in this thesis:

- The first steps are certainly the extension of the programs to the other degrees of freedom, surge, sway, roll, and yaw, and to solve the equation presented in appendix B in order to incorporate the related forward speed effects according to the present theory. The first task is an easy one since the programs were prepared to solve all the motion modes, and a couple of weeks should be enough to extend both programs, frequency domain and time domain. On the other hand the complex equation given in appendix-B requires a great deal of effort for solving.

- As mentioned, another improvement could be the evaluation in the time domain of the Froude-Krylov force over the exact wetted surface, which would certainly improve the results, especially in the range of large-high waves.

- The prediction of the linear free surface elevation on the sides of the ship could be improved by including the effects of the radiation and diffracted

potentials, which may become important in the high frequency range and certainly are important in the case of lateral waves.

- One of the advantages of the time domain approach is that it has the capability to predict the ship motions given any force for which there is an evaluation method. The force may be an arbitrary function of space and time, or a function of absolute or relative ship position, velocity and acceleration. Some forces could be included in the present method like for example bottom slamming, flare slamming, forces resulting from deck wetness, wind forces, mooring forces, rudder and propeller forces, viscous forces, etc.

- Finally the area of applicability where this method is believed to be especially useful is on the prediction of motion responses in irregular seas, if one or several non-linear effects need to be taken into account. In this case the superposition principle of frequency domain results can not be used since the motion responses to each frequency component must be linear. On the other hand the known methods use frequency dependent hydrodynamic coefficients in the non-linear equations of motion, thus the user is faced with the problem of choosing a particular frequency to be associated with the coefficients when the nature of the response is irregular. The method used in this thesis solves non-linear time domain equations of motion where the radiation forces are evaluated in the time domain, thus they are frequency independent.

REFERENCES

Beck, R. F. and **Liapis, S. J.** (1987), "*Transient Motions of Floating Bodies at Zero Forward Speed*", J. of Ship Research, Vol. 31, No. 3, pp. 164-176.

Beck, R. F. and **Magee, A. R.** (1991), "*Time-Domain Analysis for Predicting Ship Motions*", Dynamics of Marine Vehicles and Structures in Waves, Elsevier Science Publishers B. V.

Belik, O., Bishop, R.E.D. and **Price, W. G.** (1980), "*On the slamming response of ships to regular head waves*", The Royal Inst. Naval Archit., Vol. 122, pp. 325-337.

Chan, H. S. (1990), "*Prediction of Motion and Wave Loads of Twin-Hull Ships*", Marine Structures, Vol. 6, pp. 75-102.

Chang, M. S. (1977), "*Computations of three-dimensional ship motions with forward speed*", Proc. Int. Numer. Ship Hydrodyn., 2nd, pp. 124-135. University of California, Berkeley.

Chapman, R. B. (1979), "*Large-Amplitude Transient Motion of Two-Dimensional Floating Bodies*", J. of Ship Research, Vol. 23, pp. 20-31.

Chapman, R. B. (1979), "*Time-Domain Method for Computing Forces and Moments Acting on Three-Dimensional Surface-Piercing Ship Hulls with Forward Speed*", Int. Conf. Num. Ship Hydrodyn., 14th, Paris.

Cummins, W. E. (1962), "*The impulse response function and ship motions*", Schiffstechnik, Vol. 9, pp. 101-109.

Dalzell, J. F. (1962a), "*Cross-Spectral Analysis of Ship Model Motions: A Destroyer Model in Irregular Long-Crested Head Seas*", Stevens Inst. of Technology-Davidson Laboratory, Report No. 810.

Dalzell, J. F. (1962b), "*Some Further Experiments on the Application of Linear Superposition Techniques to the Responses of a Destroyer Model in Extreme Long-Crested Head Seas*", Stevens Inst. of Technology-Davidson Laboratory, Report No. 819.

Elsimillawy, N. and **Miller, N.S.** (1986), "Time Simulation of Ship Motions: A Guide to the Factors Degrading Dynamic Stability", Soc. Naval Archit. Mar.Eng., Vol. 94, pp. 215-240.

Finkelstein, A. B. (1957), "*The initial value problem for transient water waves*", Commun. on Pure and Apllied Mathem., Vol. 10, pp. 511-522.

Flokstra, C. (1974), "*Comparison of ship motion theories with experiments for a container ship*", Int. Shipbuilding Progress, Vol 21, pp. 168-189.

Frank, W. (1967), "*Oscillation of Cylinders in or Below the Free-Surface of Deep Fluids*", Report 2375, Naval Ship Research and Development Center, Washington D.C.

Froud, W. (1861), "*On the rolling of ships*", Inst. Nav. Archit., Trans. 2, pp. 180-229.

Gie, T. S. (1972), "*Wave load measurements on a model of a large container ship*", Netherlands Ship Research Centre, Report No. 173s.

Golovato (1959), "*A Study of the Transient Pitching Oscillations of a Ship*", J. of Ship Research, Vol. 2, No. 4, pp. 22-30.

Haskind, M. D. (1964), "*The hydrodynamic theory of ship oscillations in rolling and pitching*", Prikl. Mat. Mekh., Vol. 10, pp. 33-66. (Engl. transl., Tech. Res. Bull. No. 1-12, pp. 3-43, Soc. Naval Archit. Mar. Eng., New York, 1953.)

Haskind, M. D. (1964), "*The oscillation of a ship in still water*", Izv. Akad. Nauk SSSR, Otd. Tekh. Nauk 1 pp. 23-34. (Engl. transl., Tech. Res. Bull. No. 1-12, pp. 45-60, Soc. Naval Archit. Mar.Eng., New York, 1953.)

Hochmann, D. (1991), "*Calculation of Pressures on a Ship's Hull in Waves*", Ship Technology Research, Vol 38, No. 3, pp. 111-137.

Ikebuchi, T. (1981), "*Hydrodynamic forces on a body moving arbitrary in time on a free surface*", J. Kansai Society of Naval Archit., Japan, No. 181, pp. 45-53.

Ikeda Y., Himeno Y., and **Tanaka N.** (1978), "*A Prediction Method for Ship Roll Damping*", Dep. Naval Archit. Univ. of Osaka Prefecture, Report No. 405, Dec., 1978.

Inglis, R. B., and **Price W. G.** (1981), "*A Three-Dimensional Ship Motion Theory -- Comparison Between Theoretical Prediction and Experimental*

Data of the Hydrodynamic Coefficients with Forward Speed", Trans. Royal Institution of Naval Archit., Vol. 124, pp. 141-157.

Jensen, J. J. and **Pedersen, P. T.** (1979), "*Wave-induced bending moments in ships -- A quadratic theory*", The Royal Inst. Naval Archit., Vol. 121, pp 151-165.

Joosen, W. P. A. (1964), "*Oscillating Slender Ships at Forward Speed*", Publ. No. 268, Neth. Ship Model Basin, Wageningen.

Kato, H. (1958), "*On the Frictional Resistance to the Rolling Ships*", J. of Soc. Naval Archit. Japan, Vol.102, pp. 115.

Kim, Y. J. and **Hwang J. H.** (1986), "Two Dimensional Transient Motions with Large Amplitude by Time Domain Method",

Kim C. H., Frank, S. C. and **David, T.** (1980), "*Motions and Hydrodynamic Loads of a Ship Advancing in Oblique Waves*", Trans. Soc. Naval Archit. Mar. Eng., Vol. 88, pp. 225-256.

King, B. K., (1987), "*Time-Domain analysis of Wave Exciting Forces on Ships and Bodies*", Dep. of Naval Archit. Mar. Eng., The Univ. of Michigan, Report No. 306.

King, B. K., Beck, R. F. and **Magee, A. R.** (1988), "*Seakeeping Calculations with Forward Speed Using Time-Domain Analysis*", Proc. of Symp. on Naval Hydrodyn., 18th, Delft, Netherlands, pp. 577-596.

Korvin-Kroukovsky, B. V. (1955), "*Investigation of ship motions in regular waves*", Soc. Naval Archit. Mar. Eng., Trans. 63, pp. 385-435.

Korvin-Kroukovsky, B. V., and **Jacobs, W. R.** (1957), "*Pitching and heaving motions of a ship in regular waves*", Soc. Naval Archit. Mar. Eng., Trans. 65, pp. 590-632.

Krylov, A. (1896), "*A new theory of the pitching motion of ships on waves, and of the stresses produced by this motion*", Inst. Nav. Archit., Trans.65, pp. 590-632.

Lewis, F. M. (1929), "*The inertia of water surrounding a vibrating ship*", Soc. Naval Archit. Mar. Eng., Trans. 37, pp. 1-20.

Liapis, S. J. and **Beck, R. F.**(1985), "*Seakeeping Computations Using Time-Domain Analysis*", Proc. Int. Symp. on Numerical Hydrodyn., 4th, National Academy of Sciences, Washington, D.C., pp. 34-54.

Maruo, H. (1967), "*Application of the slender body theory to the longitudinal motion of ships among waves*", Bull. Fac. Eng., Yokohama Natl. Univ., Vol 16, pp. 29-61.

Maruo, H. and **Tokura, J.** (1978), "*Prediction of hydrodynamic forces and moments acting on ships in heaving and pitching oscillations by means of an improvement of the slender ship theory*", J. Soc. Naval Archit. Japan, Vol. 143, pp. 111-120.

Maskell, S. J. and **Ursell, F.** (1970), "*The transient motion of a floating body*", J. of Fluid Mechanics, Vol. 44, part 2, pp. 303-313.

Mays, J. H. (1978), "*Wave radiation and diffraction by a floating slender body*", Ph.D. Thesis, Massachusetts Institute of Technology, Cambridge, Massachusetts.

Michell, J. H. (1898), "*The wave resistance of a ship*", Philos. Mag., Vol. 45, pp. 106-123.

Nakos, D. and **Sclavounos, P. D.** (1990), "*Ship motions by a three-dimensional Rankine panel method*", Proc. Symp. Naval Hydrodyn., 18th, Ann Arbor, Michigan, USA.

Neumann, G. and **Pierson, W. J.** (1966), "*Principles of physical oceanography*", Englewood Cliffs, N. J., Prentice-Hall.

Newman, J. N. (1961), "*A linearized theory for the motion of a thin ship in regular waves*", J. Ship Res., Vol. 3, No. 1, pp. 1-19.

Newman, J. N. (1962), "The Exciting Forces on Fixed Bodies in Waves", J. Ship Res., SNAME, December, pp. 10-17.

Newman, J. N. (1964), "*A slender-body theory for ship oscillations in waves*", J. Fluid Mech., Vol 18, pp. 602-618.

Newman, J. N. (1964), "*The Exciting Forces on a Moving Body in Waves*", J. of Ship Research, Vol. 9, pp. 190-199.

Newman, J. N. (1965), "The Exciting Forces on a Moving Bodie in Waves", J. Ship Res., SNAME, December, pp. 190-199.

Newman, J. N. (1977), "*Marine Hydrodynamics*", MIT Press, Cambridge, Massachusetts.

Newman, J. N. (1978), "*The Theory of Ship Motions*", Advances in Applied Mech., Vol. 18, pp. 221-283.

Newman, J. N. (1985), "*Transient Axisymmetric Motion oa a Floating Cylinder*", J. Fluid. Mechanics, Vol. 157, pp. 17-33.

Newman, J. N., and Tuck, E. O. (1964), "*Current progress in the slender-body theory of ship motions*", Proc. Symp. Nav. Hydrodyn., 5th, pp. 129-167. Off. Nav. Res., Washington, D.C.

Ochi, M. K. (1964), "*Prediction of Occurrence and Severity of Ship Slamming at Sea*", Proc. Symp. Naval Hydrodyn., 5th.

Ogilvie, T. F. (1964), "*Recent progress toward the understanding and prediction of ship motions*", Proc. Symp. on Naval Hydrodyn., 5th, Washington D.C., pp. 3-128.

Ogilvie, T. F., and **Tuck, E. O.** (1969), "*A Rational Strip Theory for Ship Motions*", Part 1, Report No. 013, Dep. Naval Archit. Mar. Eng., Univ. of Michigan, Ann Arbor.

Ogilvie, T. F. (1974), "*The fundamental assumptions in the ship-motion theory*", Report No. 148, Dep. Naval Archit. Mar. Eng., Univ. of Michigan, Ann Arbor.

Oliver J. C. (1990), "*Advanced Methods for Ship Motion and Wave Load Prediction*", Ship Structure Committee, Report No. SSC-333.

Papanikolaou, A. and **Schellin T. E.** (1992), "*A Three-Dimensional Panel Method for Motions and Loads of Ships with Forward Speed*", Ship Technology Research, Vol. 39, No. 4, pp. 147-156.

Pauling, J. R. and **Wood, P. D.** (1974), "*Ship Motions and Capsizing in Astern Seas*", Proc. Symp. Naval Hydrodyn., 10th, pp. 93-109.

Peters, A. S., and **Stoker, J. J.** (1957), "*The motion of a ship, as a floating rigid body, in a seaway*", Commun. Pure Appl. Math., Vol. 10, pp. 399-490.

Petersen, J. B. (1992), "*Non-linear strip theories for ship response in waves*", Dep. of Ocean Eng., Technical Univ. of Denmark.

Porter, W. R. (1960), "*Pressure Distributions, Added Mass, and Damping Coefficients for Cylinders Oscillating in a Free Surface*", Univ. of California, Inst. Eng. Res., Report 82-16, Berkeley, California.

Salvesen, N., Tuck, E. O., and **Faltisen, O.** (1970), "*Ship motions and sea loads*", Soc. Naval Archit. Mar. Eng., Trans. 78, pp 250-287.

St. Denis, M. and **Pierson, W.J.** (1953), "*On the motion of ships in confused seas*", Soc. Naval Archit. Mar. Eng., Trans. 61, pp. 280-354.

Stoker, J. J. (1957), "*Water waves*", Interscience Publishers, Inc., New York.

Tasai, F. (1959), "*On the Damping Force and Added Mass of Ships Heaving and Pitching*", J. of Zosen Kiokai, Vol. 105, pp. 47-56.

Ursell, F. (1949), "*On the heaving motion of a circular cylinder on the surface of a fluid*", Q. J. Mech. Appl. Math., Vol. 2, pp. 218-231.

Ursell, F. (1964), "*The Decay of the Free Motion of a Floating Body*", J. of Fluid Mechanics, Vol. 19, pp. 305-319.

Ursell, F. (1962), "*Slender oscillating ships at zero forward speed*", J. Fluid Mechanics, Vol. 19, pp. 496-516.

Ursell, F. (1964), "*The decay of the free motion of a floating body*", J. Fluid Mechanics, Vol. 19, pp. 305-314.

Yeung, R. W. (1982), "*The transient heaving motion of floating cylinders*", J. of Eng. Mathematics, Vol. 16, pp. 97-119.

APENDIX-A: NON-LINEAR ROLL DAMPING

The roll motion, contrary to the other modes of motion, is very sensitive to the non-linear effects of fluid viscosity, especially to viscosity induced flow separations. Thus the prediction of roll damping using only the knowledge of the linear damping due to radiated waves is no longer valid as concerns this mode of motion.

Following Ikeda et. al (1978) the roll damping for the present two dimensional problem can be divided in three components, the wave, friction, and eddy components. Interferences between these components are neglected. The wave component, related with to waves generated by the oscillatory motion, has been discussed in Section-4.2. A method to predict the other two is presented here.

Friction Damping

This is related with the tangential stresses on the body surface due to the fluid viscosity. Kato (1965) showed that the skin friction laws for a flat plate in steady flow can be applied if an effective Reynolds number for roll motion is used. The friction coefficient is given by;

$$C_f = 1.328\left[\frac{3.22 r_s^2 \xi_4^{a2} \omega}{2\pi\upsilon}\right]^{-\frac{1}{2}}$$

and the damping coefficient due to surface friction is;

$$B_F = \frac{4}{3\pi}\rho S r_s^3 \xi_4^a \omega C_f$$

were r_s is the average radius of roll, S is the wetted surface area, ξ_4^a is the roll amplitude, ω is the frequency of motion, υ is the fluid kinematic viscosity, and ρ is the fluid density.

Eddy Damping

The eddy component is related to generated vortices because of flow separation from the body surface. Ikeda et. al (1978) carried out a series of experiments with two dimensional cylinders of several cross section shapes and concluded that this term depends basically on the hull shape. They then used a simple form of pressure distribution on the hull surface, and assumed that the pressure coefficient, C_p, is a function of the ratio of the maximum relative velocity to the mean one on the hull surface, $\gamma = V_{max} / V_{min}$, which can be evaluated by the potential flow theory for a rotating Lewis form cylinder in infinite fluid. The curve $C_p - \gamma$ was then obtained from the experimental results of the roll damping for two dimensional models, and a mathematical expression fitted to the curve. Finally the eddy damping component is given by;

$$B_E = \frac{4\rho d^4 \omega \xi_4^a}{3\pi}\left\{\left(1 - f_1\frac{R}{d}\right)\left(1 - \frac{Z'_G}{d}\right) + f_2\left(H_0 - \frac{R}{d}\right)^2\right\}\left\{\frac{r_{max}}{d}\right\}^2 C_p$$

where

$$H_0 = \frac{B}{2d}$$

$$f_1 = 0.5\{1 + \tanh[20(\sigma - 0.7)]\}$$

$$f_2 = 0.5\{1 - \cos(\pi\sigma)\} - 1.5\{1 - \exp[-5(1-\sigma)]\}\sin(\pi\sigma)$$

and the coefficient γ is obtained from;

$$\gamma = \frac{\sqrt{\pi} f_3}{2d\left(1 - \frac{Z'_G}{d}\right)\sqrt{H'_0\sigma'}}\left(r_{max} + \frac{2M}{H}\sqrt{A^2 + D^2}\right)$$

and

$$M = \frac{B}{2(1+a_1+a_3)} \quad , \quad H_0' = \frac{H_0}{1-\frac{Z_G}{d}} \quad , \quad \sigma' = \frac{\sigma - \frac{Z_G'}{d}}{1-\frac{Z_G'}{d}}$$

$$H = 1 + a_1^2 + 9a_3^2 + 2a_1(1-3a_3)\cos(2\psi) - 6a_3\cos(4\psi)$$

$$A = -2a_3\cos(5\psi) + a_1(1-a_3)\cos(3\psi) + \left\{(6-3a_1)a_3^2 + (a_1^2 - 3a_1)a_3 + a_1^2\right\}\cos(\psi)$$

$$D = -2a_3\sin(5\psi) + a_1(1-a_3)\sin(3\psi) + \left\{(6+3a_1)a_3^2 + (3a_1 + a_1^2)a_3 + a_1^2\right\}\sin(\psi)$$

$$\psi = \begin{cases} 0 = \psi_1 & \text{if } r_{max}(\psi_1) \geq r_{max}(\psi_2) \\ \frac{1}{2}\cos^{-1}\left\{\frac{a_1(1+a_3)}{4a_3}\right\} = \psi_2 & \text{if } r_{max}(\psi_1) < r_{max}(\psi_2) \end{cases}$$

$$f_3 = 1 + 4\exp\left\{-1.65E + 5(1-\sigma)^2\right\}$$

where ξ_4^a is the roll amplitude, ρ is the fluid density, d d is the section draft, B is the beam, ω is the motion frequency, Z_G' is the z-co-ordinate of the gravity centre on the body fixed reference system, R is the bilge radius of the section, and σ is the section area coefficient.

Evaluation of the Total Roll Damping Coefficient

As stated above the total roll damping coefficient is obtained by adding together the three components. The wave component is calculated using the Frank close fit method as explained in Section-4.2, and can be introduced directly into the equation of roll motion. However the viscous roll damping is dependent on the roll amplitude thus it must be estimated during the solution of the motion equations.

In the frequency domain solution the viscous roll damping is estimated by an iterative process, where in each iteration it is evaluated using the roll amplitude obtained on the previous one. The process stops when the difference between

$$\tilde{G}(P,Q,t-\tau)=2\int_0^{\infty}\left\{\sqrt{kg}\sin\left[\sqrt{kg}(t-\tau)\right]e^{k(z+\zeta)}J_0(kR)\right\}dk$$

$P=(x,y,z)$ is generic field point, the influenced point.

$Q=(\xi,\eta,\zeta)$ is a source point, the influencing point.

$$r=\left\{(x-\xi)^2+(y-\eta)^2+(z-\zeta)^2\right\}^{\frac{1}{2}}$$

$$r'=\left\{(x-\xi)^2+(y-\eta)^2+(z+\zeta)^2\right\}^{\frac{1}{2}}$$

$$R=\left\{\left[x-\xi+U(t-\tau)\right]^2+\left[y-\eta\right]^2\right\}^{\frac{1}{2}}$$

g = acceleration of gravity

$\delta(t)$ = delta function

$$H(t)=\begin{cases}0\ , & t<0\\ 1\ , & t>0\end{cases}\quad ,\ \text{unit step function}$$

There was no time during the period of this thesis work to solve the equation presented above, thus the time domain computer program developed is working only at the zero speed condition.